UNIVERSITAT ROVIRA I VIRGILI
NOVEL MOLECULAR CATALYSTS FOR WATER OXIDATION: TOWARDS ARTIFICIAL PHOTOSYNTHESIS
Sara Goberna Ferrón
Dipòsit Legal: T.189-2014

DOCTORAL THESIS

Novel Molecular Catalysts for Water Oxidation: Towards Artificial Photosynthesis

Sara Goberna Ferrón

UNIVERSITAT ROVIRA I VIRGILI

UNIVERSITAT ROVIRA I VIRGILI
NOVEL MOLECULAR CATALYSTS FOR WATER OXIDATION: TOWARDS ARTIFICIAL PHOTOSYNTHESIS
Sara Goberna Ferrón
Dipòsit Legal: T.189-2014

UNIVERSITAT ROVIRA I VIRGILI
NOVEL MOLECULAR CATALYSTS FOR WATER OXIDATION: TOWARDS ARTIFICIAL PHOTOSYNTHESIS
Sara Goberna Ferrón
Dipòsit Legal: T.189-2014

UNIVERSITAT ROVIRA I VIRGILI
NOVEL MOLECULAR CATALYSTS FOR WATER OXIDATION: TOWARDS ARTIFICIAL PHOTOSYNTHESIS
Sara Goberna Ferrón
Dipòsit Legal: T.189-2014

UNIVERSITAT ROVIRA I VIRGILI
NOVEL MOLECULAR CATALYSTS FOR WATER OXIDATION: TOWARDS ARTIFICIAL PHOTOSYNTHESIS
Sara Goberna Ferrón
Dipòsit Legal: T.189-2014

DOCTORAL THESIS

Novel Molecular Catalysts for Water Oxidation: Towards Artificial Photosynthesis

Sara Goberna Ferrón

Supervised by Dr. José Ramón Galán Mascarós

Institut Català d'Investigació Química (ICIQ)

Tarragona 2013

UNIVERSITAT ROVIRA I VIRGILI

UNIVERSITAT ROVIRA I VIRGILI
NOVEL MOLECULAR CATALYSTS FOR WATER OXIDATION: TOWARDS ARTIFICIAL PHOTOSYNTHESIS
Sara Goberna Ferrón
Dipòsit Legal: T.189-2014

UNIVERSITAT ROVIRA I VIRGILI
NOVEL MOLECULAR CATALYSTS FOR WATER OXIDATION: TOWARDS ARTIFICIAL PHOTOSYNTHESIS
Sara Goberna Ferrón
Dipòsit Legal: T.189-2014

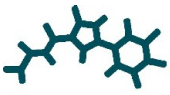

Institut Català d'Investigació Química

UNIVERSITAT ROVIRA I VIRGILI

DEPARTAMENT DE QUIMICA ANALITICA I QUIMICA ORGANICA

C/ Marcel.lí Domingo s/n
Campus Sescelades
43007 Tarragona
Tel. 34 977 55 97 69
Fax 34 977 55 84 46
e-mail: secqaqo@urv.net

Prof. Dr. José Ramón Galán Mascarós, Group Leader of the Institute of Chemical Research of Catalonia (ICIQ) and Research Professor of the Catalan Institution for Research and Advanced Studies (ICREA),

CERTIFY that the present Doctoral Thesis entitled: "**Novel Molecular Catalysts for Water Oxidation: Towards Artificial Photosynthesis**", presented by Sara Goberna Ferrón to receive the PhD degree in Chemistry, has been carried out under my supervision, in the Institute of Chemical Research of Catalonia (ICIQ).

Tarragona, 4 November 2013

PhD Thesis supervisor

Prof. Dr. José Ramón Galán Mascarós

UNIVERSITAT ROVIRA I VIRGILI
NOVEL MOLECULAR CATALYSTS FOR WATER OXIDATION: TOWARDS ARTIFICIAL PHOTOSYNTHESIS
Sara Goberna Ferrón
Dipòsit Legal: T.189-2014

UNIVERSITAT ROVIRA I VIRGILI
NOVEL MOLECULAR CATALYSTS FOR WATER OXIDATION: TOWARDS ARTIFICIAL PHOTOSYNTHESIS
Sara Goberna Ferrón
Dipòsit Legal: T.189-2014

Acknowledgements

First of all I wish to thank my supervisor, Prof. José Ramón Galán Mascarós, for giving me the opportunity to be part of his group. JR, muchas gracias por confiar en mí, por tu ayuda incondicional, tus consejos y tu apoyo. Ha sido un placer adentrarnos juntos en el mundo de *water oxidation*, y más aún recoger los frutos de tan duro trabajo. Gracias a ti, el enriquecimiento durante todos estos años no ha sido solo profesional sino personal. Ser la primera doctoranda del grupo ha sido un honor, gracias por todo.

Gracias a todos mis compañeros de laboratorio. Desde que éramos tan solo dos hasta formar parte de un grupo de más de diez personas, en el que todos y cada uno de ellos aportan algo a la esencia del grupo. En especial quiero agradecer a Laura V, por su ayuda en el laboratorio y por lo buenos momentos dentro y fuera de el, y por su amistad que va más allá de la distancia. A Ximo, perquè ja tenia ganes de que arribares quan encara no et coneixia i perquè no em vas defraudar, per els bons moments *controversial* en els congressos i per una amistat que espere que dure més enllà. A Sara, muchas gracias por tu ayuda, por tu amistad *thin-fín*! También quiero darle las gracias a Yesid, a pesar de casi no conocernos me has ayudado mucho. Y a Vero, por todos los buenos ratos que hemos pasado juntas.

A mi amiga Areli, por los buenos momentos vividos durante nuestra aventura en Tarragona y porque vivamos muchos más aunque estemos lejos.
Gracias Álvaro, por ayudarme con mi primera columna y porque eres genial.
A Laura R, quién nos iba a decir cuando estudiábamos juntas en Valencia que acabaríamos siendo vecinas en *Tarraco*. Como me hubiese gustado disfrutar más años de tu compañía. Te echaré de menos.

I would like to thank Prof. Kim Dunbar, it has been a pleasure to work in your research group and it has been one of the best experiences of my life. Gracias Bruno, por hacer de mi estancia en TX un camino de rosas.

Thanks to Prof. Marcella Bonchio, Andrea Sarotrel and Irene Bazzan. My stay in Padua was wonderful.

Many thanks to ICIQ administrative and research support units for their help. Gracias a Paula por su ayuda con el papeleo y por su paciencia.

Quiero darle las gracias a mi familia, pero en especial a mi madre, por su apoyo incondicional y por estar siempre a mi lado. Mamá, a pesar de la distancia, en cualquier momento has estado ahí, horas y horas de teléfono…Te quiero.

Gràcies Vicent. Per estar al meu costat en l'aventura del doctorat, per animar-me en tot moment. A pesar de la distancia sempre t'he sentit molt prop. Sense tu res d'açò seria possible. T'estime.

UNIVERSITAT ROVIRA I VIRGILI
NOVEL MOLECULAR CATALYSTS FOR WATER OXIDATION: TOWARDS ARTIFICIAL PHOTOSYNTHESIS
Sara Goberna Ferrón
Dipòsit Legal: T.189-2014

Table of Contents

UNIVERSITAT ROVIRA I VIRGILI
NOVEL MOLECULAR CATALYSTS FOR WATER OXIDATION: TOWARDS ARTIFICIAL PHOTOSYNTHESIS
Sara Goberna Ferrón
Dipòsit Legal: T.189-2014

UNIVERSITAT ROVIRA I VIRGILI
NOVEL MOLECULAR CATALYSTS FOR WATER OXIDATION: TOWARDS ARTIFICIAL PHOTOSYNTHESIS
Sara Goberna Ferrón
Dipòsit Legal: T.189-2014

List of publications

The results of this PhD thesis have delivered the following publications:

1 Pintado, S., Goberna-Ferrón, S., Escudero-Adán, E. & Galán-Mascarós, J. R. Fast and persistent electrocatalytic water oxidation by Co-Fe prussian blue coordination polymers. *J. Am. Chem. Soc.* **135**, 13270-13273 (2013).

2 Soriano-López, J., Goberna-Ferrón, S., Vigara, L., Carbó, J., Poblet, J. M. & Galán-Mascarós, J. R. Cobalt polyoxometalates as heterogeneous water oxidation catalysts. *Inorg. Chem.* **52**, 4753-4755 (2013).

3 Goberna-Ferrón, S., Vigara, L., Soriano-López, J. & Galán-Mascarós, J. R. Identification of a nonanuclear $\{Co(II)_9\}$ polyoxometalate cluster as a homogeneous catalyst for water oxidation. *Inorg. Chem.* **51**, 11707-11715 (2012).

4 Galán-Mascarós, J. R., Llobet, A., Vigara, L., Goberna-Ferrón, S. & Soriano-Lopez, J. Process for water oxidation comprising the use of a polyoxometalate compound as water oxidation catalyst. European Union and associated countries patent (2011).

The following publication is in preparation:

5 Goberna-Ferrón, S., Peña, B., Zhao, H., Dunbar, K. R. & Galán-Mascarós, J. R. First Metal-Metal Bonded Water Oxidation Electrocatalyst. *To be submitted.*

Nor related with this thesis publications:

1 Goberna-Ferrón, S., Lillo, V. & Galán-Mascarós, J. R. [Cu (L-prolinate)$_2$]: A catalyst for environmentally friendly oxidation of alkanes and alkenes with H_2O_2 and O_2. *Catal. Commun.* **23**, 30-33 (2012).

2 Ceolín, M., Goberna-Ferrón, S. & Galán-Mascarós, J. R. Strong hard X-ray magnetochiral dichroism in paramagnetic enantiopure molecules. *Adv. Mater.* **24**, 3120-3123 (2012).

The following publication is in preparation:

3 Rodríguez-García, B., Goberna-Ferrón, S., Yong-Sung, K., Benet-Buchholz, J., Galán-Mascarós, J. R. Synthesis, Crystal Structure and Physical Properties of the radical salt $[ET]_2[CuCl_4]$ (ET = bis(ethylenedithio)tetrathiafulvalene). *To be submitted.*

UNIVERSITAT ROVIRA I VIRGILI
NOVEL MOLECULAR CATALYSTS FOR WATER OXIDATION: TOWARDS ARTIFICIAL PHOTOSYNTHESIS
Sara Goberna Ferrón
Dipòsit Legal: T.189-2014

Abbreviations

δ	Layer thickness
Γ	Surface coverage
η	Overpotential
λ	Wavelength
μ	Micro
ν	Wavenumber
υ	Potential scan rate
A	Ampere
A	Area
abs:	Absorbance
bpy	2,2'-bipyridine
CoHCF	Cobalt hexacyanoferrate
C	Coulomb
C	Bulk solution concentration
CV	Cyclic voltammetry
CY	Chemical yield
D	diffusion coefficient
DLS	Dynamic Light Scattering
DPV	Differential Pulse Voltammetry
DTGA	Differential Thermal Analysis
e	Electron
EDX	Electron Dispersive X-ray spectroscopy
E	Potential
Eo	Standard redox potential
$E_{1/2}$	Half-wave potential
F	Faraday's constant
i	Current
ic	Catalytic peak current
ip	Peak current for a non catalytic process
I	Intensity
IR	Infrared spectroscopy
ITO	Tin doped indium oxide
FTO	Fluorine doped Tin Oxide
GC	Gas chromatography
j	Current density
K	Kelvin
K_{cat}	Effective first-order rate constant

UNIVERSITAT ROVIRA I VIRGILI
NOVEL MOLECULAR CATALYSTS FOR WATER OXIDATION: TOWARDS ARTIFICIAL PHOTOSYNTHESIS
Sara Goberna Ferrón
Dipòsit Legal: T.189-2014

KPi	Potassium phosphate buffer
M	Molar or metal
MHCM	Transition metal hexacyanometallates
MLCT	Metal-to-ligand charge transfer
MS	Mass spectroscopy
n_c	Number of electrons in a redox reaction
n_p	Number of electrons in a catalytic redox reaction
NHE	Normal Hydrogen Electrode
NaPi	Sodium phosphate buffer
OEC	Oxygen-evolving complex
PB	Prussian blue
PCET	Proton Coupled Electron Transfer
POM	Polyoxometalate
PS	Photosystem
RT	Room Temperature
SEM	Scanning electron microscopy
TCD	Thermal conductivity detector
TGA	Thermal gravimetric analysis
t	time
ton	Tonnes of oil equivalent
TON	Turnover number
TOF	Turnover frequency
UV-vis	Ultraviolet-visible spectroscopy
V	Volt
WOC	Water Oxidation Catalyst
XRD	X-ray Diffraction

UNIVERSITAT ROVIRA I VIRGILI
NOVEL MOLECULAR CATALYSTS FOR WATER OXIDATION: TOWARDS ARTIFICIAL PHOTOSYNTHESIS
Sara Goberna Ferrón
Dipòsit Legal: T.189-2014

Terms and Definitions

Cell defines a device where an oxidation−reduction (redox) reaction takes place. An electrochemical cell contains electrodes where the reactions occur. Oxidation occurs at the anode, electrons flow from the anode to the cathode, where the reduction occurs.

Chemical oxidant is an oxidant, which can be directly used in the reaction conditions, and is reduced during the oxidation of water.

Electrolyte is a substance containing free ions that make the substance electrically conductive. When electrodes are placed in an electrolyte and a voltage is applied, the electrolyte will conduct electricity.

Electron scavenging agent and **sacrificial electron acceptor** refer to the molecule that is reduced during the oxidation of water.

Gross inland energy consumption (gross inland consumption) is the total energy demand of a country or region. It represents the quantity of energy necessary to satisfy inland consumption of the geographical entity under consideration.

Oxygen yield refers to the percentage of molecular oxygen formed during the catalytic water oxidation reaction. It is expressed as the molar percent of oxygen of the total oxygen theoretically expected from total consumption of electrons taken by the scavenging agent (also called **chemical yield**, CY), the anode (also called **Faradaic efficiency**), or the photo−anode.

Photo–chemically generated oxidant is an oxidant, which is generated by light irradiation of a photosensitizing complex, and is reduced during the oxidation of water.

Photo–electrochemical cell refer to an electrochemical cell where the redox reaction is conducted by light energy.

Solar cell is a cell having a light absorbing material to absorb photons, a semiconducting material able to generate a charge separation into electrons and holes, and an anode and cathode where these electrons and holes are directed, respectively. A voltage difference is generated in the anode and cathode to yield the electrical current when the circuit is closed.

Turnover number (TON) refers to the number of moles of substrate that a mole of catalyst can convert during a certain unit of time. This term usually refers to the point where the oxidation reaction is finished, either because the oxidant has been consumed, or because the catalyst has been deactivated. TON is usually calculated as the number of moles of oxygen divided by the number of moles of catalyst.

Turnover conditions refer to the conditions in which the catalytic water oxidation reaction takes place (pH, temperature, concentration of electron scavenging agent, concentration of catalyst, etc…).

Turnover number (TON) refers to the number of moles of substrate that a mole of catalyst can convert during a certain unit of time. This term usually refers to the point where the oxidation reaction is finished, either because the oxidant has been consumed, or because the catalyst has been deactivated. TON is usually calculated as the number of moles of oxygen divided by the number of moles of catalyst.

Turnover frequency (TOF) is the turnover per unit time under turnover conditions. The TOF can be calculated by dividing the TON by the time period over which the TON was measured. The TOF is usually expressed in (time units)$^{-1}$.

Water oxidation catalyst (WOC) and **oxygen evolving center** (OEC) refer to a catalyst used to oxidize water to form molecular oxygen (O_2), hydrogen ions (H^+) and electrons (e^-).

UNIVERSITAT ROVIRA I VIRGILI
NOVEL MOLECULAR CATALYSTS FOR WATER OXIDATION: TOWARDS ARTIFICIAL PHOTOSYNTHESIS
Sara Goberna Ferrón
Dipòsit Legal: T.189-2014

UNIVERSITAT ROVIRA I VIRGILI
NOVEL MOLECULAR CATALYSTS FOR WATER OXIDATION: TOWARDS ARTIFICIAL PHOTOSYNTHESIS
Sara Goberna Ferrón
Dipòsit Legal: T.189-2014

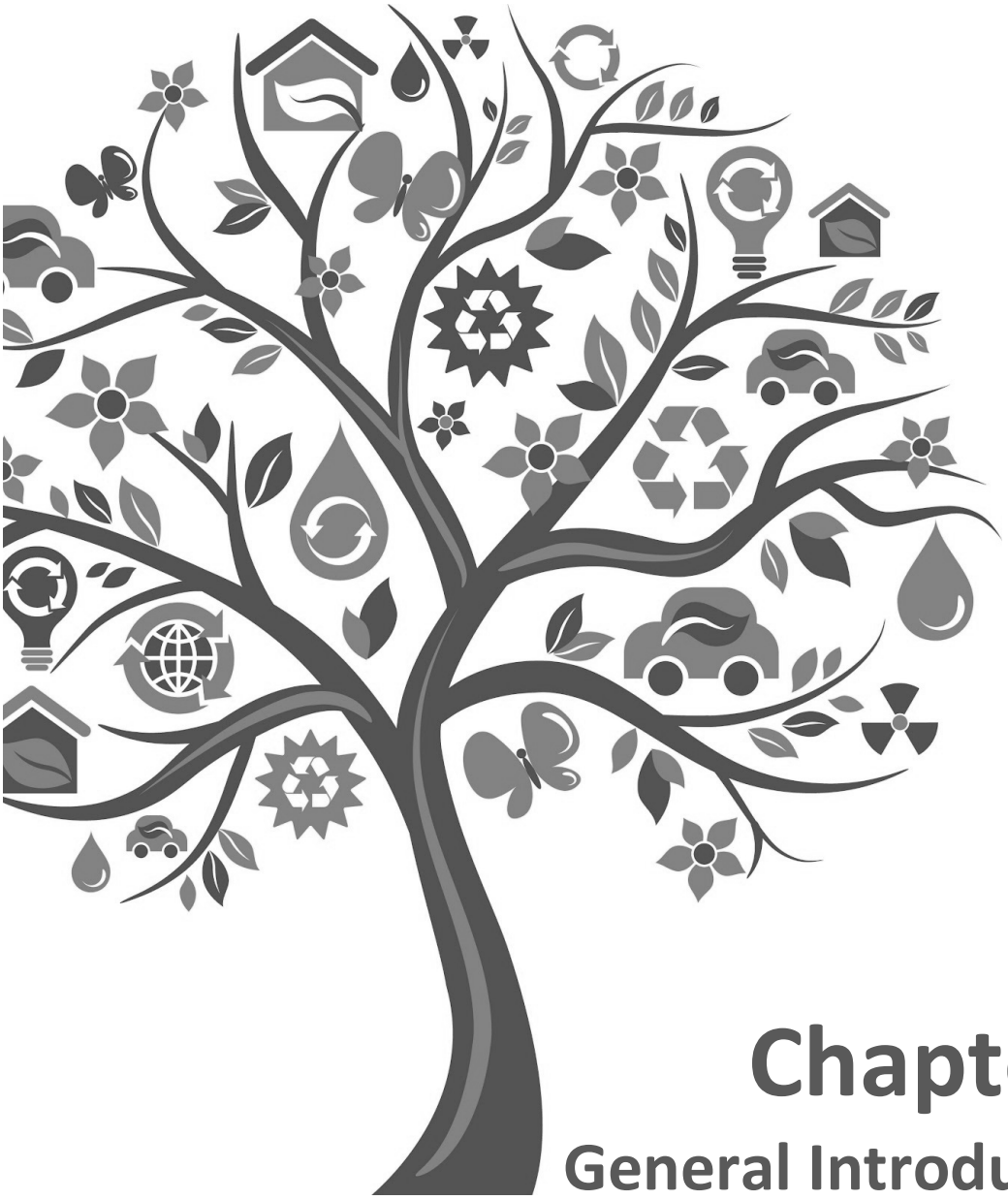

Chapter 1

General Introduction

UNIVERSITAT ROVIRA I VIRGILI
NOVEL MOLECULAR CATALYSTS FOR WATER OXIDATION: TOWARDS ARTIFICIAL PHOTOSYNTHESIS
Sara Goberna Ferrón
Dipòsit Legal: T.189-2014

UNIVERSITAT ROVIRA I VIRGILI
NOVEL MOLECULAR CATALYSTS FOR WATER OXIDATION: TOWARDS ARTIFICIAL PHOTOSYNTHESIS
Sara Goberna Ferrón
Dipòsit Legal: T.189-2014

1.1

Motivation: Energy and Environment

A competitive, reliable and sustainable energy sector is arguably the most important scientific and technical challenge facing humanity in the 21st century. The energy sector has been under the spotlight in recent years due to a number of issues that have pushed energy up the political agenda, including the volatility of oil prices, interruptions to energy supplies, and increased attention to anthropogenic (human-induced) effects on environment, in particular, greenhouse effect and deforestation. The excess in carbon dioxide (CO_2) is caused mostly by the fossil fuels burning. The atmospheric emissions of methane (CH_4) and nitrous oxide (N_2O) are mostly due to abusive agricultural practices. Global climate is already changing: average surface temperatures have increased, ocean pH has decreased, precipitation patterns have changed, and sea level has risen since the industrial revolution. [1,2]

Worldwide gross consumption of energy was 12140.9 million toe (tonnes of oil equivalent) in 2009. After three years of falling consumption that broadly coincided with the global financial and economic crisis, the European Union gross inland consumption rose from 1703.4 million toe in 2009 to 1759.0 million toe in 2010. Between 2000 and 2009 global consumption increased by 21.0 % and China's gross inland consumption more than doubled. The United States and Japan were the only to record lower gross inland consumption in 2010 than in 2000 (Table 1.1).[1]

Just over one quarter of worldwide gross consumption of energy in 2009 was coal and lignite, one third was crude oil and oil products, and one fifth was gas; combined these three fuels accounted for four fifths (80.9 %) of global energy consumption (Figure 1.1).[1]

1. General Introduction

	Consumption (million toe)		Analysis by energy type, 2009 (%)					
	2000	2009	Coal and lignite	Crude oil and oil products	Gas	Nuclear energy	Renewables and waste	Electricity and heat (1)
EU-27 (2)	1 724.9	1 759.0	15.9	35.1	25.1	13.4	10.4	0.0
Argentina	:	74.3	1.7	35.6	52.1	2.9	7.0	0.7
Australia (3)	108.1	125.8	42.0	30.8	21.6	0.0	5.6	0.0
Brazil	189.2	240.2	4.6	39.7	7.1	1.4	45.8	1.5
Canada (3)	251.4	255.3	9.4	34.6	31.0	9.3	17.0	-1.1
China	1 094.9	2 257.1	67.2	16.8	3.3	0.8	11.9	0.0
India	457.2	675.8	42.2	23.6	7.2	0.7	26.1	0.1
Indonesia	155.7	202.0	15.1	33.1	17.4	0.0	34.4	0.0
Japan (3)	518.9	494.9	21.5	42.5	17.1	15.4	3.5	0.0
Mexico (3)	145.1	169.8	4.4	56.7	27.8	1.6	9.6	0.0
Russia	619.3	646.9	14.7	21.3	54.1	6.6	3.4	-0.2
Saudi Arabia	:	157.9	0.0	61.1	38.9	0.0	0.0	0.0
South Africa	114.4	144.0	68.3	17.0	2.6	2.3	10.0	-0.1
South Korea (3)	188.1	246.5	28.3	39.5	13.8	16.8	1.5	0.0
Turkey (3)	76.3	104.8	30.5	29.8	29.6	0.0	10.2	-0.1
United States (3)	2 273.3	2 235.0	22.4	37.0	24.7	10.0	5.7	0.1
World	10 031.8	12 140.9	27.2	32.8	20.9	5.8	13.3	0.0

(1) Gross inland consumption of electricity and heat is equal to electricity net imports.
(2) Data for 2010 instead of 2009.
(3) Consumption total for 2010 instead of 2009.

Table 1.1 *Gross inland consumption, 2000 and 2009.*[1]

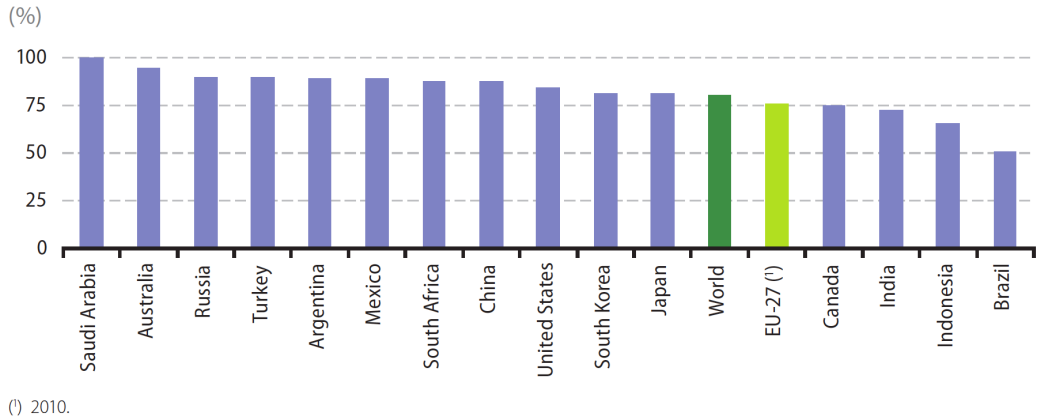

(1) 2010.

Figure 1.1. *Share of coal, lignite, oil and gas in gross inland consumption, 2009.*[1]

Renewables and waste accounted for 13.3 % of gross consumption worldwide (Figure 1.2). As for primary production, Brazil, Indonesia and India recorded above average shares for renewables and waste in gross inland consumption, as did Canada,

UNIVERSITAT ROVIRA I VIRGILI
NOVEL MOLECULAR CATALYSTS FOR WATER OXIDATION: TOWARDS ARTIFICIAL PHOTOSYNTHESIS
Sara Goberna Ferrón
Dipòsit Legal: T.189-2014

reflecting its large net exports of fossil fuels. By contrast, the European Union, Turkey and Japan recorded below average shares of renewables and waste in gross inland consumption, despite above average primary production, reflecting their net imports of fossil fuels.[1]

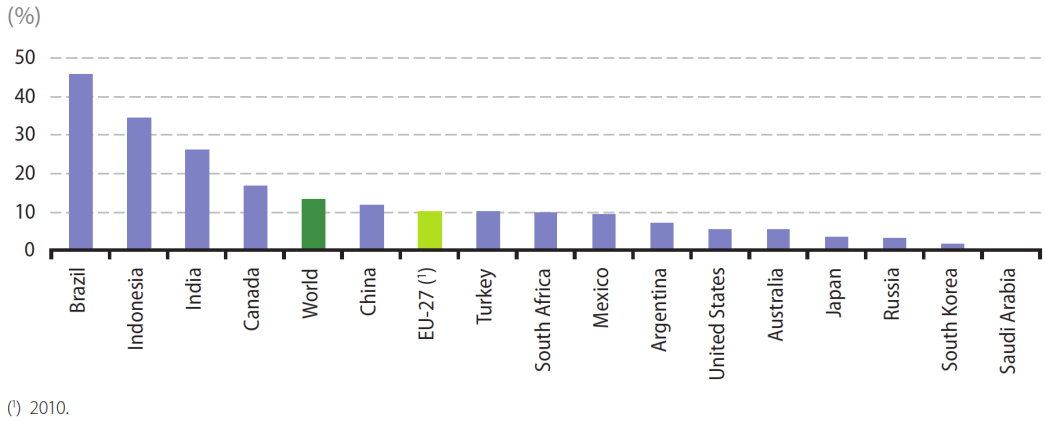

Figure 1.2. *Share of renewables and waste in gross inland consumption, 2009.*[1]

Much of this demand is driven by population growth. The world's population was approaching 7000 million in habitants at the beginning of 2010 and it is projected to increase by 0.9% yr^{-1} to ≈9.4 billion by 2050.[1,3] . With no changes in the global economic growth, the world energy consumption rate would grow by 2.3% yr^{-1}.

With this current scenario it is necessary to move towards environmentally friendly, i. e. carbon-neutral, energy sources and technologies. Among the known alternative energy sources, such as nuclear fission, hydroelectric, geothermal, wind, biomass and tidal, only solar energy have the potential to provide enough carbon-neutral energy to meet future global energy demand. [3-5]

UNIVERSITAT ROVIRA I VIRGILI
NOVEL MOLECULAR CATALYSTS FOR WATER OXIDATION: TOWARDS ARTIFICIAL PHOTOSYNTHESIS
Sara Goberna Ferrón
Dipòsit Legal: T.189-2014

UNIVERSITAT ROVIRA I VIRGILI
NOVEL MOLECULAR CATALYSTS FOR WATER OXIDATION: TOWARDS ARTIFICIAL PHOTOSYNTHESIS
Sara Goberna Ferrón
Dipòsit Legal: T.189-2014

1.2

Using Solar Energy

Sunlight is the preeminent carbon-neutral energy source for the future. Solar radiation is available at any location on the surface of the Earth. The maximum irradiance (power density) of sunlight on Earth is about 1000 watts a square meter, irrespective of location. It is common to describe the solar source in terms of insolation—the energy available per unit of area and per unit of time (such as kilo-watt-hours per square meter a year). Measured in a horizontal plane, annual insolation varies over the Earth's surface by a factor of 3—from roughly 800 kilowatt-hours per square meter a year in northern Scandinavia and Canada to a maximum of 2500 kilowatt- hours per square meter a year in some dry desert areas.[6]

The ability of solar to meet the global energy demand of the future is well documented.[7-10] Solar energy utilization requires solar capture and conversion and storage. Solar capture and conversion may be accomplished by photovoltaic solar energy conversion. Today photovoltaics generally cannot compete with conventional power plants in grid-connected applications. The challenge here is to dramatically reduce the cost per W of delivered solar electricity. Photovoltaic electricity production costs are about $0.3-1.5 a kilowatt-hour, depending on solar insolation, turnkey costs, depreciation periods, and interest rates. Under favorable conditions and at favorable sites, the lowest cost figure may come down to $0.05-0.06 a kilowatt-hour.[6]

In the absence of cost-effective storage, solar electricity can never be a primary energy source for society. Energy storage options for solar radiation arise in several forms, namely: potential energy (i.e. pumped-hydroelectric, compressed air, and charge storage); kinetic energy (flywheels); thermal energy (concentrated solar thermal and geothermal; and chemical energy (batteries and fuels). Of these

UNIVERSITAT ROVIRA I VIRGILI
NOVEL MOLECULAR CATALYSTS FOR WATER OXIDATION: TOWARDS ARTIFICIAL PHOTOSYNTHESIS
Sara Goberna Ferrón
Dipòsit Legal: T.189-2014

methods, chemical fuels stand in the forefront owing to the relatively large gravimetric and volumetric energy densities of fuels as compared to the other methods.[4,11] Moreover, current prevalent technologies and infrastructure are congruent with rapid adoption of solar-derived chemical fuels.

Chemical fuels are a sustainable solution to small-scale, distributed energy storage. Fuels achieve high energy densities through the storage of electrons in the small volume of a two-electron bond between light elements (i.e., C- H, N- H, and H- H bonds). In comparing the energy densities of hydrocarbon (C- H based), nitrogen (N- H based), and hydrogen (H_2) fuels as a function of weight and volume, a few key points emerge:

- Hydrogen (H_2) has the largest energy density by mass (143 MJ kg) but suffers in volumetric energy density because it is a gas.
- Nitrogen-based fuels have modestly high energy content by mass and volume.
- Hydrocarbon fuels provide the optimum energy supply in terms of volumetric energy density.

This latter point, along with the economic availability of fossil fuels, provides the basis for the choice of hydrocarbon-based fuels as the energy currency of modern society. The challenge currently facing our society is to shift our view of chemical fuels from that of a carbon-based energy source to that of a form of (renewable) energy storage.

UNIVERSITAT ROVIRA I VIRGILI
NOVEL MOLECULAR CATALYSTS FOR WATER OXIDATION: TOWARDS ARTIFICIAL PHOTOSYNTHESIS
Sara Goberna Ferrón
Dipòsit Legal: T.189-2014

1.3

Natural Photosynthesis

Oxygenic photosynthesis has evolved over billions of years as a means for biological organisms to convert plentiful solar radiation, water and carbon dioxide into useful biochemical fuels in the form of carbohydrates, with dioxygen as a by-product.[12]

The overall process of photosynthesis consists of two main phases, the so-called "light" and "dark" reactions. In the first, photosynthesis uses antennae compartments for light harvesting and reaction-center complexes for charge separation. Here electrochemical reactions commence that generate two vital "energy-rich" biological compounds; adenosine triphosphate (ATP) and reduced pyridine nucleotide (NADPH).[10] Oxygen is produced as a byproduct in this process and is released to the atmosphere. Photosystems catch light energy to convert it into electrically stored energy in cell membranes. The light reaction requires the participation of two photosystems, photosystem I (PSI) and photosystem II (PSII).[13] Each photosystem operates in series, to photochemically "charge" the membrane.

In the dark reactions, the products of the light phase, ATP and NADPH, are used within cells to produce carbohydrate (sugars) from carbon dioxide, via a series of biochemical intermediates. The enzyme Rubisco catalyzes the addition of carbon dioxide to ribulose diphosphate. This process is central to the progressive chemical "assembly" of sugar molecules from carbon dioxide and water.[14]

The first photosynthetic energy-transducing steps, that involves photosystem II (PSII), the cytochrome *b/f* complex, and photosystem I (PSI), generate an e^- flux and an

UNIVERSITAT ROVIRA I VIRGILI
NOVEL MOLECULAR CATALYSTS FOR WATER OXIDATION: TOWARDS ARTIFICIAL PHOTOSYNTHESIS
Sara Goberna Ferrón
Dipòsit Legal: T.189-2014

associated electrochemical gradient across the thylakoid membrane. The e^- come from water, and this oxidation of water to generate O_2 is the source of e^- utilized by organisms. The oxidation of water occurs in the oxygen-evolving complex (OEC) located in PSII (Figure 1.3).[15]

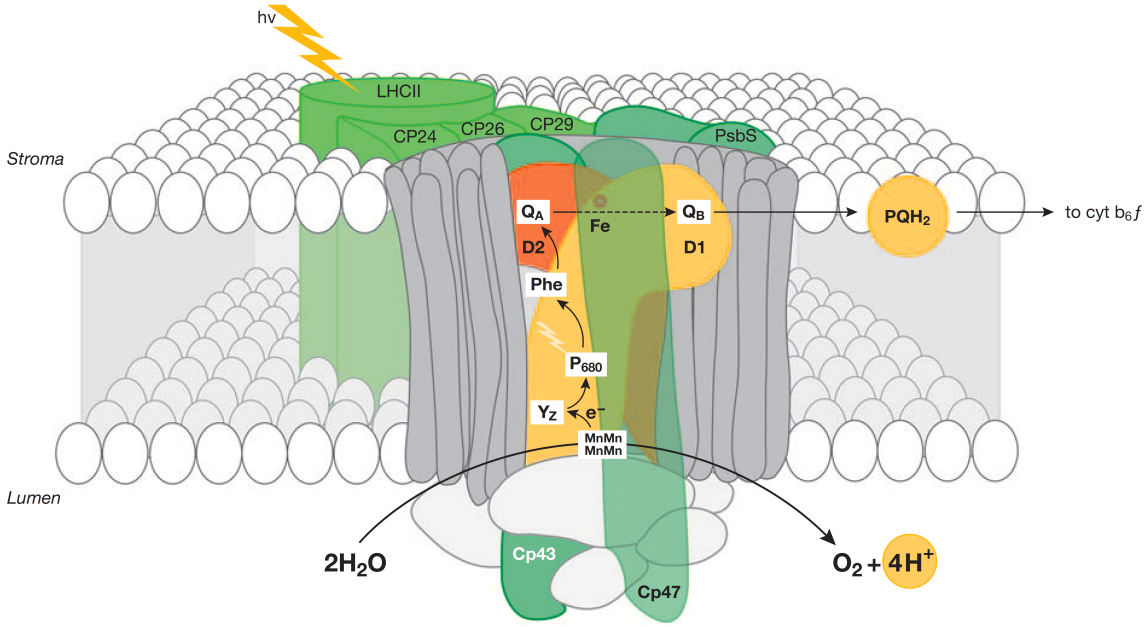

Figure 1.3. *Organization of photosystem II and light-harvesting complex II in the thylakoid membrane. Cp43, Cp47: internal antenna chlorophyll–protein complexes. D1, D2: main components of reaction centres (RCs) with binding sites for electron acceptor quinones (Q_B, Q_A). P_{680}: chlorophyll special pair. Other cofactors associated with D1/D2: pheophytin (Phe), non-haem iron (Fe), Mn-cluster. Accessory chlorophylls and β-carotene are not shown. Chl, chlorophyll; PQH_2, plastoquinone pool; cytb6f, cytochrome b6f complex; Y_Z, D1-Tyr161.*[16]

Light is harvested in large antenna arrays of chlorophyll and carotenoids towards PSII via excited-state energy transfer mechanisms. When the energy arrives at PSII, a charge separation oxidizes a chlorophyll unit P680, involved with activity at the OEC.

The OEC, located in the PSII, consists in a Mn_4O_5Ca cluster. Its structure has been recently reported from cyanobacterial PSII using crystallographic techniques (Figure 1.4).[17]

1. 3. Natural Photosynthesis

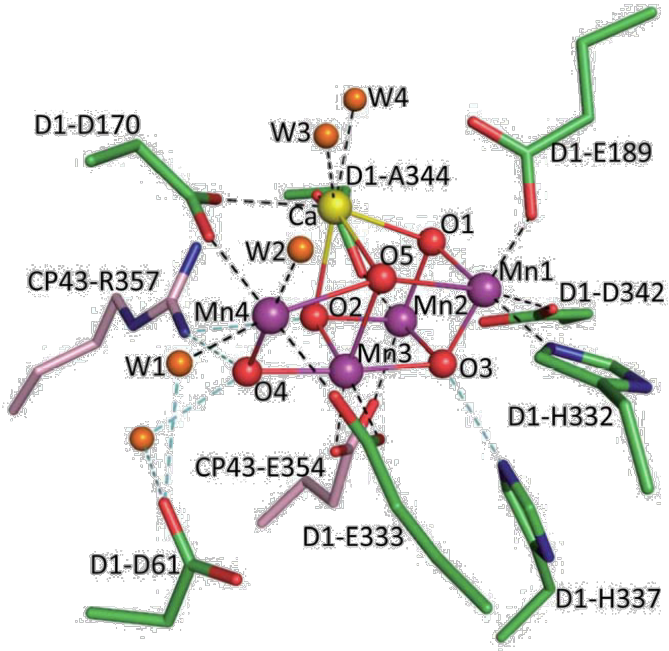

Figure 1.4. *Local structure of the OEC determined from highresolution. X-ray crystallography of PSII from cyanobacterium, Thermosynechococcus vulcanus. Relevant atoms and amino acid residues are indicated. Local water molecules are denoted as orange spheres.*[17]

Operating under mild temperature and pH conditions, the Mn-Ca cluster is the most efficient anodic "electrolysis" system known, with a maximum turnover rate of 10^3 s^{-1}. Close to the absolute thermodynamic limit, it catalyzes the reaction $2H_2O \rightarrow 4H^+ + O_2 + 4e^-$ which proceeds with a redox potential difference of at least 1.23 V (vs. NHE, pH = 0).

Arguably the most prominent feature of the OEC is the multiple and proximate oxo-bridged manganese centers, which are able to catalyze water oxidation by distributing the oxidation state changes among the four metal ions to avoid an energy-demanding accumulation of charge at a single metal. Both calcium (providing ligation sites for water and participating in proton transfer) and chloride (playing structural roles) are known to be necessary cofactors of the water oxidation cycle.[10]
Oxidation of water proceeds in the OEC through four sequential one-electron

UNIVERSITAT ROVIRA I VIRGILI
NOVEL MOLECULAR CATALYSTS FOR WATER OXIDATION: TOWARDS ARTIFICIAL PHOTOSYNTHESIS
Sara Goberna Ferrón
Dipòsit Legal: T.189-2014

oxidative steps, each step driven by an oxidation of P680, the so called Kok cycle (Figure 1.59.[15,18] The oxidized form chlorophyll unit P680, $P680^+$, is the strongest known biological oxidizing agent with a redox potential of 1.26 V for the $P680^{+/0}$ couple.[19] $P680^+$ rapidly oxidizes a tyrosine residue (Y_Z), which in turn oxidizes the manganese cluster in the Kok cycle. PSII is advanced from the lowest state, S0, progressively to the S1, S2, and S3 and S4 states, and is then spontaneously re-reduced to the S0 state as oxygen is evolved. The protein environment adjusts the proton chemical potential to the OEC catalytic sites and the resting state of the PSII is the S1 state, with one electron extracted from the OEC, stabilized by proton release. To maintain charge neutrality throughout the S-cycle for leveling of the redox potential, release of electrons into the P680 chlorophylls alternates with the release of H into the protein environment.[20,21]

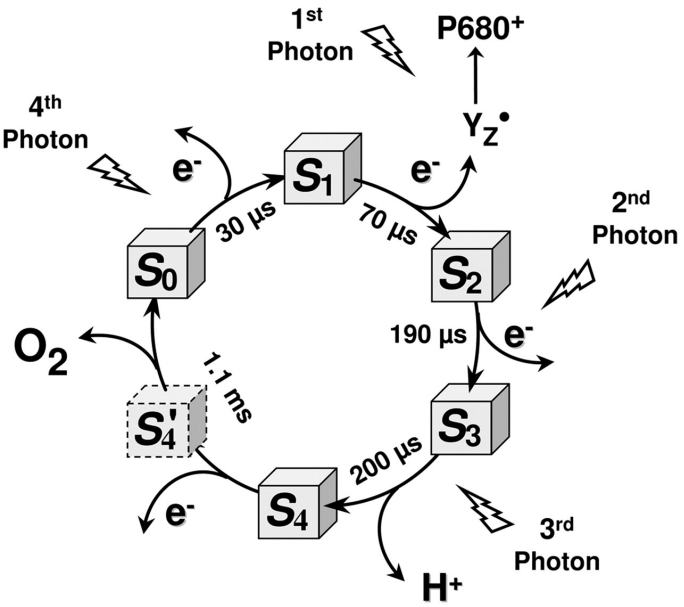

Figure 1.5. *The Kok cycle as proposed by Haumann and Dau from time-resolved X-ray absorption spectroscopy (XAS). Oxidation states of the OEC are designated the S states.*[20]

As a result of these highly energetic reactions, the OEC and surrounding structures are damaged, which are then restored and reestablished via sophisticated repair

UNIVERSITAT ROVIRA I VIRGILI
NOVEL MOLECULAR CATALYSTS FOR WATER OXIDATION: TOWARDS ARTIFICIAL PHOTOSYNTHESIS
Sara Goberna Ferrón
Dipòsit Legal: T.189-2014

mechanisms,[22] without them the OEC would degrade in about 30 minutes.

The information on how photosynthetic organisms are able to use solar energy to extract electrons from water to produce hydrogen or reduced carbon compounds can be used to design modular photocatalytic systems capable of using solar energy to produce fuels directly from sunlight using water as a raw material. Many scientists are convinced that, by using state-of-the-art knowledge from photosynthesis, the value of current technology for conversion of solar energy into electricity can be raised by adding a storage function, as in natural photosynthetic assemblies, leading to the development of novel robust photoelectrochemical solar fuel producers or "artificial leaves".

UNIVERSITAT ROVIRA I VIRGILI
NOVEL MOLECULAR CATALYSTS FOR WATER OXIDATION: TOWARDS ARTIFICIAL PHOTOSYNTHESIS
Sara Goberna Ferrón
Dipòsit Legal: T.189-2014

UNIVERSITAT ROVIRA I VIRGILI
NOVEL MOLECULAR CATALYSTS FOR WATER OXIDATION: TOWARDS ARTIFICIAL PHOTOSYNTHESIS
Sara Goberna Ferrón
Dipòsit Legal: T.189-2014

1.4

Artificial Photosynthesis and Water Splitting

The essence of artificial photosynthesis was described at the beginning of the twentieth century[23,24] by the eminent Italian chemist Giacomo Ciamician (Figure 1.6(a)) in an attempt to study whether "fossil solar energy" was the only type available or whether other methods of production could be found that rivaled the photochemical processes of the plants, Ciamician noted that

". . . the solar energy that reaches a small tropical country . . . is equal annually to the energy produced by the entire amount of coal mined in the world!"
"For our purposes the fundamental problem from the technical point of view is how to fix the solar energy through suitable photochemical reactions . . . By using suitable catalyzers, it should be possible to transform the mixture of water and carbon dioxide into oxygen and methane, or to cause other endo-energetic processes . . . On the arid lands there will spring up industrial colonies without smoke and without smokestacks; forests of glass tubes will extend over the plants and glass buildings will rise everywhere; inside of these will take place the photochemical processes that hitherto have been the guarded secret of the plants, but that will have been mastered by human industry which will know how to make them bear even more abundant fruit tan nature, for nature is not in a hurry and mankind is."

Ciamician's vision has inspired generations of researchers; one of the first scientists to use the term "artificial photosynthesis" and make seminal contributions to the field was Melvin Calvin (Figure 1.6(b)), who received a Nobel Prize for his research on photosynthetic carbon fixation.[25] Joseph J. Katz (Figure 1.6(c)) was a contemporary of Calvin, whose work on the physical chemistry of chlorophylls and other cofactors

UNIVERSITAT ROVIRA I VIRGILI
NOVEL MOLECULAR CATALYSTS FOR WATER OXIDATION: TOWARDS ARTIFICIAL PHOTOSYNTHESIS
Sara Goberna Ferrón
Dipòsit Legal: T.189-2014

found in photosynthetic proteins paved the way for future work in artificial photosynthesis.[26]

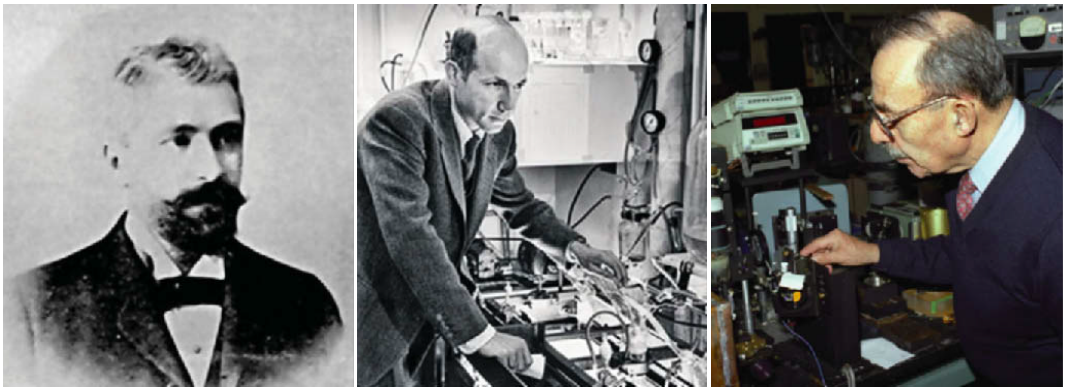

Figure 1.6. *(a) Giacomo Ciamician ; (b) Melvin Calvin and (c) Joseph J. Katz.*[2]

The "dream" of artificial photosynthesis is to technologically reproduce the components of natural photosynthesis on large scale for efficient solar energy conversion leading to totally renewable hydrogen generation from convenient water sources, such as seawater.

Following the lead of nature, it is the water splitting reaction (Eq.1.1), and not carbohydrate production (Eq.1.2), that lies at the nexus of any carbon-neutral solar fuel process.

$H_2O \rightarrow H_2 + ½\ O2$; Vrev = 1.23 V (Eq. 1.1)

$CO_2 + H_2O \rightarrow C_6H_{12}O_6 + O_2$; V_{rev} = 1.24 V (Eq. 1.2)

Note that water splitting is subsumed by the reaction in Eq.1.2. On an electron equivalency basis, therefore, the production of the carbohydrate stores only 0.01 eV more energy than water splitting. Thus, the solar energy storage in photosynthesis is achieved by water splitting; the carbohydrate is nature's method of storing the hydrogen released from the water splitting reaction.

The first step of water splitting is the most difficult; an energy input of 1.23 eV is needed to drive splitting of water (Eq.1.3):

1. 4. Artificial Photosynthesis and water Splitting

$$O_2 + 4e^- + 4H^+ \leftrightarrow 2H_2O;\ E_{anodic} = 1.23\ V - 0.059(pH)\ V\ (NHE) \qquad (Eq.\ 1.3)$$

$$4e^- + 4H^+ \leftrightarrow 2H_2;\ E_{catodic} = 0\ V - 0.059(pH)\ V\ (NHE) \qquad (Eq.\ 1.4)$$

Water oxidation involves the dissociation of protons and electrons from stable water molecules, as well as the formation of an O−O bond from formally separated water molecules. Despite the already intrinsic thermodynamic demands of water splitting, the kinetic obstacles impose significant activation energies (overpotentials) and need the development of efficient catalysts. Once protons and electrons are liberated from water, the generation of hydrogen is not limiting with existing electrode materials (eg. Ni) (although the search for inexpensive and robust catalysts remains an active field of study).[4]

The production of hydrogen fuel from electrolysis of water would become a practical strategy if a “super catalyst” for the anodic, water-oxidizing reaction could be found.[27]

UNIVERSITAT ROVIRA I VIRGILI
NOVEL MOLECULAR CATALYSTS FOR WATER OXIDATION: TOWARDS ARTIFICIAL PHOTOSYNTHESIS
Sara Goberna Ferrón
Dipòsit Legal: T.189-2014

UNIVERSITAT ROVIRA I VIRGILI
NOVEL MOLECULAR CATALYSTS FOR WATER OXIDATION: TOWARDS ARTIFICIAL PHOTOSYNTHESIS
Sara Goberna Ferrón
Dipòsit Legal: T.189-2014

1.5

Water Oxidation Catalysts

An exciting but challenging goal of inorganic chemistry is to develop a fast, stable and inexpensive water oxidation catalyst (WOC).[28] A feature of the OEC that was borrowed in the design elements of the early catalysts was the inclusion of multiple metal-centers into their frameworks. Since the first reported molecular water oxidation catalyst by Meyer et al. in 1982[29], the "blue dimer", the list of catalysts has increased exponentially more recently, but still remains a certain level of ambiguity as to the essential elements required for a molecular water oxidation catalyst. As a result, homogeneous catalysts has been preferred by researchers as they allow for a better understanding from mechanistic studies in an attempt to determine the electronic properties required for an efficient water oxidation catalyst. Once these factors have been determined, the design and synthesis of a robust and efficient catalyst should follow.

1.5.1 Molecular Water Oxidation Catalysts

Ruthenium-based WOCs

Although ruthenium is not within the active site of the OEC of PSII, several explorations of ruthenium complexes as effective catalysts for water oxidation have been conducted. Significant progress has been reported in the development of molecular catalysts for water oxidation based on the mononuclear, dinuclear, and multinuclear ruthenium complexes.

UNIVERSITAT ROVIRA I VIRGILI
NOVEL MOLECULAR CATALYSTS FOR WATER OXIDATION: TOWARDS ARTIFICIAL PHOTOSYNTHESIS
Sara Goberna Ferrón
Dipòsit Legal: T.189-2014

The Blue Dimer

The first confirmed molecular water oxidation catalyst was the μ-oxo-bridged *cis,cis* $[(bpy)(H_2O)RuORu(H_2O)(bpy)_2]^{4+}$ **1.1**, the so-called "blue dimer" (Figure 1.7).[29] Structurally the blue dimer is characterized by two-fold symmetry and a cis,cis arrangement at each Ru center with respect to the bpy ligands, allowing the aqua ligands to align in parallel through free-rotation along the the μ-oxo bridge.[30] Nearly linear geometry of the Ru atoms through the μ-oxo bridge is observed largely due to steric constraints imposed by the bpy ligands. Three possible isomers arise from chirality induced at the pseudo-octahedral Ru centres are possible with chiral Δ, Δ or Λ, Λ isomers, or the meso, Δ,Λ form. However, to date the isomers have not been separated and individually characterized.

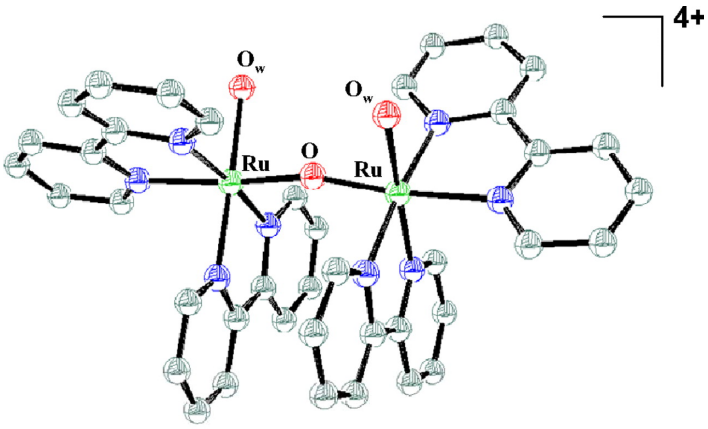

Figure 1.7. *Structure of the ruthenium blue dimer cation* ***1.1****,* cis,cis*$[(bpy)_2(H_2O)Ru^{III}ORu^{III}(OH_2)(bpy)_2]^{4+}$, in the salt $[(bpy)_2(H_2O)Ru^{III}ORu^{III}(OH_2)(bpy)_2](ClO_4)_4 \cdot 2H_2O$.*[30]

To clarify the water oxidation mechanisms of this catalyst, the blue dimer and its structurally related derivatives have been studied in detail over the past three decades.[30-38] Meyer et al. emphasized that Proton-Coupled Electron Transfer (PCET) could be the key to catalytic water oxidation by the blue dimer[39,40] which allows many oxidative equivalents to accumulate sequentially at one site without the buildup of highly charged species. [42,43]

1. 5. Water Oxidation Catalysts

Mechanistic and kinetic studies of the water oxidation activity of the blue dimer are quite complicated due to the involved series of intermediate species in the catalytic cycle.[38] Usually, water oxidation is performed in an excess of Ce^{IV} as oxidant (pH ~ 0–1).[37,38] Starting from the Ru^{III}–Ru^{III} form, the blue dimer is known to be oxidized to the Ru^{V}–Ru^{V} species to oxidize water into oxygen. The Ru^{IV}–Ru^{IV} state is unstable and oxidation of Ru^{III}–Ru^{IV} to Ru^{IV}–Ru^{IV} occurs slowly and disproportionation of Ru^{IV}–Ru^{IV} results in the doubly-oxidized Ru^{IV}–Ru^{V} that is then capable to advance along the catalytic cycle.[41]

The actual catalytic mechanism associated with the formation of molecular dioxygen by the blue dimer has been debated having been studied spectroscopically[30,38,42,43] through labeling experiments,[41] and computational methods.[41,42,44,45] As expected, the results suggested that the mechanism of water oxidation by the blue dimer is highly complex and involved not only multiple PCET reactions, higher oxidation states of the RuORu core, and cross-electron transfer between nonadjacent oxidation states but also different intermediate acid-base equilibrium reactions and some anion exchanges between the surrounding solution and the coordinated water molecules. Although water oxidation by the blue dimer is not yet understood completely and there are differing interpretations of the mechanism, a general consensus exists that the catalytically active species is the $Ru^{V}ORu^{V}$ species formed by the four−electron oxidation of $Ru^{III}ORu^{III}$, which undergoes first-order decay with the concomitant release of O_2. In the latest mechanistic proposal (Figure 1.8);[41] its characteristic features are the four PCET steps, by which the high oxidation states of Ru are accessible. At the highest oxidation state ($[O=Ru^{V}–O–Ru^{V}=O]^{4+}$) an oxido species is attacked by an ancillary water molecule, producing a hydroperoxido species. This peroxido species is oxidized intramolecularly by the second $Ru^{V}=O$ group, thus releasing O_2. Recently, another group suggested a different route for the O_2-releasing step, involving ligand participation.[46] In this alternative mechanism (Figure 1.9) the bipyridine ligand is oxidized, as a result of an attack of a molecule of water at the α-

UNIVERSITAT ROVIRA I VIRGILI
NOVEL MOLECULAR CATALYSTS FOR WATER OXIDATION: TOWARDS ARTIFICIAL PHOTOSYNTHESIS
Sara Goberna Ferrón
Dipòsit Legal: T.189-2014

position of the pyridine ring. In the mechanism of Hurst and Cape the radical is then neutralized by attack of a second water molecule at the β-position, leading to O–O bond formation after oxidation by the Ru-centers. Dioxygen is released from the ligand with the recovered aromaticity of the pyridine ring as a driving force.

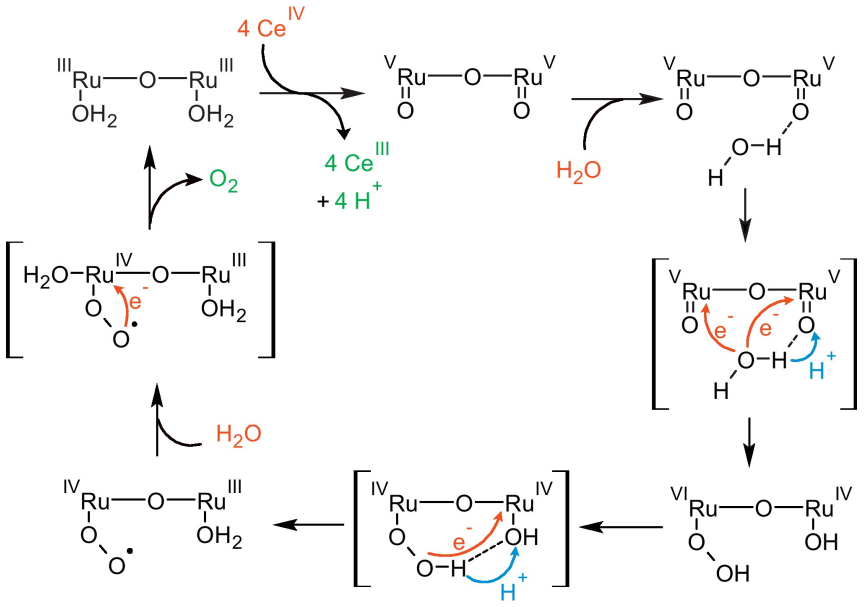

Figure 1.8. *Proposed mechanism of the "blue dimer" catalyst.*[47]

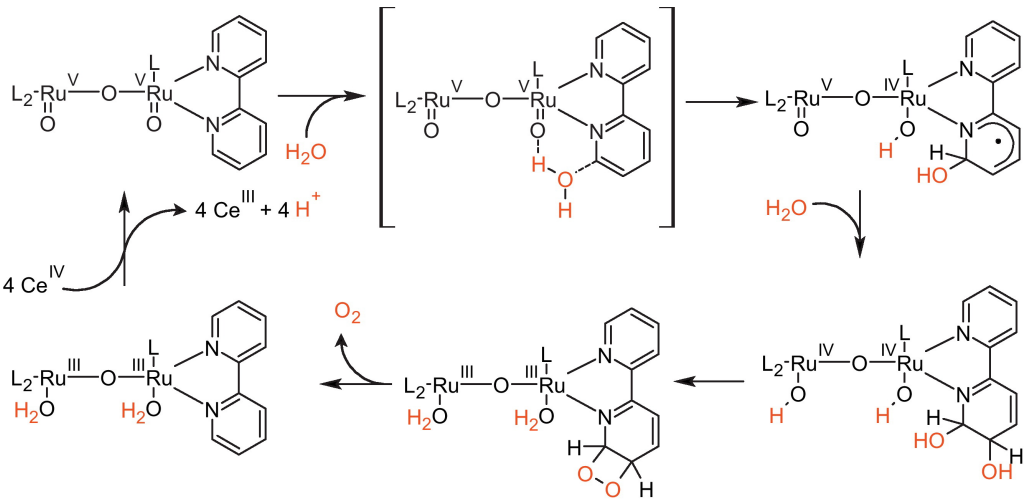

Figure 1.9. *Mechanism of O_2 release by [O = Ru^V–O–Ru^V = O],* via *ligand participation; L = 2,2'-bipyridine.*[47]

UNIVERSITAT ROVIRA I VIRGILI
NOVEL MOLECULAR CATALYSTS FOR WATER OXIDATION: TOWARDS ARTIFICIAL PHOTOSYNTHESIS
Sara Goberna Ferrón
Dipòsit Legal: T.189-2014

Regarding efficiency, the blue dimer has achieved turnover numbers (TON) of 11, with turnover frequencies (TOF) between 10^{-1} and 10^{-3} s^{-1}.[41] Methods utilizing redox mediators have been successfully employed by Meyer et al. to increase TOF by factor of 30 in solution to ~0.5 s^{-1},[48] and to ~0.6 s^{-1} when the mediator is bound to an electrode for electrocatalytic water oxidation.[49]

Dinuclear Ruthenium Complexes

As a consequence of the low TONs of the blue dimer many efforts have been devoted to improve its stability and / or activity by stabilizing the ligand frameworks. Llobet et al. reported a dinuclear Ru catalyst in 2004, $\{[Ru^{II}(tpy)(H_2O)]_2(\mu\text{-bpp})]^{3+}$ **1.2** (where tpy = 2,2′:6′,2″-terpyridine; and bpp = bis(2-pyridyl)-3,5-pyrazolate) (Figrure 1.10).[50] This new catalyst was called the "bpp dimer". Their ligand-bridged system placed the vacant water binding sites in close proximity by careful design of their ligand framework. Unlike the blue dimer **1.1** (Figure 1.7 and 1.10), the oxo bridge was replaced by a rigid pyrazolate ligand, and the two metal centers were much closer, due to the anionic nature of the bridging ligand a lower oxidation potential is required to reach the catalytically active species by over 200 mV.

Oxidative activation of the catalyst is achieved using Ce^{IV} in aqueous 0.1 M triflic acid. The starting species for the bpp dimer at pH = 1 is Ru^{II}–Ru^{II} instead of Ru^{III}–Ru^{III}, which was the case for the blue dimer. The highest oxidation state involved in the O_2 evolution is the Ru^{IV}–Ru^{IV}. A TON of ~19 was achieved, corresponding to a catalyst efficiency of 70% (according to the moles of Ce^{IV} consumed) with an oxygen evolution rate constant of 1.4 x 10^{-2} s^{-1} which, according to some accounts, is faster than that of the blue dimer. These enhanced rate is attributed to: (1) the rigid confinement of the Ru centers; (2) absence of the μ-oxo bridge avoiding decomposition routes involving reductive cleavage and a driving force for trans-dioxo formation and; (3) decreased deactivation by anation resulting from a lower overall charge on the complex. Moreover, providing a smaller pocket for incoming substrates (using bulky anions

UNIVERSITAT ROVIRA I VIRGILI
NOVEL MOLECULAR CATALYSTS FOR WATER OXIDATION: TOWARDS ARTIFICIAL PHOTOSYNTHESIS
Sara Goberna Ferrón
Dipòsit Legal: T.189-2014

such as triflate) will avoid anation. Meticulous isotopic labelling studies with $^{18}H_2O$ provided evidence of a until now uncharacterized intramolecular O-O bond forming mechanism between adjacent [Ru^{IV}=O] units.[51,52] Conversely, independent computational studies of this catalyst were reported recently by Yang and Baik,[53] and a direct oxo-coupling was found to follow a higher energy pathway than formation of an intermediate peroxide species generated from attack of a water molecule on the oxo.

Thummel et al. reported a family of dinuclear Ru complexes capable of water oxidation **1.3** (Figure 1.10) and their derivatives, which differ structurally from the above catalysts.[39,54] Two Ru^{II} ions were coordinated by bistridentate rigid bridging ligands and four axial pyridine ligands or its 4-substituted derivatives. The rates of oxygen production and the TON were studied in the presence of excess Ce^{IV} as a sacrificial oxidant at pH = 1. The results indicated that the systems having 4-methoxypyridine as an axial ligand appeared to be more active than other related species. The turnover number and the rate of oxygen production for the most active catalysts were 689 and 0.924 μmol min^{-1}, respectively.

In 2000, Tanaka et al. reported the dinuclear complex [$Ru_2^{II}(OH)_2$(3,6-tBu_2qui)$_2$(btpyan)](SbF_2)$_2$ **1.4** (Figure 1.10) with a bridging ligand bis(terpyridyl)anthracene (btpyan) and a bidentate quinone ligand.[55] Electrolysis of the complex attached to an ITO (tin-doped In_2O_3) electrode at 1.7 V (vs. Ag/AgCl) led to dioxygen evolution with a current efficiency of 95% and a final TON of 6730 before the current completely stopped after 40 h. Although the stability of this complex is very impressive the overpotential is too large according to the authors for practical application. They studied the acid-base equilibrium and redox properties of the catalyst and the analogous species [$Ru_2^{II}(OH)_2(bpy)_2$(btpyan)](SbF_2)$_2$ and compared their catalytic activities.[56,57]

UNIVERSITAT ROVIRA I VIRGILI
NOVEL MOLECULAR CATALYSTS FOR WATER OXIDATION: TOWARDS ARTIFICIAL PHOTOSYNTHESIS
Sara Goberna Ferrón
Dipòsit Legal: T.189-2014

Sun et al. reported two dinuclear complexes **1.5** and **1.6** (Figure 1.10) based on ligands that have negatively charged carboxylate groups in an attempt to lower the redox potential required for catalytic oxidation of water.[58,59] Water oxidation in the presence of Ce^{IV} as oxidant leads to TONs of 4700-10400 and TOFs of 0.281.2 s^{-1}. The visible light-water oxidation was studied for the bcppz-based complex in a system involving $Ru(bpy)_3^{2+}$ as photosensitizer and $[Co(NH_3)_5Cl]Cl_2$ or $Na_2S_2O_8$ as an electron acceptor. A TON of 1270 was obtained under these conditions.[60]

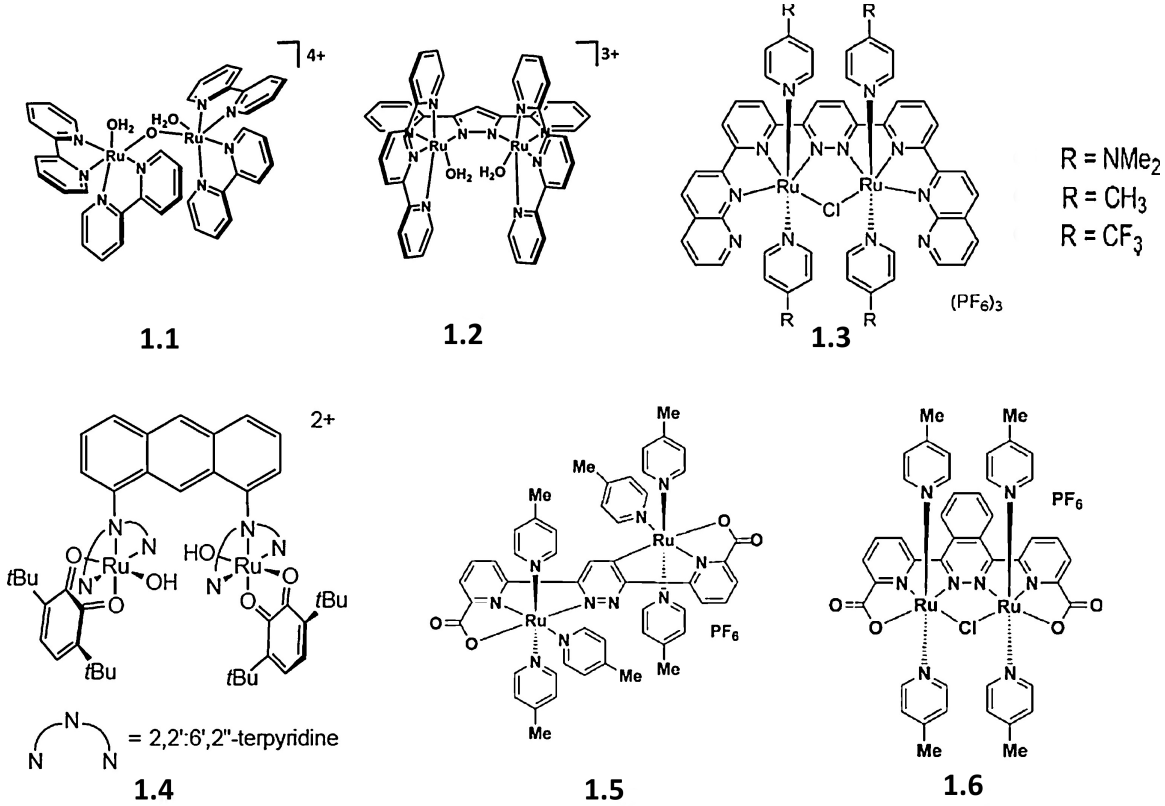

Figure 1.10. *Structures of notable dinuclear ruthenium water oxidation catalysts.*[61]

Mononuclear Ruthenium Complexes

For a long time WOCs were thought to be necessarily multinuclear in order to divide the four PCET steps required for the water oxidation reaction over several metal centers in close proximity, until Zong and Thumel[54] and Meyer[43] demonstrated

UNIVERSITAT ROVIRA I VIRGILI
NOVEL MOLECULAR CATALYSTS FOR WATER OXIDATION: TOWARDS ARTIFICIAL PHOTOSYNTHESIS
Sara Goberna Ferrón
Dipòsit Legal: T.189-2014

that "one site is enough". In 2005 by Zong and Thummel described the WOC activity of a series of three single Ru containing complexes **1.7** (Figure 1.11) using a tridentate tpy derivative, with an aqua ligand in the tridentate equatorial plane and two axially coordinated pyridine derivatives functionalized in the 4' position with $–NMe_2$, $–CH_3$, and $–CF_3$ as electron donating, neutral and withdrawing groups respectively.[54] However, as the authors noted in the report, under the highly acidic conditions required when using Ce^{IV} as oxidant for water oxidation, the tertiary amine is protonated and will act as a strong electron-withdrawing group. Reported TONs (up to 580) were highest for the $–CH_3$ derivative. The fastest turnovers, 7.8×10^{-4} s^{-1}, were found for the $–NMe_2$ derivative. This was the first demonstration of a monometallic Ru polypyridyl complex with quantified O_2 evolution. However, no mechanistic investigation was performed to determine the order in [Ru].

Subsequently, they prepared a series of mononuclear Ru complexes **1.8-1.12** (Figure 1.11) to compare their catalytic water oxidation activity.[62] The results indicated that complex **1.8** exhibited the highest TON (1170) with a rate of 3.36×10^{-5} s^{-1}. The kinetic studies of complex **1.11** indicated that the catalyst was not decomposed into ruthenium dioxide, from a comparison of the kinetic plots of **1.11** and RuO_2. The O_2 evolution rates (catalyzed by complex **1.8**, R=H) as a function of the catalyst concentration indicated that the reaction is first order. This observation was supported using also the sterically hindered complex **1.12**.

UNIVERSITAT ROVIRA I VIRGILI
NOVEL MOLECULAR CATALYSTS FOR WATER OXIDATION: TOWARDS ARTIFICIAL PHOTOSYNTHESIS
Sara Goberna Ferrón
Dipòsit Legal: T.189-2014

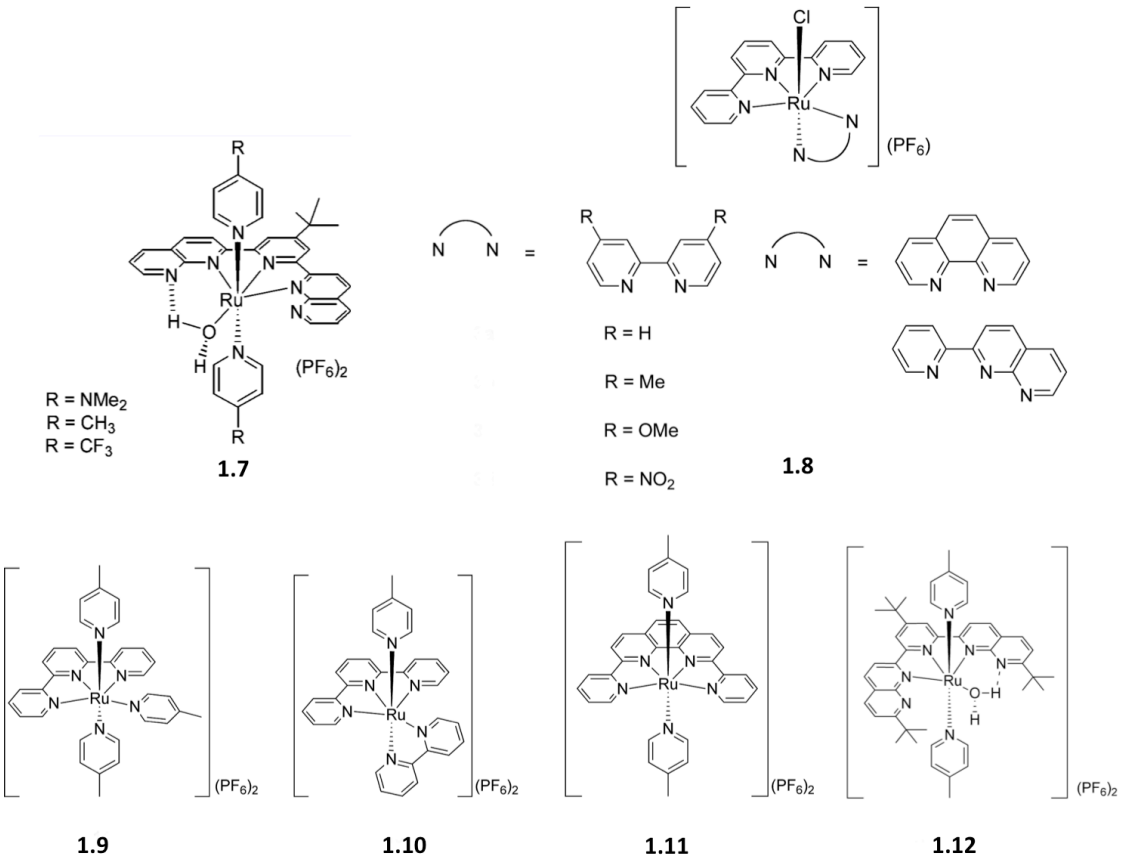

Figure 1.11. *Structures of notable mononuclear ruthenium water oxidation catalysts.*[54,62]

DFT was used to determinate a mechanism for single-site catalysis. According to this mechanism, after the catalyst had two electrons removed by Ce^{IV} and was attacked by H_2O, a seven-coordinate $Ru^{IV}(H_2O)$ species was formed. This species lost two protons and two electrons, thereby providing a resonance-stabilized Ru^{VI}=O species. Moreover, the $Ru^{VI}OOH$ species was formed by an attack of water on the Ru^{VI}=O species. The proton was then released, with the subsequently O_2 evolution (Figure 1.12).

UNIVERSITAT ROVIRA I VIRGILI
NOVEL MOLECULAR CATALYSTS FOR WATER OXIDATION: TOWARDS ARTIFICIAL PHOTOSYNTHESIS
Sara Goberna Ferrón
Dipòsit Legal: T.189-2014

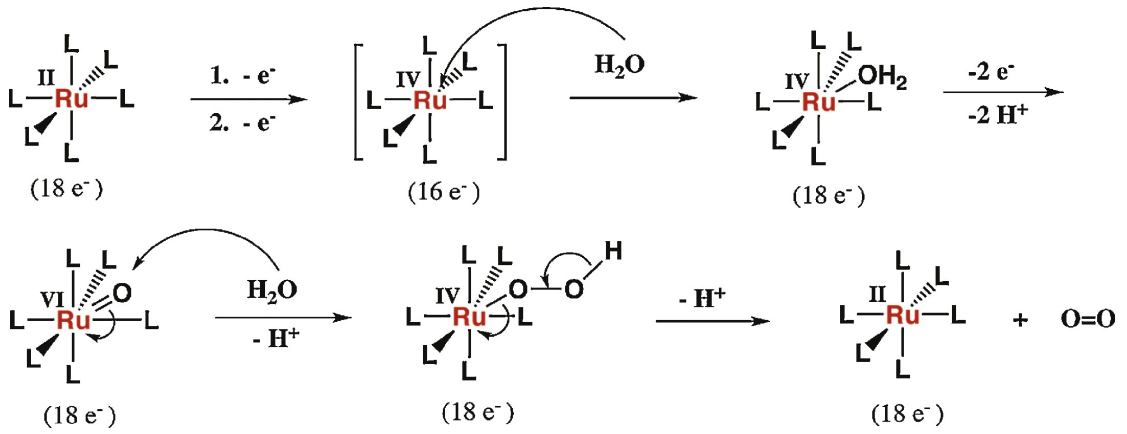

Figure 1.12. *Proposed water oxidation mechanism of **1.7**, R = CH_3.*[61]

Interestingly, the complex trans-$[Ru(tpy)(pynp)(H_2O)]^{2+}$ **1.13a** (Figure 1.13) was later studied by Yagi et al. This catalyst is an active WOC when Ce^{IV} is used as an oxidant.[63] Upon irradiation with visible light a cis-trans isomerization occurs (Figure 1.13), leading to the isomer cis-$[Ru(tpy)(pynp)(H_2O)]^{2+}$ **1.13b**. The trans isomer is one order of magnitude more active than the cis isomer, as shown by their TOFs of 3.8 x 10^{-3} s^{-1} and 4.8 x 10^{-4} s^{-1} respectively. This is reminiscent of what happens to cis-$[Ru(bpy)_2(OH_2)_2]^{2+}$ [64,65], and highlights that photoisomerization is an important cause of catalyst deactivation for Ru-based compunds.

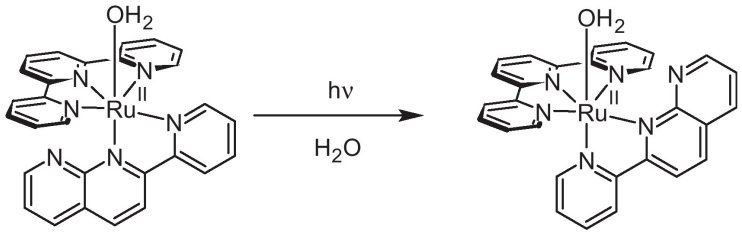

Figure 1.13. *Isomers of $[Ru^{II}(tpy)(pynap)(OH_2)]^{2+}$ that display vastly different PCET and water oxidation chemistry as a result of the proximal pyridyl group to the active Ru-O moiety.*[63,66] *The cis and trans designations refer to the orientation of the pendant base and the aqua ligand.*

A related study by Llobet et al. investigating a series of single Ru containing analogues to their dimeric catalyst **1.2** also found that geometrical influences had profound effects on the catalytic abilities of the related complexes.[67] Notably, modification of the Hbpp ligand by a phenyl ring produced the most pronounced changes, where dioxygen evolution was accompanied by carbon dioxide in a 5:1 O_2 / CO_2 ratio, demonstrating that the phenyl ring is the site of ligand deterioration. A proposed mechanism involves oxidation of the phenyl ring to add carbonyl functionalities that lead to carbon dioxide. A pyridyl group would likely be protonated under the catalytic conditions, which the authors stated might protect it from rapid oxidation. As with the study by Yagi and coworkers,[63] the Llobet group found that the *out* isomers always outperformed the in isomers with the pendant base lying in close proximity to the active Ru-O unit, shielding it from stabilizing H-bonding interactions with solvent water molecules.

Meyer et al. reported a family of mononuclear Ru complexes **1.14-1.17** (Figure 1.14) containing tpy, Mebimpy, and other ligands in this series.[36,50,52,68-70] The detailed water oxidation mechanism of one of these complexes was elucidated via stopped-flow experiments in conjunction with spectrophotometric monitoring and DFT calculations of intermediate structures (Figure 1.15).[71,72] The results of their study indicated that these complexes are promising, robust single-site water oxidation catalysts.

UNIVERSITAT ROVIRA I VIRGILI
NOVEL MOLECULAR CATALYSTS FOR WATER OXIDATION: TOWARDS ARTIFICIAL PHOTOSYNTHESIS
Sara Goberna Ferrón
Dipòsit Legal: T.189-2014

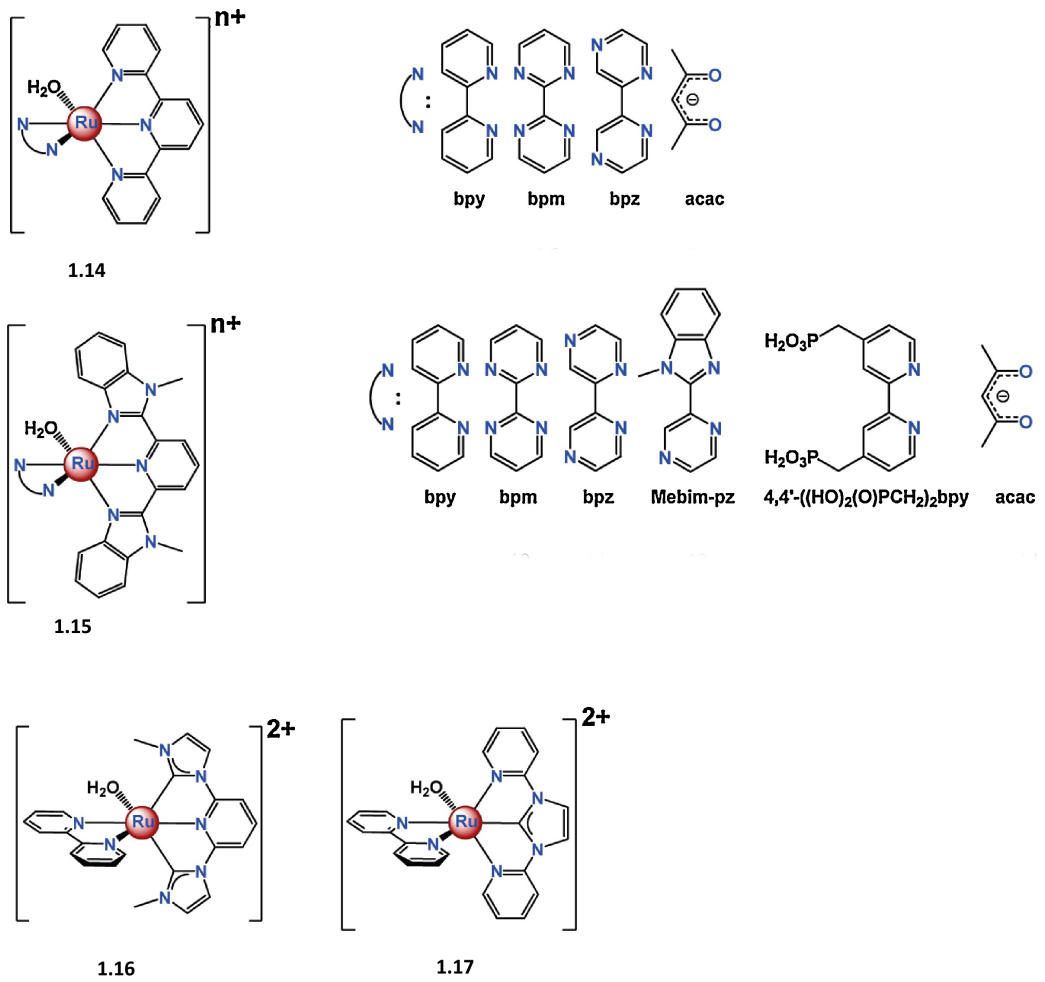

Figure 1.14. *Meyer et al. single-site Ru complexes for water oxidation.*[61]

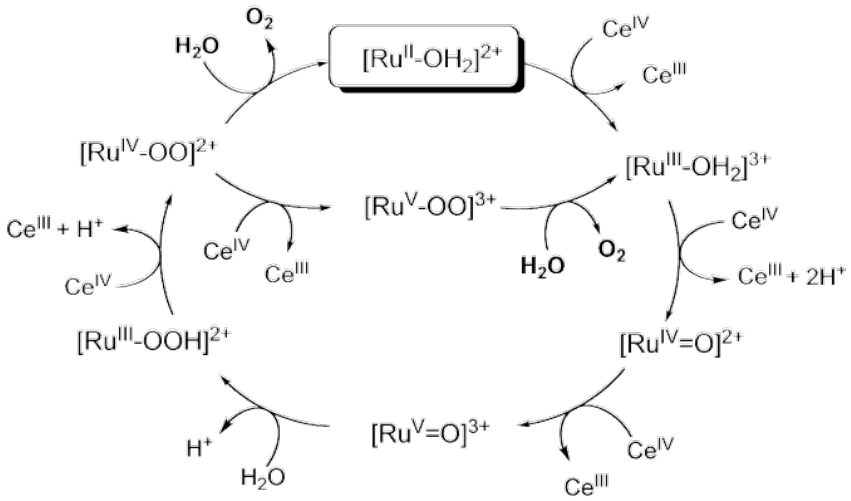

Figure 1.15. *Meyer et al. proposed mechanism of catalytic water oxidation.* [43,71]

1. 5. Water Oxidation Catalysts

The formation of O–O occurs through a nucleophilic attack of water on the $[Ru^{V}=O]^{3+}$ moiety. This $[Ru^{V}=O]^{3+}$ species was formed by continuous oxidation from $[Ru^{II}–OH2]^{2+}$ to $[Ru^{IV}–O]^{2+}$ accompanied by the loss of two electrons and two protons to avoid charge buildup. The $[Ru^{IV}=O]^{2+}$ was then oxidized by Ce^{IV}. The existence of the $Ru^{III}–O_2H$ intermediate (Eq.1.5) was experimentally demonstrated. However, this intermediate was unstable, similar to $Ru^{III}–OH^{2+}$, due to a disproportionation reaction. Kinetic studies showed that $Ru^{III}–O_2H$ undergoes a rapid oxidation accompanied by the loss of one electron and proton ($Ru^{III}–O_2H \rightarrow [Ru^{IV}(OO)]^{2+}$), followed by a competition between the first-order decomposition of $[Ru^{IV}(OO)]^{2+}$ and its further oxidation to $[Ru^{V}(OO)]^{3+}$ with rate constants of 7.4 **x** 10^{-4} s^{-1} and 10 s^{-1}, respectively. The rate-limiting reaction for the catalytic water oxidation depends on the acid concentration under catalytic conditions. The former reaction is rate-limiting in 0.1 M HNO_3; however, in 1.0 M HNO_3, the latter reaction determines the rate of water oxidation.

$$[Ru^{V}=O]^{3+} + H_2O \rightarrow Ru^{III}–O_2H + H^{+} \qquad \text{(Eq. 1.5)}$$

Meyer and coworkers have derivatized related Ru complexes with functionalities that enabled them to be attached to electrode surfaces.[73]

Sun et al. reported mononuclear complexes with electron donating carboxylate ligands that catalyze the oxidation of water at a much lower potential (difference of 0.9 V) than corresponding complexes with neutral ligands.[74] Complex **1.18** (Figure 1.16) catalyzes water oxidation with a remarkable TOF of 1.6 s^{-1} and TONs of >120. The TOF depends quadratically on the concentration of the catalyst, indicating a dinuclear process. Indeed, a crystal structure of a reaction intermediate showed a dimeric 7-coordinate Ru^{IV} compound, bridged by a $[HOHOH]^{-}$ ligand. The structural change from 6-coordinate to 7-coordinate complex appears to be rather small due to

UNIVERSITAT ROVIRA I VIRGILI
NOVEL MOLECULAR CATALYSTS FOR WATER OXIDATION: TOWARDS ARTIFICIAL PHOTOSYNTHESIS
Sara Goberna Ferrón
Dipòsit Legal: T.189-2014

the strain of the tetradentate 6,6'-dicarboxy-2,2'-bipyridine ligand, indicating that only a low-energy step needed for efficient water oxidation. They have also demonstrated a photoelectrochemical device using **1.18** as the WOC deposited in a Nafion membrane onto a TiO_2 substrate with a phosphonate functionalized dye molecule as the photosensitizer[75] and an electrocatalytic device when inmobilized onto carbon nanotubes.[76]

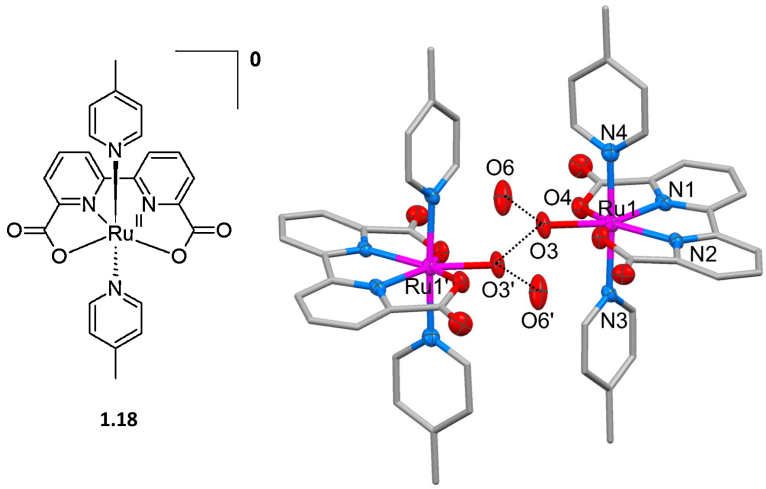

Figure 1.16. ***Left****: Chemical formula of mononuclear compound* ***1.18.*** ***Right****: Crystal structure of an intermediate in the catalytic cycle of complex* ***1.18*** *with thermal ellipsoids at 50% probability. Hydrogen atoms are omitted for clarity.*[47]

Very recently Llobet and Sun et al. reported the mononuclear ruthenium complex [Ru(bda)(isoq)$_2$] **1.19** (H_2bda = 2,2'-bipyridine-6,6'-dicarboxylic acid; isoq = isoquinoline) (Figure 1.17).[77] Water oxidation experiments were performed using Ce^{IV} as the oxidant under acidic conditions showing a high catalytic activity (TOF = 303 s^{-1}) combined with a high chemical stability (TON = 8,360). The methods used include spectroscopic, electrochemical and kinetic studies, in combination with quantum-chemical modeling.

UNIVERSITAT ROVIRA I VIRGILI
NOVEL MOLECULAR CATALYSTS FOR WATER OXIDATION: TOWARDS ARTIFICIAL PHOTOSYNTHESIS
Sara Goberna Ferrón
Dipòsit Legal: T.189-2014

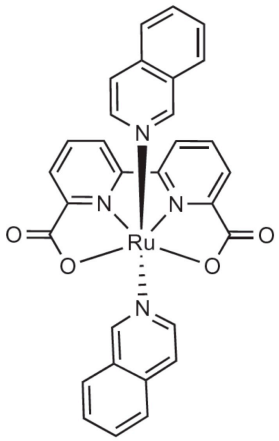

1.19

Figure 1.17. *Structure of compound 1.19.*[77]

Purely Inorganic Multinuclear Ruthenium Complexes

Many organic ligands of transition metal catalysts show degradation under the strongly oxidative conditions needed for water oxidation, which leads to relatively low TONs compared with heterogeneous.[78] In order to combine the high rate of O_2 evolution of homogeneous catalysts with the robustness of heterogeneous catalysts, catalysts were prepared with all-inorganic ligands called polyoxometalates (POMs). These polyanion ligands are excellent **σ**-donors stabilizing the high oxidation states required for water oxidation.[79]

The ruthenium polyoxometalate complex **1.20** (Figure 1.18) was simultaneously reported by two research groups to show activity toward oxidation of water.[80,81] This compound has the molecular formula $[Ru_4O_4(OH)_2(H_2O)_4(SiW_{10}O_{36})_2]^{10-}$, but water oxidation was obtained using different chemical oxidants in the two reports: Ce^{IV} [80] and $[Ru(bpy)_3]^{3+}$ [81]. The active site of the compound is the $[Ru_4O_4]$ adamantane–like core with adjacently coordinated aqua ligands, which undergo stepwise PCET steps from Ru^{IV}_4 to Ru^{V}_4.[82,83] The oxidation potentials of the intermediates lie in a close range (+0.48 V - +1.06 V vs. NHE), which makes the oxidation an efficient process.[84] The Ru^{V}_4 core is thought to release dioxygen in a rate-limiting step by intermolecular

UNIVERSITAT ROVIRA I VIRGILI
NOVEL MOLECULAR CATALYSTS FOR WATER OXIDATION: TOWARDS ARTIFICIAL PHOTOSYNTHESIS
Sara Goberna Ferrón
Dipòsit Legal: T.189-2014

attack of a molecule of water on a Ru^{V}–OH group. The intramolecular formation of the O–O bond by cooperation of two ruthenium centers is not likely, due to geometrical constraints. The stability of compound was tested by adding a second charge of Ce^{IV} after the initial catalytic run; the absence of drop in activity in this second catalytic run is indicative of the stability of the catalyst in the reaction conditions.[80-82,84,85] A TOF of 1.25 x 10^{-1} s^{-1} was found for chemical oxidation with Ce^{IV} at pH = 0.6, with an O_2 yield of 90% with respect to the oxidant. O_2 yields when using $[Ru(bpy)_3]^{3+}$ as the oxidant (pH = 7) were substantially lower (maximum of 75%)[81] due to the oxidative instability of $[Ru(bpy)_3]^{3+}$.[86] The catalyst remains stable for several months at pH = 7, but slowly decomposes at low pH (0.1 M HCl).[84] In addition, electrocatalytic oxidation of water seems to be possible at a potential of E = 0.95 V–1.05 V vs. NHE at pH = 7.[85]

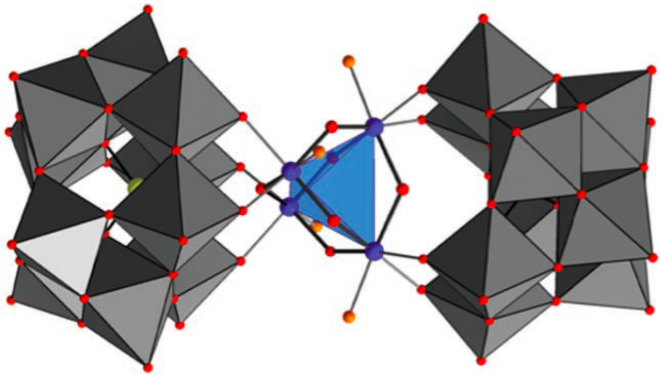

Figure 1.18. *Structure of the polyanion of **1.20**, highlighting the central $\{Ru_4(\mu\text{-}O)_4(\mu\text{-}OH)_2(H_2O)_4\}^{6+}$ core (ball-and-stick representation, Ru blue, μ-O red, $O(H_2)$ orange; hydrogen atoms omitted for clarity) and the slightly distorted $[Ru_4]$ tetrahedron (transparent blue). The polytungstate fragments are shown as gray polyhedra, and Si is in yellow*.

Manganese-based WOCs

Manganese is within the active site of the OEC in PSII and many manganese complexes have been studied extensively as possible biomimetic models of the OEC. However, only very few were catalytically active for water oxidation.[87,88]

UNIVERSITAT ROVIRA I VIRGILI
NOVEL MOLECULAR CATALYSTS FOR WATER OXIDATION: TOWARDS ARTIFICIAL PHOTOSYNTHESIS
Sara Goberna Ferrón
Dipòsit Legal: T.189-2014

Dinuclear Manganese Complexes

A di-μ-oxo bridged Mn dimer with tpy ligands $[H_2O(terpy)Mn(O)_2Mn(terpy)OH_2](NO_3)_3$ **1.21** (Figure 1.19) was demonstrated by Crabtree et al. as being the first functional model with di-μ-oxo Mn units that can catalyze homogeneous O_2 evolution, similar to those observed in the OEC.[88-90] Complex **1.21** catalyzes water oxidation starting at a TOF of 0.67 s^{-1}, and with a cumulative TON of 4 after 6 h, during which time the catalyst decomposes into permanganate. Typical water oxidation conditions involved the use sacrificial 2-electron O-atom donors such as OCl^- or HSO_5^- in aqueous solutions of pH = 8.6 and 4.5 respectively. These O-atoms donors are able to exchange with water putting into question the origin of molecular oxygen.[91-94]. The aqua ligands present in the structure can be deprotonated to form a proposed MnV = O species by PCET.[95] This oxo-manganese species is likely the reactive intermediate in the catalytic cycle of most other WOCs and in the OEC.[96]

Naruta el al. reported a series of three manganese porphyrin complexes with differing aryl substituents around the porphyrin rings **1.22** (Figure 1.19).[97] These compounds catalyze the electro-oxidation of water at a potential larger than 1.42 V (vs. NHE) in basic medium with a Faradaic efficiency of 5–17%. The TON of the most active species was 9.2 (**1.22**, Ar = C_6F_5). A suggested mechanism involves Mn^V=O species during the formation of O–O bond.[98] Evolved oxygen originating from solvent was confirmed by labeling studies with H_2O^{18}.

A more elaborate dimeric Mn complex was reported by Kurz et al. in 2008 **1.23** (Figure 1.19),[99] where they demonstrated that O-atoms in evolved dioxygen were originated from water through H_2O^{18} labeling studies. Electron paramagnetic resonance (EPR) studies suggested the formation of a Mn^{IV}-Mn^{IV} dimer as a catalytic intermediate.

More recently, the bioinspired dinuclear manganese catalyst **1.24** (Figure 1.19) was

UNIVERSITAT ROVIRA I VIRGILI
NOVEL MOLECULAR CATALYSTS FOR WATER OXIDATION: TOWARDS ARTIFICIAL PHOTOSYNTHESIS
Sara Goberna Ferrón
Dipòsit Legal: T.189-2014

reported by Akermark et al. as the most stable molecular catalyst based on manganese.[100] As in the natural PSII, OEC it consists of imidazole, carboxylate and oxygen ligands bridging two manganese centers. Water oxidation was observed using the single electron oxidant $[Ru^{III}(bpy)_3]^{3+}$ directly as the oxidant and in the presence of $S_2O_8^{2-}$ as a photocatalytic system at neutral pH. H_2O^{18} labeled studies showed that the oxygen atoms originate from water. Catalytic efficiency, however, was quite low, with moderate TOF of ~0.03 s^{-1} and TON of 25. As with the other Mn complexes discussed here, very little mechanistic information was provided, but the authors suggested that the highest oxidized state was a Mn^{V}-Mn^{V} species.

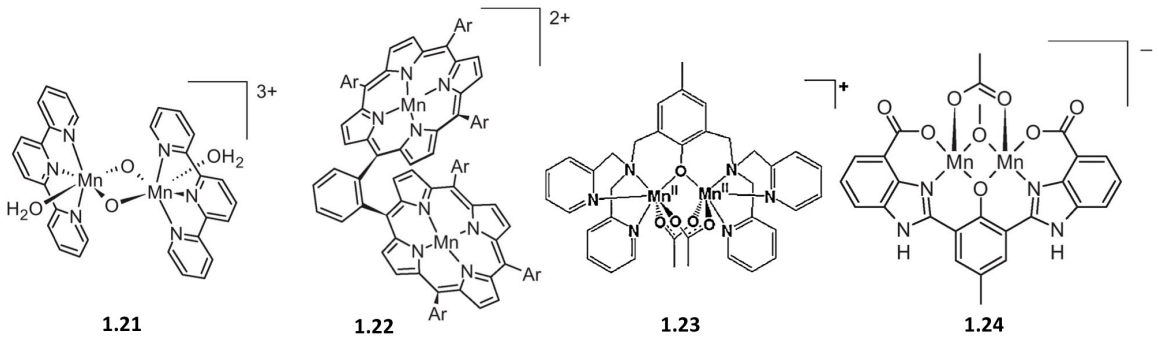

Figrue 1.19. *Structures of notable dinuclear manganese water oxidation catalysts*.[47,61]

Mononuclear Manganese Complexes

As with Ru complexes, the "one site is enough" trend also resulted viable in the case of Mn. Crabtree et al. investigated the reaction of compound **1.25** (Figure 1.20) with oxone in the pH range of 3–6, and using EPR found that a green $Mn^{III/II}$ dimer can be formed and can generate O_2 with a by-product MnO_4^-.[101] Experiments investigating the O_2 evolution were carried out with different ligands. Using dipicolinate (dpa) as the ligand **1.25**, the rate of O_2 evolution was 3.7 µmol h^{-1}, and the TON was less than 1. Considerable improvement was made by replacing dpa with terpy; the rate of O_2 evolution dramatically increased to 61 µmol h^{-1}, and the TON improved to 50. In fact, mononuclear compound **1.25** and Mn–terpy complexes are

UNIVERSITAT ROVIRA I VIRGILI
NOVEL MOLECULAR CATALYSTS FOR WATER OXIDATION: TOWARDS ARTIFICIAL PHOTOSYNTHESIS
Sara Goberna Ferrón
Dipòsit Legal: T.189-2014

precursors which formed dinuclear Mn complexes under catalytic conditions, and then the dinuclear Mn complexes catalyzed water oxidation.

Recently, Akermark et al reported a $[Mn^{III}–corrole]^{+}$ complex **1.26** (Figure 1.20) that can be converted into a $Mn^{V}=O$ complex wich undergoes reductive elimination od oxygen on attack by hydroxide ion. However, TON and TOF were not clearly reported.[102-104]

Porphyrins and corroles presented in Pacman **1.27** and Hangman **1.28** (Figure 1.20) motifs have been reported as WOCs.[105,106] Two porphyrins juxtaposed via an *o*-phenylene spacer furnish a Pacman complex that promotes water oxidation from acetonitrile/water mixture at a catalytic onset potential of 1.4 V vs NHE.[97] Electrochemical characterization of the system is minimal, making it difficult to judge the OER performance of these catalysts, although a Faradaic efficiency of only 5 – 17% is reported. These compounds have also been shown to split water electrochemically.[107] Catalytic activities of the compounds for electrochemical water oxidation were studied by cyclic voltammetry. The oxidation potentials were reported at E_{pa} = 0.79 V, and $\mathbf{E}_{pa}$ = 0.80 V [***n***-BuNOH (10% in water) in CH_2Cl_2 / CH_3CN (2/3) v/v], for **1.27** and **1.28**, respectively. The oxygen evolution was also investigated with an oxygen-sensing electrode showing that compound **1.28** has higher catalytic efficiency for water oxidation than **1.27** under basic conditions.

UNIVERSITAT ROVIRA I VIRGILI
NOVEL MOLECULAR CATALYSTS FOR WATER OXIDATION: TOWARDS ARTIFICIAL PHOTOSYNTHESIS
Sara Goberna Ferrón
Dipòsit Legal: T.189-2014

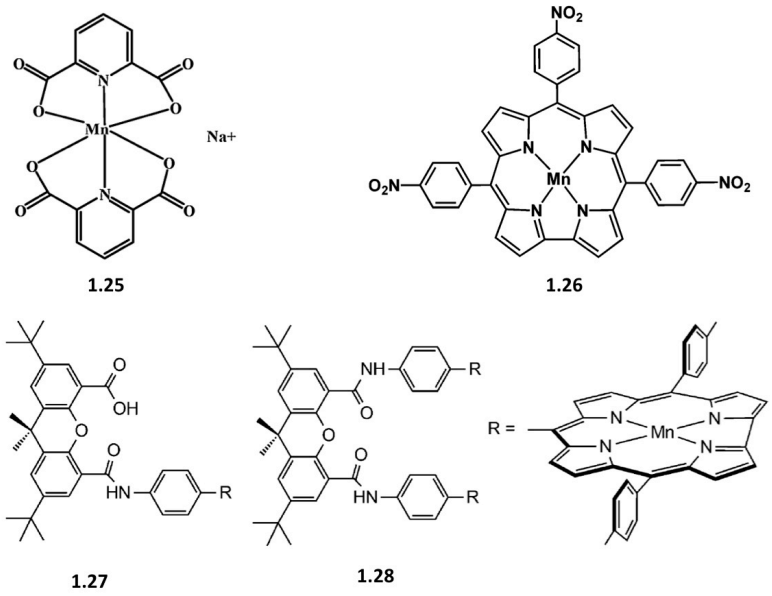

Figure 1.20. *Structures of notable mononuclear manganese water oxidation catalysts*.[61]

Tetranuclear Manganese Complexes

Motivate in large part by the structure of OEC in PSII, tetramanganese clusters have been interrogated as catalysts for water oxidation. As a Nafion composite, a Mn_4O_4 complex bridged by bis-(4-methoxyphenyl)phosphinate ligands, $[Mn_4O_4((p\text{-MeOPh})PO_2)_6]^+$ **1.29** (Figure 1.21) is proposed to drive oxygen evolution under white light irradiation and an applied potential.[108] The photocurrent scales linearly with pH when the applied potential is held at 1.2V (vs. NHE). When the electrode is illuminated with >275nm white light at pH 11, an initial photocurrent density of 9 μAcm^{-2} is reported. This current decreases 0.7 μAcm^{-2} per hour.

UNIVERSITAT ROVIRA I VIRGILI
NOVEL MOLECULAR CATALYSTS FOR WATER OXIDATION: TOWARDS ARTIFICIAL PHOTOSYNTHESIS
Sara Goberna Ferrón
Dipòsit Legal: T.189-2014

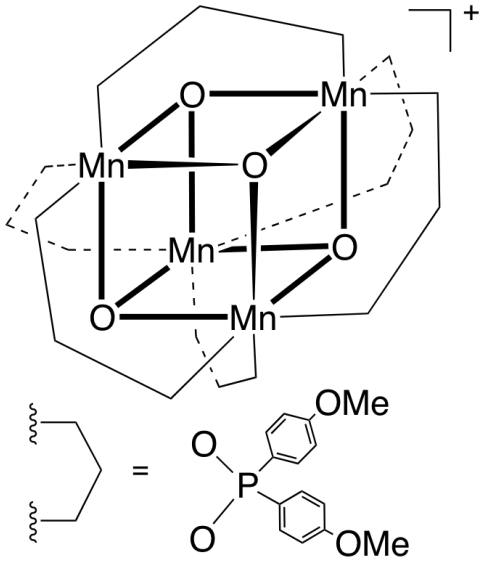

Figure 1.21. *$[Mn_4O_4((p\text{-}MeOPh)PO_2)_6]^+$ as a functional and structural model of the OEC.*[109]

Iridium-based WOCs

Numerous Iridium complexes have shown homogeneous catalytic activity for water oxidation. Bernhard et al reported a family of five cyclometalated Ir complexes composed by bis-phenylpyridines groups with solvent water occupying the two cis coordination sites, $[Ir(R_1R_2\text{-phenylpyridine})_2(H_2O)_2]$ **1.30** (Figure 1.22).[110] These complexes achieve maximum turnover frequencies of 1.5 x 10^{-3} s^{-1} and turnover numbers of 2500 using Ce^{iV} as oxidant.

The most extensively studied Ir complexes that exhibit catalytic water oxidation capabilities are the family of Cp* iridium complexes, $[(Cp^*)IrL_3]^{2+}$ (Cp*= pentamethylcyclopentadienyl, L = any monodentate or bidentate ligand) **1.31-1.42** (Figure 1.22) reported by Brudvig and Crabtree et al., which are highly active and robust water oxidation catalysts.[111] This study employed stronger donating ligand sets to improve the catalytic activity. The ^{18}O-labeling experiments confirmed that water was the source of O atoms in the evolved O_2. Complexes **1.41** and **1.42** exhibited

UNIVERSITAT ROVIRA I VIRGILI
NOVEL MOLECULAR CATALYSTS FOR WATER OXIDATION: TOWARDS ARTIFICIAL PHOTOSYNTHESIS
Sara Goberna Ferrón
Dipòsit Legal: T.189-2014

higher activities with turnover frequencies of 0.33 s^{-1} (pH = 0.89). In a proposed mechanism water attacks Ir^{V}=O species losing a proton to an adjacent water molecule. Very recently, the construction of two metal organic frameworks (MOFs) using elongated dicarboxylate bridging ligands derived from Cp*Ir(L)Cl complexes (L=dibenzoate-substituted 2,2'-bipyridine or dibenzoate-substituted 2-phenylpytidine) and $Zr_6O_4(OH)_4$(carboxylate)$_{12}$ cuboctahedral secondary building units has been reported. These MOFs provided an interesting platform to study water oxidation pathways of the Cp*Ir(L)Cl catalysts.[112]

Macchioni et al. reported the two water-soluble mononuclear Ir^{III} complexes **1.43** and **1.44** (Figure 1.22), which showed higher activity. Complexes **1.43** and **1.44** had TOF = 0.14 s^{-1} and 0.26 s^{-1} respectively.[113]

A recent work has shown that the stability of iridium-based molecular catalysts for water oxidation should not be taken for granted.[114-116] In the study of Grotjahn et al. scanning tunneling electron microscopy, powder X-ray diffraction, and UV–vis spectroscopy studies revealed the presence of nanoparticles of 2–10 nm diameter in water oxidation reaction mixtures obtained from reported iridium catalysts and large excess of Ce^{IV}.[115] Recently, Crabtree et al. studied the electrocatalytic water oxidation using mononuclear iridium catalysts.[116] Studies using an electrochemical Quartz Crystal Nanobalance showed that a thin layer of a carbon-containing iridium oxide material deposits on the electrode in water oxidizing conditions using compound **1.41** as precursor catalyst. This iridium oxide layer gives a blue color to the electrode, and it has excellent catalytic properties toward water oxidation.[117]

UNIVERSITAT ROVIRA I VIRGILI
NOVEL MOLECULAR CATALYSTS FOR WATER OXIDATION: TOWARDS ARTIFICIAL PHOTOSYNTHESIS
Sara Goberna Ferrón
Dipòsit Legal: T.189-2014

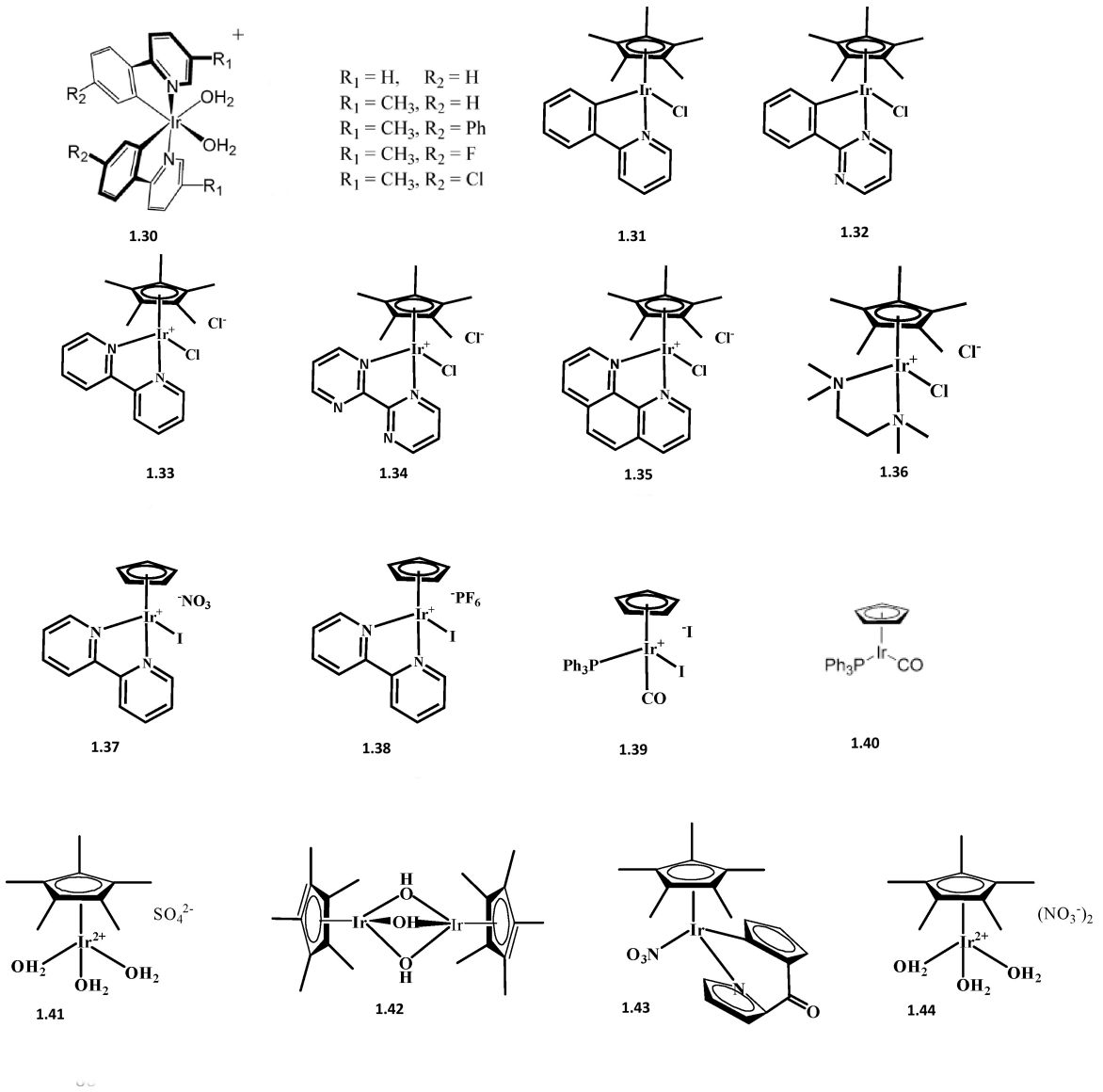

Figure 1.22. *Structures of iridium water oxidation catalysts.*[61]

Iron-based WOCs

Iron is an important element that is involved in a number of challenging biochemical oxidation processes.[118]

In 2010, Bernhard and Collins et al. reported a series of Fe-macrocyclic complexes, $[Fe^{III}(taml)]^-$ (taml = tetra amido macrocyclic ligand), **1.45** (Figure 1.23) where four were able to generate dioxygen from water using Ce^{IV} as the sacrificial oxidant.[119] The

UNIVERSITAT ROVIRA I VIRGILI
NOVEL MOLECULAR CATALYSTS FOR WATER OXIDATION: TOWARDS ARTIFICIAL PHOTOSYNTHESIS
Sara Goberna Ferrón
Dipòsit Legal: T.189-2014

ligands were substituted with electron donating or electron withdrawing groups at the aromatic ring or the alkyl bridge, the most active iron compound, R_1 = Cl and R_2 = F. Its initial TOF is 1.3 s^{-1} and TON >16, but the compound is quickly (within seconds) deactivated, most likely due to oxidation of the ligand.

A recent work reports a series of Fe complexes with various tetradentate ligands where the coordination sites were cis to each other as active catalysts using Ce^{IV} or $NaIO_4$ as the sacrificial oxidants, while the corresponding Mn, Co and Ni analogues using one of the ligands were inactive.[120] Two other complexes, with coordination sites in trans and a pentadentate ligand using Fe were not active catalysts. In the proposed mechanism high valent iron-oxo species are responsible for the O–O formation. The most active complex **1.46** (Figure 1.23) achieved TON of >1000 using $NaIO_4$ and rather impressive TOF of 0.23 s^{-1} using Ce^{IV} as the oxidant.

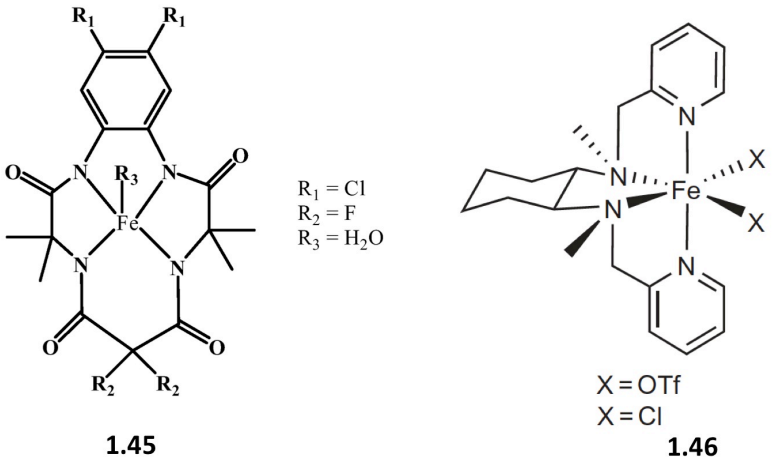

1.45 **1.46**

Figure 1.23. *Structures of iron water oxidation catalysts.*

Cobalt-based WOCs

Following their work with Ruthenium polypyridil complexes[68,121,122], Berlinguette et al. designed a complex with Co as the active metal capable of catalytically oxidize water in basic conditions, $[Co(Py5)(OH_2)](ClO_4)_2$ (Py5 = 2,6-

UNIVERSITAT ROVIRA I VIRGILI
NOVEL MOLECULAR CATALYSTS FOR WATER OXIDATION: TOWARDS ARTIFICIAL PHOTOSYNTHESIS
Sara Goberna Ferrón
Dipòsit Legal: T.189-2014

(bis(bis-2-pyridyl)methoxy-methane)-pyridine) **1.45** (Figure 1.24).[123,124] Oxygen evolution was measured with a fluorescence optical probe immersed in the solution at an applied potential of +1.59 V vs. NHE over 10 mins and TOF of 79 s^{-1} were reported.

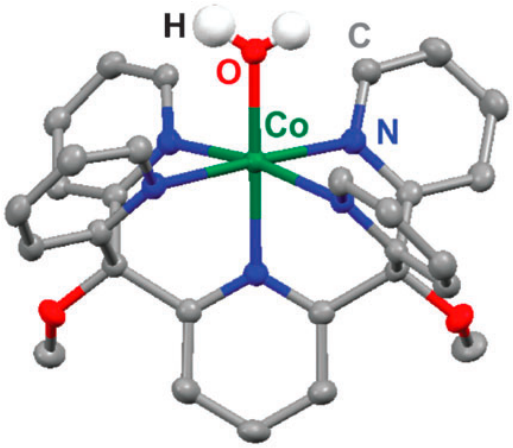

Figure 1.24. *Molecular representation of [Co(Py5)(OH$_2$)](ClO$_4$)$_2$. The counteranion and H atoms of are omitted for clarity.*[124]

Nocera et al reported a series of Co hangman corroles **1.46 (Figure 1.25)** complexes and the investigation of the electrochemical water oxidation.[125] The neutral complexes were immobilized using a Nafion membrane deposited on conducting FTO glass slides, which were used as the working electrodes. They found that octafluorination of the corrole ring significantly improved the TOFs to ≈ 1s^{-1}.

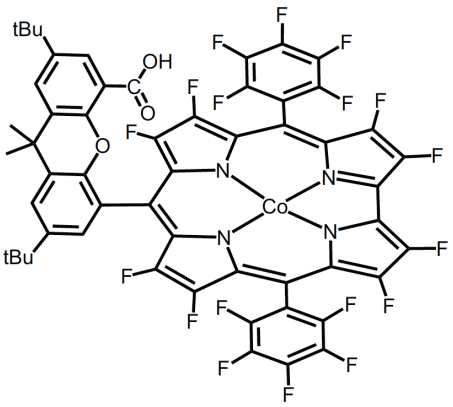

Figure 1.25. *Structure of cobalt(III) hangman corroles.*[126]

UNIVERSITAT ROVIRA I VIRGILI
NOVEL MOLECULAR CATALYSTS FOR WATER OXIDATION: TOWARDS ARTIFICIAL PHOTOSYNTHESIS
Sara Goberna Ferrón
Dipòsit Legal: T.189-2014

In early 2010, a polyoxometallate (POM) complex, $[Co_4(H_2O)_2(PW_9O_{34})_2]^{10-}$ (Co_4) **1.47** (Figure 1.27) was reported by Hill et al. as the first carbon-free homogeneous WOC obtained from abundant metals.[127] It contains a rhomb-like tetranuclear cluster of CoO_6 octahedra sharing edges encapsulated by two trivacant Keggin-type $[PW_9O_{34}]^{9-}$ units. All bridges between Co atoms are oxo groups, and two terminal water molecules complete the coordination positions. Experiments were carried out using $[Ru(bpy)_3]^{3+}$ (1.26 V) as the chemical oxidant at pH=8, or in a photocatalytic setup where $[Ru(bpy)_3]^{3+}$ is generated in situ.[128] An efficiency of ~70 % and a TOF of > 5 s^{-1} were reported. After several studies, the chemical oxidation with $[Ru(bpy)_3]^{3+}$ as oxidant has been ruled out.[129] Related Co-containing POMs were also reported, but the only active one was the Co_4 compound **1.47**.

The activity of Co-based POMs as homogeneous WOCs has been put into question. It was first reported that it decomposes during electrocatalytic water oxidation to generate a CoO_x film that rapidly becomes the major catalyst.[129,130] This is a common problem for all homogeneous catalysts because oxidative decomposition of the organic ligands yields metal oxides.[116,131-134] In POMs the origin of the CoO_x species is not decomposition of the supporting ligand but the solution equilibria that liberate traces of free Co^{2+} ions as precursors for the oxide. Indeed, the use of chelating agents able to trap free Co^{2+} ions precludes the formation of any oxide. [127,135,136]

UNIVERSITAT ROVIRA I VIRGILI
NOVEL MOLECULAR CATALYSTS FOR WATER OXIDATION: TOWARDS ARTIFICIAL PHOTOSYNTHESIS
Sara Goberna Ferrón
Dipòsit Legal: T.189-2014

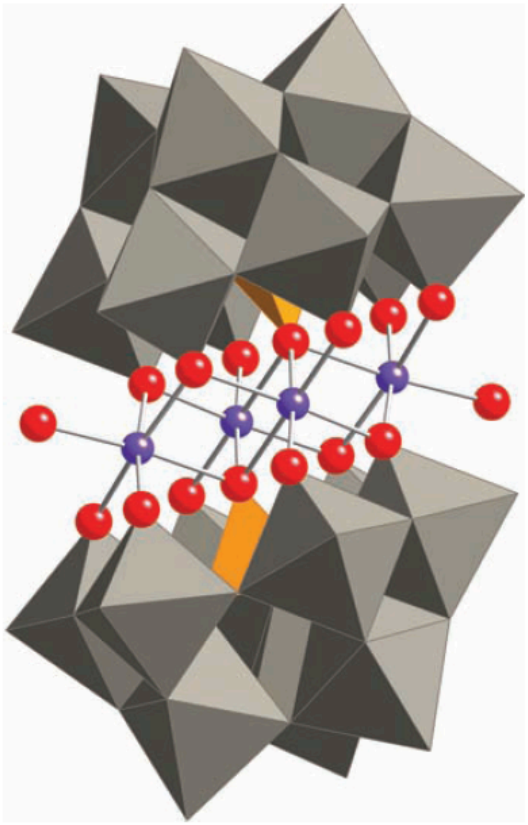

Figure 1.26. *Representation of the molecular structure of the polyanion* $[Co_4(H_2O)_2(PW_9O_{34})_2]^{10-}$, ***Co₄***. *$WO_6$ = gray octahedra; PO_4 = black octahedra; Co = pink; P = black; O = red.*[127]

Two research groups performed simultaneous, independent and complementary studies of a tetra-cobalt cubane complex, $[Co_4O_4(OAc)_4(py)_4]$ (OAc = acetate) **1.48** (Fig.1.27).[137-139] Although the complex had been previously described as an oxidation catalyst,[140] it had not been investigated as a water oxidation catalyst. A notable feature of **1.48** is that the four metals are in the Co(III) oxidation state, and a reversible one electron oxidation is observed in both MeCN and aqueous media, corresponding to oxidation to a $[3Co^{III}–Co^{IV}]$. In cyclic voltammograms, the reversible oxidation occurs prior to catalysis, suggesting another oxidation event is required to enable catalysis. Using a photocatalytic $[Ru(bpy)_3]^{2+}$ / $S_2O_8^{2-}$ system, **1.48** demonstrated TON with values over 40 after 60 minutes of illumination and TOF of ~0.02 s^{-1}.[138] The chemical yield of the process reach a 50% at pH=7, by comparing the

UNIVERSITAT ROVIRA I VIRGILI
NOVEL MOLECULAR CATALYSTS FOR WATER OXIDATION: TOWARDS ARTIFICIAL PHOTOSYNTHESIS
Sara Goberna Ferrón
Dipòsit Legal: T.189-2014

total mount of O_2 produced with the theoretical, maximum yield based on oxidant consumption.[139] Photochemical quantum yield of the process can reach the peak value of 0.30 at pH=8.[139]

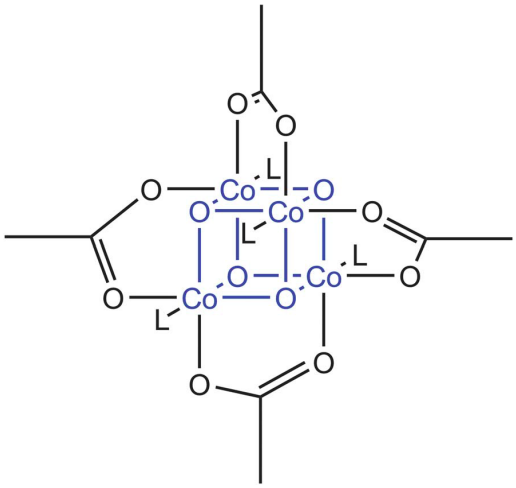

Figure 1.27. *Schematic representation of $[Co_4O_4(OAc)_4(py)_4]$. The cubane structure is highlighted in light blue. L stands for pyridine.*[139]

UNIVERSITAT ROVIRA I VIRGILI
NOVEL MOLECULAR CATALYSTS FOR WATER OXIDATION: TOWARDS ARTIFICIAL PHOTOSYNTHESIS
Sara Goberna Ferrón
Dipòsit Legal: T.189-2014

1.5.2 Solid–state Water Oxidation Catalysts

Heterogeneous catalysts have the advantage of higher stability and easier implementation in devices. An extensive range of solid-state materials is under evaluation for water oxidation catalysis, including transition metal dioxides, spinels and perovskites.[141-150] Metal oxides have long been known to catalyze water oxidation but often the most active were oxides of rare and precious metal ions, operating best in highly basic conditions. The past decade has seen major advantages in the development of highly active meta oxide catalyst based on earth–abundant elements operating under neutral or near–neutral pH conditions.[144,151-157] These metal oxides catalyze water oxidation in heterogeneous solution, driven by sacrificial oxidants and in either electrochemical[155-159] or photo-electrochemical cells. [151,160]

Ruthenium Oxide

Ruthenium oxide was reported to behave as a WOC by Grätzel el al. in 1979.[161] Colloidal RuO_2 nanoparticles catalyzed the oxidation of water in the presence of Ce^{IV} as oxidant, exceeding by two orders of magnitude the oxidation rate achieved with bulk RuO_2 powder. Colloidal RuO_2 was then implemented in a coupled redox system to catalyze water oxidation in a photo-induced system using $Ru(bpy)_3^{2+}$ as sensitizer and dimethylviologen as sacrificial oxidant.[162] A system that performed water oxidation and reduction simultaneously was constructed by deposition of RuO_2 and Pt(0) domains on photo-active TiO_2 nanoparticles.[163]

The hydration grade of RuO_2 showed an important effect in the catalytic performance, with the optimal value in the range in the 12–14% range.[164-167] An easiest method for RuO_2 nanoparticles photodeposition on titania surface has been recently reported.[167] The resulting material exhibits TON of 16 for oxygen production under dark conditions with Ce^{IV} as oxidant.

An oxygen-generating gel system induced by light has been developed using the electrostatic interactions of ionic functional groups and steric effects of a polymer

UNIVERSITAT ROVIRA I VIRGILI
NOVEL MOLECULAR CATALYSTS FOR WATER OXIDATION: TOWARDS ARTIFICIAL PHOTOSYNTHESIS
Sara Goberna Ferrón
Dipòsit Legal: T.189-2014

network. By using a graft polymer chain with photosensitizer units as sensitizers to closely arrange RuO_2 nanoparticles as catalyst, the functional groups transmit multiple electrons cooperatively to generate oxygen (Figure 1.28).[168]

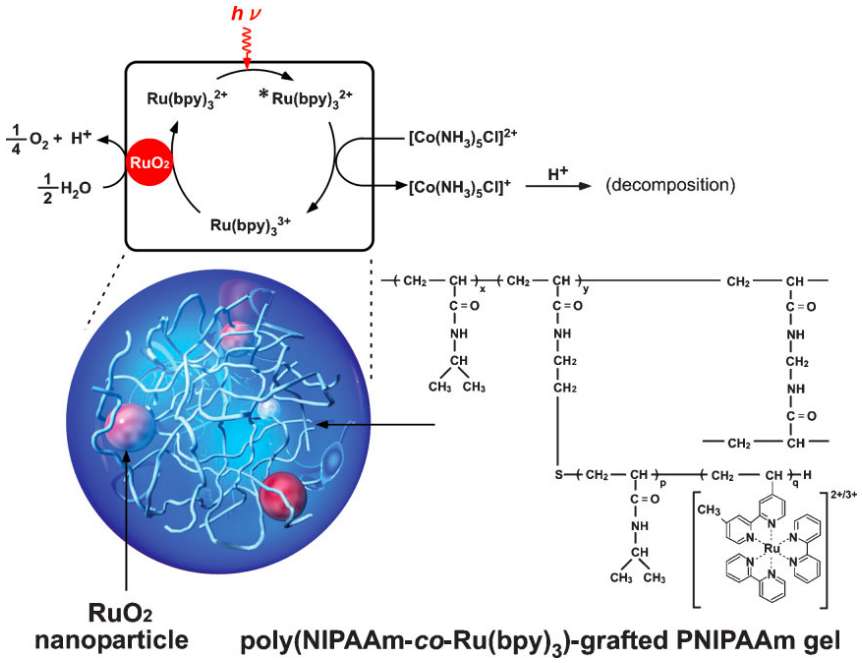

Figure 1.28. *Oxygen-generating system formed by entrapping nano-RuO_2 particles and a covalently grafted ruthenium sensitizer.*[169]

A different strategy involves oxygen evolution on a Nafion–RuO_2–$Ru(bpy)_3^{2+}$ composite electrode in acetate buffer at pH = 4.6 at 1.14 V vs. NHE.[169] The electrode was prepared by deposition of a Nafion solution containing colloidal RuO_2, and then dipped in a $Ru(bpy)_3^{2+}$ solution.

Iridium Oxide

Since more than 30 years ago,[170] iridium oxide, IrO_2, is one of the most efficient catalysts for water oxidation, it is stable and is works at low overpotentials.[164,165]

A citrate-stabilized IrO_2 colloid was self-assembled onto an indium tin oxide (ITO)

UNIVERSITAT ROVIRA I VIRGILI
NOVEL MOLECULAR CATALYSTS FOR WATER OXIDATION: TOWARDS ARTIFICIAL PHOTOSYNTHESIS
Sara Goberna Ferrón
Dipòsit Legal: T.189-2014

electrode by immersion of the electrode in the colloidal solution.[171] The self-assembly could be achieved by a chemical interaction between carboxylate groups on the citrate stabilizer and hydroxyl groups on the ITO surface to form ester bonds. Electrocatalytic water oxidation with these nano-structures electrodes (pH = 5.2) at 1.24 V vs. NHE yields TOF = 2.3-2.5 × 10^4 h^{-1} based on the surface concentration, Γ_0 (1.8-6.8 × 10^{-10} mol cm^{-2}), of IrO_2 on the electrode.

Interestingly, it has been reported the use of electro-generated nano-IrO_x on glassy carbon electrodes of diameter of 1.6-0.6 nm as electrocatalysts for water oxidation.[172,173] Controlled potential electrolysis using 2.0 nm-IrO_2 films catalyzes O_2 production at η = 0.15-0.25 V independently of pH with a current efficiency of 100 %.

Regarding light-induced water oxidation, it has been reported the use of citrate-stabilized IrO_2 colloids for water photo-oxidation in the presence of $Ru(bpy)_3^{2+}$ and persulfate in Na_2SiF_6-containing buffers.[174] At pH = 5 the turnover numbers reach values of 100. The use of polymeric ruthenium sensitizers yields TOF of 160 s^{-1} per surface iridium atom.[175,176] These systems were improved by employing dicarboxylic acid ligands to stabilize 2 nm-diameter IrO_2 particles.[177] By using sensitizer molecules that contain pendant succinate or malonate ligands for tethering to the IrO_2 nanoparticles, ET is promoted in a covalently assembled system. ET from Ir(IV) to Ru(III) occurs with a first-order rate constant of 8 × 10^2 s^{-1}, and oxygen is evolved.

These results have set the basis for the construction an overall water splitting system that uses visible light to convert water to hydrogen and oxygen assisted by a small applied voltage.[178] The photoanode integrates TiO_2 nanoparticles (anatase) with IrO_2 hydrated nanoparticles (2 nm). The authors designed a multi-functional ruthenium polypyridyl sensitizer with phosphonates substituents that are chemically selective for TiO_2 and with malonate groups, selective for $IrO_2 \cdot nH_2O$ (Figure 1.29). The quantum efficiency was limited by the slow electron transfer from the $IrO_2 \cdot nH_2O$

UNIVERSITAT ROVIRA I VIRGILI
NOVEL MOLECULAR CATALYSTS FOR WATER OXIDATION: TOWARDS ARTIFICIAL PHOTOSYNTHESIS
Sara Goberna Ferrón
Dipòsit Legal: T.189-2014

nanoparticles to the oxidized dye. The system has been improved by progress in the molecular components, in particular, the sensitizer nature[179,180] and the electrode material with respect to the semiconductor nature.[181]

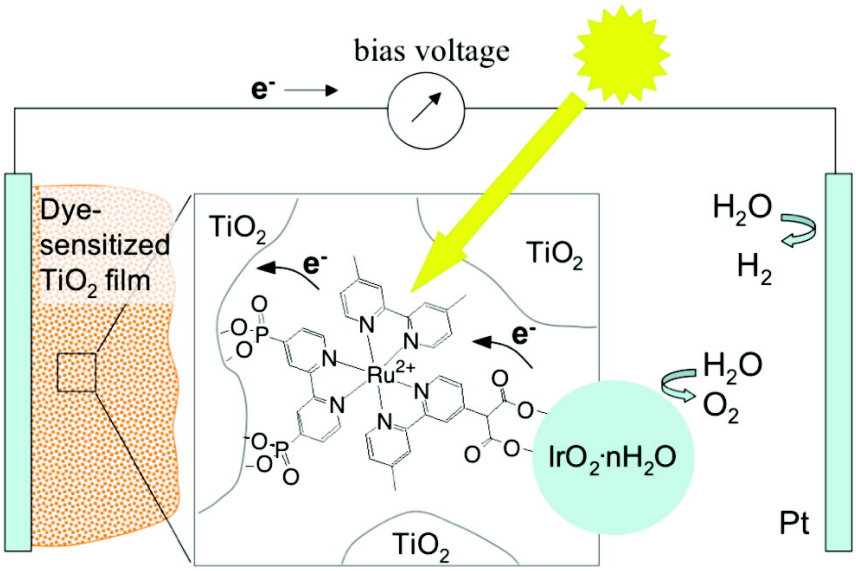

Figure 1.29. *Dye-sensitized photoelectrochemical cell containing a working electrode composed of a porous nanocrystalline TiO_2 film on F-SnO_2 and sensitized with the dye-$IrO_2 \cdot nH2O$ colloid.*[178]

While iridium oxide has almost all the requirements for a suitable WOC to be implemented in a solar conversion system, iridium is one of the rarest metals on earth, and therefore is not suitable for large-scale applications.

Manganese Oxide

With the aim to explore oxides of the much more abundant first-row transition metals and inspired by nature's Mn_4Ca cluster of photosystem II, many manganese oxides, MnO_x, has been investigated for water oxidation over a wide pH range,[182] although most commonly in alkaline medium.[144,183,184] This higher activity at basic pH is due the instability of Mn^{3+} (precursor for water oxidation) at pH > 9 due to the disproportionation reaction resulting in the formation of Mn^{2+} and Mn^{4+}, whereas in alkaline conditions it is effectively stabilized by the comproportionation of Mn^{2+}

UNIVERSITAT ROVIRA I VIRGILI
NOVEL MOLECULAR CATALYSTS FOR WATER OXIDATION: TOWARDS ARTIFICIAL PHOTOSYNTHESIS
Sara Goberna Ferrón
Dipòsit Legal: T.189-2014

and Mn^{4+}.[185]

Ohsaka et al. investigated electrocatalytic water oxidation at manganese oxide nanorods modified Au, Pt and GC electrodes in a wide range of pH values, showing a maximum activity in basic medium.[186] Very recently it has been reported the electrodeposition of MnO_x films with different phases and morphologies from protic ionic liquids.[187] In alkaline media the Mn_2O_3 and birnessite-like phases were the most active. Films of Sodium Birnessite-Type MnO_2 were electrodeposited on FTO electrodes. Direct photocatalytic activity (without sacrificial reagents) was reported in alkaline medium showing an onset for water oxidation at $\eta \approx 450$ mV but the quantum efficiency was very low (<0.1%).[188]

MacFarlane et al. published a MnO_x electrocatalyst that produces currents of the order of 1 mA cm^{-2} at 150 mV overpotential in butyl ammonium bisulfate electrolytes.[189] The major product is a solvated form of hydrogen peroxide, which was subsequently decomposed to oxygen and water.

Chemical water oxidation was also tested with manganese oxides. $CaMnO_x$ and Mn(IV) oxide colloid showed catalytic activity in the presence of sacrificial oxidants.[190,191]

Light-induced water oxidation system using $[Ru(bpy)_3]^{2+}$ as photosensitizer and $Na_2S_2O_8$ as an electron acceptor at pH ≈ 5 has been investigated. First, Dismukes et al. reported a nanoparticulate λ-MnO_2 precursor of a Mn_4O_4 water oxidation catalyst.[192].

Frei et al. synthetize high surface area mixed phases of MnO_x nanoparticles dispersed in a mesoporous silica scaffold that prevents deactivation of the nanoclusters.[193] Photodriven water oxidation is performed with a TOF of 3330 s^{-1} per catalyst cluster at $\eta \approx 350$ mV.

UNIVERSITAT ROVIRA I VIRGILI
NOVEL MOLECULAR CATALYSTS FOR WATER OXIDATION: TOWARDS ARTIFICIAL PHOTOSYNTHESIS
Sara Goberna Ferrón
Dipòsit Legal: T.189-2014

Cobalt Oxide

Since the early 80's cobalt oxides has been reported as water oxidation catalysts.[165,194-199] Photo-induced oxygen evolution was reported at nanostructured Co_3O_4 clusters in mesoporous silica in aqueous solution under mild temperature and pH (5.8) conditions using the $[Ru(bpy)_3]^{2+}$/persulfate system.[148] O_2 gas evolved with high turnover frequency of 3450 s^{-1} per Co_3O_4 nanocluster at an overpotential of 350 mV.

An important breakthrough in cobalt-based water oxidation was achieved by the discovery of highly–active cobalt phosphate (CoP_i) thin films in neutral conditions by Nocera (Figure 1.30).[156,158,200,201] Catalysis by CoO_x films has been reviewed recently.[202] These thin–films are easy to prepare, base in earth–abundant materials, and can generate O_2 under conditions of low overpotential, neutral pH, 1 atm of pressure, and room temperature. They are built from $(CoO_x)_n$ clusters stabilized by phosphate groups[203-205], and are active eletrochemically and photochemically.[206] Phosphate is a crucial component in the CoP_i catalyst because it aided in catalyst self–repair, thereby maintaining the stability of the catalyst system.[207] The self–repair is carried out by the dynamic equilibrium between $Co^{2+}HPO_4^{-2}$ in solution and $Co^{3+}HPO_4^{-2}$ on the electrode. Its current density was more than 1 mA cm^{-2} after 7–8 h when electrolysis was carried out at 1.29 V in a KP_i electrolyte (pH = 7, $[Co^{2+}]$ = 0.5 mM). This material has already been integrated into a solar cell device when combined with a silicon–based semiconductor yielding excellent results.[208,209] Although the mechanism of O–O bond formation remains to be determined, based on the studies of electrochemistry, a reaction pathway that uses a model of a molecular cobaltate cluster (Figure 1.31)[201], in which a turnover-limiting chemical step involving the evolution of O_2 is produced by a PCET equilibrium, has been proposed.[210]

UNIVERSITAT ROVIRA I VIRGILI
NOVEL MOLECULAR CATALYSTS FOR WATER OXIDATION: TOWARDS ARTIFICIAL PHOTOSYNTHESIS
Sara Goberna Ferrón
Dipòsit Legal: T.189-2014

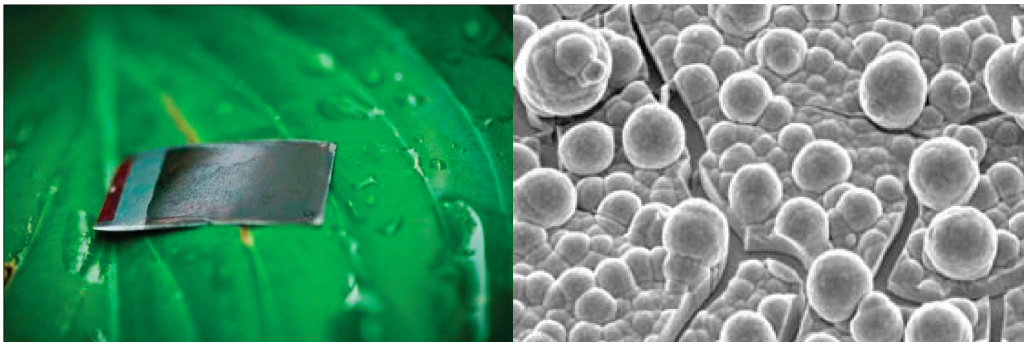

Figure 1.30. *Picture (left) and SEM image (right) of the electrodeposited CoP_i catalyst film.*[156,201]

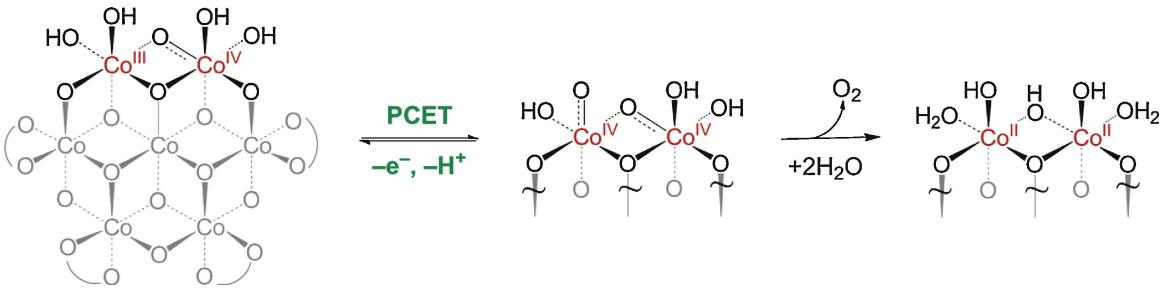

Figure 1.31. *Proposed pathway for OER by CoP_i. A PCET equilibrium proceeded by a turnoverlimiting O–O bond forming step is consistent with current dependencies on proton and electron equivalencies. Curved lines denote phosphate or OH_x terminal or bridging ligands.*[210]

Other Oxides

Among the first transition metal series, Ni, Ti, Cu and Fe oxides have been explored as water oxidation catalysts. Photodriven water oxidation has been investigated with NiO_x[211], TiO_2[212-215], Cu_2O[216] and Fe_2O_3.[217]

The activity Nickel hydroxide has been studied mainly electrochemically.[218-222] Remarkable studies were performed by Nocera et al. in a similar way than CoO_x for nickel-borate films.[155] This Ni-based catalyst that evolves O_2 at pH = 9.2 with an activity of 1 mA cm^{-2} at an overpotential of ~ 425 mV. Similar to that of Co-based films, the structure of the catalytically active material is a layered γ-NiOOH phase.[154,157,223]

UNIVERSITAT ROVIRA I VIRGILI
NOVEL MOLECULAR CATALYSTS FOR WATER OXIDATION: TOWARDS ARTIFICIAL PHOTOSYNTHESIS
Sara Goberna Ferrón
Dipòsit Legal: T.189-2014

UNIVERSITAT ROVIRA I VIRGILI
NOVEL MOLECULAR CATALYSTS FOR WATER OXIDATION: TOWARDS ARTIFICIAL PHOTOSYNTHESIS
Sara Goberna Ferrón
Dipòsit Legal: T.189-2014

1.6

Thesis Goals and Outline

As the aforementioned discussion points out, the primary technological requirements for a WOC are obvious: efficiency, stability and low-cost. The list of complexes claimed to be capable of catalytic water oxidation has now grown to >100 and much of the work reviewed in section 1.5 has been reported in the last 5 years. Still, there is no clear good enough candidate to be taken to the next step: implementation of artificial photosynthesis. The main goal of this thesis is to explore new WOCs from polyoxometalate, cyanide and metal-metal bonded chemistry in the search for novel and alternative candidates.

- The importance of Ruthenium complexes as WOCs has been discussed in section 1.5.1. **Chapter 2** involves the study of a new metal-metal bonded diruthenium complex based in inexpensive ligands, $[Ru_2(\mu\text{-}O_2CCH_3)_4]$. The capability to oxidize water electrochemically using this complex will be discussed in terms of kinetics, stability and performance.

- The motivation to acquire catalysts using more abundant first-row transition metals and taking into account the previous studies of WOCs from polyoxometalate chemistry, specially compound **Co_4** (**1.47)**, prompted the study of **Co_9 (1.48)**. **Chapter 3** will describe the study of **Co_9** for water oxidation catalysis. Chemical water oxidation is used for stability characterization, electrochemical water oxidation allow determining the performance as well as the issues associated with the true nature of the catalytically active species. Finally, photo–induced water oxidation experiments confirm the versatility of this new WOC.

UNIVERSITAT ROVIRA I VIRGILI
NOVEL MOLECULAR CATALYSTS FOR WATER OXIDATION: TOWARDS ARTIFICIAL PHOTOSYNTHESIS
Sara Goberna Ferrón
Dipòsit Legal: T.189-2014

- Finally, **Chapter 4** details the preparation and characterization of a Co-based cobalt Prussian blue type coordination polymer that possesses many of the key features deemed necessary for a robust and active WOC: it is formed from Earth-abundant metal ions in aqueous solution; it works at neutral pH and ambient conditions and it is robust in turnover conditions. Cobalt hexacyanoferrate (CoHCF) modied FTO electrodes are used for electrocatalyze the oxidation of water. The possibility of other Prussian blue-type complexes being active WOCs is investigated through heterogeneous light-induced water oxidation catalysis using the bulk compounds.

This thesis develops new attractive families of catalysts for water oxidation as well as strengthens the recent field of POM-based WOCs including a new compound to the list of POMs able to catalyze the oxidation of water.

UNIVERSITAT ROVIRA I VIRGILI
NOVEL MOLECULAR CATALYSTS FOR WATER OXIDATION: TOWARDS ARTIFICIAL PHOTOSYNTHESIS
Sara Goberna Ferrón
Dipòsit Legal: T.189-2014

1.7

References

1 *The EU in the world 2013 - A statistical portrait*. (Luxembourg: Publications Office of the European Union, 2012).

2 *Fundamentals of Materials for Energy and Environmental Sustainability*. (Cambridge University Press, 2012).

3 Lewis, N. & Nocera, D. Powering the planet: chemical challenges in solar energy utilization. *Proc. Natl. Acad. Sci. U S A* **103**, 15729-15735 (2006).

4 Cook, T., Dogutan, D., Reece, S., Surendranath, Y., Teets, T. & Nocera, D. Solar energy supply and storage for the legacy and nonlegacy worlds. *Chem. Rev.* **110**, 6474-6502 (2010).

5 Walter, M. G., Warren, E. L., McKone, J. R., Boettcher, S. W., Mi, Q. X., Santori, E. A. & Lewis, N. S. Solar Water Splitting Cells. *Chem. Rev.* **111**, 5815-5815 (2011).

6 *World Energy Assessment Report: Energy and the Challenge of Sustainability*. (United Nations Development Programme, 2003).

7 Schellnhuber, H. Global warming: stop worrying, start panicking? *Proc. Natl. Acad. Sci. U S A* **105**, 14239-14240 (2008).

8 Hoffert, M., I., Caldeira, K., Jain, A., K., Haites, E., F., Harvey, L. D., Potter, S., D., Schlesinger, M., E., Schneider, S., H., Watts, R., G., Wigley, T., M. L. & Wuebbles, D., J. Energy implications of future stabilization of atmospheric CO2 content. *Nature* **395**, 881-884 (1998).

9 Goeppert, A., Czaun, M., May, R., Prakash, G., Olah, G. & Narayanan, S. Carbon dioxide capture from the air using a polyamine based regenerable solid adsorbent. *J. Am. Chem. Soc.* **133**, 20164-20167 (2011).

10 McEvoy, J. & Brudvig, G. Water-splitting chemistry of photosystem II. *Chem. Rev.* **106**, 4455-4483 (2006).

11 Lewis, N. Toward cost-effective solar energy use. *Science* **315**, 798-801 (2007).

12 Blankenship, R. & Hartman, H. The origin and evolution of oxygenic photosynthesis. *Trends Biochem. Sci* **23**, 94-97 (1998).

13 Duysens, L. N., Amesz, J. & Kamp, B. M. Two Photochemical Systems in Photosynthesis. *Nature* **190**, 510-511 (1961).

14 *Artificial Photosynthesis-From Basic Biology to Industrial Application*. (WILEY-VCH Verlag GmbH & Co. KGaA, Weinheim, 2005).

15 Ferreira, K. N., Iverson, T., Maghlaoui, K., Barber, J. & Iwata, S. Architecture of the Photosynthetic Oxygen-Evolving Center. *Science* **303**, 1831-1838 (2004).

UNIVERSITAT ROVIRA I VIRGILI
NOVEL MOLECULAR CATALYSTS FOR WATER OXIDATION: TOWARDS ARTIFICIAL PHOTOSYNTHESIS
Sara Goberna Ferrón
Dipòsit Legal: T.189-2014

16 Szabó, I., Bergantino, E. & Giacometti, G. Light and oxygenic photosynthesis: energy dissipation as a protection mechanism against photo-oxidation. *EMBO reports* **6**, 629-634 (2005).

17 Umena, Y., Kawakami, K., Shen, J. R. & Kamiya, N. Crystal structure of oxygen-evolving photosystem II at a resolution of 1.9 angstrom. *Nature* **473**, 55-60 (2011).

18 Jordan, P., Fromme, P., Witt, H., Klukas, O., Saenger, W. & Krauss, N. Three-dimensional structure of cyanobacterial photosystem I at 2.5 A resolution. *Nature* **411**, 909-917 (2001).

19 Rappaport, F., Guergova-Kuras, M., Nixon, P., Diner, B. & Lavergne, J. r. m. Kinetics and pathways of charge recombination in photosystem II. *Biochemistry* **41**, 8518-8527 (2002).

20 Haumann, M., Liebisch, P., Muller, C., Barra, M., Grabolle, M. & Dau, H. Photosynthetic O2 Formation Tracked by Time-Resolved X-ray Experiments. *Science* **310**, 1019-1021 (2005).

21 Dau, H. & Zaharieva, I. Principles, efficiency, and blueprint character of solar-energy conversion in photosynthetic water oxidation. *Acc. Chem. Res.* **42**, 1861-1870 (2009).

22 Baranov, S., Ananyev, G., Klimov, V. & Dismukes, G. Bicarbonate accelerates assembly of the inorganic core of the water-oxidizing complex in manganese-depleted photosystem II: a proposed biogeochemical role for atmospheric carbon dioxide in oxygenic photosynthesis. *Biochemistry* **39**, 6060-6065 (2000).

23 Venturi, M., Balzani, V. & Gandolfi, M. T. Fuels from solar energy. A dream of Giacomo Ciamician, the father of photochemistry. *Proceedings of the 2005 Solar World Congress* (2005).

24 Ciamician, G. The photochemistry of the future. *Science* **36**, 385-394 (1912).

25 Calvin, M. Artificial photosynthesis. *J. Membrane Sci.* **33**, 137-149 (1987).

26 Blankenship, R. E. *Molecular Mechanisms of Photosynthesis*. (Oxford, Blackwell Science, 2002).

27 Bockris, J. O. M. *Energy – The Solar Hydrogen Alternative*. (Wiley & Sons, 1977).

28 Dau, H., Limberg, C., Reier, T., Risch, M., Roggan, S. & Strasser, P. The Mechanism of Water Oxidation: From Electrolysis via Homogeneous to Biological Catalysis. *ChemCatChem* **2**, 724-761 (2010).

29 Gersten, S. W., Samuels, G. J. & Meyer, T. J. Catalytic Oxidation of Water by an Oxo-bridged Ruthenium Dimer. *J. Am. Chem. Soc.* **104**, 4029-4030 (1982).

30 Gilbert, J., A., Eggleston, D., S., Murphy, W., R., Geselowitz, D., A., Gersten, S., W., Hodgson, D., J. & Meyer, T., J. Structure and redox properties of the water-oxidation catalyst [(bpy)2(OH2)RuORu(OH2)(bpy)2]4+. *J. Am. Chem. Soc.* **107**, 3855-3864 (1985).

UNIVERSITAT ROVIRA I VIRGILI
NOVEL MOLECULAR CATALYSTS FOR WATER OXIDATION: TOWARDS ARTIFICIAL PHOTOSYNTHESIS
Sara Goberna Ferrón
Dipòsit Legal: T.189-2014

31 Ramaraj, R., Kira, A. & Kaneko, M. Electrochemistry and stability studies of oxo-bridged dinuclear ruthenium(III) complexes for water oxidation. *J. Chem. Soc., Faraday Trans. 1* **82**, 3515-3524 (1986).

32 Rotzinger, F., P-, Munavalli, S., Comte, P., Hurst, J., K., Graetzel, M., Pern, F. J. & Frank, A., J. A molecular water-oxidation catalyst derived from ruthenium diaqua bis(2,2'-bipyridyl-5,5'-dicarboxylic acid). *J. Am. Chem. Soc.* **109**, 6619-6626 (1987).

33 Nazeeruddin, M., K., Rotzinger, F., P., Comte, P. & Grätzel, M. Spontaneous oxidation of water to oxygen by the mixed-valence μ-oxo ruthenium dimer L2(H2O)RuIII‐O‐RuIV(OH)L2(L = 2,2′ -bipyridyl-5,5′ -dicarboxylic acid) *J. Chem. Soc., Chem. Commun.*, 872-874 (1988).

34 Comte, P., Nazeeruddin, M., K., Rotzinger, F., P., Frank, A., J. & Grätzel, M. Artificial analogues of the oxygen-evolving complex in photosynthesis: the oxo-bridged ruthenium dimer L2(H2O)RuIII-O-RuIII(H2O)L2, L = 2,2'-bipyridyl-4,4'-dicarboxylate. *J. Mol. Catal.* **52**, 63-84 (1989).

35 Petach, H. H. Characterization and Catalytic Activity of Covalently Linked Bipyridyl Ruthenium OXO Dimers. *J. Electrochem. Soc.* **139**, 2217-2221 (1992).

36 Yip-Kai, L. & Kwok-Yin, W. Electrochemistry of oxo-bridged ruthenium dimers with 4,4′ -dichloro- and 5,5′ -dichloro-2,2′ -bipyridine and their catalytic properties towards water oxidation. *J. Electroanal. Chem.* **380**, 193-200 (1995).

37 Chronister, C., W., Binstead, R., A., Ni, J. & Meyer, T., J. Mechanism of Water Oxidation Catalyzed by the μ-Oxo Dimer [(bpy)2(OH2)RuIIIORuIII(OH2)(bpy)2]4+. *Inorg. Chem.* **36**, 3814-3815 (1997).

38 Binstead, R., A., Chronister, C., W., Ni, J., Hartshorn, C., M. & Meyer, T., J. Mechanism of Water Oxidation by the μ-Oxo Dimer [(bpy) 2 (H 2 O)Ru III ORu III (OH 2)(bpy) 2] 4+. *J. Am. Chem. Soc.* **122**, 8464-8473 (2000).

39 Deng, Z. P., Tseng, H. W., Zong, R. F., Wang, D. & Thummel, R. Preparation and study of a family of dinuclear Ru(II) complexes that catalyze the decomposition of water. *Inorg. Chem.* **47**, 1835-1848 (2008).

40 Huynh, M. & Meyer, T. Proton-coupled electron transfer. *Chem. Rev.* **107**, 5004-5064 (2007).

41 Liu, F., Concepcion, J. J., Jurss, J. W., Cardolaccia, T., Templeton, J. L. & Meyer, T. J. Mechanisms of water oxidation from the blue dimer to photosystem II. *Inorg. Chem.* **47**, 1727-1752 (2008).

42 Yamada, H., Siems, W., Koike, T. & Hurst, J. Mechanisms of water oxidation catalyzed by the cis,cis-[(bpy)2Ru(OH2)]2O4+ ion. *J. Am. Chem. Soc.* **126**, 9786-9795 (2004).

43 Concepcion, J. J., Jurss, J. W., Templeton, J. L. & Meyer, T. J. One Site is Enough. Catalytic Water Oxidation by Ru(tpy)(bpm)(OH(2)) (2+) and Ru(tpy)(bpz)(OH(2)) (2+). *J. Am. Chem. Soc.* **130**, 16462-16463 (2008).

UNIVERSITAT ROVIRA I VIRGILI
NOVEL MOLECULAR CATALYSTS FOR WATER OXIDATION: TOWARDS ARTIFICIAL PHOTOSYNTHESIS
Sara Goberna Ferrón
Dipòsit Legal: T.189-2014

44 Yang, X. & Baik, M.-H. cis,cis-[(bpy)2RuVO]2O4+ catalyzes water oxidation formally via in situ generation of radicaloid RuIV-O*. *J. Am. Chem. Soc.* **128**, 7476-7485 (2006).

45 Batista, E. & Martin, R. Electron localization in the ground state of the ruthenium blue dimer. *J. Am. Chem. Soc.* **129**, 7224-7225 (2007).

46 Cape, J. & Hurst, J. Detection and mechanistic relevance of transient ligand radicals formed during [Ru(bpy)2(OH2)]2O4+-catalyzed water oxidation. *J. Am. Chem. Soc.* **130**, 827-829 (2008).

47 Limburg, B., Bouwman, E. & Bonnet, S. Molecular water oxidation catalysts based on transition metals and their decomposition pathways. *Coord. Chem. Rev.* **256**, 1451-1467 (2012).

48 Concepcion, J., Jurss, J., Templeton, J. & Meyer, T. Mediator-assisted water oxidation by the ruthenium "blue dimer" cis,cis-[(bpy)2(H2O)RuORu(OH2)(bpy)2]4+. *Proc. Natl. Acad. Sci. U S A* **105**, 17632-17635 (2008).

49 Jurss, J., Concepcion, J., Norris, M., Templeton, J. & Meyer, T. Surface catalysis of water oxidation by the blue ruthenium dimer. *Inorg. Chem.* **49**, 3980-3982 (2010).

50 Sens, C., Romero, I., Rodriguez, M., Llobet, A., Parella, T. & Benet-Buchholz, J. A new Ru complex capable of catalytically oxidizing water to molecular dioxygen. *J. Am. Chem. Soc.* **126**, 7798-7799 (2004).

51 Romain, S., Bozoglian, F., Sala, X. & Llobet, A. Oxygen-Oxygen Bond Formation by the Ru-Hbpp Water Oxidation Catalyst Occurs Solely via an Intramolecular Reaction Pathway. *J. Am. Chem. Soc* **131**, 2768-2769 (2009).

52 Bozoglian, F., Romain, S., Ertem, M. Z., Todorova, T. K., Sens, C., Mola, J., Rodriguez, M., Romero, I., Benet-Buchholz, J., Fontrodona, X., Cramer, C. J., Gagliardi, L. & Llobet, A. The Ru-Hbpp Water Oxidation Catalyst. *J. Am. Chem. Soc.* **131**, 15176-15187 (2009).

53 Yang, X. & Baik, M.-H. The mechanism of water oxidation catalysis promoted by [tpyRu(IV)=O]2L3+: a computational study. *J. Am. Chem. Soc.* **130**, 16231-16240 (2008).

54 Zong, R. & Thummel, R. A new family of Ru complexes for water oxidation. *J. Am. Chem. Soc.* **127**, 12802-12803 (2005).

55 Wada, T., Tsuge, K. & Tanaka, K. Electrochemical Oxidation of Water to Dioxygen Catalyzed by the Oxidized Form of the Bis(ruthenium - hydroxo) Complex in H2O. *Angew. Chem.* **39**, 1479-1482 (2000).

56 Wada, T., Tsuge, K. & Tanaka, K. Syntheses and redox properties of bis(hydroxoruthenium) complexes with quinone and bipyridine ligands. Water-oxidation catalysis. *Inorg. Chem.* **40**, 329-337 (2001).

57 Muckerman, J., Polyansky, D., Wada, T., Tanaka, K. & Fujita, E. Water oxidation by a ruthenium complex with noninnocent quinone ligands:

UNIVERSITAT ROVIRA I VIRGILI
NOVEL MOLECULAR CATALYSTS FOR WATER OXIDATION: TOWARDS ARTIFICIAL PHOTOSYNTHESIS
Sara Goberna Ferrón
Dipòsit Legal: T.189-2014

Possible formation of an O-O bond at a low oxidation state of the metal. *Inorg. Chem.* **47**, 1787-1802 (2008).

58 Xu, Y., Akermark, T. r., Gyollai, V., Zou, D., Eriksson, L., Duan, L., Zhang, R., Akermark, B. r. & Sun, L. A new dinuclear ruthenium complex as an efficient water oxidation catalyst. *Inorg. Chem.* **48**, 2717-2719 (2009).

59 Xu, Y., Fischer, A., Duan, L., Tong, L., Gabrielsson, E., Akermark, B. & Sun, L. Chemical and light-driven oxidation of water catalyzed by an efficient dinuclear ruthenium complex. *Angew. Chem.* **49**, 8934-8937 (2010).

60 Xu, Y., Duan, L., Tong, L., Akermark, B. r. & Sun, L. Visible light-driven water oxidation catalyzed by a highly efficient dinuclear ruthenium complex. *Chem. Commun.* **46**, 6506-6508 (2010).

61 Liu, X. & Wang, F. Transition metal complexes that catalyze oxygen formation from water: 1979¬2010. *Coord. Chem. Rev.* **256**, 1115-1136 (2012).

62 Tseng, H.-W., Zong, R., Muckerman, J. & Thummel, R. Mononuclear ruthenium(II) complexes that catalyze water oxidation. *Inorg. Chem.* **47**, 11763-11773 (2008).

63 Yamazaki, H., Hakamata, T., Komi, M. & Yagi, M. Stoichiometric photoisomerization of mononuclear ruthenium(II) monoaquo complexes controlling redox properties and water oxidation catalysis. *J. Am. Chem. Soc.* **133**, 8846-8849 (2011).

64 Sala, X., Ertem, M. Z., Vigara, L., Todorova, T. K., Chen, W. Z., Rocha, R. C., Aquilante, F., Cramer, C. J., Gagliardi, L. & Llobet, A. The cis-Ru(II)(bpy)(2)(H(2)O)(2) (2+) Water-Oxidation Catalyst Revisited. *Angew. Chem.* **49**, 7745-7747 (2010).

65 John, C. D. & Thomas, J. M. Redox properties and ligand loss chemistry in aqua/hydroxo/oxo complexes derived from cis- and trans-[(bpy)2RuII(OH2)2]2+. *Inorg. Chem.* **27**, 3283-3291 (1988).

66 Boyer, J., Polyansky, D., Szalda, D., Zong, R., Thummel, R. & Fujita, E. Effects of a proximal base on water oxidation and proton reduction catalyzed by geometric isomers of [Ru(tpy)(pynap)(OH2)]2+. *Angew. Chem.* **50**, 12600-12604 (2011).

67 Roeser, S., Farrás, P., Bozoglian, F., Martínez-Belmonte, M., Benet-Buchholz, J. & Llobet, A. Chemical, electrochemical, and photochemical catalytic oxidation of water to dioxygen with mononuclear ruthenium complexes. *ChemSusChem* **4**, 197-207 (2011).

68 Wasylenko, D., Ganesamoorthy, C., Henderson, M., Koivisto, B., Osthoff, H. & Berlinguette, C. Electronic modification of the [Ru(II)(tpy)(bpy)(OH(2))](2+) scaffold: effects on catalytic water oxidation. *J. Am. Chem. Soc.* **132**, 16094-16106 (2010).

69 Sens, C., Rodríguez, M., Romero, I., Llobet, A., Parella, T. & Benet-Buchholz, J. Synthesis, structure, and acid-base and redox properties of a family of new

UNIVERSITAT ROVIRA I VIRGILI
NOVEL MOLECULAR CATALYSTS FOR WATER OXIDATION: TOWARDS ARTIFICIAL PHOTOSYNTHESIS
Sara Goberna Ferrón
Dipòsit Legal: T.189-2014

Ru(II) isomeric complexes containing the trpy and the dinucleating Hbpp ligands. *Inorg. Chem.* **42**, 8385-8394 (2003).

70 Mola, J., Dinoi, C., Sala, X., Rodriguez, M., Romero, I., Parella, T., Fontrodona, X. & Llobet, A. A new dinuclear Ru-Hbpp based water oxidation catalyst with a trans-disposition of the Ru-OH. *Dalton Trans.* **40**, 3640-3646 (2011).

71 Concepcion, J., Tsai, M.-K., Muckerman, J. & Meyer, T. Mechanism of water oxidation by single-site ruthenium complex catalysts. *J. Am. Chem. Soc.* **132**, 1545-1557 (2010).

72 Concepcion, J., Jurss, J., Norris, M., Chen, Z., Templeton, J. & Meyer, T. Catalytic water oxidation by single-site ruthenium catalysts. *Inorg. Chem.* **49**, 1277-1279 (2010).

73 Chen, Z., Concepcion, J., Jurss, J. & Meyer, T. Single-site, catalytic water oxidation on oxide surfaces. *J. Am. Chem. Soc.* **131**, 15580-15581 (2009).

74 Duan, L., Fischer, A., Xu, Y. & Sun, L. Isolated seven-coordinate Ru(IV) dimer complex with [HOHOH](-) bridging ligand as an intermediate for catalytic water oxidation. *J. Am. Chem. Soc.* **131**, 10397-10399 (2009).

75 Li, L., Duan, L., Xu, Y., Gorlov, M., Hagfeldt, A. & Sun, L. A photoelectrochemical device for visible light driven water splitting by a molecular ruthenium catalyst assembled on dye-sensitized nanostructured TiO2. *Chem. Commun.* **46**, 7307-7309 (2010).

76 Li, F., Zhang, B., Li, X., Jiang, Y., Chen, L., Li, Y. & Sun, L. Highly efficient oxidation of water by a molecular catalyst immobilized on carbon nanotubes. *Angew. Chem.* **50**, 12276-12279 (2011).

77 Duan, L., Bozoglian, F., Mandal, S., Stewart, B., Privalov, T., Llobet, A. & Sun, L. A molecular ruthenium catalyst with water-oxidation activity comparable to that of photosystem II. *Nature Chemistry* **4**, 418-423 (2012).

78 Ruttinger, W. & Dismukes, G. C. Synthetic Water-Oxidation Catalysts for Artificial Photosynthetic Water Oxidation. *Chem. Rev.* **97**, 1-24 (1997).

79 Cao, R., Ma, H., Geletii, Y. V., Hardcastle, K. I. & Hill, C. L. Structurally Characterized Iridium(III)-Containing Polytungstate and Catalytic Water Oxidation Activity. *Inorg. Chem.* **48**, 5596-5598 (2009).

80 Sartorel, A., Carraro, M., Scorrano, G., De Zorzi, R., Geremia, S., McDaniel, N., Bernhard, S. & Bonchio, M. Polyoxometalate embedding of a tetraruthenium(IV)-oxo-core by template-directed metalation of [gamma-SiW10O36]8-: a totally inorganic oxygen-evolving catalyst. *J. Am. Chem. Soc.* **130**, 5006-5007 (2008).

81 Geletii, Y., Botar, B., Koegerler, P., Hillesheim, D., Musaev, D. & Hill, C. An all-inorganic, stable, and highly active tetraruthenium homogeneous catalyst for water oxidation. *Angew. Chem.* **47**, 3896-3899 (2008).

82 Sartorel, A., Miro, P., Salvadori, E., Romain, S., Carraro, M., Scorrano, G., Di Valentin, M., Llobet, A., Bo, C. & Bonchio, M. Water Oxidation at a Tetraruthenate Core Stabilized by Polyoxometalate Ligands: Experimental and

UNIVERSITAT ROVIRA I VIRGILI
NOVEL MOLECULAR CATALYSTS FOR WATER OXIDATION: TOWARDS ARTIFICIAL PHOTOSYNTHESIS
Sara Goberna Ferrón
Dipòsit Legal: T.189-2014

Computational Evidence To Trace the Competent Intermediates. *J. Am. Chem. Soc.* **131**, 16051-16052 (2009).

83 Piccinin, S. & Fabris, S. A first principles study of water oxidation catalyzed by a tetraruthenium-oxo core embedded in polyoxometalate ligands. *Physical chemistry chemical physics : PCCP* **13**, 7666-7674 (2011).

84 Geletii, Y., Besson, C., Hou, Y., Yin, Q., Musaev, D., Quiñonero, D., Cao, R., Hardcastle, K., Proust, A., K √ ∂ gerler, P. & Hill, C. Structural, physicochemical, and reactivity properties of an all-inorganic, highly active tetraruthenium homogeneous catalyst for water oxidation. *J. Am. Chem. Soc.* **131**, 17360-17370 (2009).

85 Suss-Fink, G. Water oxidation: a robust all-inorganic catalyst. *Angew. Chem.* **47**, 5888-5890 (2008).

86 Ghosh, u., K-, Brunschwig, B., S., Chou, M., H., Creutz, C. & Sutin, N. Thermal and light-induced reduction of the ruthenium complex cation Ru(bpy)33+ in aqueous solution. *J. Am. Chem. Soc.* **106**, 4772-4783 (1984).

87 Mukhopadhyay, S., Mandal, S., Bhaduri, S. & Armstrong, W. Manganese clusters with relevance to photosystem II. *Chem. Rev.* **104**, 3981-4026 (2004).

88 Wiechen, M., Berends, H.-M. & Kurz, P. Water oxidation catalysed by manganese compounds: from complexes to "biomimetic rocks". *Dalton Trans.* **41**, 21-31 (2012).

89 Limburg, J., Vrettos, J. S., Liable-Sands, L. M., Rheingold, A. L., Crabtree, R. H. & Brudvig, G. W. A functional model for O-O bond formation by the O-2-evolving complex in photosystem II. *Science* **283**, 1524-1527 (1999).

90 Limburg, J., Vrettos, J. S., Chen, H. Y., de Paula, J. C., Crabtree, R. H. & Brudvig, G. W. Characterization of the O-2-evolving reaction catalyzed by (terpy)(H2O)Mn-III(O)(2)Mn-IV(OH2)(terpy) (NO3) (terpy=2,2 ': 6,2 ''-terpyridine). *J. Am. Chem. Soc.* **123**, 423-430 (2001).

91 Wolpher, H., Huang, P., Borgström, M., Bergquist, J., Styring, S., Sun, L. & Akermark, B. Synthesis of a Ru(bpy)3-type complex linked to a free terpyridine ligand and its use for preparation of polynuclear bimetallic complexes. *Catal. Today* **98**, 529-536 (2004).

92 Baffert, C., Romain, S., Richardot, A. l., Lepretre, J.-C., Lefebvre, B., Deronzier, A. & Collomb, M.-N. l. Electrochemical and chemical formation of [Mn4(IV)O5(terpy)4(H2O)2]6+, in relation with the photosystem II oxygen-evolving center model [Mn2(III,IV)O2(terpy)2(H2O)2]3+. *J. Am. Chem. Soc.* **127**, 13694-13704 (2005).

93 Yagi, M. & Narita, K. Catalytic O2 evolution from water induced by adsorption of [OH2)(terpy)Mn(mu-O)2Mn(terpy)(OH2)]3+ complex onto clay compounds. *J. Am. Chem. Soc.* **126**, 8084-8085 (2004).

94 Tagore, R., Crabtree, R. & Brudvig, G. Oxygen evolution catalysis by a dimanganese complex and its relation to photosynthetic water oxidation. *Inorg. Chem.* **47**, 1815-1823 (2008).

UNIVERSITAT ROVIRA I VIRGILI
NOVEL MOLECULAR CATALYSTS FOR WATER OXIDATION: TOWARDS ARTIFICIAL PHOTOSYNTHESIS
Sara Goberna Ferrón
Dipòsit Legal: T.189-2014

95 Cady, C., Shinopoulos, K., Crabtree, R. & Brudvig, G. [(H2O)(terpy)Mn(mu-O)2Mn(terpy)(OH2)](NO3)3 (terpy = 2,2':6,2''-terpyridine) and its relevance to the oxygen-evolving complex of photosystem II examined through pH dependent cyclic voltammetry. *Dalton Trans.* **39**, 3985-3989 (2010).

96 Vrettos, J., Limburg, J. & Brudvig, G. Mechanism of photosynthetic water oxidation: combining biophysical studies of photosystem II with inorganic model chemistry. *Biochim. Biophys. Acta* **1503**, 229-245 (2001).

97 Yoshinori, N., Masa-aki, S. & Takao, S. Oxygen Evolution by Oxidation of Water with Manganese Porphyrin Dimers. *Angew. Chem.* **33**, 1839-1841 (1994).

98 Poulsen, A., Rompel, A. & McKenzie, C. Water oxidation catalyzed by a dinuclear Mn complex: a functional model for the oxygen-evolving center of photosystem II. *Angew. Chem.* **44**, 6916-6920 (2005).

99 Beckmann, K., Uchtenhagen, H., Berggren, G., Anderlund, M., F., Thapper, A., Messinger, J., Styring, S. & Kurz, P. Formation of stoichiometrically 18O-labelled oxygen from the oxidation of 18O-enriched water mediated by a dinuclear manganese complex - a mass spectrometry and EPR study. *Energy Environ. Sci.* **1**, 668-676 (2008).

100 Karlsson, E., Lee, B. L., Akermark, T., Johnston, E., Kärkäs, M. D., Sun, J., Hansson, O., Bäckvall, J. E. & Akermark, B. Photosensitized water oxidation by use of a bioinspired manganese catalyst. *Angew. Chem.* **50**, 11715-11718 (2011).

101 Limburg, J., Brudvig, G. W. & Crabtree, R. H. O2 evolution and permanganate formation from high-valent manganese complexes. *J. Am. Chem. Soc.* **119**, 2761-2762 (1997).

102 Shimazaki, Y., Nagano, T., Takesue, H., Ye, B.-H., Tani, F. & Naruta, Y. Characterization of a dinuclear MnV=O complex and is efficient evolution of O2 in the presence of water. *Angew. Chem.* **43**, 98-100 (2004).

103 Gao, Y., Akermark, T. r., Liu, J., Sun, L. & Akermark, B. r. Nucleophilic attack of hydroxide on a Mn(V) oxo complex: a model of the O-O bond formation in the oxygen evolving complex of photosystem II. *J. Am. Chem. Soc.* **131**, 8726-8727 (2009).

104 Privalov, T., Sun, L., Akermark, B. r., Liu, J., Gao, Y. & Wang, M. A computational study of O-O bond formation catalyzed by mono- and bis-MnIV-corrole complexes. *Inorg. Chem.* **46**, 7075-7086 (2007).

105 Rosenthal, J. & Nocera, D. Role of proton-coupled electron transfer in O-O bond activation. *Acc. Chem. Res.* **40**, 543-553 (2007).

106 Rosenthal, J. & Nocera, D. G. Oxygen activation chemistry of pacman and hangman porphyrin architectures based on xanthene and dibenzofuran spacers. *Progress in Inorganic Chemistry, Volume 55*, 483-544 (2007).

1. 7. References

107 Gao, Y., Liu, J., Wang, M., Na, Y., Akermark, B. & Sun, L. Synthesis and characterization of manganese and copper corrole xanthene complexes as catalysts for water oxidation. *Tetrahedron* **63**, 1987-1994 (2007).

108 Brimblecombe, R., Swiegers, G., Dismukes, G. & Spiccia, L. Sustained water oxidation photocatalysis by a bioinspired manganese cluster. *Angew. Chem.* **47**, 7335-7338 (2008).

109 Ulloa, O. A. Modeling the Oxygen Evolving Complex of Photosystem II. (UIUC, 2011).

110 McDaniel, N., Coughlin, F., Tinker, L. & Bernhard, S. Cyclometalated iridium(III) Aquo complexes: efficient and tunable catalysts for the homogeneous oxidation of water. *J. Am. Chem. Soc.* **130**, 210-217 (2008).

111 Blakemore, J. D., Schley, N. D., Balcells, D., Hull, J. F., Olack, G. W., Incarvito, C. D., Eisenstein, O., Brudvig, G. W. & Crabtree, R. H. Half-Sandwich Iridium Complexes for Homogeneous Water-Oxidation Catalysis. *J. Am. Chem. Soc.* **132**, 16017-16029 (2010).

112 Wang, C., Wang, J.-L. & Lin, W. Elucidating molecular iridium water oxidation catalysts using metal-organic frameworks: a comprehensive structural, catalytic, spectroscopic, and kinetic study. *J. Am. Chem. Soc.* **134**, 19895-19908 (2012).

113 Savini, A., Bellachioma, G., Ciancaleoni, G., Zuccaccia, C., Zuccaccia, D. & Macchioni, A. Iridium(III) molecular catalysts for water oxidation: the simpler the faster. *Chem. Commun.* **46**, 9218-9219 (2010).

114 Savini, A., Belanzoni, P., Bellachioma, G., Zuccaccia, C., Zuccaccia, D. & MacChioni, A. Activity and degradation pathways of pentamethyl-cyclopentadienyl-iridium catalysts for water oxidation. *Green Chem.* **13**, 3360-3374 (2011).

115 Grotjahn, D. B., Brown, D. B., Martin, J. K., Marelius, D. C., Abadjian, M.-C., Tran, H. N., Kalyuzhny, G., Vecchio, K. S., Specht, Z. G., Cortes-Llamas, S. A., Miranda-Soto, V., van Niekerk, C., Moore, C. E. & Rheingold, A. L. Evolution of Iridium-Based Molecular Catalysts during Water Oxidation with Ceric Ammonium Nitrate. *J. Am. Chem. Soc* **133**, 19026-19027 (2011).

116 Schley, N. D., Blakemore, J. D., Subbaiyan, N. K., Incarvito, C. D., D'Souza, F., Crabtree, R. H. & Brudvig, G. W. Distinguishing Homogeneous from Heterogeneous Catalysis in Electrode-Driven Water Oxidation with Molecular Iridium Complexes. *J. Am. Chem. Soc.* **133**, 10473-10481 (2011).

117 Blakemore, J. D., Schley, N. D., Olack, G. W., Incarvito, C. D., Brudvig, G. W. & Crabtree, R. H. Anodic deposition of a robust iridium-based water-oxidation catalyst from organometallic precursors. *Chemical Science* **2**, 94-98 (2011).

118 Tiago de Oliveira, F., Chanda, A., Banerjee, D., Shan, X., Mondal, S., Que, L., Bominaar, E., Münck, E. & Collins, T. Chemical and spectroscopic evidence for an FeV-oxo complex. *Science* **315**, 835-838 (2007).

UNIVERSITAT ROVIRA I VIRGILI
NOVEL MOLECULAR CATALYSTS FOR WATER OXIDATION: TOWARDS ARTIFICIAL PHOTOSYNTHESIS
Sara Goberna Ferrón
Dipòsit Legal: T.189-2014

119 Ellis, W. C., McDaniel, N. D., Bernhard, S. & Collins, T. J. Fast Water Oxidation Using Iron. *J. Am. Chem. Soc.* **132**, 10990-10991 (2010).

120 Fillol, J. L., Codola, Z., Garcia-Bosch, I., Gomez, L., Jose Pla, J. & Costas, M. Efficient water oxidation catalysts based on readily available iron coordination complexes. *Nature Chemistry* **3**, 807-813 (2011).

121 Wasylenko, D., Ganesamoorthy, C., Koivisto, B., Henderson, M. & Berlinguette, C. Insight into water oxidation by mononuclear polypyridyl Ru catalysts. *Inorg. Chem.* **49**, 2202-2209 (2010).

122 Wasylenko, D., Ganesamoorthy, C., Henderson, M. & Berlinguette, C. Unraveling the roles of the acid medium, experimental probes, and terminal oxidant, (NH4)2[Ce(NO3)6], in the study of a homogeneous water oxidation catalyst. *Inorg. Chem.* **50**, 3662-3672 (2011).

123 Wasylenko, D., Ganesamoorthy, C., Borau-Garcia, J. & Berlinguette, C. Electrochemical evidence for catalytic water oxidation mediated by a high-valent cobalt complex. *Chem. Commun.* **47**, 4249-4251 (2011).

124 Wasylenko, D., Palmer, R., Schott, E. & Berlinguette, C. Interrogation of electrocatalytic water oxidation mediated by a cobalt complex. *Chem. Commun.* **48**, 2107-2109 (2012).

125 Dogutan, D. K., McGuire, R. & Nocera, D. G. Electocatalytic Water Oxidation by Cobalt(III) Hangman beta-Octafluoro Corroles. *J. Am. Chem. Soc.* **133**, 9178-9180 (2011).

126 Singh, A. & Spiccia, L. Water oxidation catalysts based on abundant 1st row transition metals. *Coord. Chem. Rev.* **257**, 2607–2622 (2013).

127 Yin, Q. S., Tan, J. M., Besson, C., Geletii, Y. V., Musaev, D. G., Kuznetsov, A. E., Luo, Z., Hardcastle, K. I. & Hill, C. L. A Fast Soluble Carbon-Free Molecular Water Oxidation Catalyst Based on Abundant Metals. *Science* **328**, 342-345 (2010).

128 Huang, Z., Luo, Z., Geletii, Y. V., Vickers, J. W., Yin, Q., Wu, D., Hou, Y., Ding, Y., Song, J., Musaev, D. G., Hill, C. L. & Lian, T. Efficient Light-Driven Carbon-Free Cobalt-Based Molecular Catalyst for Water Oxidation. *J. Am. Chem. Soc.* **133**, 2068-2071 (2011).

129 Natali, M., Berardi, S., Sartorel, A., Bonchio, M., Campagna, S. & Scandola, F. Is [Co4(H2O)2([alpha]-PW9O34)2]10- a genuine molecular catalyst in photochemical water oxidation? Answers from time-resolved hole scavenging experiments. *Chem. Commun.* **48**, 8808-8810 (2012).

130 Stracke, J. J. & Finke, R. G. Electrocatalytic Water Oxidation Beginning with the Cobalt Polyoxometalate [Co(4)(H(2)O)(2)(PW(9)O(34))(2)](10-): Identification of Heterogeneous CoO(x) as the Dominant Catalyst. *J. Am. Chem. Soc.* **133**, 14872-14875 (2011).

131 Artero, V. & Fontecave, M. Solar fuels generation and molecular systems: is it homogeneous or heterogeneous catalysis? *Chem. Soc. Rev.* **42**, 2338-2356 (2013).

1. 7. References

132 Hintermair, U., Hashmi, S., Elimelech, M. & Crabtree, R. Particle formation during oxidation catalysis with Cp* iridium complexes. *J. Am. Chem. Soc.* **134**, 9785-9795 (2012).

133 Hong, D., Murakami, M., Yamada, Y. & Fukuzumi, S. Efficient water oxidation by cerium ammonium nitrate with [IrIII(Cp*)(4,4[prime or minute]-bishydroxy-2,2[prime or minute]-bipyridine)(H2O)]2+as a precatalyst. *Energy Environ. Sci.* **5**, 5708-5716 (2012).

134 Hong, D., Jung, J., Park, J., Yamada, Y., Suenobu, T., Lee, Y.-M., Nam, W. & Fukuzumi, S. Water-soluble mononuclear cobalt complexes with organic ligands acting as precatalysts for efficient photocatalytic water oxidation. *Energy Environ. Sci.* **5**, 7606-7616 (2012).

135 Car, P.-E., Guttentag, M., Baldridge, K. K., Alberto, R. & Patzke, G. R. Synthesis and characterization of open and sandwich-type polyoxometalates reveals visible-light-driven water oxidation via POM-photosensitizer complexes. *Green Chem.* **14**, 1680-1688 (2012).

136 Goberna-Ferrón, S., Vigara, L., Soriano-López, J. & Galán-Mascarós, J. R. Identification of a nonanuclear {Co(II)9} polyoxometalate cluster as a homogeneous catalyst for water oxidation. *Inorg. Chem.* **51**, 11707-11715 (2012).

137 Sartorel, A., Bonchio, M., Campagna, S. & Scandola, F. Tetrametallic molecular catalysts for photochemical water oxidation. *Chem. Soc. Rev.* **42**, 2262-2280 (2013).

138 McCool, N. S., Robinson, D. M., Sheats, J. E. & Dismukes, G. C. A Co(4)O(4) "Cubane" Water Oxidation Catalyst Inspired by Photosynthesis. *J. Am. Chem. Soc.* **133**, 11446-11449 (2011).

139 Ganga, G. L., Puntoriero, F., Campagna, S., Bazzan, I., Berardi, S., Bonchio, M., Sartorel, A., Natali, M. & Scandola, F. Light-driven water oxidation with a molecular tetra-cobalt(iii) cubane cluster. *Faraday Discuss.* **155**, 177-190 (2012).

140 Chakrabarty, R., Bora, S. & Das, B. Synthesis, structure, spectral and electrochemical properties, and catalytic use of cobalt(III)-oxo cubane clusters. *Inorg. Chem.* **46**, 9450-9462 (2007).

141 Matsumoto, Y. & Sato, E. Electrocatalytic properties of transition metal oxides for oxygen evolution reaction. *Mater. Chem. Phys.* **14**, 397-426 (1986).

142 Bockris, J., O. & Otagawa, T. Mechanism of oxygen evolution on perovskites. *J. Phys. Chem. C* **87**, 2960–2971 (1983).

143 Bockris, J. O. M. & Otagawa, T. The Electrocatalysis of Oxygen Evolution on Perovskites. *J. Electrochem. Soc.* **131**, 290-302 (1984).

144 Trasatti, S. Electrocatalysis in the anodic evolution of oxygen and chlorine. *Electrochim. Acta* **29**, 1503–1512 (1984).

145 Rasiyah, P. The Role of the Lower Metal Oxide/Higher Metal Oxide Couple in Oxygen Evolution Reactions. *J. Electrochem. Soc.* **131**, 803-808 (1984).

UNIVERSITAT ROVIRA I VIRGILI
NOVEL MOLECULAR CATALYSTS FOR WATER OXIDATION: TOWARDS ARTIFICIAL PHOTOSYNTHESIS
Sara Goberna Ferrón
Dipòsit Legal: T.189-2014

146 Jasem, S. M. A Potentiostatic Pulse Study of Oxygen Evolution on Teflon-Bonded Nickel-Cobalt Oxide Electrodes. *J. Electrochem. Soc.* **126**, 1353-1360 (1979).

147 Aron Walsh, S.-H. W., Yanfa Yan, M. M. Al-Jassim, and John A. Turner Structural, magnetic, and electronic properties of the Co-Fe-Al oxide spinel system: Density-functional theory calculations. *Phys Rev B Condens Matter* **76**, 165119-165128 (2007).

148 Jiao, F. & Frei, H. Nanostructured cobalt oxide clusters in mesoporous silica as efficient oxygen-evolving catalysts. *Angew. Chem.* **48**, 1841-1844 (2009).

149 Hocking, R. K., Brimblecombe, R., Chang, L. Y., Singh, A., Cheah, M. H., Glover, C., Casey, W. H. & Spiccia, L. Water-oxidation catalysis by manganese in a geochemical-like cycle. *Nature Chemistry* **3**, 461-466 (2011).

150 Sivula, K., Le Formal, F. & Gratzel, M. Solar Water Splitting: Progress Using Hematite (alpha-Fe(2)O(3)) Photoelectrodes. *Chemsuschem* **4**, 432-449 (2011).

151 Pinaud, B., A., Zhebo, C., Abram, D., N. & Jaramillo, T., F. Thin Films of Sodium Birnessite-Type MnO 2 : Optical Properties, Electronic Band Structure, and Solar Photoelectrochemistry. *J. Phys. Chem. C* **115**, 11830-11838 (2011).

152 Morita, M., Iwakura, C. & Tamura, H. The anodic characteristics of massive manganese oxide electrode. *Electrochim. Acta* **24**, 357-362 (1979).

153 Trasatti, S. Electrocatalysis by oxides - Attempt at a unifying approach. *J. Electroanal. Chem.* **111**, 125-131 (1980).

154 Bediako, D., Lassalle-Kaiser, B., Surendranath, Y., Yano, J., Yachandra, V. & Nocera, D. Structure-activity correlations in a nickel-borate oxygen evolution catalyst. *J. Am. Chem. Soc.* **134**, 6801-6809 (2012).

155 Dinca, M., Surendranath, Y. & Nocera, D. Nickel-borate oxygen-evolving catalyst that functions under benign conditions. *Proc. Natl. Acad. Sci. U S A* **107**, 10337-10341 (2010).

156 Kanan, M. W. & Nocera, D. G. In situ formation of an oxygen-evolving catalyst in neutral water containing phosphate and Co(2+). *Science* **321**, 1072-1075 (2008).

157 Risch, M., Klingan, K., Heidkamp, J., Ehrenberg, D., Chernev, P., Zaharieva, I. & Dau, H. Nickel-oxido structure of a water-oxidizing catalyst film. *Chem. Commun.* **47**, 11912-11914 (2011).

158 Kanan, M. W., Yano, J., Surendranath, Y., Dinca, M., Yachandra, V. K. & Nocera, D. G. Structure and valency of a cobalt− phosphate water oxidation catalyst determined by in situ X-ray spectroscopy. *J. Am. Chem. Soc.* **132**, 13692-13701 (2010).

159 Zhou, F., Izgorodin, A., Hocking, R., K, Spiccia, L. & MacFarlane, D., R. Electrodeposited MnOx Films from Ionic Liquid for Electrocatalytic Water Oxidation. *Adv. Energy Mater.* **2**, 1013-1021 (2012).

1. 7. References

160 Sakai, N., Ebina, Y., Takada, K. & Sasaki, T. Photocurrent generation from semiconducting manganese oxide nanosheets in response to visible light. *J. Phys. Chem. B* **109**, 9651-9655 (2005).

161 Kiwi, J. & Grätzel, M. Colloidal Redox Catalysts for Evolution of Oxygen and for Light-Induced Evolution of Hydrogen from Water. *Angew. Chem.* **18**, 624-626 (1979).

162 Kalyanasundaram, K. & Grätzel, M. Cyclic Cleavage of Water into H2 and O2 by Visible Light with Coupled Redox Catalysts. *Angew. Chem.* **18**, 701-702 (1979).

163 Kiwi, J., Borgarello, E., Pelizzetti, E., Visca, M. & Grätzel, M. Cyclic Water Cleavage by Visible Light: Drastic Improvement of Yield of H2 and O2 with Bifunctional Redox Catalysts. *Angew. Chem.* **19**, 646-648 (1980).

164 Harriman, A., Richoux, M.-C., Christensen, P., A, Mosseri, S. & Neta, P. Redox reactions with colloidal metal oxides. Comparison of radiation-generated and chemically generated RuO2.2H2O. *J. Chem. Soc., Faraday Trans. 1* **83**, 3001–3014 (1987).

165 Harriman, A., Pickering, I., J., Thomas, J., M. & Christensen, P., A. Metal oxides as heterogeneous catalysts for oxygen evolution under photochemical conditions. *J. Chem. Soc., Faraday Trans. 1* **84**, 2795–2806 (1988).

166 Mills, A. Heterogeneous redox catalysts for oxygen and chlorine evolution. *Chem. Soc. Rev.* **18**, 285-316 (1989).

167 Mills, A., Duckmanton, P. & Reglinski, J. A simple, novel method for preparing an effective water oxidation catalyst. *Chem. Commun.* **46**, 2397-2398 (2010).

168 Okeyoshi, K. & Yoshida, R. Oxygen-Generating Gel Systems Induced by Visible Light. *Adv. Funct. Mater.* **20**, 708–714 (2010).

169 Pillai, K., Kumar, A. & Zen, J. Nafion–RuO2 –Ru(bpy)32+ composite electrodes for efficient electrocatalytic water oxidation. *J. Mol. Catal. A: Chem.* **160**, 277–285 (2000).

170 Kiwi, J. & Grätzel, M. Oxygen Evolution from Water via Redox Catalysis. *Angew. Chem.* **17**, 860–861 (1978).

171 Yagi, M., Tomita, E., Sakita, S., Kuwabara, T. & Nagai, K. Self-assembly of active IrO2 colloid catalyst on an ITO electrode for efficient electrochemical water oxidation. *J. Phys. Chem. B* **109**, 21489-21491 (2005).

172 Nakagawa, T., Bjorge, N. & Murray, R. Electrogenerated IrO(x) nanoparticles as dissolved redox catalysts for water oxidation. *J. Am. Chem. Soc.* **131**, 15578-15579 (2009).

173 Nakagawa, T., Beasley, C., A. & Murray, R., W. . Efficient Electro-Oxidation of Water near Its Reversible Potential by a Mesoporous IrO x Nanoparticle Film. *J. Phys. Chem. C* **113**, 12958-12961 (2009).

174 Hara, M., Waraksa, C., C., Lean, J., T., Lewis, B., A. & Mallouk, T., E. Photocatalytic Water Oxidation in a Buffered Tris(2,2'-bipyridyl)ruthenium Complex-Colloidal IrO 2 System. *J. Phys. Chem. A* **104**, 5275-5280 (2000).

UNIVERSITAT ROVIRA I VIRGILI
NOVEL MOLECULAR CATALYSTS FOR WATER OXIDATION: TOWARDS ARTIFICIAL PHOTOSYNTHESIS
Sara Goberna Ferrón
Dipòsit Legal: T.189-2014

175 Hara, M., Lean, J., T. & Mallouk, T., E. Photocatalytic Oxidation of Water by Silica-Supported Tris(4,4'-dialkyl-2,2'-bipyridyl)ruthenium Polymeric Sensitizers and Colloidal Iridium Oxide. *Chem. Mater.* **13**, 4668-4675 (2001).

176 Morris, N. D., Suzuki, M. & Mallouk, T. E. Kinetics of Electron Transfer and Oxygen Evolution in the Reaction of [Ru(bpy) 3] 3+ with Colloidal Iridium Oxide. *J. Phys. Chem. A* **108**, 9115-9119 (2004).

177 Hoertz, P., Kim, Y.-I., Youngblood, W. & Mallouk, T. Bidentate dicarboxylate capping groups and photosensitizers control the size of IrO2 nanoparticle catalysts for water oxidation. *J. Phys. Chem. B* **111**, 6845-6856 (2007).

178 Youngblood, W., Lee, S.-H. A., Kobayashi, Y., Hernandez-Pagan, E., Hoertz, P., Moore, T., Moore, A., Gust, D. & Mallouk, T. Photoassisted overall water splitting in a visible light-absorbing dye-sensitized photoelectrochemical cell. *J. Am. Chem. Soc.* **131**, 926-927 (2009).

179 Han, H. & Frei, H. In Situ Spectroscopy of Water Oxidation at Ir Oxide Nanocluster Driven by Visible TiOCr Charge-transfer Chromophore in Mesoporous Silica. *J. Phys. Chem. C* **112**, 16156–16159 (2008).

180 La Ganga, G., Nastasi, F., Campagna, S. & Puntoriero, F. Photoinduced water oxidation sensitized by a tetranuclear Ru(II) dendrimer. *Dalton Trans.*, 9997-9999 (2009).

181 Tilley, S., Cornuz, M., Sivula, K. & Grätzel, M. Light-induced water splitting with hematite: improved nanostructure and iridium oxide catalysis. *Angew. Chem.* **49**, 6405-6408 (2010).

182 Najafpour, M. M. & Allakhverdiev, S. I. Manganese compounds as water oxidizing catalysts for hydrogen production via water splitting: from manganese complexes to nano-sized manganese oxides. *Int. J. Hydrogen Energy* **37**, 8753-8764 (2012).

183 Morita, M., Iwakura, C. & Tamura, H. The anodic characteristics of massive manganese oxide electrode. *Electrochim. Acta* **24**, 357–362 (1979).

184 Morita, M., Iwakura, C. & Tamura, H. The anodic characteristics of manganese dioxide electrodes prepared by thermal decomposition of manganese nitrate. *Electrochim. Acta* **22**, 325-328 (1977).

185 Takashima, T., Hashimoto, K. & Nakamura, R. Mechanisms of pH-dependent activity for water oxidation to molecular oxygen by MnO2 electrocatalysts. *J. Am. Chem. Soc.* **134**, 1519-1527 (2012).

186 Mohammad, A. M., Awad, M. I., El-Deab, M. S., Okajima, T. & Ohsaka, T. Electrocatalysis by nanoparticles: Optimization of the loading level and operating pH for the oxygen evolution at crystallographically oriented manganese oxide nanorods modified electrodes. *Electrochim. Acta* **53**, 4351-4358 (2008).

187 Zhou, F., Izgorodin, A., Hocking, R., K., Spiccia, L. & MacFarlane, D., R. Electrodeposited MnOx Films from Ionic Liquid for Electrocatalytic Water Oxidation. *Adv. Energy Mater.* **2**, 1013–1021 (2012).

1. 7. References

188 Pinaud, B., A., Chen, Z., Abram, D., N. & Jaramillo, T., F. Thin Films of Sodium Birnessite-Type MnO 2 : Optical Properties, Electronic Band Structure, and Solar Photoelectrochemistry. *J. Phys. Chem. C* **115**, 11830–11838 (2011).

189 Izgorodin, A., Izgorodina, E. & MacFarlane, D., R. Low overpotential water oxidation to hydrogen peroxide on a MnOx catalyst. *Energy Environ. Sci.* **5**, 9496-9501 (2012).

190 Najafpour, M., Nayeri, S. & Pashaei, B. Nano-size amorphous calcium-manganese oxide as an efficient and biomimetic water oxidizing catalyst for artificial photosynthesis: back to manganese. *Dalton Trans.* **40**, 9374-9378 (2011).

191 Najafpour, M., Tabrizi, M., Haghighi, B. & Govindjee. A manganese oxide with phenol groups as a promising structural model for water oxidizing complex in Photosystem II: a 'golden fish'. *Dalton Trans.* **41**, 3906-3910 (2012).

192 Robinson, D., Go, Y., Greenblatt, M. & Dismukes, G. Water oxidation by lambda-MnO2: catalysis by the cubical Mn4O4 subcluster obtained by delithiation of spinel LiMn2O4. *J. Am. Chem. Soc.* **132**, 11467-11469 (2010).

193 Jiao, F. & Frei, H. Nanostructured manganese oxide clusters supported on mesoporous silica as efficient oxygen-evolving catalysts. *Chem. Commun.* **46**, 2920-2922 (2010).

194 Shafirovich, V. Y., Khannanov, N. K. & Strelets, V. V. Chemical and light-induced catalytic water oxidation. *Nouv. J. Chim.* **4**, 81–84 (1980).

195 Brunschwig, B., S., Chou, M., H., Creutz, C., Ghosh, P. & Sutin, N. Mechanisms of water oxidation to oxygen: cobalt(IV) as an intermediate in the aquocobalt(II)-catalyzed reaction. *J. Am. Chem. Soc.* **105**, 4832–4833. (1983).

196 Artero, V., Chavarot-Kerlidou, M. & Fontecave, M. Splitting water with cobalt. *Angew. Chem.* **50**, 7238-7266 (2011).

197 Iwakura, C., Honji, A. & Tamura, H. The anodic evolution of oxygen on Co3 O 4 film electrodes in alkaline solutions. *Electrochim. Acta* **26**, 1319-1326 (1981).

198 Schmidt, T. & Wendt, H. Electrocatalysis of cathodic hydrogen and anodic oxygen evolution in alkaline water electrolysis by in situ activation procedures. *Electrochim. Acta* **39**, 1763-1767 (1994).

199 Rasiyah, P. & Tseung, A. C. C. A Mechanistic Study of Oxygen Evolution on Li-Doped Co3O4. *J. Electrochem. Soc.* **130**, 365-368. (1983).

200 Kanan, M. W., Surendranath, Y. & Nocera, D. G. Cobalt-phosphate oxygen-evolving compound. *Chem. Soc. Rev.* **38**, 109-114 (2009).

201 Nocera, D. The artificial leaf. *Acc. Chem. Res.* **45**, 767-776 (2012).

202 McAlpin, J. G., Stich, T. A., Casey, W. H. & Britt, R. D. Comparison of cobalt and manganese in the chemistry of water oxidation. *Coord. Chem. Rev.* **256**, 2445-2452 (2012).

203 McAlpin, J. G., Stich, T. A., Ohlin, C. A., Surendranath, Y., Nocera, D. G., Casey, W. H. & Britt, R. D. Electronic Structure Description of a [Co(III)(3)Co(IV)O(4)]

UNIVERSITAT ROVIRA I VIRGILI
NOVEL MOLECULAR CATALYSTS FOR WATER OXIDATION: TOWARDS ARTIFICIAL PHOTOSYNTHESIS
Sara Goberna Ferrón
Dipòsit Legal: T.189-2014

Cluster: A Model for the Paramagnetic Intermediate in Cobalt-Catalyzed Water Oxidation. *J. Am. Chem. Soc.* **133**, 15444-15452 (2011).

204 Kanan, M., Yano, J., Surendranath, Y., DincƒÉ, M., Yachandra, V. & Nocera, D. Structure and valency of a cobalt-phosphate water oxidation catalyst determined by in situ X-ray spectroscopy. *J. Am. Chem. Soc.* **132**, 13692-13701 (2010).

205 Gerken, J., McAlpin, J., Chen, J., Rigsby, M., Casey, W., Britt, R. & Stahl, S. Electrochemical water oxidation with cobalt-based electrocatalysts from pH 0-14: the thermodynamic basis for catalyst structure, stability, and activity. *J. Am. Chem. Soc.* **133**, 14431-14442 (2011).

206 Young, E. R., Nocera, D. G. & Bulovic, V. Direct formation of a water oxidation catalyst from thin-film cobalt. *Energy Environ. Sci.* **3**, 1726-1728 (2010).

207 Risch, M., Khare, V., Zaharieva, I., Gerencser, L., Chernev, P. & Dau, H. Cobalt-oxo core of a water-oxidizing catalyst film. *J. Am. Chem. Soc.* **131**, 6936-6937 (2009).

208 Reece, S. Y., Hamel, J. A., Sung, K., Jarvi, T. D., Esswein, A. J., Pijpers, J. J. H. & Nocera, D. G. Wireless Solar Water Splitting Using Silicon-Based Semiconductors and Earth-Abundant Catalysts. *Science* **334**, 645-648 (2011).

209 Pijpers, J. J. H., Winkler, M. T., Surendranath, Y., Buonassisi, T. & Nocera, D. G. Light-induced water oxidation at silicon electrodes functionalized with a cobalt oxygen-evolving catalyst. *Proc. Natl. Acad. Sci.* **108**, 10056-10061 (2011).

210 Surendranath, Y., Kanan, M. W. & Nocera, D. G. Mechanistic Studies of the Oxygen Evolution Reaction by a Cobalt-Phosphate Catalyst at Neutral pH. *J. Am. Chem. Soc.* **132**, 16501-16509 (2010).

211 Ke, S., Namseok, P., Zhelin, S., Jigang, Z., Jian, W., Xiaolu, P., Shaohua, S., Sun Young, N., Yi, J., Sungho, J., Paul, K. L. Y. & Deli, W. Nickel oxide functionalized silicon for efficient photo-oxidation of water. *Energy Environ. Sci.* **5**, 7872-7877 (2012).

212 Gao, X., Chen, P. & Liu, J. Enhanced visible-light absorption of nitrogen-doped titania induced by shock wave. *Mater. Lett.*, 685–687 (2011).

213 Pore, V., Heikkilä, M., Ritala, M., Leskelä, M. & Areva, S. Atomic layer deposition of TiO2- x Nx thin films for photocatalytic applications. *J. Photochem. Photobiol. A: Chemistry* **177**, 68-75 (2006).

214 Ohno, T., Akiyoshi, M., Umebayashi, T., Asai, K., Mitsui, T. & Matsumura, M. Preparation of S-doped TiO 2 photocatalysts and their photocatalytic activities under visible light. *Appl. Catal. A: General* **265**, 115-121 (2004).

215 Grätzel, M. Photoelectrochemical cells. *Nature* **414**, 338-344 (2001).

216 Rai, B. Cu2O solar cells: A review. *Sol. Cells* **25**, 265-272 (1988).

217 Shinar, R. & Kennedy, J. H. Competition Reactions at Fe2O3 Photoanodes. *J. Electrochem. Soc.* **130**, 860-863 (1983).

1. 7. References

218 Lu, P. W. T. & Srinivasan, S. Electrochemical-Ellipsometric Studies of Oxide Film Formed on Nickel during Oxygen Evolution. *J. Electrochem. Soc.* **125**, 1416-1422 (1978).

219 Gennero de Chialvo, M. & Chialvo, A. Oxygen evolution reaction on thick hydrous nickel oxide electrodes. *Electrochim. Acta* **33**, 825-830 (1988).

220 Wang, X., Luo, H., Yang, H., Sebastian, P. & Gamboa, S. Oxygen catalytic evolution reaction on nickel hydroxide electrode modified by electroless cobalt coating. *Int. J. Hydrogen Energy* **29**, 967-972 (2004).

221 Lyons, M. E. & Brandon, M. P. The oxygen evolution reaction on passive oxide covered transition metal electrodes in aqueous alkaline solution. Part 1-Nickel. *Int. J. Electrochem. Sci.* **3**, 1386 - 1424 (2008).

222 Yeo, B. S. & Bell, A., T. In Situ Raman Study of Nickel Oxide and Gold-Supported Nickel Oxide Catalysts for the Electrochemical Evolution of Oxygen. *J. Phys. Chem. C* **116**, 8394−8400 (2012).

223 Singh, A., Chang, S., L. Y., Hocking, R., K., Bach, U. & Spiccia, L. Highly active nickel oxide water oxidation catalysts deposited from molecular complexes. *Energy Environ. Sci.* **6**, 579-586 (2013).

UNIVERSITAT ROVIRA I VIRGILI
NOVEL MOLECULAR CATALYSTS FOR WATER OXIDATION: TOWARDS ARTIFICIAL PHOTOSYNTHESIS
Sara Goberna Ferrón
Dipòsit Legal: T.189-2014

UNIVERSITAT ROVIRA I VIRGILI
NOVEL MOLECULAR CATALYSTS FOR WATER OXIDATION: TOWARDS ARTIFICIAL PHOTOSYNTHESIS
Sara Goberna Ferrón
Dipòsit Legal: T.189-2014

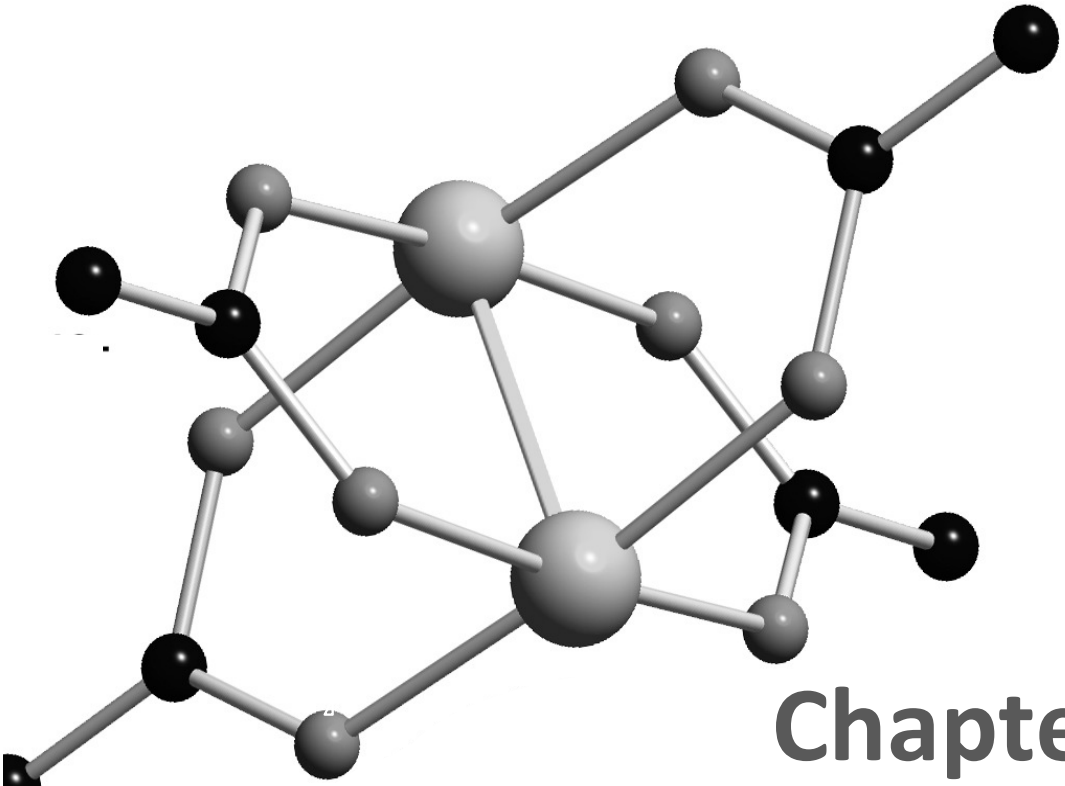

Chapter 2

Metal-Metal Bonded Diruthenium Water Oxidation Catalyst

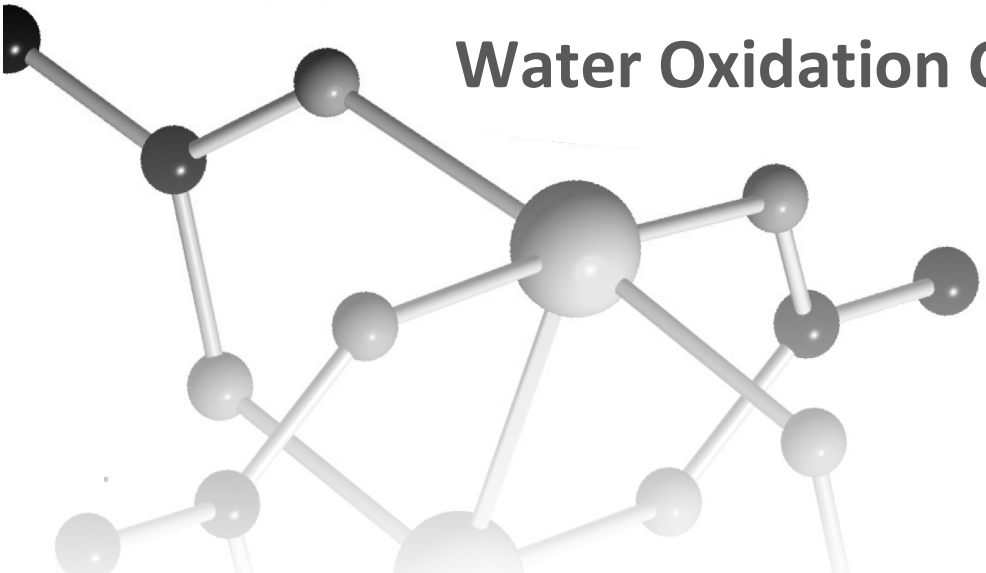

UNIVERSITAT ROVIRA I VIRGILI
NOVEL MOLECULAR CATALYSTS FOR WATER OXIDATION: TOWARDS ARTIFICIAL PHOTOSYNTHESIS
Sara Goberna Ferrón
Dipòsit Legal: T.189-2014

UNIVERSITAT ROVIRA I VIRGILI
NOVEL MOLECULAR CATALYSTS FOR WATER OXIDATION: TOWARDS ARTIFICIAL PHOTOSYNTHESIS
Sara Goberna Ferrón
Dipòsit Legal: T.189-2014

2.1

Introduction

The demonstration of the existence of multiple bonds between transition metal atoms began in the period of 1963-1966.[1-5] From the earliest observations in 1844 of a compound which contains a quadruple bond, $Cr_2(O_2CCH_3)_4(H_2O)_2$, to the recognition that quadruple bonds exists by Albert Cotton's discovery in 1964 of $Re_2Cl_8^{2-}$ that caused the birth of this new area in chemistry (Figure 2.1).[4-6] *Multicenter chemistry* constitutes an important step in the progress of inorganic chemistry. Metal-metal bonded species are known for a large family of transition metal complexes including hetero- as well as homo-metallic examples. Their structures tolerate a large variety of ligands allowing for an excellent control of the electronic properties of these dinuclear species.[7]

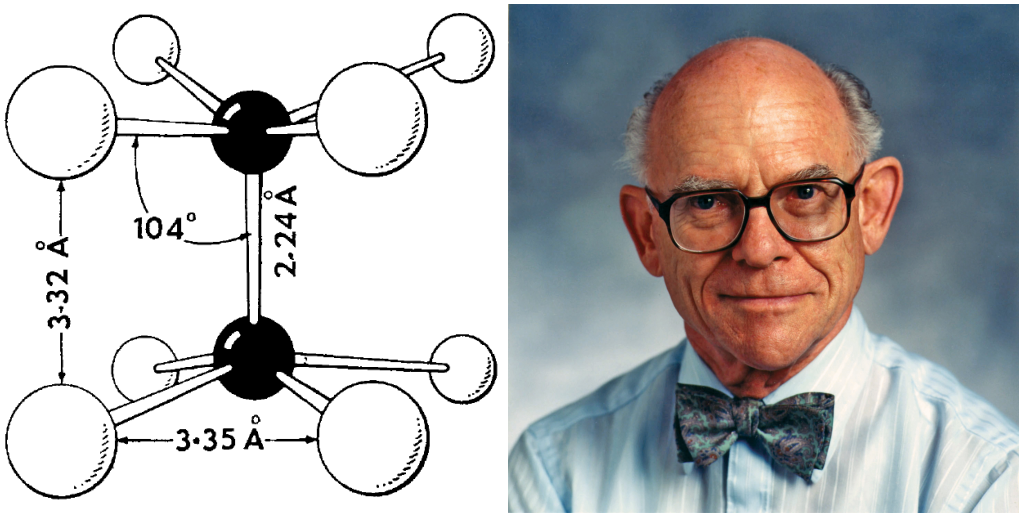

Figure 2.1. ***Left****: The structure of the* $Re_2Cl_8^{2-}$ *ion.*[8] ***Right****: F. Albert Cotton.*[9]

- 2. M–M Bonded Diruthenium WOC -

The design of metal–metal bonded materials with desired structural and physical properties[7] has had a profound impact in diverse fields ranging from crystal engineering,[10] magnetism,[11-14] spectroscopy,[15,16] optical properties,[17] anticancer therapy[18,19] and catalysis.[20-22] These compounds are highly stable and possess multiple and reversible oxidation states. From the perspective of catalysis it is remarkable that stable multielectron chemistry of the late transition metal complexes has been exploited for numerous catalytic applications including C–H activation,[23] halogen photoelimination,[24-26] and organometallic transformations.[27] In the renewable energy field, metal–metal bonded materials have been shown to be good catalysts for hydrogen production[28-30] and oxygen reduction.[30-33] Surprisingly, the application of M–M bonded species to water oxidation catalysis has not been investigated.

Given the importance of ruthenium chemistry in this field (see 1.5.1.1), we rationalized that metal–metal bonded diruthenium complexes could offer some advantages if they exhibit catalytic activity for water oxidation:

- These species are easily stabilized by available inexpensive ligands such as carboxylates and do not require the design and multi-step preparation of complex organic groups.

- Usually, Ru_2 complexes adopt the Ru_2L_4 paddlewheel configuration, in which four bidentate ligands are bridging two Ru–bonded atoms. The Ru=Ru double bond in the paddlewheel tetracarboxylate compounds, based on the Ru_2^{4+} core with the electronic configuration $\sigma^2\pi^2\delta^2\delta^{*2}\pi^{*2}$, increases in strength upon oxidation since anti–bonding orbitals are being depopulated. Thus, it is expected a high stability for intermediates.[7]

- The Ru_2^{4+} tetracarboxylates have a high affinity for axial coordination, exhibiting open and / or labile sites for water ligation.

UNIVERSITAT ROVIRA I VIRGILI
NOVEL MOLECULAR CATALYSTS FOR WATER OXIDATION: TOWARDS ARTIFICIAL PHOTOSYNTHESIS
Sara Goberna Ferrón
Dipòsit Legal: T.189-2014

2. 1. Introduction

In the present chapter, the catalytic activity towards water oxidation of the [Ru_2(μ-O_2CCH_3)$_4$] (**Ru_2**, Figure 2.2), with the axial positions available for water ligations / interactions, has been explored in a collaboration with Prof. Kim R. Dunbar's Group (Texas A&M University).

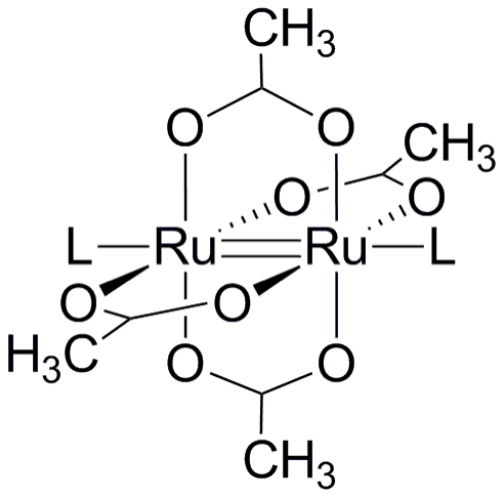

Figure 2.2. *Schematic representation of the molecular structure of [Ru_2(μ-O_2CCH_3)$_4$], **Ru_2**. L denotes open axial positions for solvent or anion binding.*

UNIVERSITAT ROVIRA I VIRGILI
NOVEL MOLECULAR CATALYSTS FOR WATER OXIDATION: TOWARDS ARTIFICIAL PHOTOSYNTHESIS
Sara Goberna Ferrón
Dipòsit Legal: T.189-2014

UNIVERSITAT ROVIRA I VIRGILI
NOVEL MOLECULAR CATALYSTS FOR WATER OXIDATION: TOWARDS ARTIFICIAL PHOTOSYNTHESIS
Sara Goberna Ferrón
Dipòsit Legal: T.189-2014

2.2

Results and Discussion

The electrochemistry in water and the electrocatalytic activity of **Ru_2** towards water oxidation has been investigated, giving unequivocal insights of the catalytic performance of this compound.

Electrochemistry of Ru_2

In order to determine the catalytic activity of **Ru_2** for water oxidation, the electrochemistry of **Ru_2** has been studied in aqueous solutions. It is well–known that the electrochemical properties of diruthenium tetracarboxylate–bridged species are highly solvent dependent.[34] The presence of coordinating anions or neutral ligands in the axial positions exerts a strong influence on the redox potentials. In organic solvents, **Ru_2** typically exhibits a single $Ru_2^{+5/+4}$ reversible couple in the 0.2 to 0.5 V range vs NHE (all potentials in this thesis are referenced to NHE).[35-37] A perusal of the literature revealed that the aqueous electrochemistry of **Ru_2** has not been well investigated, although in one report it was described to be analogous to that observed in organic solvents,[38] a different behavior was found (Figure 2.3). At pH = 1 (H_2SO_4 0.1 M), no distinct reversible redox processes were evident in the cyclic voltammograms of **Ru_2** (0.5 mM) but a feature indicative of a catalytic water oxidation wave above 1.40 V was present (Figure 2.3, left). When the sweep was extended to cathodic potentials, a broad irreversible peak was observed below –0.3 V which corresponds to the irreversible O_2 / O_2^- reduction.[39] The feature appears only after successive scans, in support of effective catalytic O_2 evolution. When the pH was slowly increased by addition of NaOH, a quasi–irreversible redox couple appeared above pH = 2 with peak potentials at E_{ox} = 1.24 V and E_{red} = 1.05 V (E_{ox}–E_{rd} = 200 mV)

UNIVERSITAT ROVIRA I VIRGILI
NOVEL MOLECULAR CATALYSTS FOR WATER OXIDATION: TOWARDS ARTIFICIAL PHOTOSYNTHESIS
Sara Goberna Ferrón
Dipòsit Legal: T.189-2014

which is assigned to the $Ru_2^{+5/+4}$ couple. The large E_{ox}–E_{red} difference in water suggests that electron transfer is associated with proton transfer and the change in going from H_2O to OH^- in the axial position stabilizes the Ru_2^{+5} redox state.

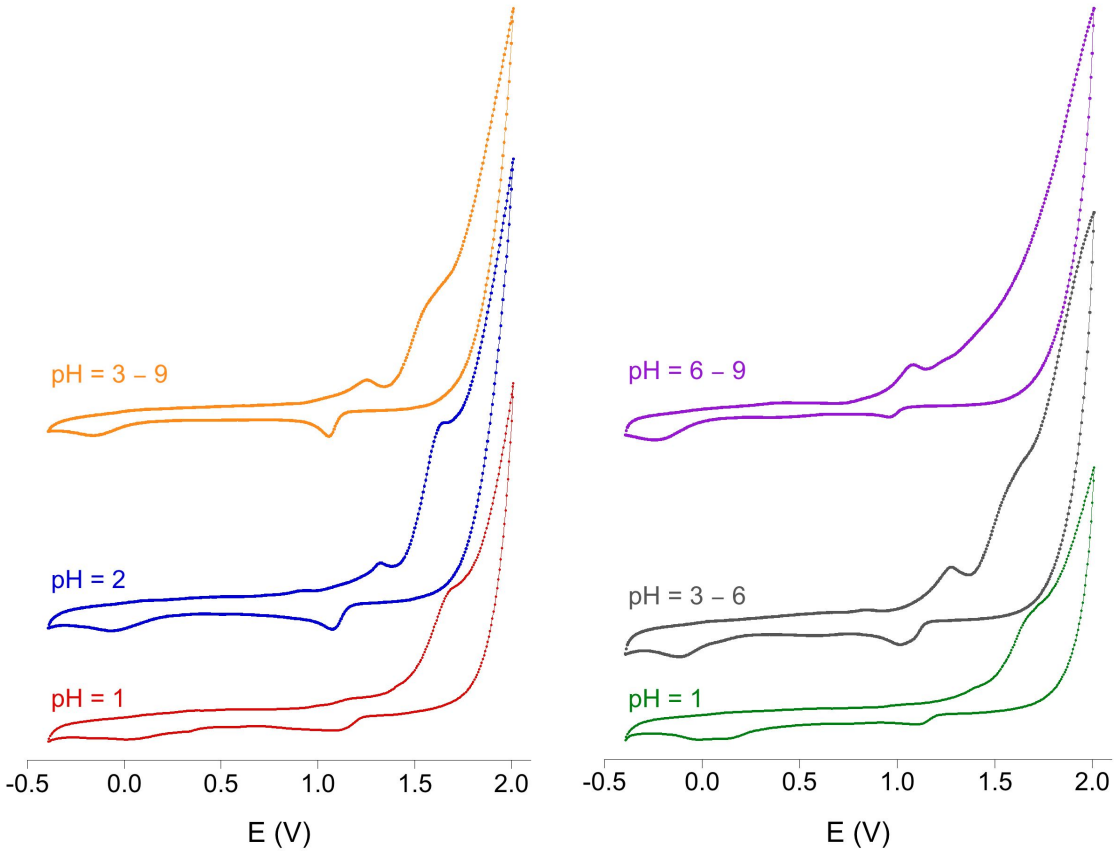

Figure 2.3. *Cyclic voltammetry scans (100 mV/s) of* ***Ru_2*** *(0.5 mM) as a function of different pH values (left) in dilute sulfuric acid solutions adding NaOH to adjust the pH and (right) in a 50 mM NaP_i buffer solution containing 1 M $NaNO_3$ as electrolyte at pH = 7 and adding H_3PO_4/ NaOH to adjust the pH. Glassy Carbon working electrode, Pt wire counter electrode and Ag/AgCl (NaCl 3M) reference electrode.*

The current associated with the catalytic water oxidation wave also increased, exhibiting a small shoulder at ~ 1.4 V. As the pH was increased to pH = 9, no significant changes were observed. Identical results were also obtained by varying the

UNIVERSITAT ROVIRA I VIRGILI
NOVEL MOLECULAR CATALYSTS FOR WATER OXIDATION: TOWARDS ARTIFICIAL PHOTOSYNTHESIS
Sara Goberna Ferrón
Dipòsit Legal: T.189-2014

pH from basic to acid media or vice versa, supporting the conclusion that the catalyst is unaffected by pH variations.

The aforementioned experiments were repeated in a 50 mM sodium phosphate (NaP_i) buffer (pH = 7) with 1 M $NaNO_3$ as electrolyte at different pH values (Figure 2.3, right). When pH is lowered with H_3PO_4 below pH = 5, the cyclic voltammograms are analogous to those observed for the buffer–free experiments. Above this pH, however, the $Ru_2^{+5/+4}$ couple becomes reversible with $i_{ox}/i_{red} \approx 1$ and 75 mV peak separation values that are independent of scan rate. In addition, the shoulder on the water oxidation wave disappears, suggesting faster water oxidation kinetics in the presence of NaP_i buffer. The reversibility of the $Ru_2^{+5/+4}$ couple at neutral pH values in the presence of NaP_i also supports the participation of proton transfer associated with electron transfer, given that phosphate axial binding would lead to deprotonation of the phosphate group instead of the water molecule. No significant changes were observed for the voltammograms recorded at pH > 6.

It is important to note that the cyclic voltammograms revert to the original irreversible form when the pH is lowered to less than 5 by addition of phosphoric acid. The electrochemical data acquired in the presence of excess phosphoric or sulfuric acid support the contention that phosphate or sulfate groups do not replace acetate ligands in the equatorial positions. Acetate substitution by highly charged bridging ligands in water requires extreme conditions[40,41] and, most importantly, the electrochemical properties of sulfate and phosphate bridged diruthenium complexes do not match the present data. Moreover, the catalytic water oxidation wave is stable with time. Although the different chemical environments of the axial positions affect the electrochemistry in the 0.0 – 1.0 V region, there is no significant effect on the catalytic process. This behavior of **Ru_2** is a remarkable feature indicative of a high robustness, since most WOCs operate under very strict conditions, particularly with respect to pH and buffer nature. A complete study of the pH–dependence in the catalytic activity of Ru_2 will be discussed later.

UNIVERSITAT ROVIRA I VIRGILI
NOVEL MOLECULAR CATALYSTS FOR WATER OXIDATION: TOWARDS ARTIFICIAL PHOTOSYNTHESIS
Sara Goberna Ferrón
Dipòsit Legal: T.189-2014

Kinetics of Ru_2 Water Oxidation Catalysis

As mentioned above, cyclic voltammetry of a diluted **Ru_2** solution in 50 mM NaP_i buffer containing 1 M $NaNO_3$ as electrolyte at pH = 7 shows an irreversible current wave signature of catalytic water oxidation (Figure 2.4). Compared with a blank experiment, the appearance of a prominent catalytic oxidation wave in the presence of **Ru_2** demonstrate that water oxidation is enhanced by the presence of this compound. In addition, the $Ru_2^{+5/+4}$ couple becomes reversible above pH > 6 (Figure 2.4, inset).

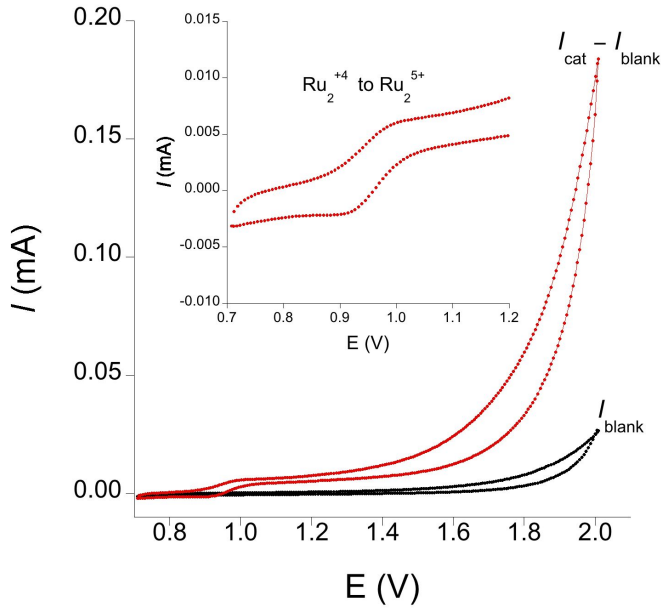

Figure 2.4. *Blank corrected cyclic voltammetry of 0.5 mM **Ru_2** in a 50 mM NaP_i buffer solution containing 1 M $NaNO_3$ as electrolyte at pH = 7. Scan rate = 100 mV s^{-1}. Inset: Detail of the the $Ru_2^{+5/+4}$ redox pair. Glassy Carbon working electrode, Pt wire counter electrode and Ag/AgCl (NaCl 3M) reference electrode*

In electrochemical water oxidation, homogeneous catalysts require count only the catalyst present in the reaction layer. In contrast with chemical or photochemical water oxidation, where the catalyst present in the whole solution is used to determinate turnover numbers (TON) and TOF, in electrochemistry only the moles of

UNIVERSITAT ROVIRA I VIRGILI
NOVEL MOLECULAR CATALYSTS FOR WATER OXIDATION: TOWARDS ARTIFICIAL PHOTOSYNTHESIS
Sara Goberna Ferrón
Dipòsit Legal: T.189-2014

catalyst present in the thin reaction–diffusion layer adjacent to the electrode are participating in the reaction. Cyclic voltammograms (CVs) are valuable to estimate the limiting turnover frequencies (TOF). For this purpose, two methodologies can be used for the estimation of TOF from CVs.

Estimation of TOF from CVs, Method 1:

The non-catalytic reversible couple observed in the phosphate buffer experiments at pH > 6 can be used to estimate the thickness of the diffusion layer from the Randles-Sevcik equation (equation 2.1 and 2.2). This equation describes the effect of the scan rate (v) on the peak current intensity of a simple redox event, following a linear dependence with $v^{1/2}$ (Figure 2.5).

$$i_p = 0.4463\, n_p\, FAC \left(\frac{n_p\, F\nu D}{RT}\right)^{1/2} \quad \text{(Eq. 2.1)}$$

At room temperature:

$$i_p = (2.687 \times 10^5) n_p{}^{3/2} \nu^{1/2} D^{1/2} AC \quad \text{(Eq. 2.2)}$$

Where i_p is the peak current for the non–catalytic process (A), n_p is the number of electrons in the redox reaction (n_p = 1 for the $Ru_2^{+5/+4}$ couple), *F* is the Faraday's constant (C mol^{-1}), v is the scan rate (V s^{-1}), *D* is the diffusion coefficient (cm^2 s^{-1}), *A* is the area of the electrode (cm^3), and *C* the bulk catalyst concentration (mol cm^3).

By measuring the peak intensity at different scan rates, *D* can be extracted from the slope of i_p vs $v^{1/2}$ (Figure 2.5).

UNIVERSITAT ROVIRA I VIRGILI
NOVEL MOLECULAR CATALYSTS FOR WATER OXIDATION: TOWARDS ARTIFICIAL PHOTOSYNTHESIS
Sara Goberna Ferrón
Dipòsit Legal: T.189-2014

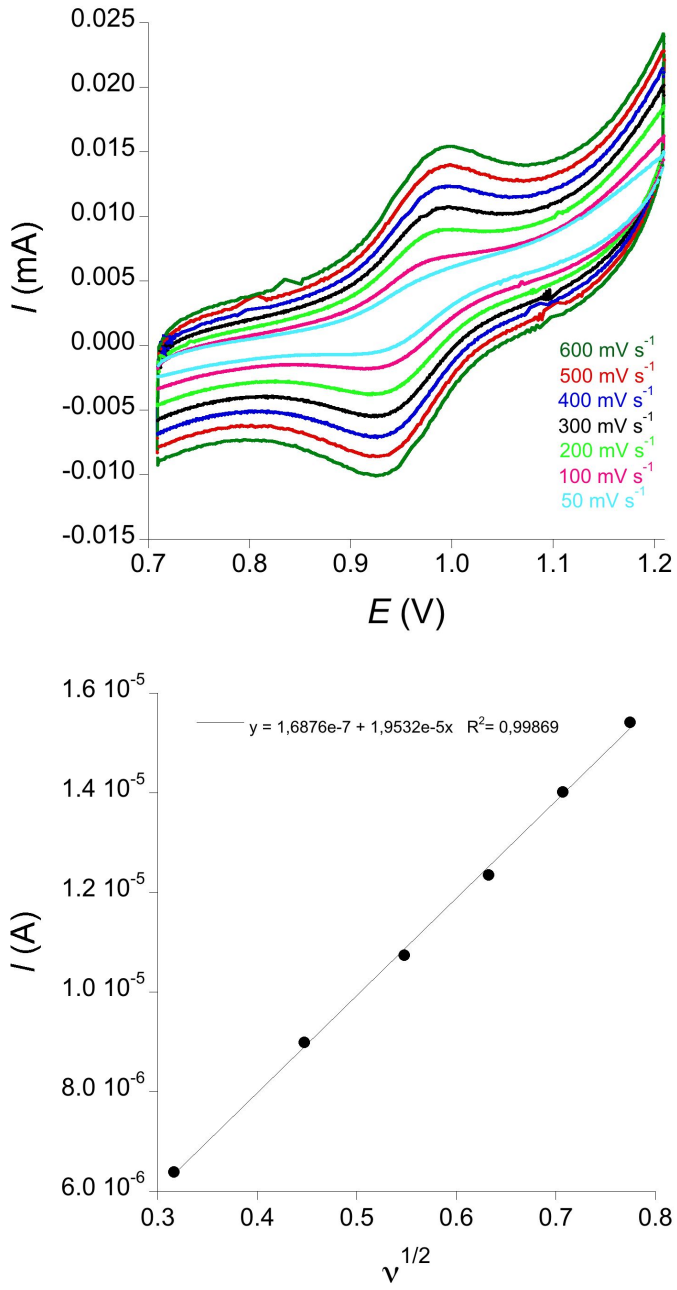

Figure 2.5. ***Top:*** *Cyclic voltammograms at different scan rates of 0.5 mM* ***Ru_2*** *in a 50 mM NaP_i buffer solution containing 1 M $NaNO_3$ as electrolyte at pH = 7.* ***Bottom:*** *Linear fit of i_p vs $v^{1/2}$. Glassy Carbon working electrode, Pt wire counter electrode and Ag/AgCl (NaCl 3M) reference electrode.*

The layer thickness, δ, can be estimated from the relationship $\delta \approx [Dt]^{1/2}$, where *t* is time. The diffusion layer should be close to the length of the effective active layer in contact with the electrode in diffusion–controlled experiments. Accordingly, the

UNIVERSITAT ROVIRA I VIRGILI
NOVEL MOLECULAR CATALYSTS FOR WATER OXIDATION: TOWARDS ARTIFICIAL PHOTOSYNTHESIS
Sara Goberna Ferrón
Dipòsit Legal: T.189-2014

maximum number of available molecules of catalyst in the diffusion layer per second (t = 1) can be conveniently calculated taking into account layer thickness, electrode surface area, and bulk concentration. This would give an upper limit for the theoretical maximum number of molecules of catalyst interacting with the electrode at a given time in a diffusion−controlled experiment. Therefore, with these data a minimum limit to the TOF can be estimated directly from chronoamperometric measurements. It is important to note that TOF estimation was performed under the same steady diffusion controlled conditions used for the cyclic voltammograms (without stirring). Steady-state current density was measured for 10 minutes of water electrolysis at different constant applied potentials using a glassy carbon working electrode (Figure 2.6) and the average current was used to convert current into turnover frequency (TOF), assuming that all current is caused by the 4 e^- oxidation of water to produce O_2 (Equation 2.3).

$$TOF = \frac{i}{Fn} \times \frac{1}{4} \qquad \text{(Eq. 2.3)}$$

Where i is the averaged current (A), F is the Faraday's cobstant (C mol^{-1}), n is the number of molecules of catalyst participating in the oxidation reaction (mol) and 4 is the number of electrons in the catalytic reaction.

TOF values are function of the electrode potential and, therefore, of the overpotential ($\eta = E_{appl} - E_0$). Significant catalytic current density (i) appears above 0.9 V and it increases exponentially as a function of overpotential (η), reaching i > 1 mA cm^{-2} (Figure 2.6 and 2.7). A linear logTOF – η dependence is expected in the absence of side phenomena, that is, for low TOF and low η.[42] Linear fitting of logTOF in the low η range (Figure 2.7, inset) yields an intrinsic turnover frequency of 600 h^{-1}, which is the theoretical catalytic rate at the thermodynamic water oxidation potential (η = 0). The plot deviates from linearity above η = 1.0 V reaching a maximum TOF over 7 s^{-1}

UNIVERSITAT ROVIRA I VIRGILI
NOVEL MOLECULAR CATALYSTS FOR WATER OXIDATION: TOWARDS ARTIFICIAL PHOTOSYNTHESIS
Sara Goberna Ferrón
Dipòsit Legal: T.189-2014

(>25000 h^{-1}). The slope of the linear fit is well over 300 mV $decade^{-1}$. Such a high value for a Tafel slope (see Appendix I) suggests that the apparent rate-limiting process is not catalytic. This situation may be due to the influence of bubble formation, inefficient homogeneity or local defects as noted in other electrochemical catalysts.[43] This approach is more commonly used for heterogeneous catalysts[44], but it is theoretically correct for diffusion–controlled conditions. These TOF values are an estimation of the minimum theoretical TOF, as not all catalyst molecules in the diffusion layer will be active, this estimation may include more molecules than the real active ones, but never the opposite.

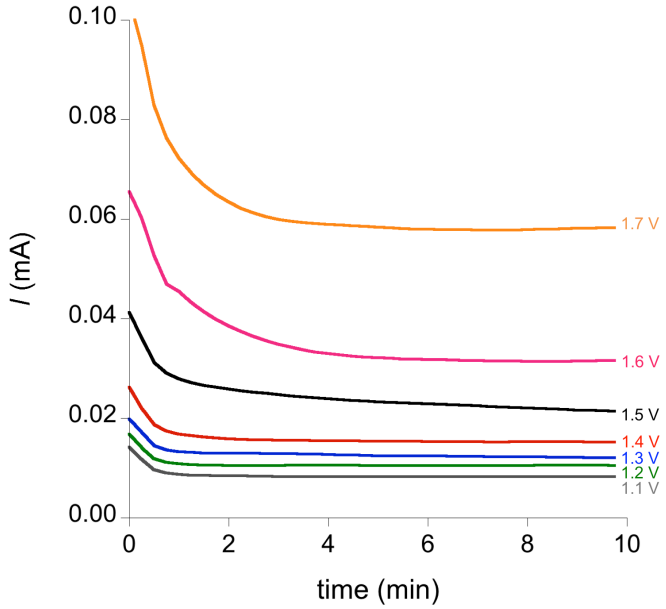

Figure 2.6. *Chronoamperometry without stirring in a 0.5 mM* ***Ru_2*** *solution, 50 mM NaP_i buffer (pH = 7) with 1M $NaNO_3$. Applied voltages vs NHE. Same conditions than cyclic voltammetry experiments: Glassy Carbon working electrode and without stirring.*

UNIVERSITAT ROVIRA I VIRGILI
NOVEL MOLECULAR CATALYSTS FOR WATER OXIDATION: TOWARDS ARTIFICIAL PHOTOSYNTHESIS
Sara Goberna Ferrón
Dipòsit Legal: T.189-2014

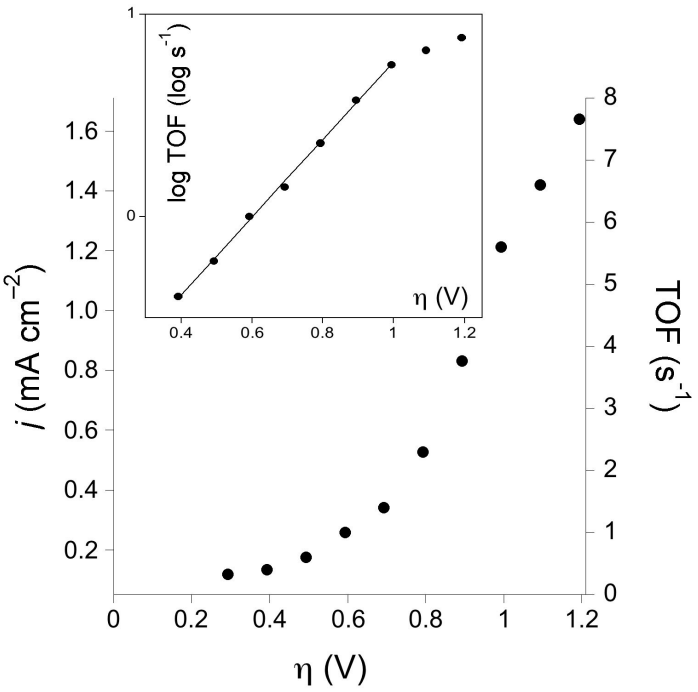

Figure 2.7. *Current density and TOF for* ***Ru₂*** *(0.5 mM) catalyzed water oxidation as a function of overpotential in a 50 mM NaP_i buffer (pH = 7) with 1M $NaNO_3$. Inset: linear dependence of logTOF at low overpotentials. Same conditions than cyclic voltammetry experiments: Glassy Carbon working electrode and without stirring.*

Estimation of TOF from CVs, Method 2:

Under purely kinetic conditions, when the current is limited only by catalytic steps in solution, cyclic voltammograms are predicted to show a S−like wave and reach a limiting catalytic current i_c (Equation 2.4).[45] In order to guarantee pseudo−first−order kinetics, low scan rates and high substrate / catalyst ratios are required.

$$i_c = n_c FAC(K_{cat}D)^{1/2} \qquad \text{(Eq. 2.4)}$$

Where i_c is the limiting catalytic current (A), n_c is the number of electrons in the catalytic redox reaction (n = 4 for water oxidation), F is Faraday's constant (C mol^{-1}), D

UNIVERSITAT ROVIRA I VIRGILI
NOVEL MOLECULAR CATALYSTS FOR WATER OXIDATION: TOWARDS ARTIFICIAL PHOTOSYNTHESIS
Sara Goberna Ferrón
Dipòsit Legal: T.189-2014

is the diffusion coefficient ($cm^2\ s^{-1}$), *A* is the area of the electrode (cm^3), and *C* the bulk catalyst concentration (mol cm^3).

As previously described, the peak current for the $Ru_2^{+5/+4}$ varies linearly with the square root of the scan rate (Figure 2.5), this result is consistent with the Randles–Sevcik equation (Equation 2.1) for a diffusion controlled current, i_p. The ratio between Equations 2.4 and 2.1 gives Equation 2.5.[46]

$$\frac{i_c}{i_p} = 0.359 \frac{n_c}{n_p^{3/2}} \sqrt{\frac{k_{cat}}{\nu}} \qquad \text{(Eq. 2.5)}$$

Where i_c is the limiting catalytic current and i_p is the peak current for the non catalytic process, both obtained after background subtraction (A). n_p is the number of electrons in the non-catalytic redox reaction (n = 1 for the $Ru_2^{+5/+4}$ couple) and n_c is the number of electrons in the catalytic redox reaction (n = 4 for water oxidation). For water oxidation, with water as the substrate, the value of k_{cat} is also the catalytic TOF for catalytic water oxidation.

Cyclic voltammograms were obtained at 10 mV s^{-1} for different concentrations of **Ru_2** in 50 mM NaP_i buffer at pH = 7. The limiting catalytic current (background corrected) varies linearly with the catalyst concentration (Figure 2.8), consistent with pseudo–first–order kinetics (Equation 2.4).

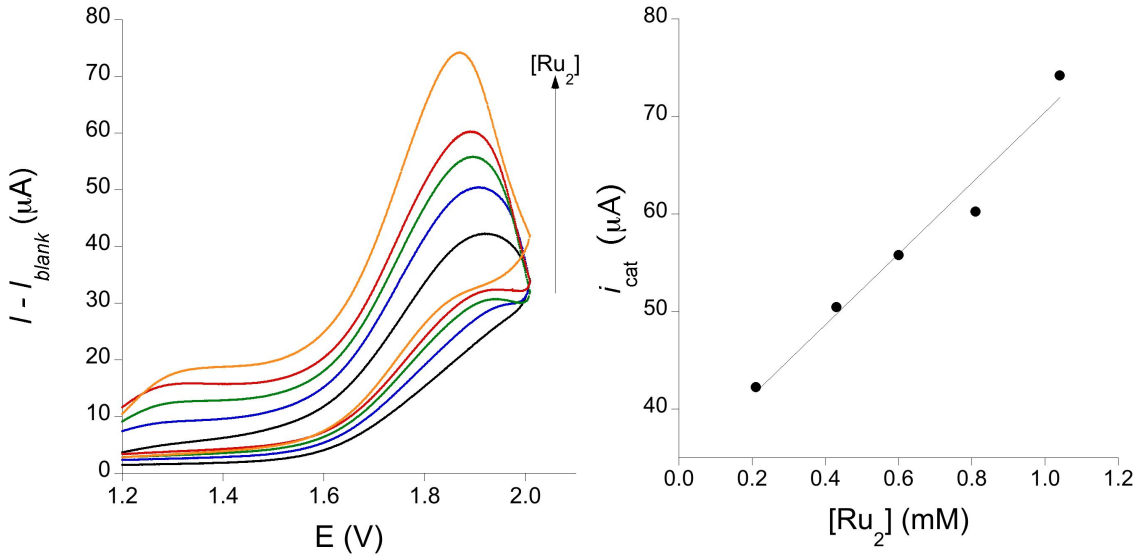

Figure 2.8. ***Left:*** *Blank corrected cyclic voltammogram at scan rate = 10 mV s^{-1} in a 50 mM NaP_i buffer (pH = 7) with 1 M $NaNO_3$ with different concentrations of* ***Ru_2*** *(between 0.2 and 1.1 mM). Glassy Carbon working electrode, Pt wire counter electrode and Ag/AgCl (NaCl 3M) reference electrode.* ***Right****: Plot of catalytic peak current at $E_{p,a}$ = 1.9 V (vs NHE) vs the concentration of* ***Ru_2****.*

In order to estimate a limiting TOF, cyclic voltammograms were performed at different scan rates (between 2 and 10 mV s^{-1}) for 0.85 mM **Ru_2** in 50 mM NaP_i buffer at pH = 7 (Figure 2.9). A concentration–independent TOF (k_{cat}) can be directly estimated from the linear relationship of the ratio between the catalytic current peak and the current peak of the non–catalytic redox couple as a function of $v^{-1/2}$ (Equation 2.5). The slope was substituted for $i_c/i_p - v^{-1/2}$, and then k_{cat} was solved for (Figure 2.10). A TOF of 77 s^{-1} was observed in the linear region at low scan rates. This should be the limiting TOF for the **Ru_2** catalyst, a value that cannot be extracted from the steady state bulk electrolysis data because of the experimental conditions. Most Ru catalysts achieve rates well below 1 s^{-1}, the notable exception being the family of complexes containing the 6,6'-dicarboxylate-2,2'-dipyridyl ligand (TOF > 300 s^{-1}).[47,48]

UNIVERSITAT ROVIRA I VIRGILI
NOVEL MOLECULAR CATALYSTS FOR WATER OXIDATION: TOWARDS ARTIFICIAL PHOTOSYNTHESIS
Sara Goberna Ferrón
Dipòsit Legal: T.189-2014

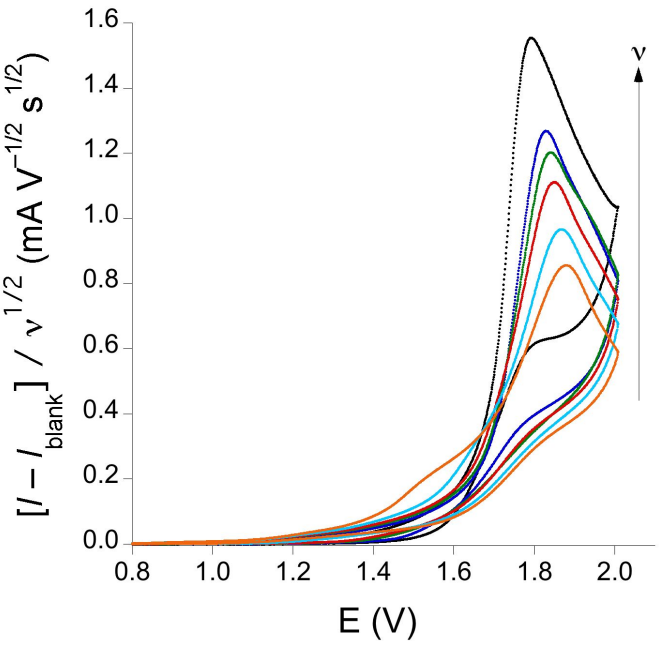

Figure 2.9. *Blank corrected and normalized cyclic voltammograms at different scan rates (between 2 and 10 mV s^{-1}) of 0.85 mM* ***Ru₂*** *in a 50 mM NaP_i buffer (pH = 7) with 1 M $NaNO_3$. Glassy Carbon working electrode, Pt wire counter electrode and Ag/AgCl (NaCl 3M).*

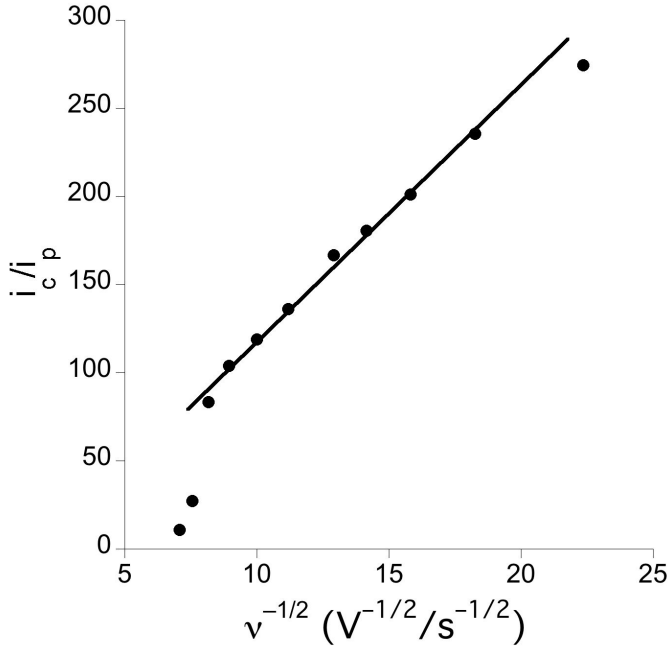

Figure 2.10. *Plot of the catalytic current peak to the reversible non–catalytic peak as a function of $\nu^{-1/2}$. Same conditions than Figure 2.9.*

UNIVERSITAT ROVIRA I VIRGILI
NOVEL MOLECULAR CATALYSTS FOR WATER OXIDATION: TOWARDS ARTIFICIAL PHOTOSYNTHESIS
Sara Goberna Ferrón
Dipòsit Legal: T.189-2014

Bulk Water Oxidation with Ru_2

In order to examine the catalytic activity and stability of **Ru_2** towards water oxidation, bulk electrolysis experiments were performed in water with a FTO–coated glass working electrode by applying a constant potential of 1.5 V to a well–stirred neutral 50 mM NaP_i buffer solution with 1 M $NaNO_3$ containing 1 mM **Ru_2** (Figure 2.11, left) in a two-chamber cell to separate reduction and oxidation electrodes. Oxygen evolution during bulk electrolysis was monitored in the oxidation compartment with the use of a fluorescence probe (See 2.4 Experimental). Comparing the amount of O_2 measured with the theoretical (Faraday's law) assuming that all current is caused by the 4 e^- oxidation of water to produce O_2, the oxygen levels match the expected yield calculated from Faraday's law, an indication of quantitative efficiency for the catalytic process (Figure 2.11, right). This result confirms that current density measurements can be directly used to quantify catalytic performance.

During electrolysis, a slow but constant decrease in current suggests catalyst decomposition. After 10 hours of continuous electrolysis, the rate reaches about 10% of the initial value. Mass spectrometric measurements detect traces of CO_2 in the gas phase in addition to the dominant O_2 content (Figure 2.12) during this bulk electrolysis experiments. The CO_2 fraction is very small but increases with time, albeit at a much slower rate than oxygen evolution. This suggest that oxidative deactivation of the catalyst is occurring via acetate loss. Decomposition eventually leads to a black powder, presumably some form of ruthenium oxide.

UNIVERSITAT ROVIRA I VIRGILI
NOVEL MOLECULAR CATALYSTS FOR WATER OXIDATION: TOWARDS ARTIFICIAL PHOTOSYNTHESIS
Sara Goberna Ferrón
Dipòsit Legal: T.189-2014

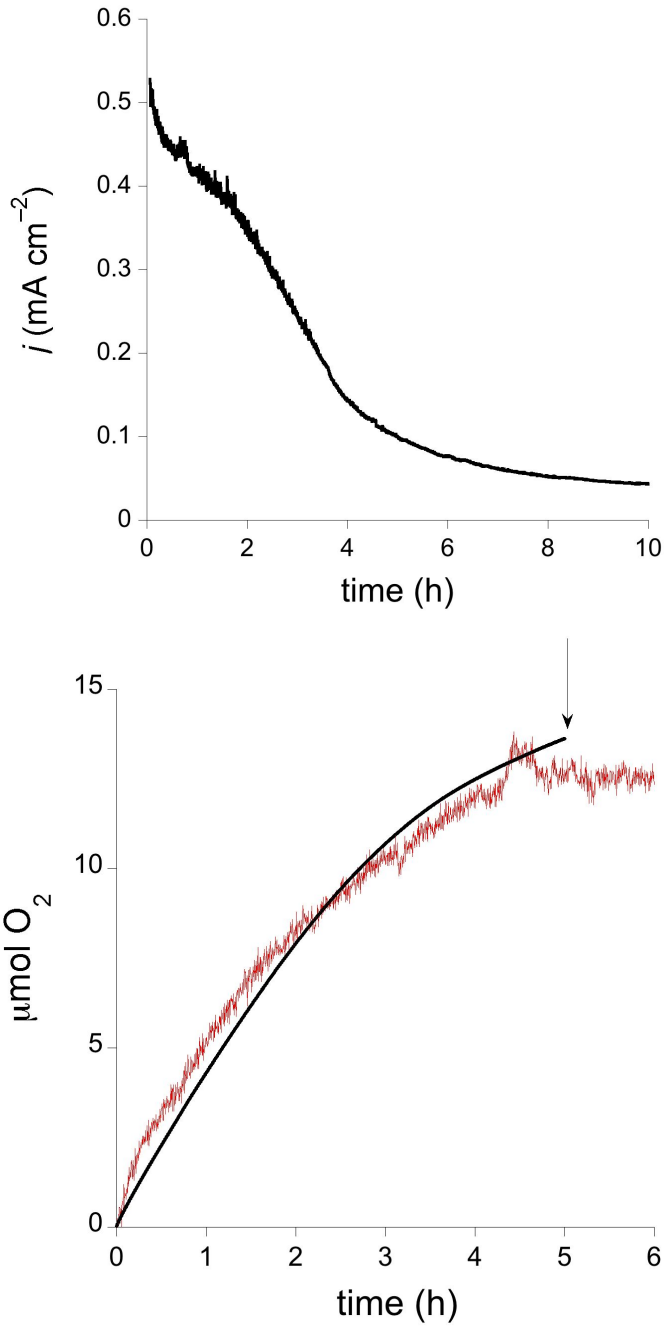

Figure 2.11. ***Top:*** *Current density profile during bulk water electrolysis under a constant applied potential of 1.5 V (vs NHE) in a 50 mM NaP_i buffer (pH = 7) with 1M $NaNO_3$ containing 1.0 mM of* ***Ru_2*****.** ***Bottom****: Corresponding catalytic O_2 evolution measured with a fluorescence sensor (red line) and theoretical production calculated for a quantitative Faradaic efficiency (black line). The arrow indicates the termination of electrolysis. FTO working electrode, Pt mesh counter electrode and Ag/AgCl (NaCl 3 M) reference electrode.*

UNIVERSITAT ROVIRA I VIRGILI
NOVEL MOLECULAR CATALYSTS FOR WATER OXIDATION: TOWARDS ARTIFICIAL PHOTOSYNTHESIS
Sara Goberna Ferrón
Dipòsit Legal: T.189-2014

It is important to point out, however, that although ruthenium oxide is a well-known WOC, the black solid formed *in situ* is not participating in the catalysis as supported by several key facts:

- The catalytic activity decreases with time while at the same time the solid particles are becoming more abundant.
- The "as used" electrode exhibits no catalytic activity when used for water electrolysis in a **Ru_2**–free solution with intensities very close to the original blank (Figure 2.13).
- The electrode is not coated with any residue as determined by EDX (Figure 2.14).

The latter fact is key, since the significant participation of heterogeneous catalysts formed during water oxidation requires their deposition on the electrode surface. Electron transfer between colloidal nanoparticles and the electron surface is very low efficient,[49] specially for multielectron processes. All these experimental evidences confirm that **Ru_2** is the only specie participating in the catalytic process. However, an additional comparison was performed, in a control experiment, bulk water electrolysis was performed under the same experimental conditions but with $RuCl_3$ (2 mM) instead of **Ru_2** (Figure 2.15). This experiment showed negligible catalytic activity in the presence of $RuCl_3$, confirming that ruthenium oxide nanoparticles are not participating in the catalysis under these experimental conditions.

UNIVERSITAT ROVIRA I VIRGILI
NOVEL MOLECULAR CATALYSTS FOR WATER OXIDATION: TOWARDS ARTIFICIAL PHOTOSYNTHESIS
Sara Goberna Ferrón
Dipòsit Legal: T.189-2014

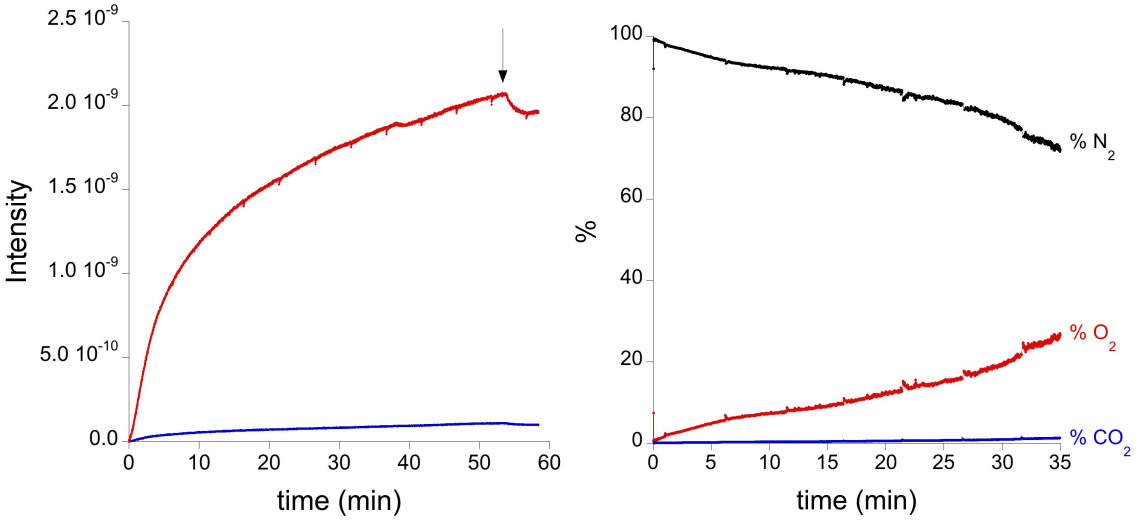

Figure 2.12. ***Left:*** *On-line mass spectroscopy signal for O_2 and CO_2 of 1.0 mM Ru_2 catalyzed bulk electrolysis at 1.5 V (vs NHE) in a 50 mM NaP_i buffer (pH = 7) with 1M $NaNO_3$. The arrow indicates the termination of electrolysis.* ***Right:*** *Percent abundance in the head–space obtained from mass spectroscopy data in the same experiment. FTO working electrode, Pt mesh counter electrode and Ag/AgCl (NaCl 3 M) reference electrode.*

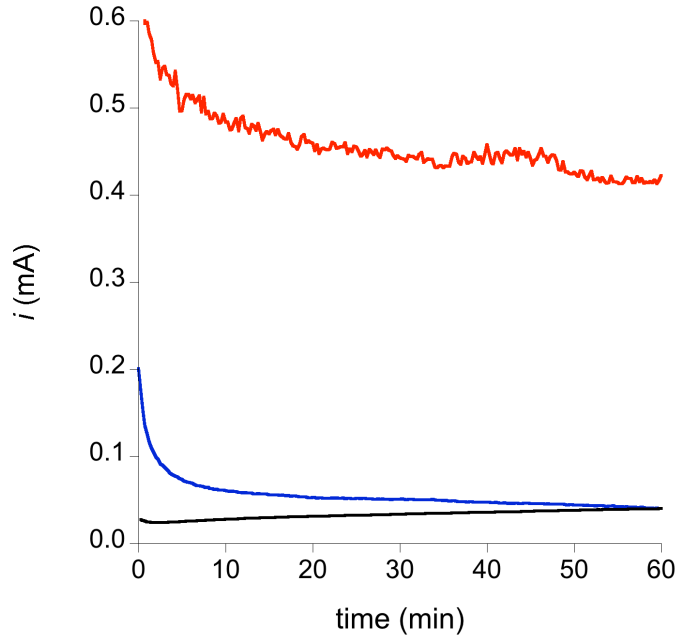

Figure 2.13. *Current density profile during bulk water electrolysis under a constant applied potential of 1.5 V with 1mM* ***Ru_2*** *(red line) in a 50 mM NaP_i buffer (pH = 7) with 1M $NaNO_3$. Blank experiment before (black line) and after (blue line) water electrolysis with the same working electrode. FTO working electrode, Pt mesh counter electrode and Ag/AgCl (NaCl 3 M) reference electrode.*

UNIVERSITAT ROVIRA I VIRGILI
NOVEL MOLECULAR CATALYSTS FOR WATER OXIDATION: TOWARDS ARTIFICIAL PHOTOSYNTHESIS
Sara Goberna Ferrón
Dipòsit Legal: T.189-2014

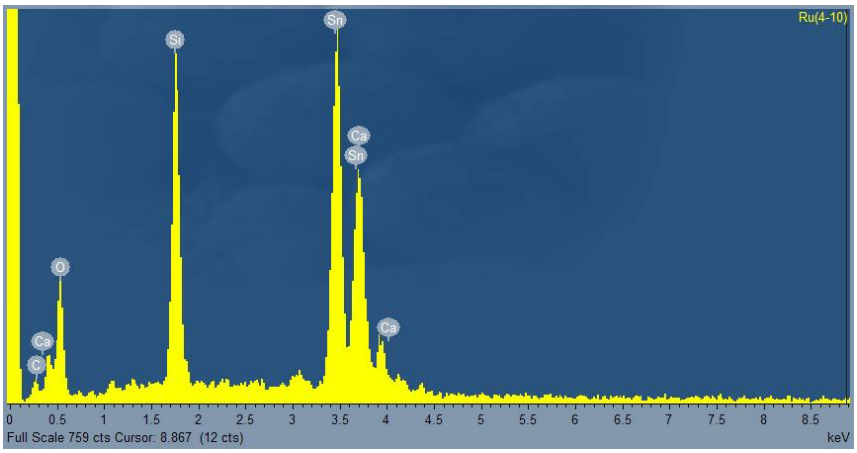

Figure 2.14. *EDX histogram acquired for an "as used" FTO electrode after 4 hours–bulk water electrolysis under a constant applied potential of 1.5 V (vs NHE) in a 50 mM NaP_i buffer (pH = 7) with 1M $NaNO_3$ containing 1.0 mM of* ***Ru_2****. The absence of any Ru residue demonstrates no oxide is being deposited on the electrode.*

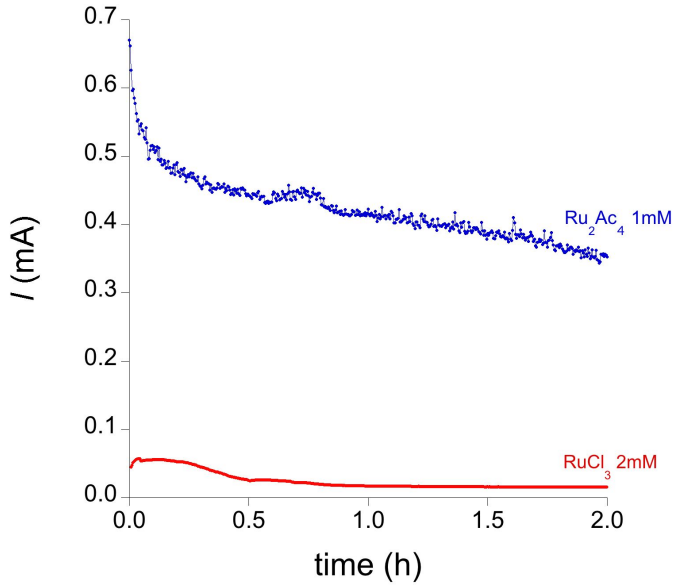

Figure 2.15. *Current profile during bulk water electrolysis in a 50 mM NaP_i buffer (pH = 7) with 1M $NaNO_3$. Applied voltage = 1.5 V (vs NHE) with 1 mM* ***Ru_2*** *(red line) and 2 mM $RuCl_3$ (black line). FTO working electrode, Pt mesh counter electrode and Ag/AgCl (NaCl 3 M) reference electrode.*

UNIVERSITAT ROVIRA I VIRGILI
NOVEL MOLECULAR CATALYSTS FOR WATER OXIDATION: TOWARDS ARTIFICIAL PHOTOSYNTHESIS
Sara Goberna Ferrón
Dipòsit Legal: T.189-2014

Effect of pH in the Catalytic Performance of Ru_2

Although previous experiments suggests that pH is not affecting the catalytic activity of **Ru_2**, a complete study of bulk water electrolysis at different pH was performed in order to determinate how pH affects the catalytic rates. Water electrolysis experiments were performed at a constant applied potential (1.5 V) with constant stirring using a glassy carbon working electrode at different pH values for the NaP_i buffer obtained by addition of aqueous solutions of H_3PO_4 or NaOH in the presence of 0.5 mM **Ru_2** (Figure 2.16, top). After 10 minutes–bulk water electrolysis (when current values are stable) the average of the current density (i / A cm^{-2}) values is used to plot log$i$ against the corresponding pH. Current densities indicated very little pH dependence and maintained the same magnitude in the 1 < pH < 10 range. Analogous results were obtained by lowering or increasing the pH value in the 1 < pH < 10 range. Moreover, in order to discard the possibility of small **Ru_2** concentration variations (by addition of H_3PO_4 or NaOH), these experiments were repeated with independently prepared solutions at each pH (Figure 2.16, bottom). Very similar results were obtained. This is a unique finding among homogeneous WOCs given that pH is typically a key parameter (Equation 2.6) regarding activity and also stability with very strict pH control requirements being operative.

$$E = +1.23 - 0.059(pH)\ V\ vs\ (NHE)\ at\ 25°C \qquad (Eq.\ 2.6)$$

These data also indicate that **Ru_2** achieves limiting catalytic rates at low pH values since, although overpotential increases with pH, this effect does not significantly alter the reaction kinetics. This fact has been demonstrated by repeating identical experiments at constant overpotential ($\eta = E_{appl} - E_0$) (Figure 2.17). In order to calculate the needed applied potential at each pH, equation 2.6 was used.

UNIVERSITAT ROVIRA I VIRGILI
NOVEL MOLECULAR CATALYSTS FOR WATER OXIDATION: TOWARDS ARTIFICIAL PHOTOSYNTHESIS
Sara Goberna Ferrón
Dipòsit Legal: T.189-2014

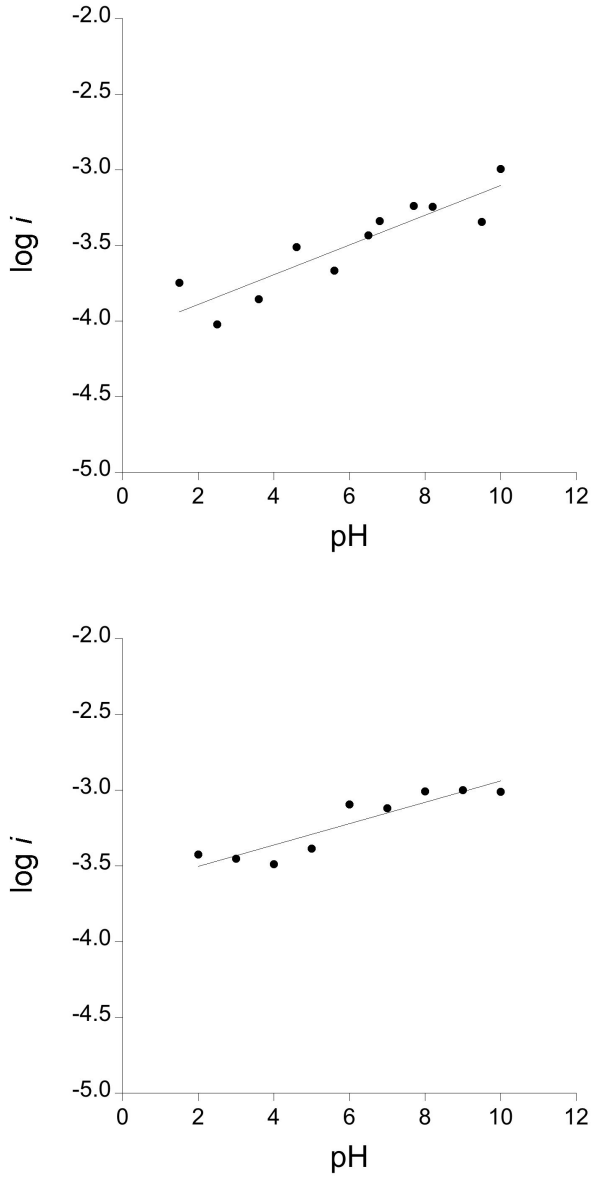

Figure 2.16. *pH dependence current density for bulk water electrolysis applying 1.5 V (vs NHE) to (top) 0.5 mM of* ***Ru₂*** *in 50 mM NaP_i buffer / 1M $NaNO_3$ adding H_3PO_4 or NaOH to adjust pH, and (bottom) to independently prepared 0.5 mM* ***Ru₂*** *solution at each pH in a 50 mM NaP_i buffer with 1M $NaNO_3$. Glassy Carbon working electrode, Pt wire counter electrode and Ag/AgCl (NaCl 3M) reference electrode.*

The evolution current density with pH at constant overpotential shows very little pH dependence, confirming that the catalytic rates for water oxidation are practically

UNIVERSITAT ROVIRA I VIRGILI
NOVEL MOLECULAR CATALYSTS FOR WATER OXIDATION: TOWARDS ARTIFICIAL PHOTOSYNTHESIS
Sara Goberna Ferrón
Dipòsit Legal: T.189-2014

pH–independent when **Ru_2** is used as catalyst. In addition, TOF values can be estimated at different pH from pH = 6 to pH = 10, where the $Ru_2^{+5/+4}$ couple is reversible, using cyclic voltammetry. As described above (Method 1), the number of molecules of catalyst interacting with the electrode in a diffusion–controlled conditions were calculated and used to estimate TOF following equation 2.3. The values of TOF, of the same order of magnitude, are practically independent of pH (Table 2.1), confirming the pH–independence of the catalytic activity of **Ru_2**.

One final important point is that all of the experiments described in this work yield identical results when the mixed-valence Ru_2^{+5} derivative $Ru_2(\mu\text{-}O_2CCH_3)_4Cl$ is used as the catalyst, a result that is in accord with the fact that the initial oxidation state of the complex does not affect its catalytic activity or electrochemical behavior.

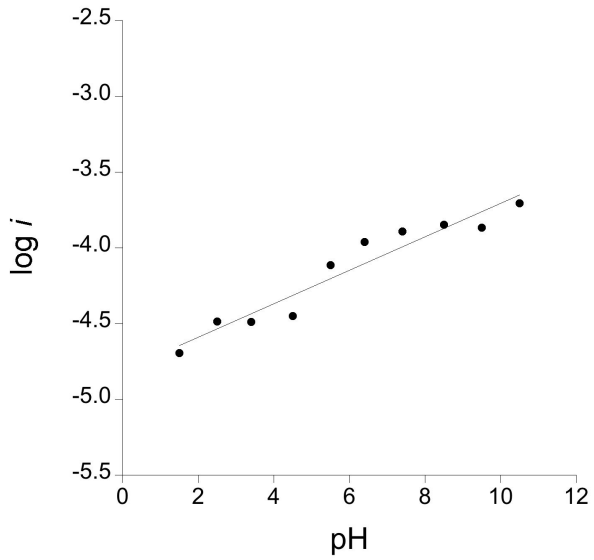

Figure 2.17. *Plot of the pH dependence of the current density for bulk water electrolysis under a constant applied overpotential of 338 mV to independently prepared 0.5 mM **Ru_2** solution at each pH in a 50 mM NaP_i buffer with 1M $NaNO_3$. Glassy Carbon working electrode, Pt wire counter electrode and Ag/AgCl (NaCl 3M) reference electrode.*

UNIVERSITAT ROVIRA I VIRGILI
NOVEL MOLECULAR CATALYSTS FOR WATER OXIDATION: TOWARDS ARTIFICIAL PHOTOSYNTHESIS
Sara Goberna Ferrón
Dipòsit Legal: T.189-2014

pH	TOF at E_{appl} = 2.0 V (vs NHE) (s^{-1})
6	2.1
7	7.6
8	4.1
9	6.3
10	4.5

Table 2.1. *TOF values for* ***Ru_2*** *(0.5 mM) catalyzed water oxidation at different pH values in a 50 mM NaP_i buffer with 1M $NaNO_3$ (pH adjusted adding H_3PO_4 or NaOH).*

UNIVERSITAT ROVIRA I VIRGILI
NOVEL MOLECULAR CATALYSTS FOR WATER OXIDATION: TOWARDS ARTIFICIAL PHOTOSYNTHESIS
Sara Goberna Ferrón
Dipòsit Legal: T.189-2014

2. M–M Bonded Diruthenium WOC

UNIVERSITAT ROVIRA I VIRGILI
NOVEL MOLECULAR CATALYSTS FOR WATER OXIDATION: TOWARDS ARTIFICIAL PHOTOSYNTHESIS
Sara Goberna Ferrón
Dipòsit Legal: T.189-2014

2.3

Conclusions

The results of this chapter reveal that metal-metal bonded diruthenium complexes are viable water oxidation catalysts. The **Ru_2** paddlewheel compound catalyzes water electrolysis over a wide pH range (1 - 10) at high catalytic rates with quantitative efficiencies in dilute solutions. Although it is detected a low oxidative deactivation due to the instability of the acetate ligands observed at high potentials, this disadvantage can be overcome by increasing metal–metal bond stability by employing different bridging ligands as well as other transition metals to tune the performance. The possibility of ruthenium oxide being participating in the catalysis is ruled out by several control experiments and characterization of the "as used" electrode.

The advantage of this approach is that the metal–metal bond platform allows for the use of common ligands such as acetate to develop new WOCs without the need for complex organic chelating agents. The rich chemistry and versatility of metal–metal bonded molecules clearly opens a great opportunity to find exceptional WOC activity in this field, developing an attractive new family of fast water oxidation electrocatalysts.

UNIVERSITAT ROVIRA I VIRGILI
NOVEL MOLECULAR CATALYSTS FOR WATER OXIDATION: TOWARDS ARTIFICIAL PHOTOSYNTHESIS
Sara Goberna Ferrón
Dipòsit Legal: T.189-2014

UNIVERSITAT ROVIRA I VIRGILI
NOVEL MOLECULAR CATALYSTS FOR WATER OXIDATION: TOWARDS ARTIFICIAL PHOTOSYNTHESIS
Sara Goberna Ferrón
Dipòsit Legal: T.189-2014

2.4

Experimental

Synthesis

All reagents are commercially available (> 99.9 %, Sigma-Aldrich) and used without further purification. $Ru_2(\mu\text{-}O_2CCH_3)_4$ (**Ru_2**) and $Ru_2(\mu\text{-}O_2CCH_3)_4Cl$ were prepared according to literature methods.[20-22]

- $Ru_2(\mu\text{-}O_2CCH_3)_4$ (**Ru_2**) synthesis was performed in two steps.

  Step 1. Preparation of $Ru^{II}Cl_2$: $Ru^{III}Cl_3$ (2.15 g, 10.3 mmol) was reduced by H_2 under slight pressure (≈1.06 atm.) catalyzed by Pt black (0.002 g, 0.01 mmol) in a 200 mL methanol solution during 1.5 days (non-stop reaction), during this time the solution goes form brown to blue. The dark blue solution ($Ru^{II}Cl_2$) is collected by filtration under N_2 atmosphere.

  Step 2. Preparation of $Ru_2(\mu\text{-}O_2CCH_3)_4$: Refluxing the solution of $RuCl_2$ in the presence of an excess of NaOAc (2.3 g, 28.03 mmol) during 18 hours. The dark brown powder of compound $Ru_2(\mu\text{-}O_2CCH_3)_4$ was collected by filtration under nitrogen, washed with methanol and dried under vacuum (yield = 40 %).

- $Ru_2(\mu\text{-}O_2CCH_3)_4Cl$ was synthetized by mixing $RuCl_3$ (1.14 g, 4.34 mmol) and LiCl (1.0 g, 0.024 mol) in 35 mL of CH_3COOH + 7.0 mL of $C(CH_3CO)_2$. The reaction mixture was refluxed under slow O_2 stream overnight. The resulting orange powder of compound $Ru_2(\mu\text{-}O_2CCH_3)_4Cl$ was collected by filtration, washed with cold methanol and ether, and dried under vacuum (yield 50 %).

UNIVERSITAT ROVIRA I VIRGILI
NOVEL MOLECULAR CATALYSTS FOR WATER OXIDATION: TOWARDS ARTIFICIAL PHOTOSYNTHESIS
Sara Goberna Ferrón
Dipòsit Legal: T.189-2014

Electrochemistry

All experiments were performed with a Biologic SP-150 potentiostat. Cyclic voltammetry experiments were performed with a 0.07 cm^2 glassy carbon button working electrode, a Pt wire counter electrode and a Ag/AgCl (NaCl 3M) reference in a 50 mM NaP_i buffer (pH 7) with 1 M $NaNO_3$ in milli-Q. The working electrodes were polished with 3 μm and 1 μm diamond paste and rinsed with distilled water prior to use.

Cyclic voltammograms were collected in the -0.4 - 2 V range (vs NHE) at different scan rates between 1 and 100 mV/s and different **Ru_2** concentrations between 0.2 and 1.1 mM.

Bulk water electrolysis were carried out with stirring in a two-chamber cell, with a porous frit connecting both chambers (Figure 2.18). A Pt mesh counter electrode (99.9 % Pt Goodfellow plain weave mesh, 0.25 mm nominal aperture, 0.06 mm wire diameter, 82 x 82 wires/inch, 65 % open area) was placed in one chamber. The other chamber contained a FTO-coated glass working electrode (Pilkington NSG TEC 15A 2.3 mm slides with 12-14 Ω/sq. surface resistivity) and a BASi Ag/AgCl (NaCl 3 M) reference electrode. FTO slides were cleaned prior use by sonication for 10 minutes in alkaline soapy solution *(LABWASH),* deionized water and isopropanol, followed by annealing at 400 ºC for 30 minutes. Typical electrolysis experiments were carried out in a 50 mM NaP_i buffer (pH = 7) with 1 M $NaNO_3$. Ohmic drop was compensated by using the positive feedback compensation implemented in the instrument.

UNIVERSITAT ROVIRA I VIRGILI
NOVEL MOLECULAR CATALYSTS FOR WATER OXIDATION: TOWARDS ARTIFICIAL PHOTOSYNTHESIS
Sara Goberna Ferrón
Dipòsit Legal: T.189-2014

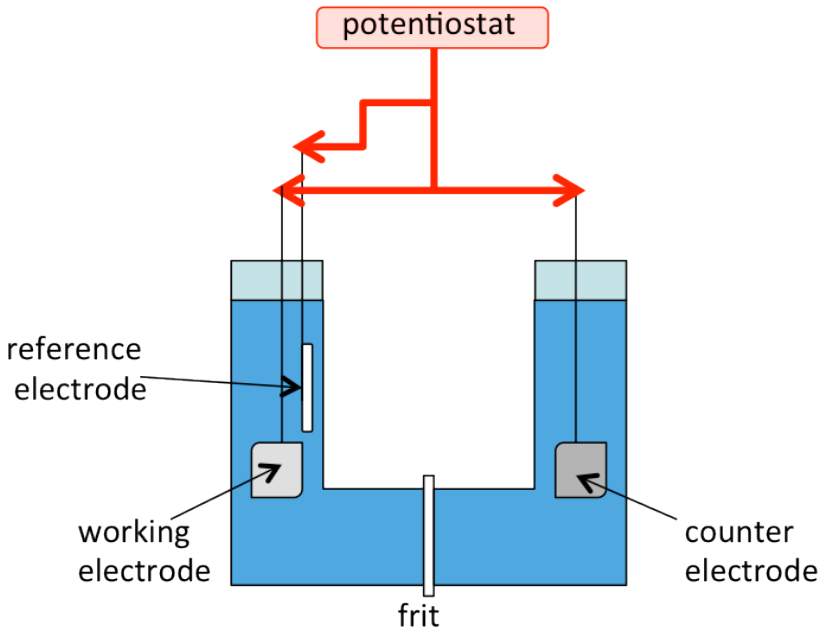

Figure 2.18. *Schema of a water electrolysis cell*

Oxygen evolution was determined with an Ocean Optics NeoFOX oxygen sensing system equipped with a FOXY probe during controlled potential electrolysis at 1.5V (*vs* NHE) using a FTO-coated glass working electrode. A two compartment H-cell separated by a frit (Figure 2.18) was used for these experiments. The working compartment contained the FTO-coated glass working electrode, the Ag/AgCl reference electrode and the FOXY probe and was filled with 20 mL of a $Ru_2(\mu\text{-}O_2CCH_3)_4$ 1 mM solution in 50 mM NaP_i buffer with 1 M $NaNO_3$ as the electrolyte. The second compartment of the electrochemical cell contained the platinum mesh auxiliary electrode and was filled with 20 mL of buffer. The solutions were capped with a septum and stirred vigorously. The system is degassed by an N_2 flow through the gas-space while stirring during 30 minutes to achieve gas–liquid equilibria. The set–up was calibrated using the same procedure substitung the reaction solutions by water. By addition of known quantities of the corresponding pure gas, a calibration slope was obtained. The slope was employed for the quantification of oxygen in the

UNIVERSITAT ROVIRA I VIRGILI
NOVEL MOLECULAR CATALYSTS FOR WATER OXIDATION: TOWARDS ARTIFICIAL PHOTOSYNTHESIS
Sara Goberna Ferrón
Dipòsit Legal: T.189-2014

catalysis experiments carried out.

Mass spectroscopy measurements were performed using an Omnistar TM GSD 301 C (Pfeiffer) quadrupole mass spectrometer apparatus. The system is degassed by a N_2 flow through the gas-space while stirring during 30 minutes. The composition of the gas phase (O_2 *m/z*=32; N_2 *m/z*=28 and CO_2 *m/z*=44) was measured during controlled potential electrolysis experiments by inserting the MS-spectrometer cannula in the head-space of the anodic compartment through a septum.

Physical Methods.

Scanning electron microscopy (SEM) and electron dispersive x-ray spectroscopic (EDX) analysis were performed with a JEOL-JSM6400 microscope equipped with an Oxford EDX analyzer (Oxford Instruments).

UNIVERSITAT ROVIRA I VIRGILI
NOVEL MOLECULAR CATALYSTS FOR WATER OXIDATION: TOWARDS ARTIFICIAL PHOTOSYNTHESIS
Sara Goberna Ferrón
Dipòsit Legal: T.189-2014

2.5

References

1 Bertrand, J. A., Cotton, F. A. & Dollase, W. A. The Metal-Metal Bonded, Polynuclear Complex Anion in CsReCl4. *J. Am. Chem. Soc.* **85**, 1349-1350 (1963).

2 Bennett, M. J., Cotton, F. A. & Walton, R. A. A Rhenium-to-Rhenium Triple Bond. *J. Am. Chem. Soc.* **88**, 3866-3867 (1966).

3 Bennett, M. J., Cotton, F. A. & Walton, R. A. A Structural and Magnetic Study of Pentachloro-bis(1,5-Dithiahexane) Dirhenium. *Proc. R. Soc. Lond. A.* **303**, 175-192 (1968).

4 Cotton, F., Curtis, N., Harris, C., Johnson, B., Lippard, S., Mague, J., Robinson, W. & Wood, J. Mononuclear and Polynuclear Chemistry of Rhenium (III): Its Pronounced Homophilicity. *Science* **145**, 1305-1307 (1964).

5 Cotton, F. A. Metal-Metal Bonding in [Re2X8]2- Ions and Other Metal Atom Clusters. *Inorg. Chem.* **4**, 334-336 (1965).

6 E. Peligot. Sur un Nouvel Oxyde de Chrome. *Compt. Rendus* **19**, 609-611 (1844).

7 Cotton, F. A., Murillo, C. A., and Walton, R. A. *Multiple Bonds Between Metal Atoms*. 3rd edn, (Springer, 2005).

8 Cotton, F. Centenary Lecture. Quadruple bonds and other multiple metal to metal bonds. *Chem. Soc. Rev.* **4**, 27-53 (1975).

9 <http://www.science.tamu.edu/articles/548> (

10 Cotton, F., Lin, C. & Murillo, C. Supramolecular arrays based on dimetal building units. *Acc. Chem. Res.* **34**, 759-771 (2001).

11 Miyasaka, H., Asai, Y., Motokawa, N., Kubo, K. & Yamashita, M. Magnetic/conducting bifunctionality due to pi/sigma-conjugated functional moieties in a stacked ferrimagnetic chain. *Inorg. Chem.* **49**, 9116-9118 (2010).

12 Miyasaka, H., Clérac, R., Campos-Fernández, C. & Dunbar, K. Metal-metal bonded diruthenium(II, III) assemblies with the polycyano anionic linkers N(CN)2-, C(CN)3-, and 1,4-dicyanamido-2,5-dimethylbenzene (DM-dicyd2-): syntheses, structures, and magnetic properties. *Inorg. Chem.* **40**, 1663-1671 (2001).

13 Motokawa, N., Matsunaga, S., Takaishi, S., Miyasaka, H., Yamashita, M. & Dunbar, K. Reversible magnetism between an antiferromagnet and a ferromagnet related to solvation/desolvation in a robust layered [Ru2]2TCNQ charge-transfer system. *J. Am. Chem. Soc.* **132**, 11943-11951 (2010).

UNIVERSITAT ROVIRA I VIRGILI
NOVEL MOLECULAR CATALYSTS FOR WATER OXIDATION: TOWARDS ARTIFICIAL PHOTOSYNTHESIS
Sara Goberna Ferrón
Dipòsit Legal: T.189-2014

14 Miyasaka, H., Izawa, T., Takahashi, N., Yamashita, M. & Dunbar, K. Long-range ordered magnet of a charge-transfer Ru2(4+)/TCNQ two-dimensional network compound. *J. Am. Chem. Soc.* **128**, 11358-11359 (2006).

15 Kadish, K., Wang, L.-L., Thuriere, A., Van Caemelbecke, E. & Bear, J. Factors affecting the electrochemical and spectroelectrochemical properties of diruthenium(III,II) complexes containing four identical unsymmetrical bridging ligands. *Inorg. Chem.* **42**, 834-843 (2003).

16 Baxter, D., V., Chisholm, M., H. , Lynn, M., A. , Putilina, E., F. , Trzaska, S., T. & Swager, T. Studies of Thermotropic Properties and the Mesophase of Mixtures of n -Alkanoates and Perfluoro- n -alkanoates of Dimolybdenum (MM). *Chem. Mater.* **10**, 1758-1763 (1998).

17 Mashima, K., Tanaka, M., Kaneda, Y., Fukumoto, A., Mizomoto, H., Tani, K., Nakano, H., Nakamura, A., Sakaguchi, T., Kamada, K. & Ohta, K. Large Third-Order Nonlinear Optical Susceptibilities of Multiply-Bonded M2(pyphos)4 and M2Pd2Cl2(pyphos)4 (M = Cr, Mo; Pyphos = 6-Diphenylphosphino-2-pyridonate) by Picosecond Degenerate Four-Wave Mixing Method *Chem. Lett.* **26**, 411-415 (1997).

18 Aguirre, J., Angeles-Boza, A., Chouai, A., Pellois, J.-P., Turro, C. & Dunbar, K. Live cell cytotoxicity studies: documentation of the interactions of antitumor active dirhodium compounds with nuclear DNA. *J. Am. Chem. Soc.* **131**, 11353-11360 (2009).

19 Chifotides, H. & Dunbar, K. Interactions of metal-metal-bonded antitumor active complexes with DNA fragments and DNA. *Acc. Chem. Res.* **38**, 146-156 (2005).

20 Doyle, M., Duffy, R., Ratnikov, M. & Zhou, L. Catalytic carbene insertion into C-H bonds. *Chem. Rev.* **110**, 704-724 (2010).

21 Hansen, J. r. & Davies, H. High Symmetry Dirhodium(II) Paddlewheel Complexes as Chiral Catalysts. *Coord. Chem. Rev.* **252**, 545-555 (2008).

22 Daren J. Timmons & Doyle, M. P. in *Multiple Bonds Between Metal Atoms* Ch. 13, 591-632 (2005).

23 Doyle, M. Perspective on dirhodium carboxamidates as catalysts. *J. Org. Chem* **71**, 9253-9260 (2006).

24 Heyduk, A., F. , Macintosh, A., M. & Nocera, D., G. . Four-Electron Photochemistry of Dirhodium Fluorophosphine Compounds. *J. Am. Chem. Soc.* **121** (1999).

25 Cook, T. R., Esswein, A., J. & Nocera, D. G. Metal-halide bond photoactivation from a PtIII-AuII complex. *J. Am. Chem. Soc.* **129**, 10094-10095 (2007).

26 Teets, T. S., Lutterman, D. A. & Nocera, D. G. Halogen photoreductive elimination from metal-metal bonded iridium(II)-gold(II) heterobimetallic complexes. *Inorg. Chem.* **49**, 3035-3043 (2010).

27 Esswein, A., J. , Veige, A., S. , Piccoli, P., M., Schultz, A., J. & Nocera, D., G. . Intramolecular C-H Bond Activation and Redox Isomerization across Two-

UNIVERSITAT ROVIRA I VIRGILI
NOVEL MOLECULAR CATALYSTS FOR WATER OXIDATION: TOWARDS ARTIFICIAL PHOTOSYNTHESIS
Sara Goberna Ferrón
Dipòsit Legal: T.189-2014

Electron Mixed Valence Diiridium Cores. *Organometallics* **27**, 1073-1083 (2008).

28 Esswein, A. J., Veige, A. S. & Nocera, D. G. A photocycle for hydrogen production from two-electron mixed-valence complexes. *J. Am. Chem. Soc.* **127**, 16641-16651 (2005).

29 Heyduk, A. F. & Nocera, D. G. Hydrogen produced from hydrohalic acid solutions by a two-electron mixed-valence photocatalyst. *Science* **293**, 1639-1641 (2001).

30 Kampa, M., Pandelia, M.-E., Lubitz, W., van Gastel, M. & Neese, F. A metal-metal bond in the light-induced state of [NiFe] hydrogenases with relevance to hydrogen evolution. *J. Am. Chem. Soc.* **135**, 3915-3925 (2013).

31 Teets, T. S. & Nocera, D. G. Mechanistic studies of O2 reduction effected by group 9 bimetallic hydride complexes. *J. Am. Chem. Soc.* **133**, 17796-17806 (2011).

32 Teets, T. S. & Nocera, D. G. Oxygen reduction reactions of monometallic rhodium hydride complexes. *Inorg. Chem.* **51**, 7192-7201 (2012).

33 Teets, T. S., Cook, T. R., McCarthy, B. D. & Nocera, D. G. Oxygen reduction to water mediated by a dirhodium hydrido-chloride complex. *J. Am. Chem. Soc.* **133**, 8114-8117 (2011).

34 Aquino, M. A. S. Diruthenium and diosmium tetracarboxylates: synthesis, physical properties and applications. *Coord. Chem. Rev.* **170**, 141-202 (1998).

35 Cotton, F. A. & Pedersen, E. Magnetic and electrochemical properties of transition metal complexes with multiple metal-to-metal bonds. IV. Octachlorodimolybdate(n-) with n = 3 and 4 and tetrabutyratodimolybdate(n+) with n = 0 and 1. *Inorg. Chem.* **14**, 388-391 (1975).

36 Cotton, F. A., Marek, M. & Bianxiao, Z. Oxidation states available to the diruthenium n+ core in tetracarboxylato-bridged species. *Inorg. Chem.* **27**, 4368-4372 (1988).

37 Lindsay, A., J., Wilkinson, G., Motevalli, M. & Hursthouse, M., B. The synthesis, magnetic, electrochemical, and spectroscopic properties of diruthenium(II,II) tetra-u-carboxylates and their adducts. X-Ray structures of Ru2(O2CR)4L2(R = Me, L = H2O or tetrahydrofuran; R = Et, L = Me2CO). *J. Chem. Soc., Dalton Trans.*, 2321-2326 (1985).

38 Wilson, C. R. & Taube, H. Acetate complexes of dirhodium and diruthenium. Aquation and reduction-oxidation. *Inorg. Chem.* **14**, 2276-2279 (1975).

39 Yeager, E. Electrocatalysts for O 2 reduction. *Electrochim. Acta* **29**, 1527-1537 (1984).

40 Collin, J. P., Abdelaziz, J., Jean Pierre, S., William, C. K., Margaret, A. M., Nancy, L. K., William, T. A. H. & Galen, D. S. Synthesis and electrochemical characterization of binuclear rhodium and ruthenium complexes with 1,8-naphthyridine-2,7-dicarboxylate. X-ray molecular structure of tris(.mu.-

UNIVERSITAT ROVIRA I VIRGILI
NOVEL MOLECULAR CATALYSTS FOR WATER OXIDATION: TOWARDS ARTIFICIAL PHOTOSYNTHESIS
Sara Goberna Ferrón
Dipòsit Legal: T.189-2014

acetato)(1,8-naphthyridine-2,7-dicarboxylato)diruthenium. *Inorg. Chem.* **29**, 2238-2241 (1990).

41 Cotton, F. A., Datta, T., Labella, L. & Shang, M. Stabilizing of the Ru 2(6+) core. Use of highly charged ligands such as sulfate and phosphate. *Inorg. Chim. Acta* **203**, 55-60 (1993).

42 Costentin, C., Drouet, S., Robert, M. & Saveant, J.-M. Turnover numbers, turnover frequencies, and overpotential in molecular catalysis of electrochemical reactions. Cyclic voltammetry and preparative-scale electrolysis. *J. Am. Chem. Soc.* **134**, 11235-11242 (2012).

43 Blakemore, J. D., Schley, N. D., Olack, G. W., Incarvito, C. D., Brudvig, G. W. & Crabtree, R. H. Anodic deposition of a robust iridium-based water-oxidation catalyst from organometallic precursors. *Chemical Science* **2**, 94-98 (2011).

44 Sun, L., Tong, L. & Göthelid, M. Oxygen Evolution at Functionalized Carbon Surface: A Strategy for Immobilization of Molecular Water Oxidation Catalysts. *Chem. Commun.* **48**, 10025–10027 (2012).

45 Zanello, P. *Inorganic electrochemistry : theory, practice and applications*. (The Royal Society of Chemistry: Cambridge, UK, 2003).

46 Barnett, S., Goldberg, K. & Mayer, J. A soluble copper-bipyridine water-oxidation electrocatalyst. *Nature Chem.* **4**, 498-502 (2012).

47 Jiang, Y., Li, F., Zhang, B., Li, X., Wang, X., Huang, F. & Sun, L. Promoting the activity of catalysts for the oxidation of water with bridged dinuclear ruthenium complexes. *Angew. Chem.* **52**, 3398-3401 (2013).

48 Duan, L., Bozoglian, F., Mandal, S., Stewart, B., Privalov, T., Llobet, A. & Sun, L. A molecular ruthenium catalyst with water-oxidation activity comparable to that of photosystem II. *Nature Chemistry* **4**, 418-423 (2012).

49 Schley, N. D., Blakemore, J. D., Subbaiyan, N. K., Incarvito, C. D., D'Souza, F., Crabtree, R. H. & Brudvig, G. W. Distinguishing Homogeneous from Heterogeneous Catalysis in Electrode-Driven Water Oxidation with Molecular Iridium Complexes. *J. Am. Chem. Soc.* **133**, 10473-10481 (2011).

UNIVERSITAT ROVIRA I VIRGILI
NOVEL MOLECULAR CATALYSTS FOR WATER OXIDATION: TOWARDS ARTIFICIAL PHOTOSYNTHESIS
Sara Goberna Ferrón
Dipòsit Legal: T.189-2014

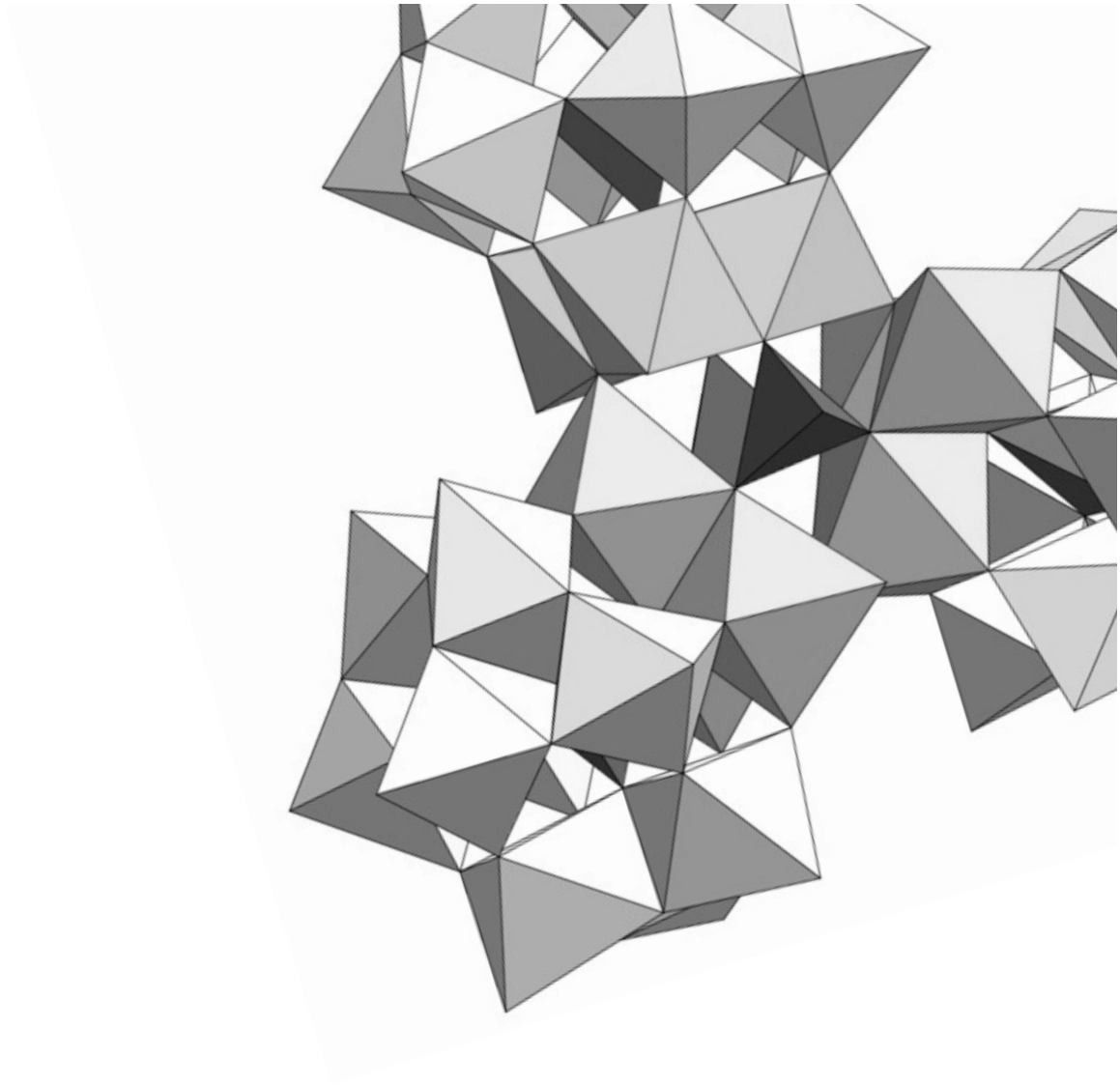

Chapter 3

Nonanuclear Cobalt Polyoxometalate Water Oxidation Catalyst

UNIVERSITAT ROVIRA I VIRGILI
NOVEL MOLECULAR CATALYSTS FOR WATER OXIDATION: TOWARDS ARTIFICIAL PHOTOSYNTHESIS
Sara Goberna Ferrón
Dipòsit Legal: T.189-2014

UNIVERSITAT ROVIRA I VIRGILI
NOVEL MOLECULAR CATALYSTS FOR WATER OXIDATION: TOWARDS ARTIFICIAL PHOTOSYNTHESIS
Sara Goberna Ferrón
Dipòsit Legal: T.189-2014

3.1

Introduction

Polyoxometalates (POMs) are early−transition metal (especially vanadium molybdenum and tungsten) oxygen anion clusters.[1-4] Although they have been investigated since the last third of the 19th century, it is only since the early fifties that more and more techniques have greatly aided the research in this field, enabling the relation between solid−state and solution species, and the link between structure and reactivity. The chemically robust nature of POMs, coupled with their highly tunable physicochemical properties lead to applications in several areas including medicine,[5-14] magnetism,[15-19] chirality,[20-27] and others.[28]

Polyaoxometallates are constructed of linked polyhedra MO_x (usually octahedra or tetrahedra). Among the wide variety of POMs, the class of isopoly– ($[M_mO_y]^{p-}$) and heteropolyoxoanions ($[X_xM_mO_y]^{q-}$) of the early transition metals are hydrolytically stable. M and X are called *addenda atom* and *heteroatom* respectively, M = molybdenum, tungsten, vanadium, niobioum or tantalum or mixture of them; X = p or d block elements found in one or more polyhedral positions in the polyanion unit (Figure 3.1). Heteropolyoxoanions tend to be stable over a wider pH range than the isopolyanions. In the common Keggin structure $[XM_{12}O_{40}]^{n-}$ (Figure 3.1, bottom left), structurally determined by Keggin in the 1930s,[29,30] four trimetallic M_3O_{13} groups are arranged around a central tetrahedron (XO_4). Each MO_6 octahedra is sharing two edges with other MO_6 and the four M_3O_{13} groups are attached to one another by corner sharing bridges. The total assembly contains 40 close−packed oxygen and a tetrahedral pocket in its center for the heteroatom. There are five isomers, designated by the prefixes α-, β-, γ-, δ- and ε- depending on the different rotational orientations of the M_3O_{13} units. The original Keggin structure, the α isomer, is the

UNIVERSITAT ROVIRA I VIRGILI
NOVEL MOLECULAR CATALYSTS FOR WATER OXIDATION: TOWARDS ARTIFICIAL PHOTOSYNTHESIS
Sara Goberna Ferrón
Dipòsit Legal: T.189-2014

most prevalent and thermodynamic stable isomer.

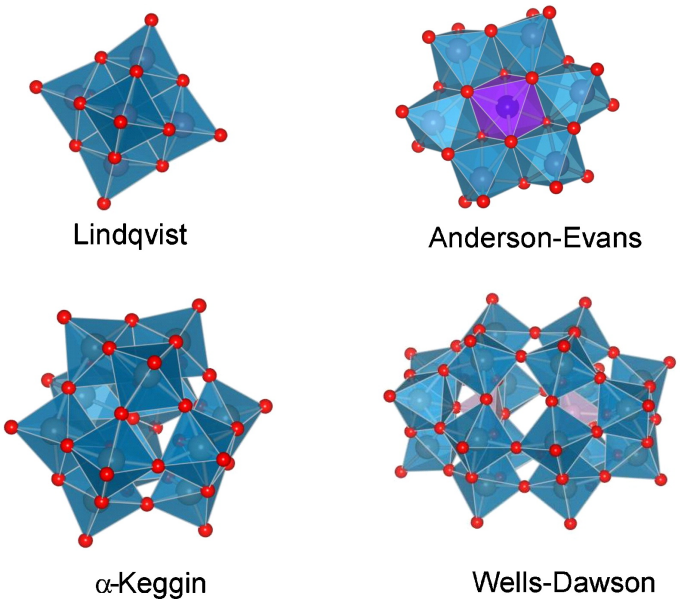

Figure 3.1. *Some classical structures of polyoxometalates. Top right: Lindqvist* $[M_6O_{19}]^{2-}$*; Top left: Anderson- Evans* $[TeMo_6O_{24}]^{6-}$*; Bottom right: Keggin* $[XM_{12}O_{40}]^{n-}$*, Bottom left: Wells –Dawson* $[X_2M_{18}O_{62}]^{n-}$*.*[31]

Keggin-type units are particularly convenient for preparing lacunary species, "defect" structures where one or more *addenda atoms* have been removed along with the corresponding terminal oxygen atoms. These lacunary POMs have high negative charge densities, and are good inorganic multidentate ligands to stabilize multi−metal oxide clusters. Thus, the robust and redox inert structure of the lacunary Keggin ligands has been exploited for the preparation of redox active cores, with many applications in catalysis. For example, excellent catalytic activity has been achieved in selective oxidation of organic substrates and sulfoxidation.[2,32-38] Very recently, POMs has been considered promising candidates as catalysts for water oxidation for several reasons:

- They are C-free complexes, being perfectly stable towards oxidative degradation in aqueous media.

UNIVERSITAT ROVIRA I VIRGILI
NOVEL MOLECULAR CATALYSTS FOR WATER OXIDATION: TOWARDS ARTIFICIAL PHOTOSYNTHESIS
Sara Goberna Ferrón
Dipòsit Legal: T.189-2014

- Their oxo−bridged structure allows for reversible proton exchange with the solvent, a feature usually combined with the subsequent oxidation steps in the reaction mechanism of WOCs.
- The ligands proximal to the redox-active metal center(s), that can be protonated or deprotonated under the conditions of catalytic turnover, allows for a better PCET capability.

Since Shannon and coworkers discover in 2004 the electrochemical production of oxygen in the presence of a Ruthenium−substituted POM, $Na_{14}[Ru^{III}_2Zn_2(H_2O)_2(ZnW_9O_{34})_2]$,[39] there has been several reports of other POMs as WOCs.[40-42] One of the major breakthroughs was achieved in 2008, when $[Ru_4O_4(OH)_2(H_2O)_4(SiW_{10}O_{36})_2]^{10-}$ (**1.20**, Figure 1.18) was simultaneously reported by two research groups. This cluster showed an extraordinary activity and stability towards water oxidation.[43,44] However, the oxygen evolving core was still made of Ru, an expensive material, rendering it unsuitable for use on a technologically relevant process. For this reason, $[Co_4(H_2O)_2(PW_9O_{34})_2]^{10-}$ (**Co_4**, **1.47**, Figure 1.27), reported by Hill et al., was one of the most important discoveries in the field of water oxidation, since it was defined as the first carbon−free homogeneous WOC obtained from abundant metals.[45] The activity of **Co_4** as a homogeneous WOC has been put into question. It was first reported that it decomposes during electrocatalytic water oxidation to generate a cobalt oxide film that rapidly becomes the major catalyst.[46] Its activity as a catalyst for photo-induced water oxidation with $[Ru(bpy)_3]^{2+}$ as sensitizer and persulfate as oxidant has been the subject of contradictory reports.[47,48]

Surprisingly, seven other cobalt−containing POMs were tested by Hill's group, but none of them showed any significant activity, although their reactivity should not differ much from that of **Co_4** based on their structural features. Among all the POMs tested, the main difference seems to be the pH range in which these polyanions are stable in solution. **Co_4** is prepared at the highest pH among them. More recently,

UNIVERSITAT ROVIRA I VIRGILI
NOVEL MOLECULAR CATALYSTS FOR WATER OXIDATION: TOWARDS ARTIFICIAL PHOTOSYNTHESIS
Sara Goberna Ferrón
Dipòsit Legal: T.189-2014

another cobalt-containing polymolybdate has been reported as a WOC but with very different structural features.[49]

In this chapter it is presented the catalytic activity towards water oxidation of a cobalt-containing POM with higher nuclearity: the nonanuclear $[Co_9(H_2O)_6(OH)_3(HPO_4)_2(PW_9O_{34})_3]^{16-}$ cluster (**Co_9**, Figure 3.2). This POM is prepared and stable at a higher pH than **Co_4**. It forms in a solution of sodium tungstate, sodium phosphate, and cobalt(II) acetate at pH > 7. Its molecular structure[50] contains nine exchange–coupled Co(II) ions in octahedral sites: three triangular entities Co_3O_{12} belonging to the three Keggin fragments are connected by two oxygen bridges and two HPO_4^{2-} anions in order to form a triangle of triangles (Figure 3.2). In the Co_3O_{12} triangles the three $Co^{II}O_6$ octahedra are sharing edges. Six of the Co ions complete their coordination sphere with terminal water molecules. The structural differences with **Co_4** are (i) a triangle of triangles versus rhombohedral core structure, (ii) the presence of hydroxyl bridges versus only oxo bridges, (iii) available hydrogen phosphate bridges that are not embedded in the POM structure, and (iv) a higher percentage of terminal water molecules.

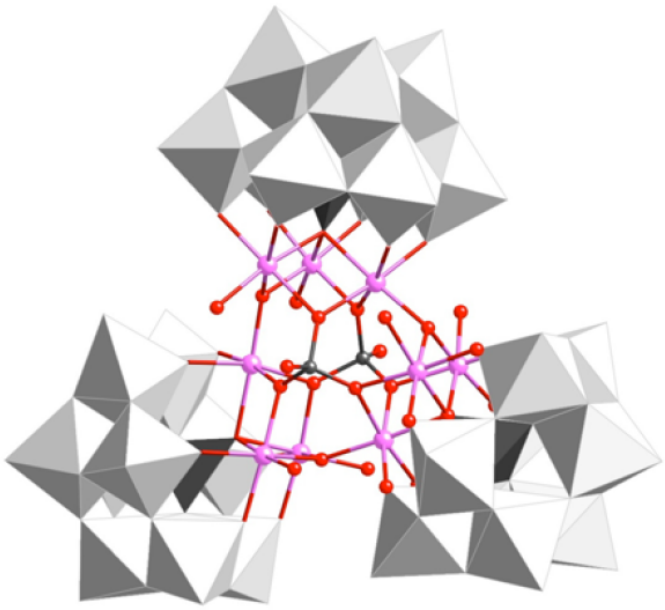

Figure 3.2. *Structure of the **Co_9** polyanion, $[Co_9(H_2O)_6(OH)_3(HPO_4)_2(PW_9O_{34})_3]^{16-}$, WO_6 = gray octahedra; PO_4 = black octahedra; Co = pink; P = black; O = red.*

UNIVERSITAT ROVIRA I VIRGILI
NOVEL MOLECULAR CATALYSTS FOR WATER OXIDATION: TOWARDS ARTIFICIAL PHOTOSYNTHESIS
Sara Goberna Ferrón
Dipòsit Legal: T.189-2014

3.2 Results and Discussion

3.2.1 Chemical Water Oxidation Using Sodium Hypochlorite as Oxidant

The homogeneous catalytic activity of **Co_9** for chemical water oxidation has been investigated. In this approach, a chemical oxidant is directly used as electron scavenging agent to be reduced during the oxidation of water in the presence of the catalyst.

The Oxidant: ClO^-

Catalytic water oxidation at neutral pH is an important technological objective. Nevertheless, few homogeneous WOCs work in these conditions. Maybe because of this, most chemical oxidants commonly used for the characterization of new WOCs are only active at very low pH. For example, Ce^{iV}, a preferred oxidant, precipitates out of solution at pH > 3. At neutrality, $[Ru(bpy)_3]^{3+}$ has been a typical oxidant of choice, but it has an important drawback: $[Ru(bpy)_3]^{3+}$ is easily reduced by hydroxyl anions.[51] In fact, trying to reproduce the conditions reported by Hill et al.[45] using $[Ru(bpy)_3]^{3+}$ as oxidant, we obtained very surprising results. In our experiments, O_2 evolution was monitored by manometric measurements in a sodium phosphate / borate buffer (7 < pH < 8) $[Ru(bpy)_3]^{3+}$. It was found that O_2 evolution occurs even in the absence of any catalyst (Figure 3.3). At this pH range, the $[Ru(bpy)_3]^{3+}$ specie is quite insoluble and also unstable, since it is already able to oxidize water. Furthermore, addition of **Co_4**, decreases the oxygen evolution rate. These results has also been observed by other research groups, and communicated in private

UNIVERSITAT ROVIRA I VIRGILI
NOVEL MOLECULAR CATALYSTS FOR WATER OXIDATION: TOWARDS ARTIFICIAL PHOTOSYNTHESIS
Sara Goberna Ferrón
Dipòsit Legal: T.189-2014

communications. Unfortunately, it has not been published. Thus, $[Ru(bpy)_3]^{3+}$ is not a reliable oxidant for the characterization of oxidation catalysts in such conditions.

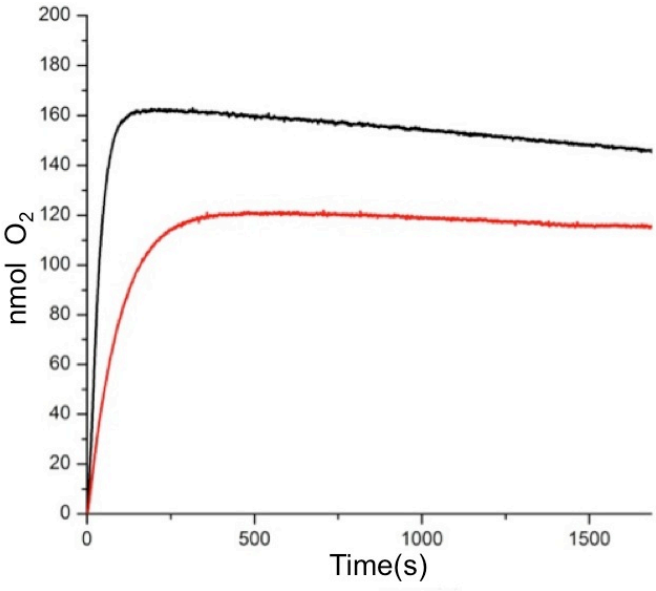

Figure 3.3. *Oxygen evolution profile for a 0.5 mM $[Ru(bpy)_3]^{3+}$ solution in sodium buffer at pH = 8 (black) and with the addition of 1 mM of* ***Co_4*** *(red).*

We tested other oxidants such as periodate,[52] oxone,[53] persulfate or even chlorine at neutral pH, but no oxygen evolution was detected with any of them. It has been reported that **Co_4** does not react with periodate either, suggesting that it is not a good primary oxidant for POM oxidation catalysts.[52] We finally found POM–catalyzed oxygen evolution with sodium hypochlorite. NaClO is kinetically inert towards water oxidation, highly soluble in water and stable in a large pH range. It has been used for the characterisation of homogeneous WOCs at neutral pH in the past, although as an O–containing oxidant, it has some drawbacks related with the nature of the O_2 evolved during water oxidation experiments. This will be discussed in detail later.

UNIVERSITAT ROVIRA I VIRGILI
NOVEL MOLECULAR CATALYSTS FOR WATER OXIDATION: TOWARDS ARTIFICIAL PHOTOSYNTHESIS
Sara Goberna Ferrón
Dipòsit Legal: T.189-2014

Catalytic activity of Co_9

We studied the oxygen evolution catalyzed by **Co_9** with sodium hypochlorite as oxidant. When sodium hypochlorite is added to a 0.9 M sodium phosphate (NaP_i) buffer solution at pH = 8, negligible increment of pressure was observed. However, when NaClO is added to a 1.0 mM solution of **Co_9** in 0.9 M NaP_i buffer (pH = 8) the pressure increases immediately (Figure 3.4).

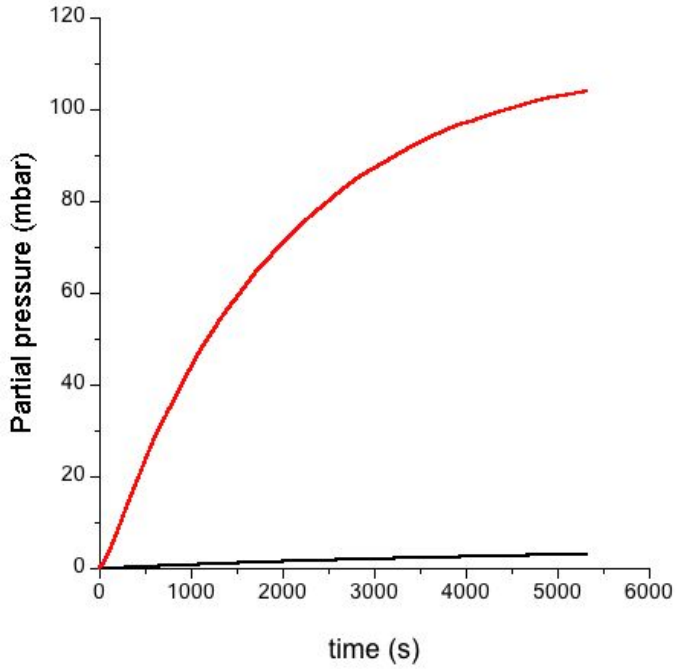

Figure 3.4. *Manometric measurement during chemical water oxidation using 100 equivalents of hypochlorite as oxidant in 0.9 M NaP_i buffer at pH = 8 and at 25 °C, with 1.0 mM **Co_9** (red), and without **Co_9** (black).*

We optimized this catalytic process based on the oxidant / catalyst ratio. The O_2 evolution was quantitatively monitored with differential manometry at various oxidant / catalyst ratios in 0.9 M NaP_i buffer at pH = 8 (Table 3.1 and Figure 3.5). A maximum turnover number (TON) of 20 is reached for a 100 : 1 oxidant / **Co_9** ratio after 1 hour, with an initial turnover frequency (TOF) over 40 h^{-1}. NaClO is a two-electron oxidant, so, this TON reflects a 40% efficiency. This efficiency, far from being

UNIVERSITAT ROVIRA I VIRGILI
NOVEL MOLECULAR CATALYSTS FOR WATER OXIDATION: TOWARDS ARTIFICIAL PHOTOSYNTHESIS
Sara Goberna Ferrón
Dipòsit Legal: T.189-2014

quantitative, indicates that there are competing reactions, probably disproportionation of ClO^- (see below). The TON and TOF increase dramatically when increasing the oxidant equivalents, whereas efficiency decreases. For example, a 3.3×10^3 : 1 oxidant / **Co_9** ratio yields a TON over 400 and an initial TOF of 350 h^{-1}, for a rough efficiency of 2.5%. Although faster WOCs have been reported, it is important to note that TOF depends not only on the catalyst, but also on the oxidant. Hypochlorite is particularly slow. The fastest WOC reported for hypochlorite water oxidation showed a much slower TOF of 12 h^{-1}.[54] We repeated all experiments at least twice, and the oxygen yield was confirmed with gas chromatography (GC). The GC and manometry data show excellent agreement (Table 3.1).

Co_9 shows good stability in the pH range from 4.5 to 9, as confirmed by UV-vis spectroscopy (Figure 3.6). Outside this pH range, a pronounced absorption decrease was detected and the appearance of isosbestic points indicates that new species are being formed. As model reaction, the 100 : 1 oxidant / catalyst ratio was chosen and water oxidation was studied at different pH. When the 100:1 catalytic oxidation is performed at pH = 7 or pH = 9 in 0.9 M NaP_i buffer, comparable TON are obtained (Figure 3.7, left), although some differences are observed for initial rates. The reaction is slower at lower pH (19 h^{-1}), and the catalytic cycle is twice as fast at higher pH (73 h^{-1}). As described in equation 3.1, the thermodynamic potential for water oxidation is pH−dependent and, therefore, pH should influence the catalytic performance.

$$E = +1.23 - 0.059(pH)\ V\ vs\ (NHE)\ at\ 25°C \qquad \text{(Eq. 3.1)}$$

UNIVERSITAT ROVIRA I VIRGILI
NOVEL MOLECULAR CATALYSTS FOR WATER OXIDATION: TOWARDS ARTIFICIAL PHOTOSYNTHESIS
Sara Goberna Ferrón
Dipòsit Legal: T.189-2014

[Co_9] (mM)	Eq. NaClO	[NaClO] (mM)	Reaction time (h)	TON	TOF_i (h^{-1})
1.0	10^2	10^2	1.7	20 (23)	42
10^{-1}	10^3	10^3	3.5	75 (72)	70
10^{-1}	3.3×10^3	3.3×10^2	1.4	121	246
10^{-2}	3.3×10^4	3.3×10^2	5.5	410	351

Table 3.1. *Manometry data for catalytic oxygen evolution in 0.9 M NaP_i buffer solution at pH = 8 with NaClO as oxidant, after the addition of* ***Co_9****. Reaction time refers to the time when oxygen evolution stops. TON = mol O_2 / mol* ***Co_9*** *→ total turnover number at the final reaction time, compared GC data in brackets. TOF → slope of the oxygen evolution curve at the starting time.*

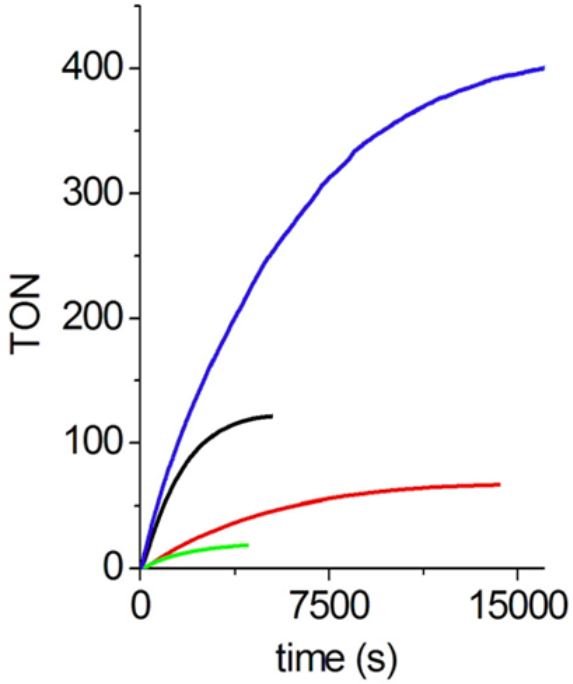

Figure 3.5. *Oxygen evolution profile for a 1.0 mM Co9 solution after the addition of different equivalents of NaClO as the oxidant (10^2, green; 10^3, red; 3.3×10^3, black; 3.3×10^4, blue) in a 0.9 M NaP_i buffer at pH = 8.0. The reaction was stopped in each case once a constant oxygen partial pressure was reached.*

Although temperature–dependence is not usually studied for the characterization of WOCs, we also found an influence in the oxygen evolution as a function of temperature. The 100:1 catalytic oxidation in 0.9 M NaP_i buffer at pH = 8 (Figure 3.7, right) is faster by increasing the temperature. The total yield doubles from 15 to 25 °C,

UNIVERSITAT ROVIRA I VIRGILI
NOVEL MOLECULAR CATALYSTS FOR WATER OXIDATION: TOWARDS ARTIFICIAL PHOTOSYNTHESIS
Sara Goberna Ferrón
Dipòsit Legal: T.189-2014

and an optimum performance with a 50% efficiency was found at 35 °C. Therefore, water oxidation catalyzed by **Co_9** is influenced by both, pH and temperature in this reaction conditions.

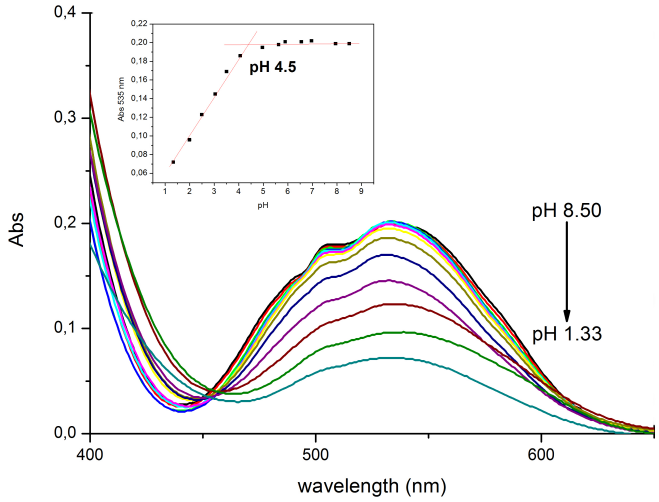

Figure 3.6. *pH titration for a 1.0 mM **Co_9** solution in water. Inset: Absorvance at 535 nm vs pH.*

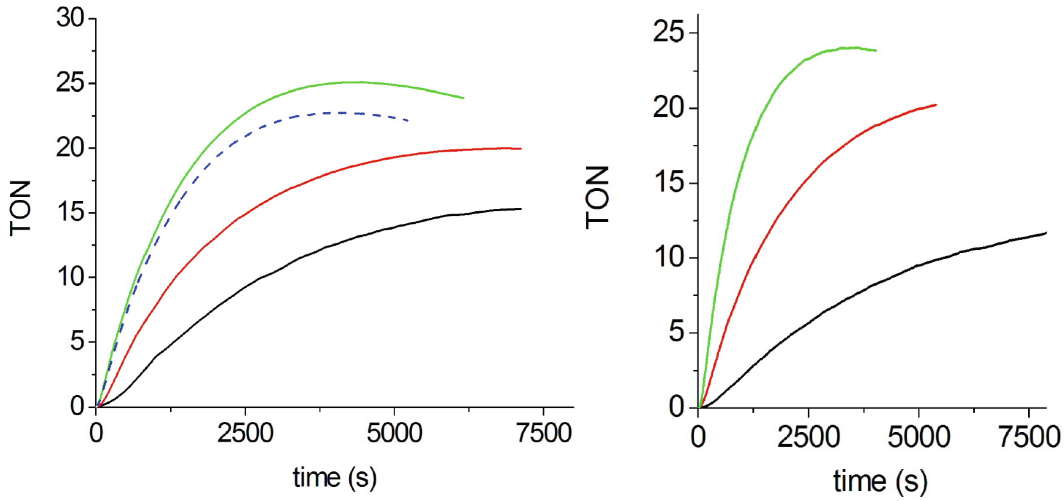

Figure 3.7. *Oxygen evolution profile for a 1.0 mM **Co_9** solution after the addition of 100 equivalents of NaClO as the oxidant in a 0.9 M NaPi buffer, **left**: as a function of the pH (7.0: black line, 8.0: red line, 9.0: green line, 9.0 in the presence of a 10-fold excess of bpy: dotted blue line; T = 25 °C). **Right:** as a function of the temperature (15 °C: black, 25 °C: red, 35 °C: green; pH = 8.0).*

- 3. 2. Results and Discussion -

An important concern in homogeneous cobalt containing WOCs is the possibility of *in situ* formation of cobalt phosphate or cobalt hydroxide, known to be solid state WOCs. For this reason, it is important to confirm that **Co_9** is not decomposing or forming cobalt phosphate / hydroxide. For this purpose, we analyzed the reaction solution after the catalysis. UV-Vis spectroscopy shows the signature absorption bands of Co_9, without appearance of any additional band from any other species. Dynamic light scattering (DLS) analysis also ruled out the presence of heterogeneous naonoparticles because identical data were found before and after oxygen evolution (See 3.4.1 Synthesis and Characterization). Indeed, after the water oxidation is completed, **Co_9** can be recovered from solution by precipitation with additional K^+. This salt is identical to the starting **Co_9** sample, as confirmed by the X-ray diffraction pattern and IR spectra. Even single crystals could be grown from the solution once the oxidation is complete. After catalysis, traces of an insoluble black powder were found, but this powder did not contain cobalt. The EDX analysis showed a mixture of sodium chloride and tungstate, and this powder had no catalytic activity (Figure 3.8). This suggests that some Co^{2+} cations could be liberated in turnover conditions and participate in the catalytic cycle. The addition of a chelating agent, such as 2,2**'** -bipyridyl (bpy), can prevent their participation. The free cations would be rapidly trapped by the chelating ligands to form $[Co(bpy)_3)]^{2+}$, which in oxidation conditions yields the highly inert $[Co(bpy)_3)]^{3+}$ species. The experiments described above were repeated adding a 10-fold excess of 2,2′-bipyridyl (bpy) per Co atom. The results are consistent, no significant differences in TON or TOF were found in the presence of bpy. This confirms that **Co_9** is the main active species throughout the oxidation. Only at pH = 9 a small decrease in activity was observed. (Figure 3.7, left). This decrease in activity should be due to a decomposition of the POM into a new species that does not improve the catalytic performance. All this evidences confirm that the *in situ* formation of cobalt phosphate or cobalt hydroxide does not occur in the case of **Co_9**, at least in these reaction conditions.

UNIVERSITAT ROVIRA I VIRGILI
NOVEL MOLECULAR CATALYSTS FOR WATER OXIDATION: TOWARDS ARTIFICIAL PHOTOSYNTHESIS
Sara Goberna Ferrón
Dipòsit Legal: T.189-2014

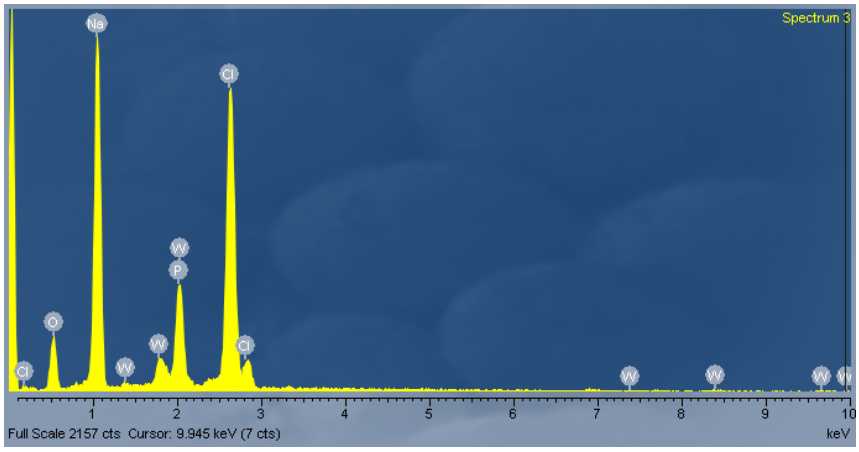

Figure 3.8. *EDX histogram of the black powder recovered from the bottom of the reactor after* ***Co₉*** *catalyzed water oxidation with NaClO in* NaP_i *buffer at pH = 8.*

Long-Term stability of Co_9 in Turnover Conditions

The stability and continuous catalytic performance of **Co_9** is remarkable. Once O_2 evolution stops, the addition of catalyst did not show any effect. On the contrary, successive additions of oxidant re-start the O_2 evolution maintaining identical TON and TOF through multiple additions (Table 3.2). This demonstrates that **Co_9** remains quantitatively intact in solution in the long term. As shown before, the rate and yield of the catalytic oxidation of water with hypochlorite are very sensitive to changes in the oxidant / **Co_9** ratio, and a significant decrease in catalyst concentration is expected to affect the results. Furthermore, decomposition to other species would result in important changes in the catalytic activity.[46] The addition of 1000 equivalents of oxidant to a **Co_9** (0.1 mM) in 0.9 M NaP_i buffer at pH = 8 solution every two hours yielded a final cumulative TON of 180, and a constant initial TOF of 69 ± 2 h^{-1} (after three cycles). The addition of 3.3×10^3 equivalents of oxidant every ≈2 hours yielded a total cumulative TON > 880, and a constant initial TOF ≈ 370 ± 20 h^{-1} (after five cycles). The mean TOF over the reaction time holds over 100 h^{-1}.

In order to test the stability limits of **Co_9** in solution, these experiments were repeated in the presence of a 10-fold excess of bpy, and adding the additional equivalents of

UNIVERSITAT ROVIRA I VIRGILI
NOVEL MOLECULAR CATALYSTS FOR WATER OXIDATION: TOWARDS ARTIFICIAL PHOTOSYNTHESIS
Sara Goberna Ferrón
Dipòsit Legal: T.189-2014

oxidant after much longer periods of time (Figure 3.9). The results indicate that the **Co_9** solution remains completely active for over a week, without any signal of fatigue or decomposition. To date, no other reported WOC can remain active for such a long time either under chemical, electrochemical or photo-induced water oxidation conditions.

[Co_9] (mM)	**Eq. NaClO**	**$t_i - t_f$ (h)**	**TON**	**TOF (h^{-1})**	**TON_C**
10^{-1}	10^3(x3)	0.0 – 2.5	75	70	75
"	"	2.5 – 5.0	53	69	130
"	"	5.0 – 7.3	50	67	180
10^{-2}	3.3 x 10^4 (x3)	0.0 – 1.6	148	391	148
"	"	1.6 – 3.0	158	379	306
"	"	3.0 – 4.5	217	367	523
"	"	4.5 – 6.0	200	355	723
"	"	6.0 – 7.0	165	343	888
1^{-2}	*3.3 x 10^4 (x3)*	*0.0 – 84*	*255*	*391*	*255*
8 x 10^{-3}	"	*84 – 108*	*215*	*468*	*470*
6 x 10^{-3}	"	*108 – 131*	*180*	*586*	*650*
5 x 10^{-3}	"	*131 – 137*	*173*	*689*	*823*

Table 3.2. *Manometry data for **Co_9**–catalyzed oxygen evolution in 0.9 M NaP_i buffer solutions at pH = 8 after successive additions of NaClO as the oxidant at 25 °C. Data in italic corresponds to an experiment carried out in presence of 1.0 mM bpy (bpy = 2,2'-bipyridyl). TON = mol O_2 / mol **Co_9** → total turnover number at the next addition or final time; TOF → slope of the oxygen evolution curve at the oxidant addition time; TON_C → cumulative TON.*

UNIVERSITAT ROVIRA I VIRGILI
NOVEL MOLECULAR CATALYSTS FOR WATER OXIDATION: TOWARDS ARTIFICIAL PHOTOSYNTHESIS
Sara Goberna Ferrón
Dipòsit Legal: T.189-2014

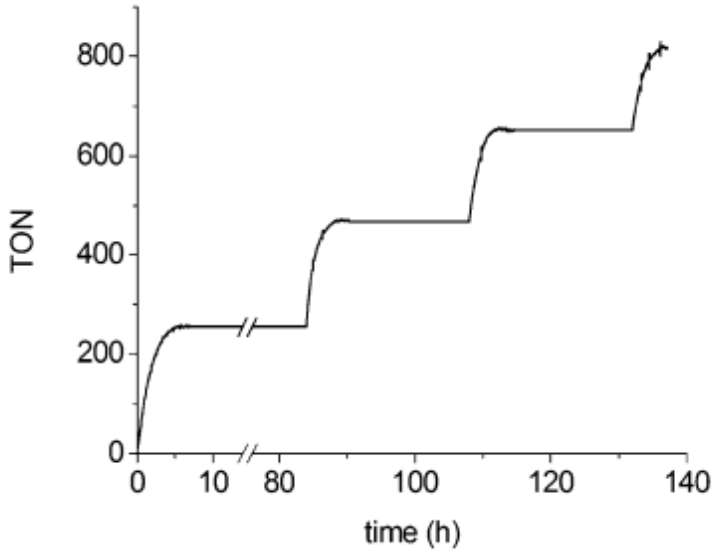

Figure 3.9. *Oxygen evolution profile catalyzed by* ***Co_9*** *after successive additions of NaClO as the oxidant in 0.9 M NaP_i buffer at pH = 8 and 10-fold excess of bpy at 25 °C.*

Comparison between Co_9 and Co_4

The catalytic performance of **Co_9** was compared, in the same experimental conditions, with the first cobalt–based POM that showed catalytic activity for water oxidation **Co_4** (Table 3.3)**.**[45] Our results put into perspective the remarkable catalytic performance of **Co_9**. When **Co_4** is added to a sodium hypochlorite solution in a 100:1 ratio in 0.9 M NaP_i buffer at pH = 8 a TON of only 2 is reached (Figure 3.10). This corresponds to 4% efficiency. Calculated initial TOF data indicates that **Co_9** is at least eight times faster than **Co_4**. These differences are maintained for a 1000:1 ratio, giving 75 and 5 TON, respectively, although the initial **Co_9** TOF is just twice that of **Co_4.** Since these experiments were carried out with the same POM concentration, it can be argued that the different cobalt content might account for the observed differences. Calculating the catalytic activity numbers per cobalt atom, the superior performance of **Co_9** is corroborated, with a 2.2 vs 0.5 and 7.4 vs 1.3 TON for a 100:1 and 1000:1 ratio respectively, although the turns per WOC get closer. From a technological perspective, it is also interesting to compare the activity per gram of catalyst, since

UNIVERSITAT ROVIRA I VIRGILI
NOVEL MOLECULAR CATALYSTS FOR WATER OXIDATION: TOWARDS ARTIFICIAL PHOTOSYNTHESIS
Sara Goberna Ferrón
Dipòsit Legal: T.189-2014

not only the Co content is important regarding costs. Taking into account the *Mw* of the POM salts, an estimation of 250 and 29 mg of O_2 per gram of POM can be obtained with a 1000:1 oxidant/POM ratio for **Co_9** and **Co_4**, respectively. These data demonstrates that both catalysts show comparable kinetics. But, the total O_2 yield indicates that **Co_9** is much more efficient. This might be related to **Co_9** being more robust in turnover conditions. Indeed, the instability of **Co_4** has been subject of several communications.[46,47]

Catalyst	[cat] (mM)	Eq. NaClO	TON	TOF_i (h^{-1})
Co_9	1	10^2	20	42
	10^{-1}	10^3	67	70
Co_4	1	10^2	2	6
	10^{-1}	10^2	5	34

Table 3.3. *Comparison of manometry data for catalytic oxygen evolution in 0.9M NaP_i buffer solutions at pH = 8 with $_{NaClO}$ as the oxidant, after the addition of **Co_9** or **Co_4** at 25 °C. TON = mol O_2 / mol catalyst → total turnover number at the final reaction time. TOF → slope of the oxygen evolution curve at the starting time.*

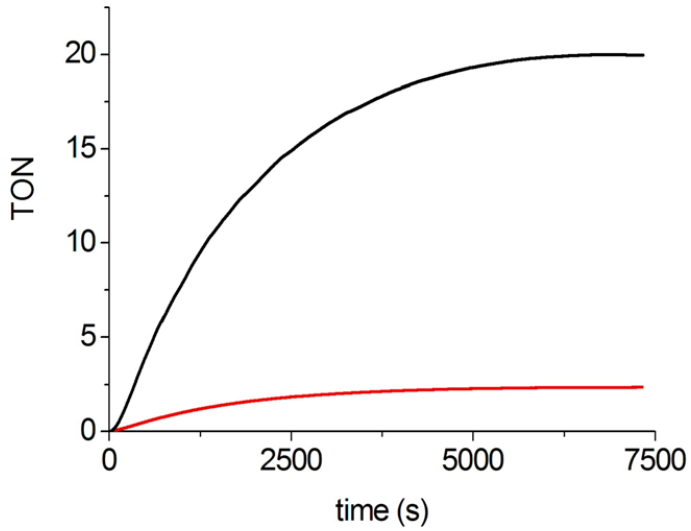

Figure 3.10. *Oxygen evolution profile for 1.0 mM **Co_9** (black) and **Co_4** (red) solutions respectively, after the addition of 100 equivalents of NaClO as the oxidant in a 0.9 M NaP_i buffer solution at pH = 8.*

UNIVERSITAT ROVIRA I VIRGILI
NOVEL MOLECULAR CATALYSTS FOR WATER OXIDATION: TOWARDS ARTIFICIAL PHOTOSYNTHESIS
Sara Goberna Ferrón
Dipòsit Legal: T.189-2014

Oxygen evolution from catalytic water oxidation?

Although hypochlorite has been used as a model water oxidant,[54] it has some drawbacks. The first concern regarding the use of ClO^- as oxidant for the characterization of WOCs is the possible generation of other gases as byproducts. Hypochlorite is known to disproportionate into chloride and chlorate (Cl^- and ClO_3^-) and to slowly evolve Cl_2 gas. We carried out mass spectroscopy experiments to confirm that the gas evolved in all previous experiments is essentially O_2. We found a very small fraction of CO_2 (<3%), and only traces of Cl_2 and $HClO_3$ (<0.01%) (Figure 3.11). The CO_2 should come from adventitious carbonate from dissolved atmospheric CO_2 in the basic media.

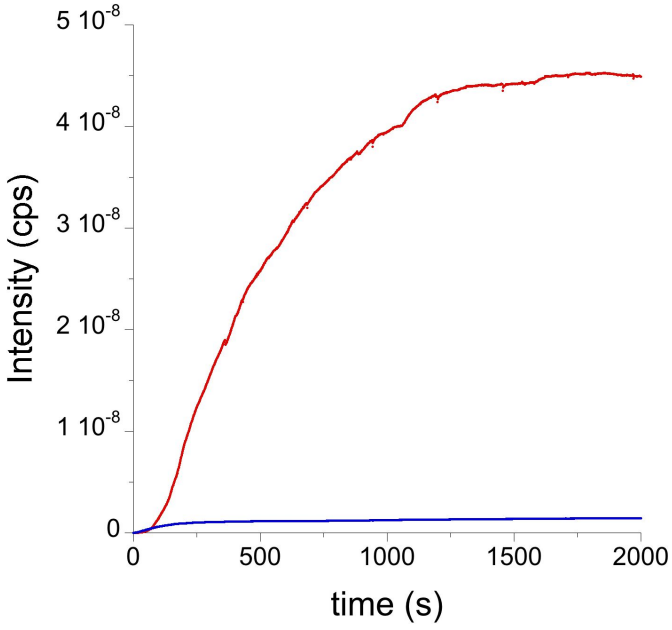

Figure 3.11. *Mass spectra obtained for 1.0 mM Co9 solution after addition of 200 µL of 0.9 M NaClO solution (100 equivalents). The composition of the gas phase (O_2, m/z = 32; N_2, m/z = 44) was monitored on–line.*

The second, and most important concern in the use of hypochlorite as oxidant for WOC characterization is the unambiguous determination of the source of O_2 atoms. It is of critical importance to establish whether the oxygens in the evolved O_2 arise from water or from disproportionation of the oxidant itself. One method to achieve this is

UNIVERSITAT ROVIRA I VIRGILI
NOVEL MOLECULAR CATALYSTS FOR WATER OXIDATION: TOWARDS ARTIFICIAL PHOTOSYNTHESIS
Sara Goberna Ferrón
Dipòsit Legal: T.189-2014

the use of ^{18}O-isotope labelled water. When we performed analogous water oxidation reactions with 19.4% $H_2{}^{18}O$-labelled water as solvent, the O_2 evolution (Figure 3.12) for the different possible isotopes ($^{32}O_2$, $^{34}O_2$ and $^{36}O_2$) is in excellent agreement with the expected statistical distribution (Table 3.4). This suggests that water is the main source of O atoms.

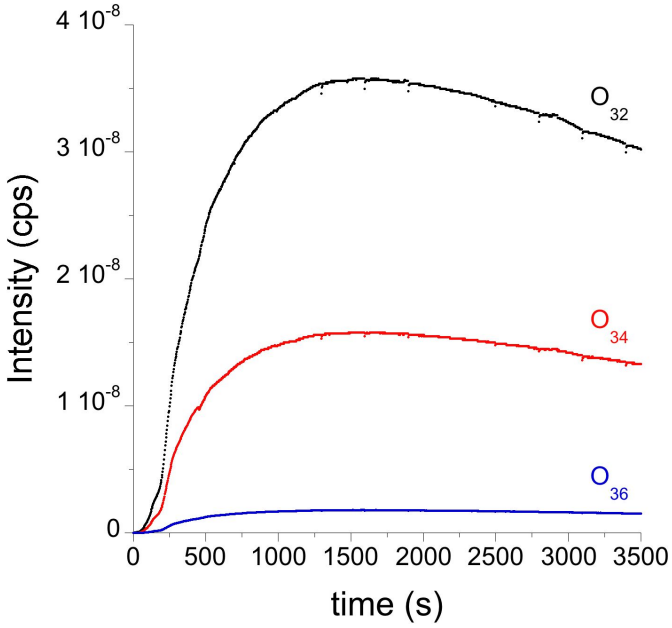

Figure 3.12. *Mass spectra obtained for 1.0 mM* ***Co$_9$*** *solution after addition of 100 equivalents of 0.9 M NaClO (NaClO dissolve in $H_2{}^{18}O$ and* ***Co$_9$*** *dissolved in $H_2{}^{16}O$). The composition of the gas phase ($^{16}O_2$, m/z = 32; $^{16}O^{18}O$, m/z = 34 and $^{18}O_2$, m/z = 36) was monitored on–line.*

	Isotopic Ratios			Isotopic Ratios	
	Teor.	**Expl.**		**Teor.**	**Expl.**
O_{32}/O_{34}	2.1	2.3	**$^{16}O_2$**	64.9	67.0
O_{32}/O_{36}	17.1	19.7	**$^{16}O^{18}O$**	31.3	29.6
O_{34}/O_{36}	8.2	8.7	**$^{18}O_2$**	3.8	3.4

Table 3.4. *Ratio of O_{32}/O_{34}, O_{32}/O_{36} and O_{34}/O_{36} (left) and relative isotopic ratios (right) of O_2 evolved, NaClO dissolve in $H_2{}^{18}O$ and* ***Co$_9$*** *dissolved in $H_2{}^{16}O$. Theoretical values calculated assuming a fase O atom exchange between the catalyst and the solvent.*

However, ClO^- exchanges the O atom with solvent very fast, reaching equilibrium at

UNIVERSITAT ROVIRA I VIRGILI
NOVEL MOLECULAR CATALYSTS FOR WATER OXIDATION: TOWARDS ARTIFICIAL PHOTOSYNTHESIS
Sara Goberna Ferrón
Dipòsit Legal: T.189-2014

30 s, for a half-life of about 10 s,[53] and this puts into question the isotope-labeling experiments. This is a common problem for all oxidants containing oxygen, including the lately accepted periodate that also shows rapid oxo-exchange.[52] In the case of ClO^-, it has been well established that the main dismutation pathway yields chloride, oxygen and chlorates (Equations 2–3). The oxygen-evolving pathway is much slower, and typically negligible.[55-57]

$$3\ ClO^- \rightarrow ClO_3^- + 2Cl^- \qquad \text{(Eq. 3.2)}$$

$$2\ ClO^- \rightarrow O_2 + 2Cl^- \qquad \text{(Eq. 3.3)}$$

In order to get additional evidence about the source of oxygen atoms, we designed a set of experiments using labeled or unlabeled $^{18}OCl^-$ to look at differences in the very first seconds of oxygen evolution. Compared studies of the very initial kinetics of the oxygen evolving reaction were performed dissolving either the oxidant or the catalyst in isotope-labeled water. If water is the main O_2 source, the oxygen evolution should be identical in both cases (diffusion control), since the labeled water ratio will be the same in both cases. On the contrary, if ClO^- is the main O_2 source, the initial dynamics should be different (exchange control). For instance, when using 97% ^{18}O-labeled water for the preparation of the ClO^- solution, an initial 97% $Cl^{18}O^-$ content would be observed. After mixing it with a non-labeled **Co_9** solution, if $Cl^{18}O^-$ is the main oxygen source, higher $^{34}O_2$ and $^{36}O_2$ initial ratios should be observed, since the $Cl^{18}O^-$ content would actually decrease from its initial maximum value down to the 19.4% ^{18}O content at equilibrium, because of exchange with solvent. When using non-labeled water for the preparation of the ClO^- solution, after mixing it with a 97% ^{18}O-labeled **Co_9** solution, much slower $^{34}O_2$ and $^{36}O_2$ evolution dynamics should be observed initially, since the $Cl^{18}O^-$ content would increase up to 19.4% ^{18}O at equilibrium. Although the MS data needs a few seconds to become stable, both experiments

UNIVERSITAT ROVIRA I VIRGILI
NOVEL MOLECULAR CATALYSTS FOR WATER OXIDATION: TOWARDS ARTIFICIAL PHOTOSYNTHESIS
Sara Goberna Ferrón
Dipòsit Legal: T.189-2014

showed identical $^{32}O_2$:$^{34}O_2$:$^{36}O_2$ dynamic evolution at very short times (< 30 s), that is, before equilibria is reached (Figure 3.13). This is additional evidence that water is the main oxygen source, and that **Co_9** is catalyzing water oxidation by hypochlorite.

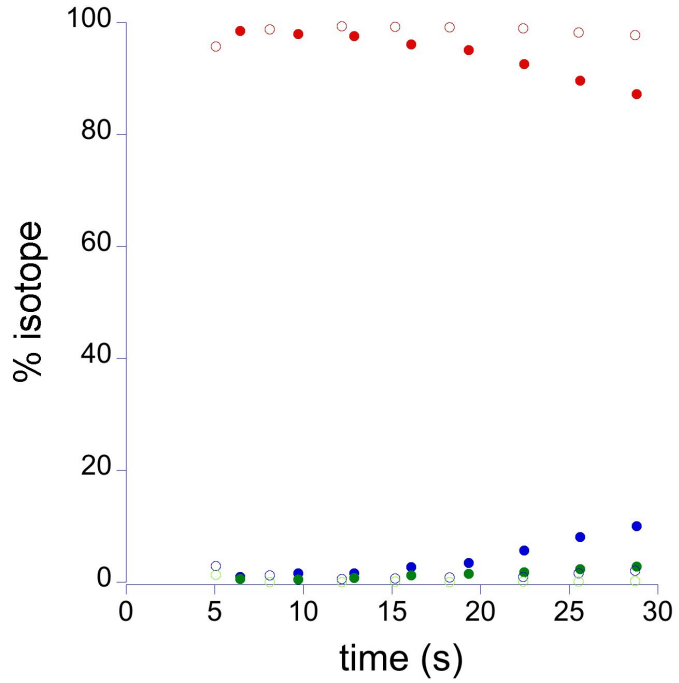

Figure 3.13. *Mass spectra of the $^{32}O_2$ (red), $^{34}O_2$ (blue) and $^{36}O_2$ (green) dynamic content obtained after addition of 100 equivalents of NaClO in a 0.6 mL of water to 1.4 mL of NaP_i buffer solution at pH = 8 containing 2.0 µmol of the **Co_9** catalyst in the first 30 seconds. Full circles: NaClO dissolve in $H_2{}^{18}O$ and **Co_9** dissolved in $H_2{}^{16}O$. Empty circles: **Co_9** dissolved in $H_2{}^{18}O$ and NaClO dissolved in $H_2{}^{16}O$. In both cases the final $H_2{}^{18}O$ labeled solvent is 19.4%. The composition of the gas phase ($^{16}O_2$, m/z = 32; $^{16}O^{18}O$, m/z = 34 and $^{18}O_2$, m/z = 36) was monitored on−line.*

Nevertheless, as Crabtree concludes,[52,58] the use of primary oxidants gives solid information on the catalytic water oxidation activity, including rates and stability, even if the real source of oxygen cannot be unambiguously determined. In our experiments with hypochlorite as oxidant, the results indicate that the most plausible origin for oxygen gas is water oxidation. But even if not, the data demonstrates that **Co_9** is a stable and robust catalyst in water oxidation conditions. To confirm , beyond

UNIVERSITAT ROVIRA I VIRGILI
NOVEL MOLECULAR CATALYSTS FOR WATER OXIDATION: TOWARDS ARTIFICIAL PHOTOSYNTHESIS
Sara Goberna Ferrón
Dipòsit Legal: T.189-2014

any reasonable doubt, that **Co_9** is a WOC, we will need to study the catalytic activity of **Co_9** in other reaction conditions, such as electrochemical (section 3.2.2) or photo−induced (section 3.2.3) water oxidation. In these cases, the oxidation is promoted by external sources to the reaction, voltage or photo-induction, offering a clean procedure for the analysis of the oxygen production. Furthermore, in terms of artificial photosynthesis, water oxidation would always be performed (photo)electrochemically, giving additional interest to these experiments.

UNIVERSITAT ROVIRA I VIRGILI
NOVEL MOLECULAR CATALYSTS FOR WATER OXIDATION: TOWARDS ARTIFICIAL PHOTOSYNTHESIS
Sara Goberna Ferrón
Dipòsit Legal: T.189-2014

3.2.2 Electrochemical Water Oxidation

Cyclic voltammetry experiments allow determining if a given compound is a good WOC candidate since the water oxidation wave should be significantly increased in the presence of the compound. The cyclic voltammogram (CV) of a diluted **Co_9** solution in 50 mM NaP_i buffer at pH = 8 using a Pt working electrode shows an irreversible current wave signature of catalytic water oxidation (Figure 13). This wave shows higher current intensity at lower potentials when compared with a **Co_4** solution under the same experimental conditions. Thus, suggesting that **Co_9** possess also higher electrocatalytic activity in the same conditions (Figure 3.14).

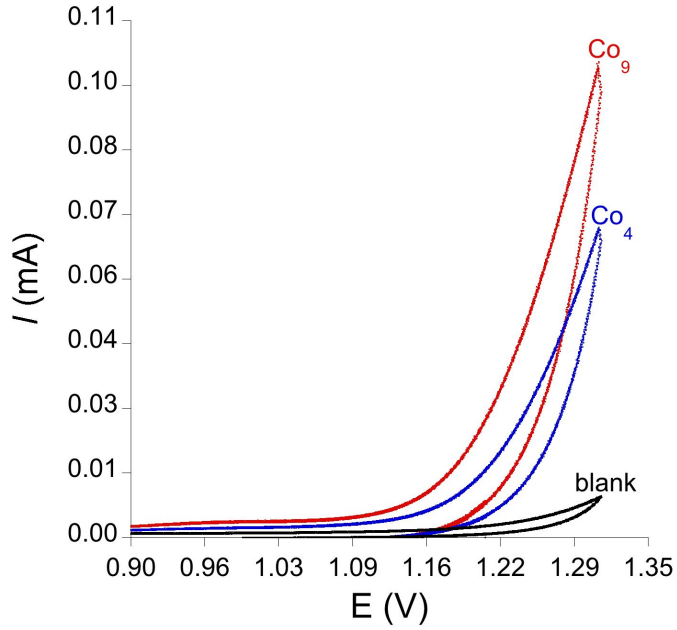

Figure 3.14. *Cyclic voltammetry of a 1.0 mM Co_9 (red) or Co_4 (blue) in 50 mM NaP_i buffer with 1 M $NaNO_3$ as electrolyte at pH = 8 solution. Pt working electrode, Ag/AgCl (NaCl 3 M) reference electrode and Pt wire counter electrode. Scan rate = 100 mV s^{-1}. Potentials reported vs NHE.*

It has been reported that **Co_4** decomposes rapidly in other electrochemical conditions,[46] as confirmed by the continuous increase of the water oxidation wave intensity with time. Such observation indicates that a "better" catalyst is formed in situ. We monitored successive cyclic voltammograms for thw **Co_9** and **Co_4** catalyzed water oxidation during hours without significant changes in current (Figure 3.15). Still,

UNIVERSITAT ROVIRA I VIRGILI
NOVEL MOLECULAR CATALYSTS FOR WATER OXIDATION: TOWARDS ARTIFICIAL PHOTOSYNTHESIS
Sara Goberna Ferrón
Dipòsit Legal: T.189-2014

the studies that showed decomposition with time for **Co_4** due to CoO_x formation were performed with amorphous carbon working electrode,[46] We used Pt anodes and deposition could be much slower. Therefore, we cannot completely rule out CoO_x formation.

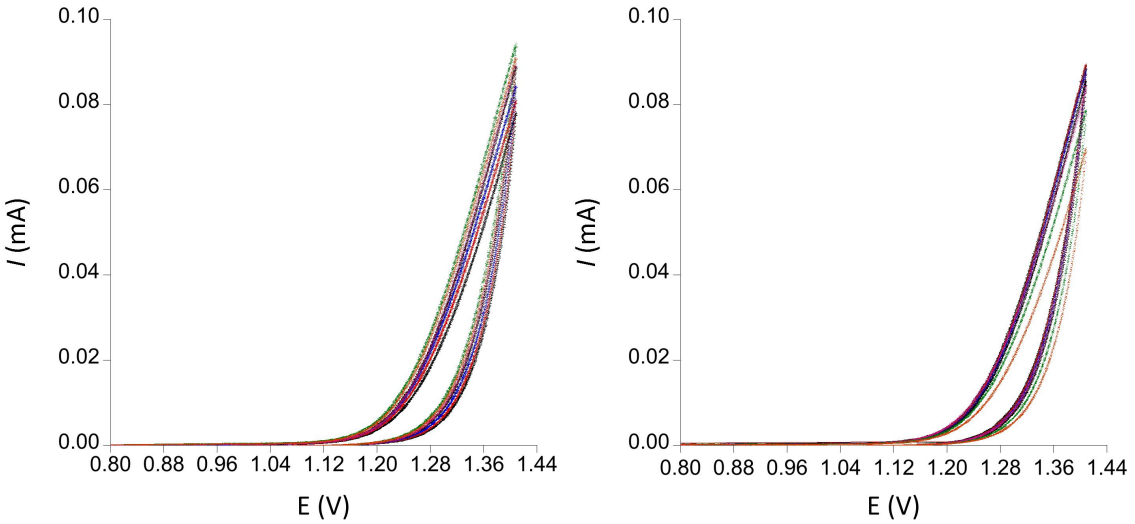

Figure 3.15. *Cyclic voltammograms recorded continuously during 3 hours of a 1.0 mM Co_9 (**left**) or Co_4 (**right**) in 50 mM NaP_i buffer with 1 M $NaNO_3$ as electrolyte at pH = 8 solution. Pt working electrode, Ag/AgCl (NaCl 3 M) reference electrode and Pt wire counter electrode. Scan rate = 100 mV s^{-1}. Potentials reported vs NHE.*

Bulk Water Electrolysis with Co_9 and / or CoO_x

Bulk water electrolysis experiments were carried out in a U-shape two-chamber cell with both chambers connected through a glass frit. Platinum mesh electrodes were used as anode and cathode. Negligible current values were obtained in a 50 mM NaP_i buffer at pH = 8 with 1 M **$NaNO_3$** as electrolyte solution when an anodic voltage of of 1.3 V was applied in the absence of catalyst. With the addition of **Co_9** (1 mM) to the anode compartment, the current rapidly reached over 1 mA, and then it decreased down to a stable value that remained constant for hours (Figure 3.16). The applied potential corresponds to an overpotential (η) of 500 mV when compared with the thermodynamic value (Equation 3.4). Most homogeneous WOCs

UNIVERSITAT ROVIRA I VIRGILI
NOVEL MOLECULAR CATALYSTS FOR WATER OXIDATION: TOWARDS ARTIFICIAL PHOTOSYNTHESIS
Sara Goberna Ferrón
Dipòsit Legal: T.189-2014

require η in the 600-900 mV range.[59]

E = + 0.816 vs (NHE) at pH = 7 and 25°C (Eq. 3.4)

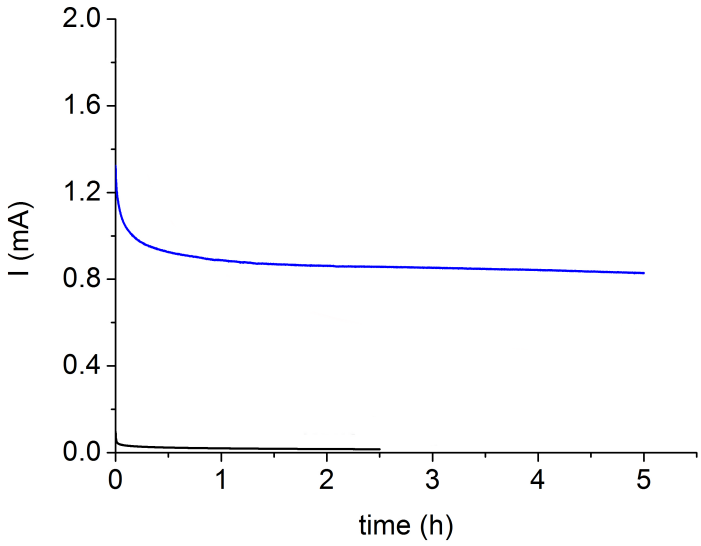

Figure 3.16. ***Co_9*** *(1.0 mM) catalyzed bulk water electrolysis in a 50 mM NaP_i buffer with 1 M $NaNO_3$ as electrolyte at pH = 8, applying a constant potential of 1.3 V (vs NHE) (blue) and blank experiment (black) in the same conditions. Pt mesh working and counter electrodes and Ag/AgCl (NaCl 3 M) reference electrode.*

During bulk water electrolysis, the Pt anode was covered by a thin black film. This film was characterized as a Co oxide (CoO_x), since neither P, K or W were detected in EDAX elemental analysis. In addition to being a decomposition product of the POM, this film is an active WOC, so it is important distinguish between the activity of **Co_9** and / or film. The fact that the current remains constant after just one hour suggests that once the CoO_x thin film covers the entire anode surface, no further **Co_9** decomposition occurs. If the same covered electrode is used after 1 hour of **Co_9**-catalyzed water oxidation to perform water electrolysis in a **Co_9**-free solution, a much lower current was observed (Figure 3.17). A third cycle using the very same electrode in a new **Co_9**

UNIVERSITAT ROVIRA I VIRGILI
NOVEL MOLECULAR CATALYSTS FOR WATER OXIDATION: TOWARDS ARTIFICIAL PHOTOSYNTHESIS
Sara Goberna Ferrón
Dipòsit Legal: T.189-2014

buffered solution shows increased activity. These distinc activity suggests that both, **Co_9** and CoO_x are active in these experiments (Figure 16). Thus, the formation of the CoO_x film reduces the activity of **Co_9**, that becomes negligible after five 1-hour cycles, once CoO_x is the main and only WOC in these conditions.

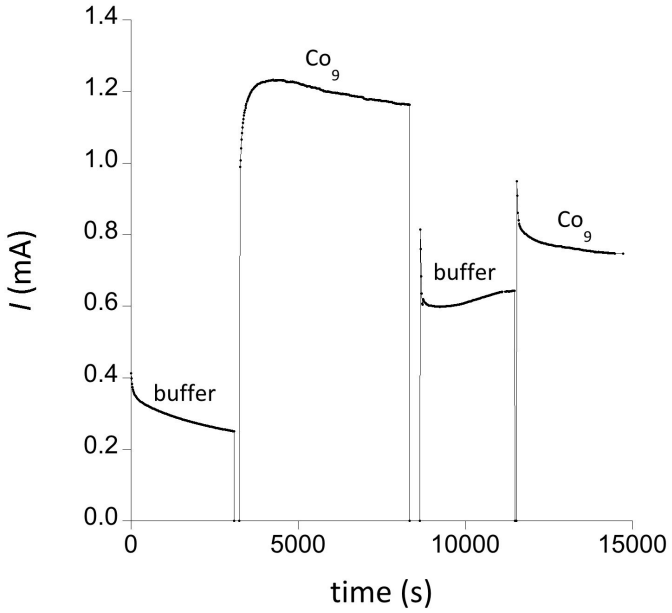

Figure 3.17. ***Co_9*** *(1.0 mM) catalyzed bulk water electrolysis in a 50 mM NaP_i buffer with 1 M $NaNO_3$ as electrolyte at pH = 8, applying a constant potential of 1.3 V (vs NHE). Each 1 hour the* ***Co_9*** *solution was changed by a buffer solution without catalyst but maintaining the Co oxide–covered Pt mesh working electrode. Pt counter electrode and Ag/AgCl (NaCl 3 M) reference electrode.*

The *in situ* oxygen evolution in the gas phase was monitored at constant pressure with a fluorescence probe in these bulk electrolysis. Comparing the experimental amount of O_2 generated with the theoretically expected (Faraday's law), assuming that all the electrons are used to oxidize water into O_2, the faradaic efficiency (measured mol O_2 / theoretical mol O_2) of **Co_9** / CoO_x catalyzed reaction was found to be quantitative for > 4 hours (Figure 3.18). This means that all electrons removed in the anodic reaction are indeed coming from water molecules. After this time, the

UNIVERSITAT ROVIRA I VIRGILI
NOVEL MOLECULAR CATALYSTS FOR WATER OXIDATION: TOWARDS ARTIFICIAL PHOTOSYNTHESIS
Sara Goberna Ferrón
Dipòsit Legal: T.189-2014

efficiency slowly decreases down to ≈ 80 % probably because of the effect of the CoO_x film coverage. Still, the oxygen pressure in the cell headspace continuously increases without significant changes in slope. The experiments described above were performed at pH = 8, as it was found an optimal pH in chemical water oxidation. In contrast to chemical oxidation, analogous performance was observed for analogous bulk water electrolysis experiments at neutral pH (Figure 3.19). For this reason, pH = 7 was chosen for future experiments, as neutral pH is preferable from a technological point of view.

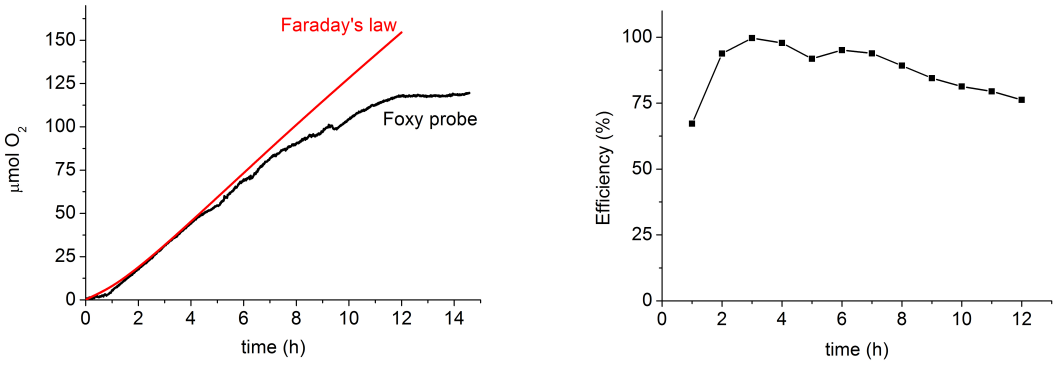

Figure 3.18. ***Left:*** *Catalytic O_2 evolution (black) during bulk electrolysis at 1.3 V (vs NHE) with 1.0 mM Co_9 in 50 mM NaP_i buffer solution containing 1 M $NaNO_3$ as electrolyte at pH = 8, and theoretical O_2 assuming Faradaic behavior (red). Pt mesh working and counter electrodes and Ag/AgCl (NaCl 3 M) reference electrode.* ***Right:*** *Relation between the theoretical and experimental O_2 evolution in the same experimental conditions.*

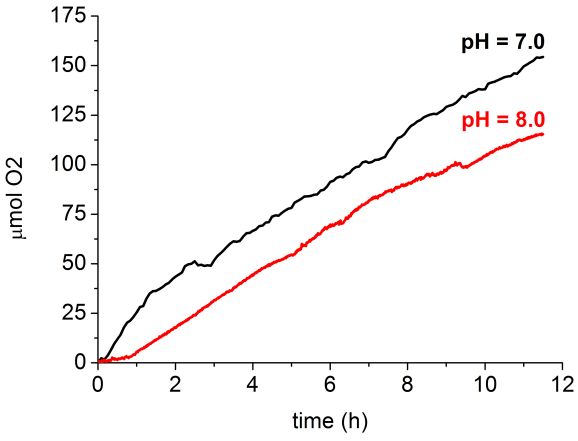

UNIVERSITAT ROVIRA I VIRGILI
NOVEL MOLECULAR CATALYSTS FOR WATER OXIDATION: TOWARDS ARTIFICIAL PHOTOSYNTHESIS
Sara Goberna Ferrón
Dipòsit Legal: T.189-2014

Figure 3.19. *Catalytic O_2 evolution during bulk electrolysis at 1.3 V (vs NHE) with 1.0 mM Co_9 in 50 mM NaP_i buffer solution containing 1 M $NaNO_3$ as electrolyte at pH = 8 (red) and pH = 7 (black). Pt mesh working and counter electrodes and Ag/AgCl (NaCl 3 M) reference electrode.*

If O_2 is being formed at the anodic compartment, H_2 should be produced in the cathodic compartment (Equations 3.5-3.6).

$2H_2O \rightarrow O_2 + 4H^+ + 4e^-$ ***Oxidation*** (Eq. 3.5)

$4H^+ + 4e^- \rightarrow 2H_2$ ***Reduction*** (Eq. 3.6)

$2H_2O \rightarrow 2H_2 + O_2$ ***Total Reaction*** (Eq. 3.7)

The hydrogen evolution in the cathode compartment headspace was monitored with a Clark-type hydrogen sensor (Figure 3.20). The data is in complete agreement with the oxygen evolution curve, indicating that the catalyzed water oxidation reaction is indeed responsible for increasing the hydrogen production rate.

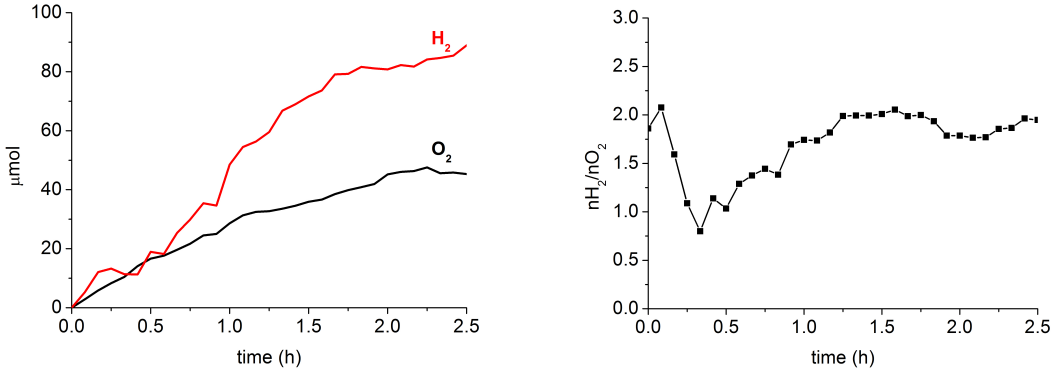

Figure 3.20. ***Left:*** *Evolved O_2 (black) and H_2 (red) during bulk electrolysis at 1.3 V (vs NHE) with 1.0 mM Co_9 in 50 mM NaP_i buffer solution containing 1 M $NaNO_3$ as electrolyte at pH = 8. Pt mesh working and counter electrodes and Ag/AgCl (NaCl 3 M) reference electrode.* ***Right:*** *Relation between moles of O_2 and moles of H_2 in in the same experimental conditions.*

Stability during long-term bulk water electrolysis

3. $\{Co^{II}_9\}$ Polyoxometalate WOC

In order to study in detail the real activity of **Co_9**, successive 2-5 hour bulk electrolysis cycles were performed changing the Pt mesh electrode in the anode for a new one (Figure 3.21, left; Table 3.5), to periodically remove the CoO_x contribution.

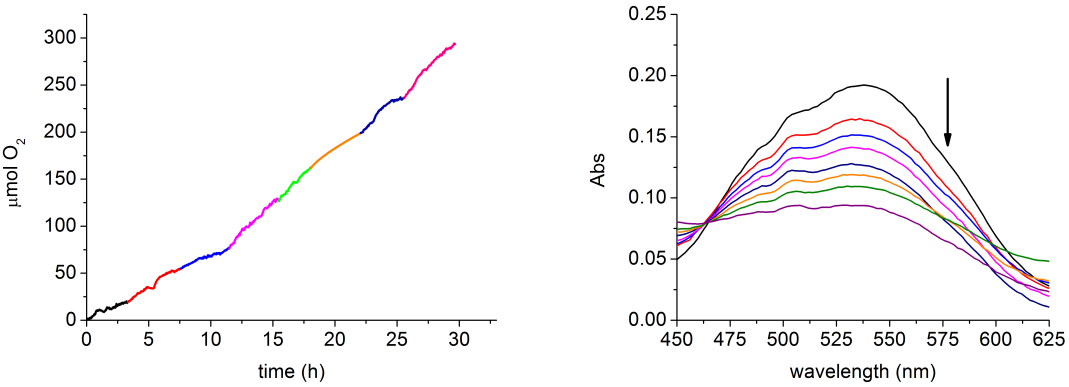

Figure 3.21. ***Left:*** *Successive* ***Co_9*** *(initially 1.0 mM) catalyzed bulk electrolysis at 1.3 V (vs NHE) with 1.0 mM Co_9 in 50 mM NaP_i buffer solution containing 1 M $NaNO_3$ as electrolyte at pH = 7. Pt mesh working and counter electrodes and Ag/AgCl (NaCl 3 M) reference electrode.* ***Right:*** *Corresponding UV-vis spectra of the solution after each electrolysis process. Color codes correspond to each successive cycle.*

cycle	% catalyst	cycle time (h)	µmol O_2	total time (h)	total µmol O_2
1	100	3	19	3	19
2	85	5	36	8	55
3	79	4	21	12	76
4	73	4	53	16	129
5	66	2	33	18	162
6	62	4	36	22	198
7	57	4	38	26	236
8	48	4	59	30	295

Table 3.5. *Experimental data for successive catalytic bulk electrolysis at 1.3 V (vs NHE)* ***Co_9*** *in 50 mM NaP_i buffer solution containing 1 M $NaNO_3$ as electrolyte at pH = 7. Pt mesh working and counter electrodes and Ag/AgCl (NaCl 3 M) reference electrode. % catalyst = % of Co_9 remaining in solution respect to the initial one, calculated by the absorbance at λ = 538 nm.*

UNIVERSITAT ROVIRA I VIRGILI
NOVEL MOLECULAR CATALYSTS FOR WATER OXIDATION: TOWARDS ARTIFICIAL PHOTOSYNTHESIS
Sara Goberna Ferrón
Dipòsit Legal: T.189-2014

The **Co_9** content after each cycle was estimated through UV-Vis spectroscopy (Figure 20, right). The concentration of **Co_9**, estimated by the absorbance at λ = 538 nm, slowly decreases during each electrolysis at a rate ≈1.7 % per hour, maintaining about 50% of the starting value after seven cycles (30 hours). More diluted conditions yield higher catalytic activity, as the oxygen evolution rate increases continuously with each cycle as [**Co_9**] decreases. It is noteworthy that this experiment corresponds to 30 hours of continuous water oxidation catalysis, and that each cycle was carried out in a different day, showing how the **Co_9** solution is stable for long periods of time (at least over one week).

Comparison between Co_9 and Co_4 as electrocatalyst

The performance of **Co_9** was compared, in the same experimental conditions, with **Co_4**.[45] Bulk water electrolysis experiments were repeated using 1 mM **Co_4** in a 50 mM NaP_i buffered solution at pH 8. When an anodic voltage of 1.3 V is applied, continuous and faster current decrease is observed as the Co oxide thin film deposits. In this case stability is not reached even after 5 hours (Figure 3.22). This suggests that anode deposition is not the only process promoting **Co_4** decomposition, since it still occurs through the whole water electrolysis.

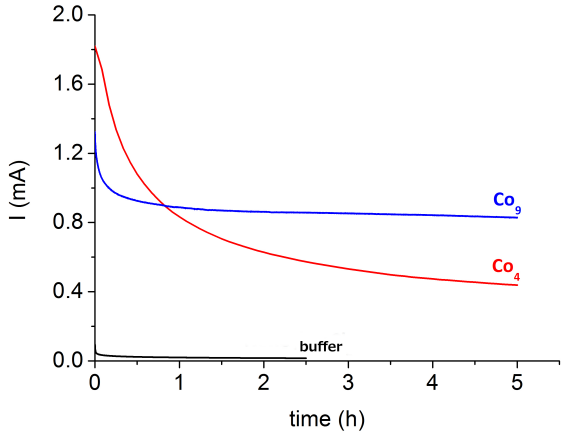

Figure 3.22. ***Co_9*** *(blue)* ***or Co_4*** *(red) (1.0 mM) catalyzed bulk water electrolysis in a 50 mM NaP_i buffer with 1 M $NaNO_3$ as electrolyte at pH = 8, applying a constant potential of 1.3 V (vs NHE) and blank experiment (black) in the same conditions. Pt*

UNIVERSITAT ROVIRA I VIRGILI
NOVEL MOLECULAR CATALYSTS FOR WATER OXIDATION: TOWARDS ARTIFICIAL PHOTOSYNTHESIS
Sara Goberna Ferrón
Dipòsit Legal: T.189-2014

mesh working and counter electrodes and Ag/AgCl (NaCl 3 M) reference electrode.

The monitored *in situ* oxygen evolution catalyzed by **Co_4** is also quite different than for **Co_9** (Figure 3.23). In the same experimental conditions describe above, the O_2 generation was quantified with a fluorescence probe. In the case of **Co_4**, the oxygen evolution is maintained for 1 hour, and after 3 hours the oxygen content reaches a maximum constant value as the catalytic water oxidation is over. This deactivation of the catalyst indicates than **Co_4** decomposes faster than **Co_9**.

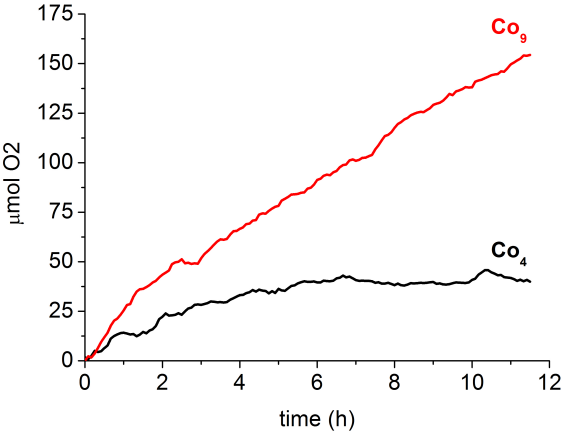

Figure 3.23. *Catalytic O_2 evolution (black) during bulk electrolysis at 1.3 V (vs NHE) with 1.0 mM **Co_9** (red) or **Co_4** (black) in 50 mM NaPi buffer solution containing 1 M $NaNO_3$ as electrolyte at pH = 8. Pt mesh working and counter electrodes and Ag/AgCl (NaCl 3 M) reference electrode.*

The experiments above, with a Pt mesh electrode as anode, indicate that **Co_9** is active as water oxidation catalyst, but the in situ formation of a CoO_x oxide film covering the electrode surface precludes the quantification of its genuine catalytic activity. Oxide formation should be avoided, or at least controlled, to properly characterize the homogeneous catalytic activity of **Co_9**.

Bulk water electrolysis with Co_9 on a FTO working electrode

- 3. 2. Results and Discussion -

Since the formation of the CoO_x film depends on the nature of the anode (faster on carbon than on Platinum), a possible strategy could be the use of a different electrode surface. For this purpose, fluorine-doped tin oxide (FTO) coated glass electrode was chosen as working electrode. This material is optically transparent and electrically conductive. The transparency allows for a better characterization of the deposited materials by direct spectroscopic techniques. Moreover, FTO electrodes are more inert, ensuring a minimal background activity for O_2 production. Bulk water electrolysis experiments were carried out in a U-shape two-chamber cell with both chambers connected through a glass frit. Fluorine-doped tin oxide (FTO) coated glass electrode was used as anode and a platinum mesh was used as cathode (Figure 3.24). Negligible current values were obtained in a 50 mM NaP_i buffer at pH = 7 with 1 M $NaNO_3$ as electrolyte when an anodic overpotential of ≈ 600 mV was applied (1.41 V). With the addition of **Co_9** (1.0 mM) to the anode compartment, the current rapidly increases over 1 order of magnitude, reaching typical values over 3 mA. However, as it was observed using a Pt mesh working electrode, through this process a brown film deposits on the surface of the FTO electrode. However, in this case the film deposits quicker. As oxidation proceeds, the film grows thicker reaching a maximum current value in 20 minutes. This increase of current until a maximum value of intensity corresponds with the CoO_x film formation, as reported by Nocera and coworkers.[60] Once the cobalt oxide is form, the current intensity decreases until it reaches a constant value after 1 h. The activity of this film was tested with a successive bulk electrolysis using the CoO_x covered anode in the absence of **Co_9**. In this case, no significant change in the current is observed (Figure 3.24), demonstrating that the deposited cobalt oxide is the main catalyst, even when **Co_9** is present in solution.

The cobalt oxide film on the electrode was characterized by electron microscopy. EDX analysis confirmed cobalt was the only metallic component with some phosphate traces, in good agreement with the reported data (Figure 3.25).[46] The **Co_9** content in

UNIVERSITAT ROVIRA I VIRGILI
NOVEL MOLECULAR CATALYSTS FOR WATER OXIDATION: TOWARDS ARTIFICIAL PHOTOSYNTHESIS
Sara Goberna Ferrón
Dipòsit Legal: T.189-2014

solution, after water electrolysis, was estimated through UV-Vis spectroscopy (Figure 3.26). Concentration stays about 60%. No further decomposition occurs once the electrode is completely covered, even at very long times (>8 h). This result suggests that the oxide formation occurs only on the surface of the electrode. Once the electrode is completely covered, decomposition quantitatively stops. This process is much faster than the procedures reported by Nocera and coworkers,[60] where 8-hour electrolysis is needed to completely cover the electrode with cobalt oxide.

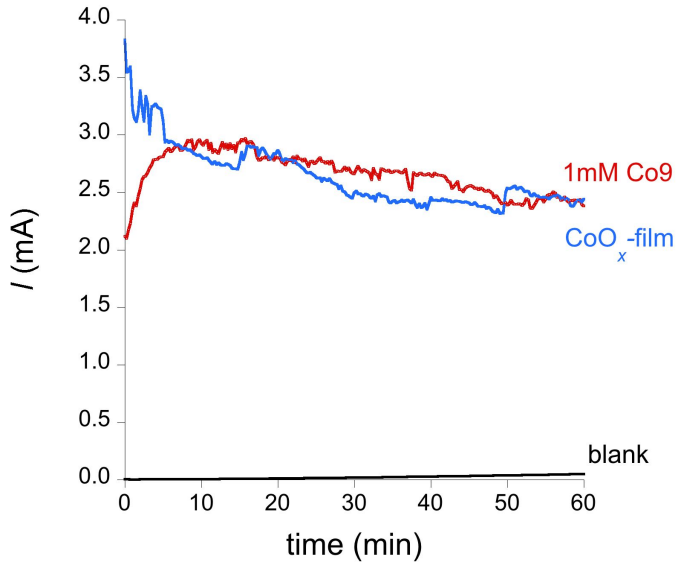

Figure 3.24. *Catalyzed bulk water electrolysis in a 50 mM NaP_i buffer with 1 M $NaNO_3$ as electrolyte at pH = 7, applying a constant potential of 1.41 V (vs NHE). Initial blank (black), 1.0 mM* ***Co_9*** *(red) and blank after* ***Co_9****–catalyzed electrolysis (blue). FTO working electrode, Pt mesh counter electrode and Ag/AgCl (NaCl 3 M) reference electrode.*

UNIVERSITAT ROVIRA I VIRGILI
NOVEL MOLECULAR CATALYSTS FOR WATER OXIDATION: TOWARDS ARTIFICIAL PHOTOSYNTHESIS
Sara Goberna Ferrón
Dipòsit Legal: T.189-2014

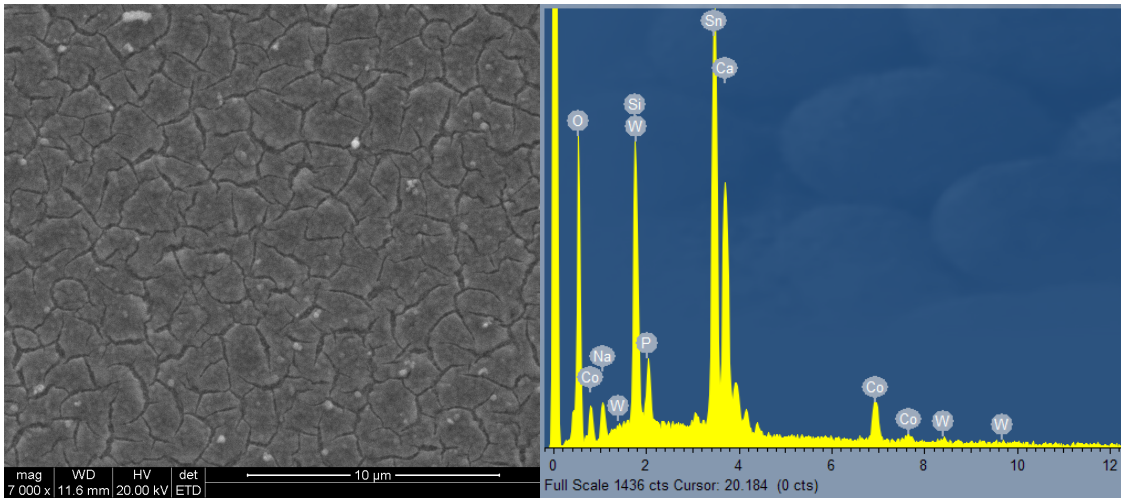

Figure 3.25. *SEM image and EDX analysis of the surface of a FTO electrode after 1 hour of catalytic water oxidation under an applied voltage of 1.41 V (vs NHE) with 1.0 mM* ***Co$_9$*** *in 50 mM NaP$_i$ buffer solution containing 1 M NaNO$_3$ as electrolyte at pH = 7.*

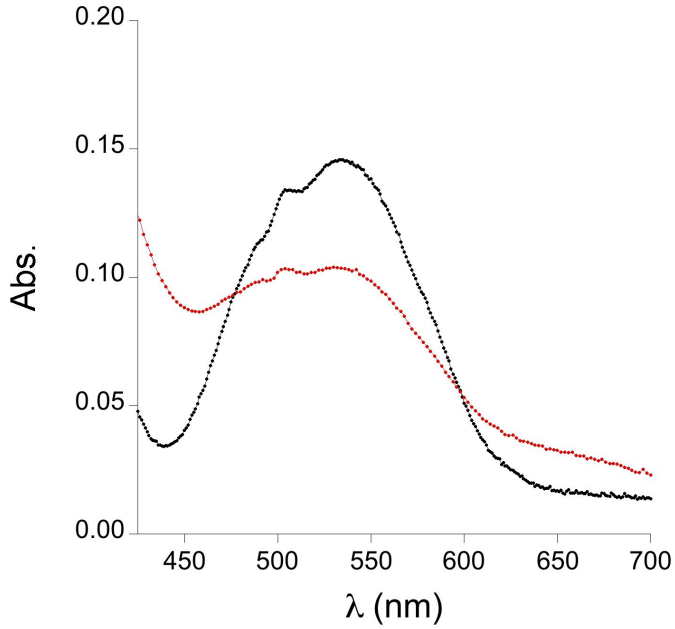

Figure 3.26. *UV-vis spectra of a solution before (black) and after (red) 1 hour of catalytic water oxidation under an applied voltage of 1.41 V (vs NHE) with 1.0 mM* ***Co$_9$*** *in 50 mM NaP$_i$ buffer solution containing 1 M NaNO$_3$ as electrolyte at pH = 7.*

Bulk Water Oxidation using a Dye-Sensitized Solar Cell

- 3. $\{Co^{II}_9\}$ Polyoxometalate WOC -

Analogous experiments using a Co_9 solution and a FTO electrode can be performed using a dye-sensitized solar cell (DSSC) as power source, mimicking photosynthesis. In this case, sunlight is first converted into electrical power by the DSSC, and this is used to split water with the help of our Co9 catalyst. We used two DSSCs provided by Prof. Emilio Palomares Group (ICIQ) forming a tandem device.

The DSSC comprises a dye sensitized porous, nanocrystalline titanium dioxide film interpenetrated by a liquid electrolyte containing an I^- / I^{3-} redox couple. The main charge-transfer events take place at the TiO_2 / dye / electrolyte interface. Photoinduced electron injection from the sensitizer dye into the TiO_2 conduction band initiates charge separation. The injected electrons are transported through the metal oxide film to one electrode, while the redox-active electrolyte is employed to reduce the dye cation to its original state. And the resulting positive charge is transported to a platinum counter electrode. Each DSSC yields a potential difference between 0.6 and 0.7 V. Since this voltage is not enough to oxidize water at neutral pH, we connected two DSSCs cells as in a tandem scheme to reach a voltage difference over 1.2 V. The working electrode of the tandem DSSC was connected to the FTO electrode immersed in the Co_9 solution of the anodic compartment, while the counter electrode was connected to the Pt mesh of the cathode compartment. Once irradiation starts, oxygen starts to evolve in the anodic compartment, while H_2 is produced in the cathodic compartment (Equations 3.5-3.6).The hydrogen evolution in the cathode compartment headspace was monitored with a Clark-type hydrogen sensor (Figure 3.27). As we know, during this reaction part of the Co9 will be transformed into CoOx on the surface of the FTO. But still this experiment is an interesting proof-of-concept that demonstrates that hydrogen can be produced using exclusively solar energy with the help of our Co9 catalyst. We will continue investigating this hydrogen production scheme.

UNIVERSITAT ROVIRA I VIRGILI
NOVEL MOLECULAR CATALYSTS FOR WATER OXIDATION: TOWARDS ARTIFICIAL PHOTOSYNTHESIS
Sara Goberna Ferrón
Dipòsit Legal: T.189-2014

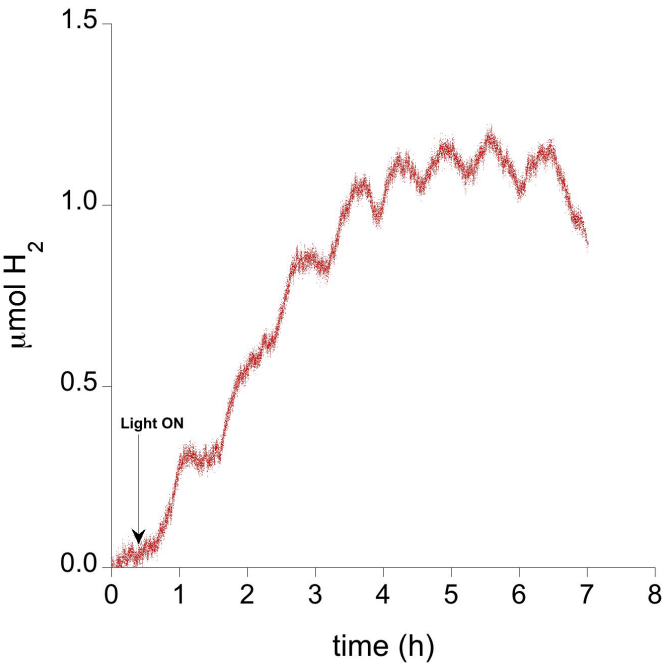

Figure 3.27. *Evolved H_2 during bulk electrolysis using a DSSC with 1.0 mM Co_9 in 50 mM NaP_i buffer solution containing 1 M $NaNO_3$ as electrolyte at pH = 7. FTO working electrode and Pt mesh counter electrode.*

Water Oxidation with Cobalt Oxide films prepared from Co_9

Although the main objective of this chapter is the characterization of **Co_9** as a WOC, it is interesting to study the catalytic activity of the CoO_x film prepared using **Co_9** as a precursor, since this preparation may have some advantages.

The procedure for electrodeposition of an amorphous cobalt oxide from **Co_9** was carried out in a U-shape two-chamber cell. As described above, a FTO working electrode was used as anode for the deposition of the cobalt oxide film, by applying a a constant oxidation voltage in the 1.05−1.5 V range to a 50 mM NaP_i buffer at pH = 7 with 1 M $NaNO_3$ with a 1mM concentration of **Co_9**. When catalyst films were grown by controlled potential electrolysis at E_{appl} > 1.05 V, the growth of the film is accompanied by significant O_2 evolution. Thereby, the charge passed in a deposition is not representative of the number of Co atoms deposited. When films are prepared by controlled potential electrolysis at 1.05 V (Figure 3.28, left), negligible water oxidation

UNIVERSITAT ROVIRA I VIRGILI
NOVEL MOLECULAR CATALYSTS FOR WATER OXIDATION: TOWARDS ARTIFICIAL PHOTOSYNTHESIS
Sara Goberna Ferrón
Dipòsit Legal: T.189-2014

catalysis occurs. Accordingly, the charge that passes through the electrode (C) during the deposition is proportional to the Co^{II} to Co^{III} oxidation reaction. Therefore, the measured charge allows to estimate [Q (C) / F (C/mol)] the number of moles of CoO_x incorporated into the film[61] (Table 3.6).

Bulk water electrolysis experiments were performed using these CoO_x modified electrodes applying an oxidation potential of 1.4 V in a 50 mM sodium phosphate (NaP_i) buffer at pH = 7. Using equation 8, turnover frequency values, TOF, can be calculated:

$$TOF = \frac{I}{4Fn} \qquad \text{(Eq. 3.8)}$$

Where n = number of moles of CoO_x deposited into the film, I = intensity (A) and F = Faraday's constant (C mol^{-1}). TOF numbers were calculated for electrodes after different deposition times and the values compared (Figure 3.28, right and Table 3.5). The TOF values obtained and the similarity among films of varying cobalt content are in agreement with the literature data, where TOFs ≈2 × 10^{-3} s^{-1} at an overpotential of 410 mV are reported for different film thickness[61]. This TOF estimation is a lower limit since assumes that every Co center in the film is catalytically active.

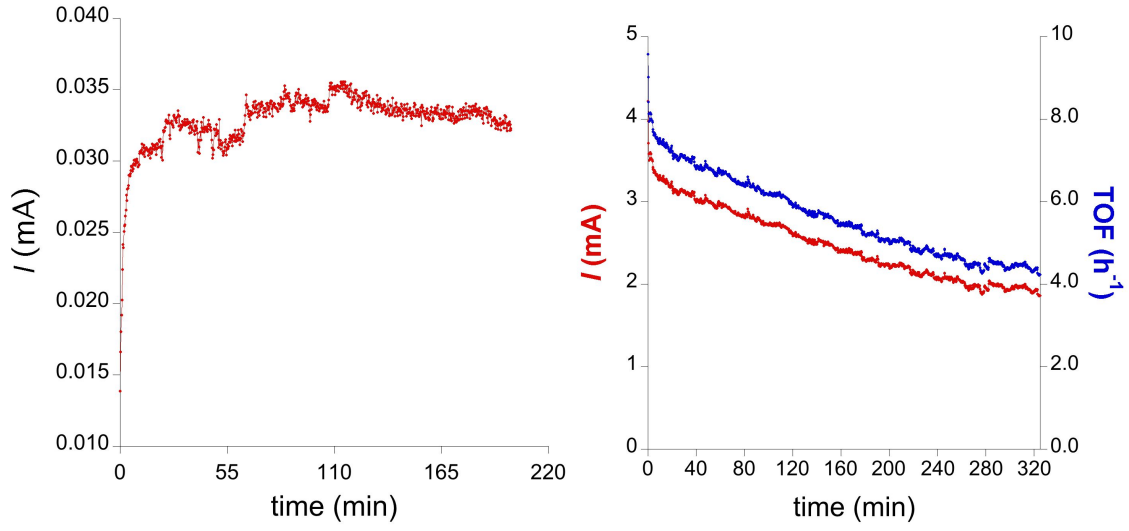

UNIVERSITAT ROVIRA I VIRGILI
NOVEL MOLECULAR CATALYSTS FOR WATER OXIDATION: TOWARDS ARTIFICIAL PHOTOSYNTHESIS
Sara Goberna Ferrón
Dipòsit Legal: T.189-2014

Figure 3.28. ***Left:*** *Current profile of the electrodeposition of CoO_x on FTO electrode by applying a constant potential of 1.05 V (vs NHE) in a 50 mM NaP_i buffer with 1 M $NaNO_3$ as electrolyte at pH = 7 solution containing 1.0 mM* ***Co_9****.* ***Right:*** *Current (red) and TOF (blue) profile of catalyzed bulk water applying a constant potential of 1.41 V using the CoO_x modified FTO as catalyst in a* ***Co_9****–free 50 mM NaP_i buffer with 1 M $NaNO_3$ as electrolyte at pH = 7 solution. Pt mesh counter electrode and Ag/AgCl (NaCl 3 M) reference electrode.*

Deposition time (h)	Charge (C)	µmol CoO_x	TOF (s^{-1})	TOF (h^{-1})
12	1.63	17	6×10^{-3}	2.2
4	0.68	7.1	1.8×10^{-2}	6.5
3.5	0.40	4.1	1.9×10^{-2}	6.8

Table 3.6. *Experimental data for electrodeposited CoO_x on FTO electrodes (constant potential of 1.05 V (vs NHE) in a 50 mM NaP_i buffer with 1 M $NaNO_3$ as electrolyte at pH = 7 solution containing 1.0 mM* ***Co_9****) and the corresponding TOF values after charge = 5 C of catalytic bulk electrolysis at 1.41 V (vs NHE) using the CoO_x modified FTO as catalyst in a* ***Co_9****–free 50 mM NaP_i buffer with 1 M $NaNO_3$ as electrolyte at pH = 7 solution. Pt mesh counter electrode and Ag/AgCl (NaCl 3 M) reference electrode.*

The effect of the overpotential (η) on the current density (*i*) has been investigated. The set–up for these experiments is exactly the same than the one used for bulk water electrolysis. However, in this case, different potentials were applied for 10 minutes, and the average of the steady state current values is plotted against the overpotential (Tafel plot, see Appendix I for details). The Tafel behavior of the catalyst in the region of water oxidation follows the expected linear trend (Figure 3.29).

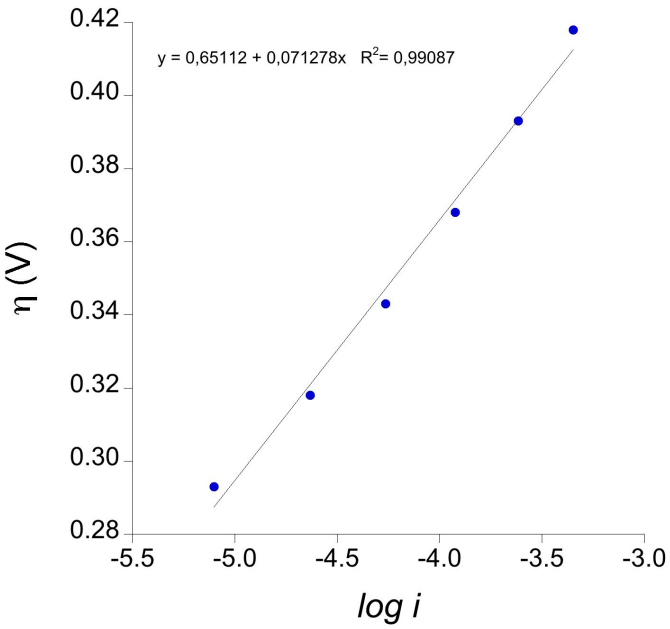

Figure 3.29 *Tafel plot of the steady state current density in a* ***Co_9****–free 50 mM NaP_i buffer solution containing 1 M $NaNO_3$ as electrolyte at pH = 7 using a CoO_x film electrodeposited by applying a constant potential of 1.05 V (vs NHE) during 3.5 hours in a solution containing 1.0 mM* ***Co_9****. Calculated slope = 71 mV decade^{-1}.*

Electrolysis was conducted at each overpotential in a **Co_9**–free 50 mM NaP_i buffer at pH = 7. Tafel data were collected using freshly prepared films that were deposited at different reaction conditions (Table 3.7). The optimized reaction conditions to prepare the CoO_x film are an applied voltage of 1.05 V and 3.5 hours of deposition time. In this case, the Tafel slope (70 mV decade^{-1}) and the overpotential that would be needed to reach 1 mA cm^{-2} (420 mV) are very similar to the data reported by Nocera and coworkers.[60,61] This slope is characteristic of a chemical rate-limiting step. A chronoamperometric pre–treatment at 1.4 V in a **Co_9**–free buffered solution is not improving the value of the Tafel slope (95 mV decade^{-1}), indicating that the film could be altered during bulk water electrolysis. The deposition time also affects the activity of the films. Better results were obtained for shorter deposition times. This suggest that, once the film is formed, an extra-deposition time is decomposing the film or that higher CoO_x incorporated in the film have an influence in the reaction kinetics by barriers to electron and/or mass transport within the film. Higher deposition voltages

UNIVERSITAT ROVIRA I VIRGILI
NOVEL MOLECULAR CATALYSTS FOR WATER OXIDATION: TOWARDS ARTIFICIAL PHOTOSYNTHESIS
Sara Goberna Ferrón
Dipòsit Legal: T.189-2014

do not improve the Tafel slope, possibly because the competition with the water oxidation reaction during incorporation of the CoO_x film leads to less-quality films.

Deposition time (h)	**E_{appl} (V)**	**1.4 V pre-treatment time (h)**	**Tafel slope mV decade^{-1}**	**η (V) (i = 1mA cm^{-2})**
3.5	1.05	✗	71	0.42
3.5	1.05	12	95	0.53
12	1.05	✗	90	0.47
4	1.4	4	114	0.51
12	1.4	✗	100	0.49
4	1.3	4	93	0.51
8 (Nocera's film)[60]	*1.3*	✗	*60*	*0.41*

Table 3.7. *Electrodeposition conditions for different CoO_x modified FTO electrodes in a 50 mM NaP_i buffer with 1 M $NaNO_3$ as electrolyte at pH = 7 solution containing 1.0 mM Co_9 and the corresponding Tafel slope and overpotential (η) needed to reach 1mA cm^{-2} values using the CoO_x modified FTO as catalyst in a Co_9–free 50 mM NaP_i buffer with 1 M $NaNO_3$ as electrolyte at pH = 7 solution. Pt mesh counter electrode and Ag/AgCl (NaCl 3 M) reference electrode.*

In order to determine the faradic efficiency of the catalyst, O_2 evolution was measured with a fluorescence probe O_2 sensor during bulk water electrolysis experiments (Figure 3.30) applying a constant voltage of 1.41 V to a 50 mM NaP_i buffer solution at pH = 7 using the optimized CoO_x film as working electrode. The percentage of oxygen detected agrees with the expected values assuming that all the current was caused by 4 e^- oxidation of water to produce oxygen. The efficiency is quantitative during the first 4 hours. Then the experimental line deviates from the theoretical one, probably due to film decomposition during the experiments.

UNIVERSITAT ROVIRA I VIRGILI
NOVEL MOLECULAR CATALYSTS FOR WATER OXIDATION: TOWARDS ARTIFICIAL PHOTOSYNTHESIS
Sara Goberna Ferrón
Dipòsit Legal: T.189-2014

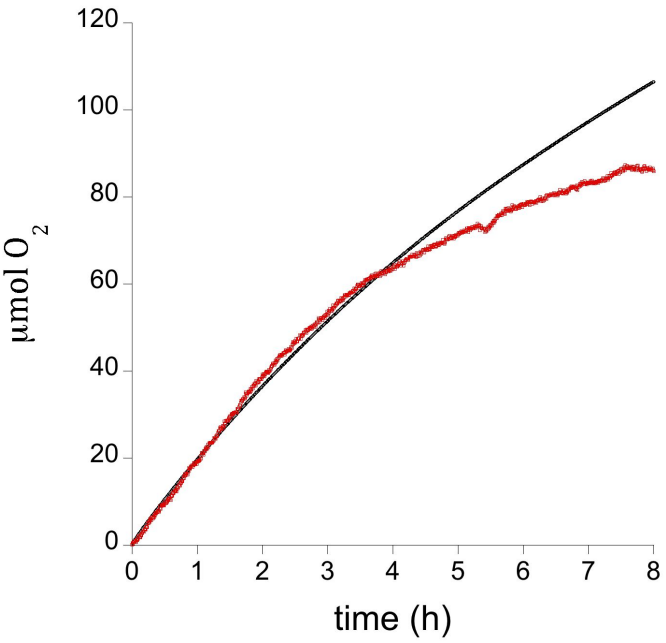

Figure 3.30. *Catalytic O_2 evolution (red) during bulk electrolysis at 1.41 V (vs NHE) in a* ***Co_9****–free (50 mM NaP_i buffer containing 1 M $NaNO_3$ as electrolyte at pH = 7) solution using the CoO_x film electrodeposited on FTO (constant potential of 1.05 V (vs NHE) during 3.5 hours in a solution containing 1.0 mM* ***Co_9****) and theoretical O_2 (black) assuming Faradaic behavior. Pt counter electrode and Ag/AgCl (NaCl 3 M) reference electrode.*

In summary, the use of **Co_9** as a precursor for the preparation of active heterogeneous CoO_x film has some advantages; films are prepared in a few hours by applying low voltages.

Homogeneous Electrocatalytic Water Oxidation: Co_9 is a genuine WOC

If free Co^{II} ions are a needed intermediate between decomposition of the POM and formation of the cobalt oxide, the addition of 2,2’ -bipyridyl (bpy) could prevent film deposition. Following this hypothesis, bulk electrolysis experiments were

repeated with the addition of bpy to account for a 30% loss of **Co_9**. In this case, catalytic current also appears, but it does not reach such high values as in the previous conditions. Stable current values remain below 1 mA, less than one-third that observed in the absence of bpy. This already suggests that the main catalyst is different in both experiments. After 1 h cycles, the catalytic activity of the anode was checked by repeating the electrolysis experiments with the same **"**as used**"** electrode in a buffer solution without the addition of **Co_9**. No significant activity was observed (Figure 3.31) in this case, with intensities very close to the original blank. In addition, no traces of cobalt were detected on the surface of the electrodes. The peaks that appear in the EDX histogram (Figure 3.32, right) belong exclusively to the composition of the FTO-coated glass electrode itself. The electrode surface appears clean, as it can be observed in the SEM image (Figure 3.32, left), with no sign of film deposition, in contrast with the same bpy-free experiment (Figure 3.25).

All this experimental evidence confirms that, in these conditions, **Co_9** is a genuine homogeneous WOC. The efficiency for oxygen evolution of this electrocatalytic reaction was determined with a fluorescence probe (Figure 3.33). It is quantitative for the first 15 min, and then it maintains ≈ 90% efficiency for over 1 h.

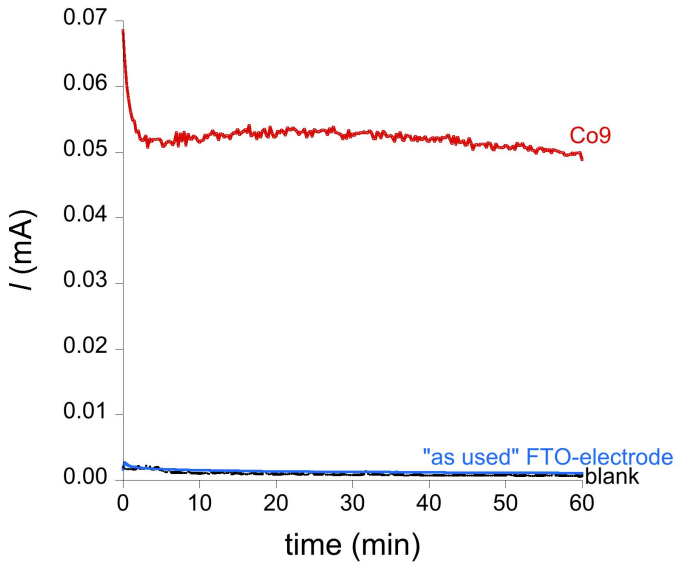

UNIVERSITAT ROVIRA I VIRGILI
NOVEL MOLECULAR CATALYSTS FOR WATER OXIDATION: TOWARDS ARTIFICIAL PHOTOSYNTHESIS
Sara Goberna Ferrón
Dipòsit Legal: T.189-2014

Figure 3.31. *Catalyzed bulk water electrolysis in a 50 mM NaP_i buffer with 1 M $NaNO_3$ as electrolyte at pH = 7, applying a constant potential of 1.41 V (vs NHE). Initial blank (black), 1.0 mM* ***Co_9*** *+ 2.8 mM bpy (red) and blank after* ***Co_9****–catalyzed electrolysis (blue). FTO working electrode, Pt mesh counter electrode and Ag/AgCl (NaCl 3 M) reference electrode.*

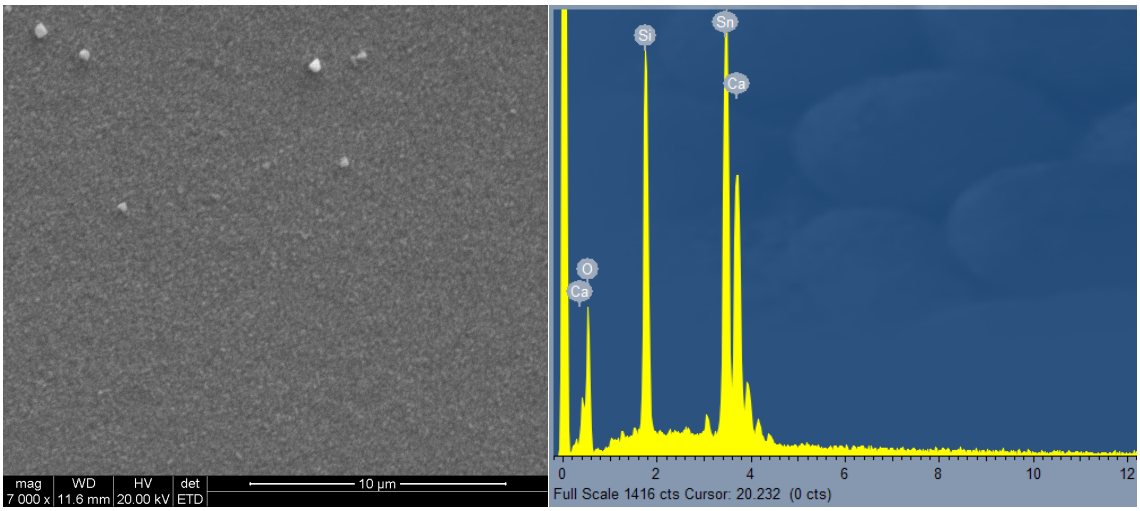

Figure 3.32. *SEM image and EDX analysis of the surface of a FTO electrode after 1 hour of catalytic water oxidation under an applied voltage of 1.41 V (vs NHE) with 1.0 mM* ***Co_9*** *+ 2.8 mM bpy in 50 mM NaPi buffer solution containing 1 M $NaNO_3$ as electrolyte at pH = 7.*

UNIVERSITAT ROVIRA I VIRGILI
NOVEL MOLECULAR CATALYSTS FOR WATER OXIDATION: TOWARDS ARTIFICIAL PHOTOSYNTHESIS
Sara Goberna Ferrón
Dipòsit Legal: T.189-2014

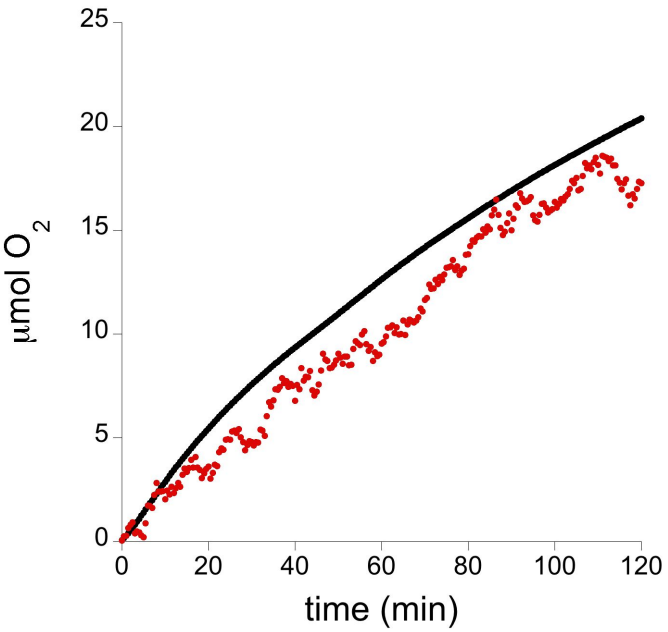

Figure 3.33. *Catalytic O_2 evolution (red) during bulk electrolysis at 1.41 V (vs NHE) in a* ***Co₉*** *1.0 mM + 2.8 mM bpy (50 mM NaP_i buffer containing 1 M $NaNO_3$ as electrolyte at pH = 7) solution and theoretical O_2 (black) assuming Faradaic behavior. FTO working electrode, Pt mesh counter electrodes and Ag/AgCl (NaCl 3 M) reference electrode.*

The current not involved in water oxidation probably comes from the expected oxidation of the $[Co(bpy)_3)]^{2+}$ species generated in solution. Indeed, at the end of the catalytic cycle, a fine pink precipitate appeared at the bottom of the reactor. This precipitate was characterized as a $[Co(bpy)_3)]^{3+}$ salt of the **Co_9** polyanion. IR spectrometry shows typical spectra of **Co_9**, with some additional bands that can be assigned to a tris(bipyridyl)metal complex (Figure 3.34). Metal analysis showed a 1:2 Co/W ratio, consistent with $[Co^{3+}(bpy)_3)]_4A_4[Co_9]$ stoichiometry, where A = Na^+ or K^+ (Figure 3.35 and Table 3.8). This highly insoluble precipitate can also be prepared by the addition of $[Co(bpy)_3)]^{3+}$ to a **Co_9** solution.

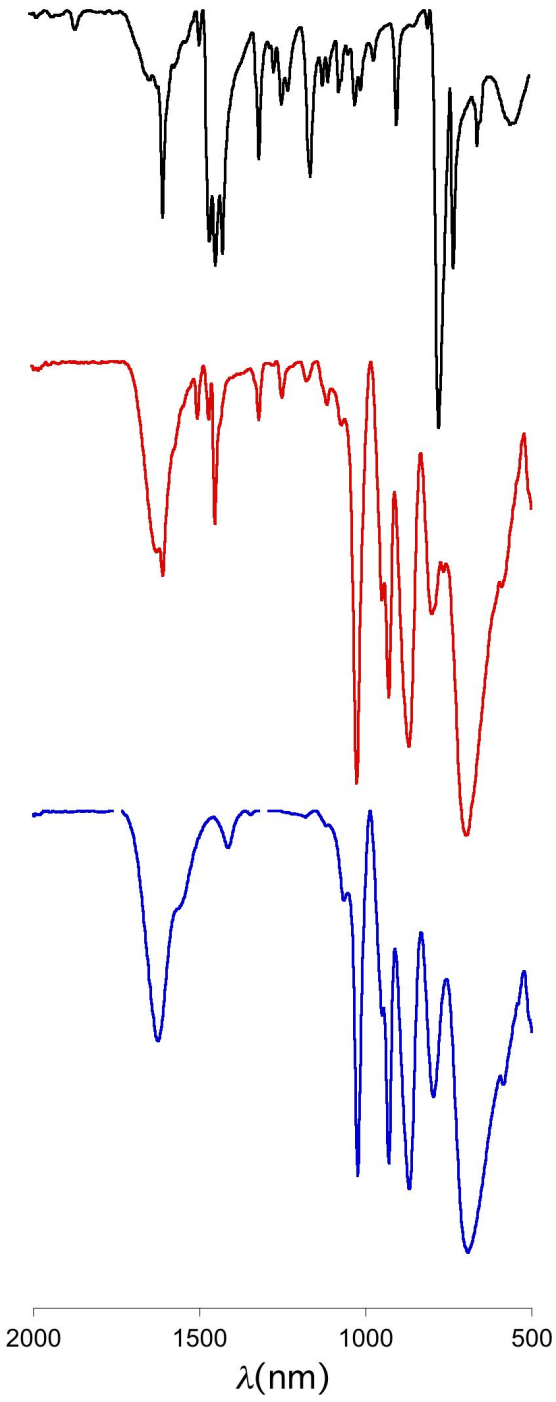

Figure 3.34. *Comparison between the IR spectra of $[Co(bpy)_3)]Cl_3$ (black);* ***Co_9*** *(blue) and the pink powder (red) recovered from the bottom of the reactor after 2 hours–bulk water oxidation with* ***Co_9*** *1.0 mM + 2.8 mM bpy (50 mM NaP_i buffer, 1 M $NaNO_3$, pH = 7) solution applying a constant voltage of 1.41V vs NHE.*

UNIVERSITAT ROVIRA I VIRGILI
NOVEL MOLECULAR CATALYSTS FOR WATER OXIDATION: TOWARDS ARTIFICIAL PHOTOSYNTHESIS
Sara Goberna Ferrón
Dipòsit Legal: T.189-2014

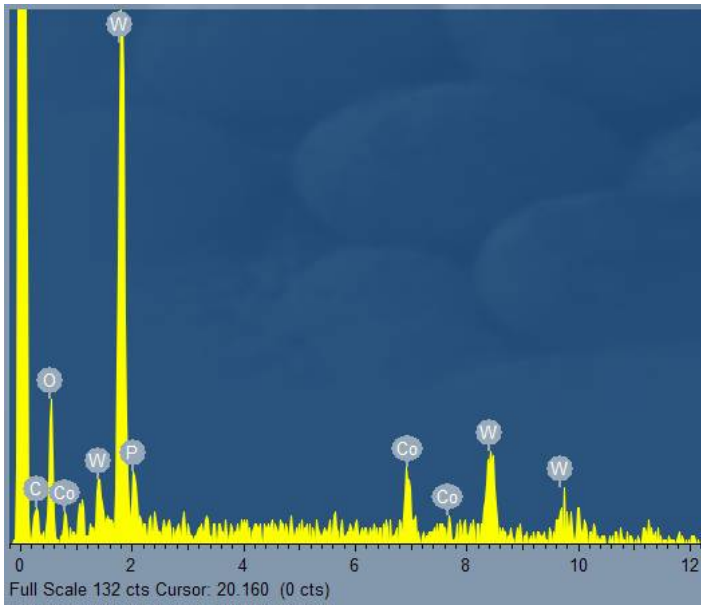

Figure 3.35. Typical EDX histogram *the pink powder recovered from the bottom of the reactor after 2 hours–bulk water oxidation with* ***Co_9*** *1.0 mM + 2.8 mM bpy (50 mM NaP_i buffer, 1 M $NaNO_3$, pH = 7) solution applying a constant voltage of 1.41V vs NHE.*

Element	Atomic %	Estimated Ratio	Theoretical Ratio
P	13.3	6.16	5
Co	28.1	13	13
W	58.6	27.1	27

Table 3.8. *Metal analysis summary results calculated from EDX analysis corresponding to Figure 33.*

Catalyst concentration and applied voltage have significant effect in analogous bulk electrolysis experiments (Table 3.9). As expected, O_2 evolution decreases by decreasing the concentration of catalyst. On the other hand, O_2 generation increases at higher potentials. In all the experiments the surface of the FTO electrode was analyzed after the catalysis using EDX to ensure that there was no trace of cobalt oxide.

UNIVERSITAT ROVIRA I VIRGILI
NOVEL MOLECULAR CATALYSTS FOR WATER OXIDATION: TOWARDS ARTIFICIAL PHOTOSYNTHESIS
Sara Goberna Ferrón
Dipòsit Legal: T.189-2014

[Co_9] (mM)	E_{appl} vs NHE (V)	I_{max} (mA)	µmol O_2 (Faraday's Law)
1	1.4	0.06	0.6
0.25	"	0.012	0.09
0.06	"	0.005	0.04
1	1.5	0.5	4.0
"	1.3	0.05	0.4
"	1.1	0.04	0.32
"	1.0	0.03	0.26

Table 3.9. *Summary of results obtained for with **Co_9** + 30% bpy (50 mM NaP_i buffer, 1 M $NaNO_3$, pH = 7) solution. FTO working electrode, Pt mesh counter electrode and Ag/AgCl (NaCl 3 M) reference electrode. I_{max} corresponds to the current at 1000 seconds and it used to calculate the moles of oxygen using Faraday's Law [Q (C) / 4Fn].*

Kinetics of Co_9-catalyzed water oxidation

Returning to cyclic voltammetry measurements, we repeated CVs using a glassy carbon working electrode and in the presence of bpy. A catalytic water oxidation wave appears (Figure 3.36), when the curve deviates from the blank above 1.10 V, at the onset of the catalytic water oxidation wave. On the contrary, when bpy is not present in solution, the current signal deviates from the blank just above 0.75 V. This voltage is not enough to oxidize water, and this current should be related to the formation of a cobalt oxide film without any water oxidation occurring, as already stated by Nocera and co-workers.[61] The current increases much faster after 1.10 V, indicating the onset of catalytic water oxidation. The current values are higher than those in the Co_9-only catalyzed case. These features corroborate again the presence of a cobalt oxide catalyst in the absence of bpy and they also support the negligible participation of CoO_x when a chelating agent is present in solution.

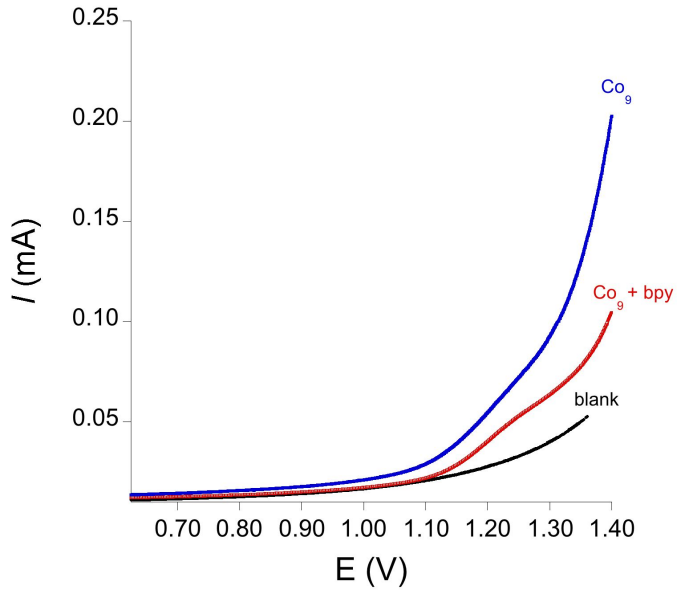

Figure 3.36. *Cyclic voltammetry using a glassy carbon electrode, 100 mV scan rate, of a 1.0 mM* ***Co₉*** *(50 mM NaP_i buffer, 1 M $NaNO_3$, pH = 7) (black line) and in the presence of 1.4 mM bpy (red line). Potentials reported vs NHE.*

The Tafel plot from steady current density data follows the expected linear trend for a catalytic process (Figure 3.37). For a 1 mM catalyst concentration (añadir concentración de bpy), a measurable current density was observed over 1.15 V, corresponding to an overpotential η = 353 mV. The calculated Tafel slope is consistent in the 130–140 mV decade^{-1} range. This slope implies that the rate-determining step is electrochemical,[62,63] arising from electron- or mass-transport issues. A η = 776 mV would be needed to reach 1 mA s^{-1} cm^{-2}. In more dilute conditions, the kinetics of the catalyzed water electrolysis change as the Tafel slope decreases. Below 0.25 mM, the slope is in the 55-65 mV decade^{-1} range, consistent with a chemical step becoming the rate-limiting one.[61,64] Thus, a lower overpotential is needed to reach the same current densities. For example, η = 695 mV would be needed to reach 1 mA s^{-1} cm^{-2} with a 0.06 mM Co9 concentration. We want to stress that the current densities obtained in these experimental conditions are lower than those observed for cobalt oxides, where an overpotential below 450 mV typically allows to reach analogous current values. It is also worth mentioning that this

UNIVERSITAT ROVIRA I VIRGILI
NOVEL MOLECULAR CATALYSTS FOR WATER OXIDATION: TOWARDS ARTIFICIAL PHOTOSYNTHESIS
Sara Goberna Ferrón
Dipòsit Legal: T.189-2014

comparison is not fair to the homogeneous catalyst because current density is concentration-dependent.

The **Co_9** content after Tafel plot experiments was estimated through UV-Vis spectroscopy (Figure 3.38). The concentration of **Co_9** lost was estimated at about 23% of the initial **Co_9**. The loss of **Co_9** in solution comes from the precipitation of the $[Co(bpy)_3)]^{3+}$ salt of the **Co_9** polyanion, that occurs during water electrolysis experiments.

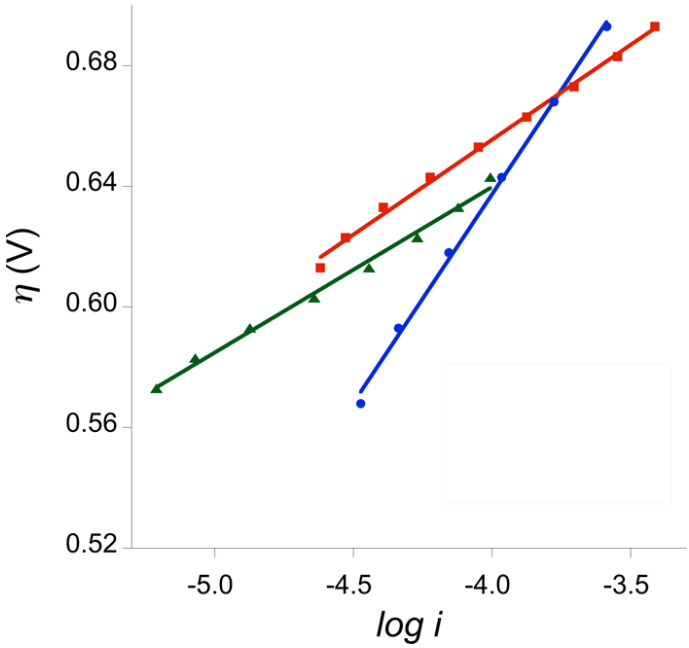

Figure 3.37. *Steady-state Tafel data acquired in a 50 mM NaP_i buffer solution with 1 M $NaNO_3$ at pH = 7 at different **Co_9**/bpy concentrations: 1.00/2.80 mM, Tafel slope = 138 mV $decade^{-1}$ (blue); 0.25/0.68 mM, Tafel slope = 63 mV $decade^{-1}$ (red); 0.06/0.16 mM, Tafel slope = 55 mV$decade^{-1}$ (green). FTO working electrode, Pt mesh counter electrode and Ag/AgCl (NaCl 3 M) reference electrode.*

UNIVERSITAT ROVIRA I VIRGILI
NOVEL MOLECULAR CATALYSTS FOR WATER OXIDATION: TOWARDS ARTIFICIAL PHOTOSYNTHESIS
Sara Goberna Ferrón
Dipòsit Legal: T.189-2014

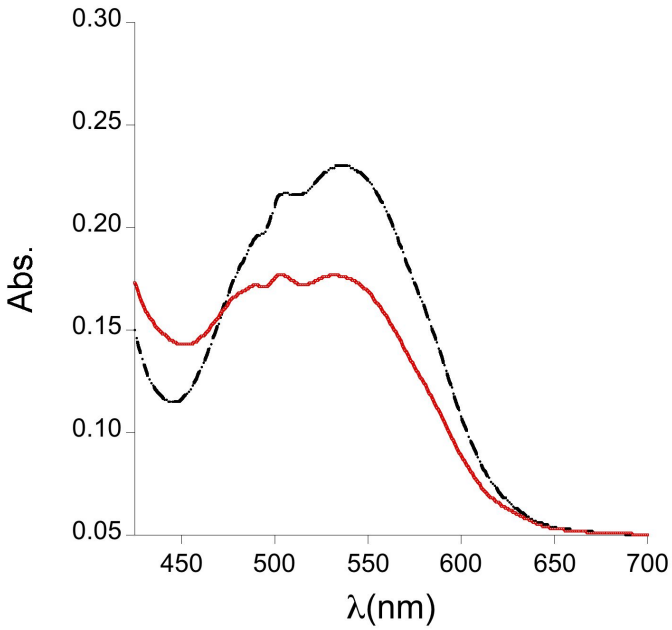

Figure 3.38. *UV-vis spectra of a solution before (black) and after (red) Tafel plot studies wit 1.0 mM* ***Co₉*** *+ 30 % bpy (per cobalt atom) in a 50 mM NaP_i buffer solution with 1 M $NaNO_3$ at pH = 7.*

UNIVERSITAT ROVIRA I VIRGILI
NOVEL MOLECULAR CATALYSTS FOR WATER OXIDATION: TOWARDS ARTIFICIAL PHOTOSYNTHESIS
Sara Goberna Ferrón
Dipòsit Legal: T.189-2014

UNIVERSITAT ROVIRA I VIRGILI
NOVEL MOLECULAR CATALYSTS FOR WATER OXIDATION: TOWARDS ARTIFICIAL PHOTOSYNTHESIS
Sara Goberna Ferrón
Dipòsit Legal: T.189-2014

3.2.3 Photo-induced Water Oxidation.

Co_9 catalyzed water oxidation in a totally homogeneous light−induced system was investigated in a collaboration with Prof. Marcella Bonchio's Group (University of Padova, Italy) to determine if **Co_9** is a viable component of a future solar cell: it works under light irradiation, and it can participate in electron tranfer processes with a photosensitizer. In photo-induced water oxidation, a solution containing a photosensitizer ($[Ru(bpy)_3]^{2+}$), a sacrificial oxidant ($[S_2O_8]^{2-}$), and the catalyst is irradiated to monitor oxygen evolution. $[Ru(bpy)_3]^{2+}$ absorbs light to populate an excited electronic state $*[Ru(bpy)_3]^{2+}$. The $*[Ru(bpy)_3]^{2+}$ state passes to the oxidized $[Ru(bpy)_3]^{3+}$, through electron transfer to $[S_2O_8]^{2-}$. The $SO_4^{-\bullet}$ radical ion produced by the quenching process reacts with another $[Ru(bpy)_3]^{2+}$ species to form a second $[Ru(bpy)_3]^{3+}$ molecule. The $[Ru(bpy)_3]^{3+}$ species will remove electrons from the catalyst that will subsequently oxidize water to re-start the catalytic cycle (Figure 3.39). This well-established procedure is based on the facile generation of $Ru(bpy)_3^{3+}$ by photoinduced electron transfer between $Ru(bpy)_3^{2+}$ and the sacrificial electron sink (Equations 3.9−3.12).[65] Providing a convenient way to evaluate the performance of **Co_9** under continuous light irradiation.

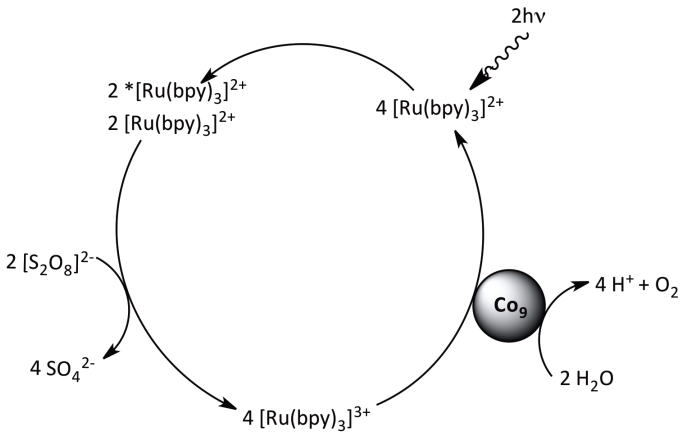

Figure 3.39. *Schematic representation of the photo−induced oxidation of water*

UNIVERSITAT ROVIRA I VIRGILI
NOVEL MOLECULAR CATALYSTS FOR WATER OXIDATION: TOWARDS ARTIFICIAL PHOTOSYNTHESIS
Sara Goberna Ferrón
Dipòsit Legal: T.189-2014

$Ru(bpy)_3^{2+} + hv \rightarrow * Ru(bpy)_3^{2+}$ (Eq. 3.9)

$*Ru(bpy)_3^{2+} + S_2O_8^{2-} \rightarrow Ru(bpy)_3^{3+} + SO_4^{2-} + SO_4^{-\bullet}$ (Eq. 3.10)

$Ru(bpy)_3^{2+} + SO_4^{-\bullet} \rightarrow Ru(bpy)_3^{3+} + SO_4^{2-}$ (Eq. 3.11)

$Ru(bpy)_3^{3+} + 2H_2O + catalyst \rightarrow 4\ Ru(bpy)_3^{2+} + 4H^+ + O_2$ (Eq. 3.12)

We monitored the time evolution of molecular oxygen production occurring in a 12.5 mL 6.6 µM solution of **Co_9** containing $[Ru(bpy)_3]^{2+}$ (1 mM) and persulfate ions (5 mM), at pH 8 in borate buffer ($[Na_2B_4O_7]$ = 40 mM, adjusted at pH 8 with HCl), upon light irradiation (λ > 400 nm). The production rate decreases with time to reach a plateau, once oxygen evolution stops (Figure 3.40, left). Negligible O_2 evolution was observed by repeating the same procedure without the presence of **Co_9** in solution. The final O_2 chemical yield (CY = $[O_2]$ / $2[S_2O_8^{2-}]$) was 1.6 %. TON ($[O_2]$ / $[\mathbf{Co_9}]$) was 25 with an initial TOF = 34 h^{-1}. A control experiment was performed monitoring the O_2 evolution in the very same conditions, but using $Co(NO_3)_2$ as precursor for the CoO_x catalyst, taking into account the same total concentration of cobalt atoms: $Co(NO_3)_2$ 60 µM vs **Co_9** 6.6 µM (Figure 3.40, right). The O_2 generation only doubles with $Co(NO_3)_2$. This experiment confirms that CoO_x is not participating in the **Co_9** catalysis. On one hand the kinetics of O_2 evolution are significantly different, and at least half of the **Co_9** should decompose to produce the same oxygen evolution. This is refuted by the analysis of the catalyst after the experiment, as it will be discussed later.

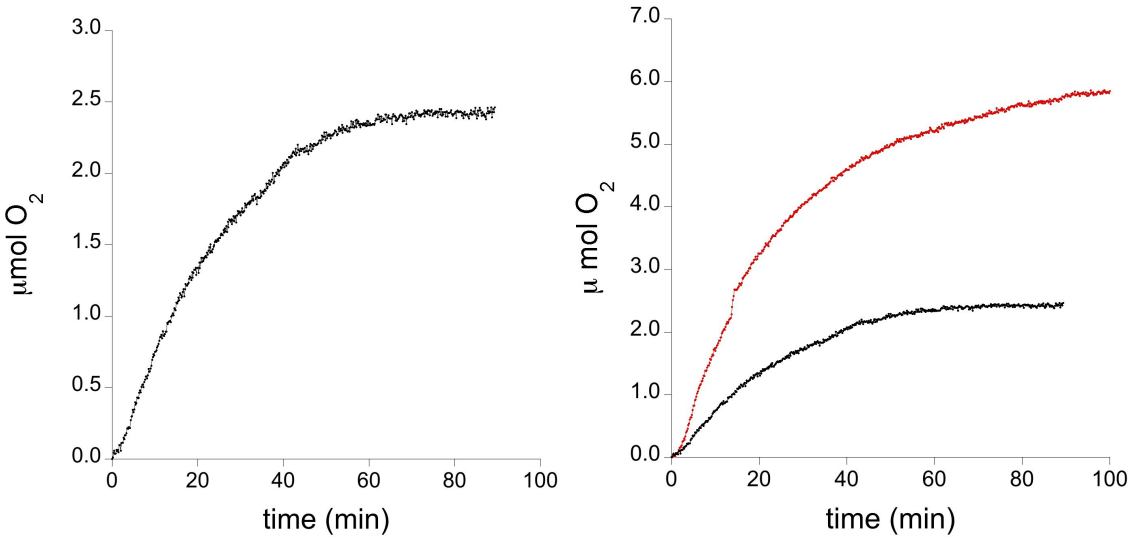

Figure 3.40. *Kinetics of O_2 formation upon light irradiation (λ > 400 nm) to the reaction solution (40 mM borate buffer at pH = 8) containing 1 mM $[Ru(bpy)_3]^{2+}$, 5 mM $[S_2O_8]^{2-}$ and 60 μM in total cobalt atoms of catalyst. Black line: 6.6 μM* ***Co₉****. Red line: 60 μM $Co(NO_3)_2$.*

The effects of the catalyst concentration on this photo-induced water oxidation have been investigated keeping constant all the other parameters. (Table 3.10 and Figure 3.41). Higher TONs (up to 40) were achieved at lower catalyst concentration, whereas little changes were observed for CYs.

[Co₉] μM	**TON**	**TOF (h^{-1})**	**Yield (%)**
60	4.3	4.8	2.5
30	6.7	8.8	2.0
6.6	25	33.7	1.6
3.3	43.4	64.5	1.4

Table 3.10. *Turnover numers (TON) and Turnover Frequency numbers (TOF) for homogeneous light–driven water oxidation system catalyzed by Co_9. Reaction conditions: 40 mM borate buffer at pH = 8 containing 1 mM $[Ru(bpy)_3]^{2+}$, 5 mM $[S_2O_8]^{2-}$ and different* ***Co₉*** *concentrations.*

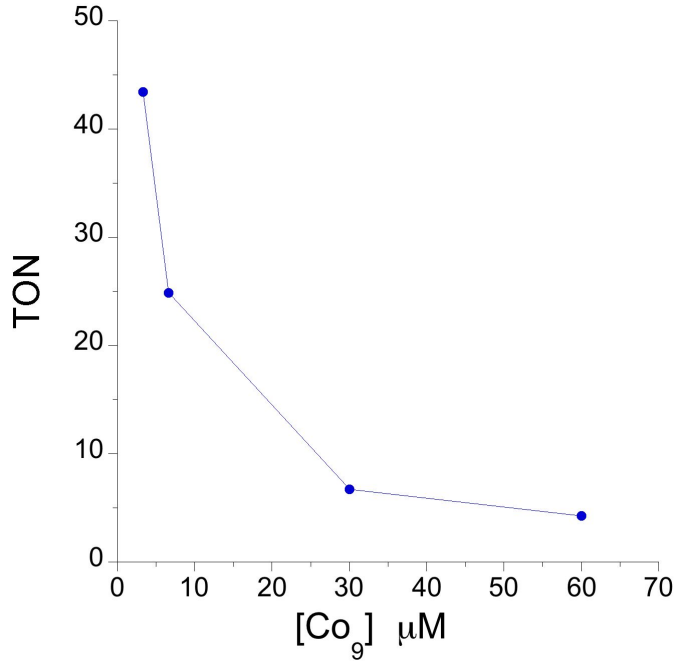

Figure 3.41. *Dependence of Turnover number (TON) on catalyst concentration in the same experimental conditions described in Table 11.*

The chemical yield is essentially limited by the decomposition of $Ru(bpy)_3^{3+}$ in neutral or basic conditions, mostly returning to $Ru(bpy)_3^{2+}$ but also undergoing irreversible decomposition (Equation 3.13), which depends on pH and buffer nature.[66]

$Ru(bpy)_3^{3+}$ + nucleophiles (*i.e.*, OH^-) → decomposition products (Eq. 3.13)

This decomposition process competes with electron transfer from the catalyst (Equation 3.12), and a significant decomposition of the photosensitizer reduces the chemical yield. When the catalyst concentration increases up to 30 μM a precipitate of an adduct between Co_9 and $[Ru(bpy)_3]^{2+}$ appears, this precipitate was characterized through IR spectroscopy (Figure 3.42), where the main bands in the W–O region (600-920 cm^{-1}) characteristics of **Co_9** are maintained.

UNIVERSITAT ROVIRA I VIRGILI
NOVEL MOLECULAR CATALYSTS FOR WATER OXIDATION: TOWARDS ARTIFICIAL PHOTOSYNTHESIS
Sara Goberna Ferrón
Dipòsit Legal: T.189-2014

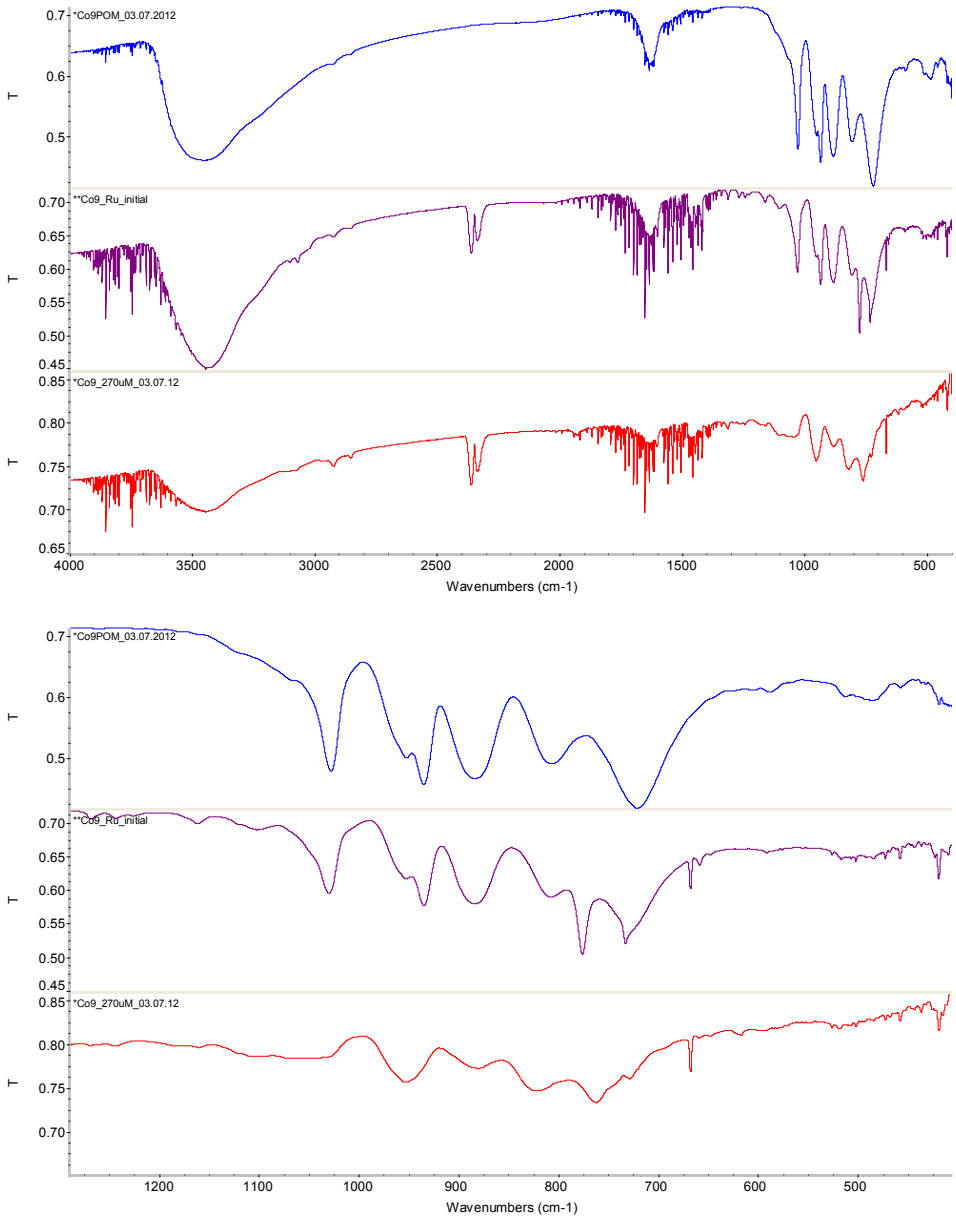

Figure 3.42. *Comparison between the IR spectra of (blue)* ***Co₉****; (purple)* ***Co₉****–[Ru(bpy)₃)]²⁺ adduct prepared by the addition of [Ru(bpy)₃)]²⁺ to a* ***Co₉*** *solution and (red) the powder recovered from the bottom of the reactor after light–driven water oxidation catalyzed by 30 µM* ***Co₉*** *(40 mM borate buffer at pH = 8, containing 1 mM [Ru(bpy)₃]²⁺and 5 mM [S₂O₈]²⁻).*

The formation of sensitizer–catalyst ion–pairing species affects the amount of $[Ru(bpy)_3]^{3+}$ formed, as only the fraction of excited $[Ru(bpy)_3]^{2+}$ that is not ion-paired with the catalyst is able to generate $[Ru(bpy)_3]^{3+}$ by reaction with persulfate. This is a

UNIVERSITAT ROVIRA I VIRGILI
NOVEL MOLECULAR CATALYSTS FOR WATER OXIDATION: TOWARDS ARTIFICIAL PHOTOSYNTHESIS
Sara Goberna Ferrón
Dipòsit Legal: T.189-2014

reasonable explanation of the decrease in TON by increasing the [Co_9]. Another effect is that by increasing the catalyst concentration, the $SO_4^{-\bullet}$ radical ion produced in equation 2 starts to oxidize the catalyst instead of $[Ru(bpy)_3]^{2+}$.

Effect of buffer on the catalytic activity

The stability of the catalyst by itself is demonstrated by recording successive UV–vis spectra each 15 minutes during 8 hours of a Co_9 solution in borate or phosphate buffer at pH = 8 (Figure 3.43). The absorption at 530 nm, characteristic of Co_9, does not change with time. This result confirms the stability of the catalyst in either borate or phosphate buffers.

In order to determinate the effect of buffer nature and concentration in the catalytic activity of Co_9, light–driven water oxidation experiments were performed in different buffer conditions. A decreasing of buffer concentration from 40 mM to 10 mM slightly increases the turnover number (Table 3.11), suggesting that the photosensitizer is subject to accelerated decomposition (Equation 3.13) in concentrated buffer solutions. For reasons to be understood, the nature of buffer also affects the efficiency of O_2 formation. A clear decrease in the photocatalytic activity of the system occurs on passing from borate to phosphate buffer (Figure 3.44 and Table 3.11). The decomposition of $[Ru(bpy)_3]^{3+}$ involves nucleophilic OH^- attack on the bipyridine ring,[67] because phosphate is a relatively weak nucleophile, it is difficult to understand why it should accelerate the decomposition reaction to a much greater extent than other oxyanions as borate.

UNIVERSITAT ROVIRA I VIRGILI
NOVEL MOLECULAR CATALYSTS FOR WATER OXIDATION: TOWARDS ARTIFICIAL PHOTOSYNTHESIS
Sara Goberna Ferrón
Dipòsit Legal: T.189-2014

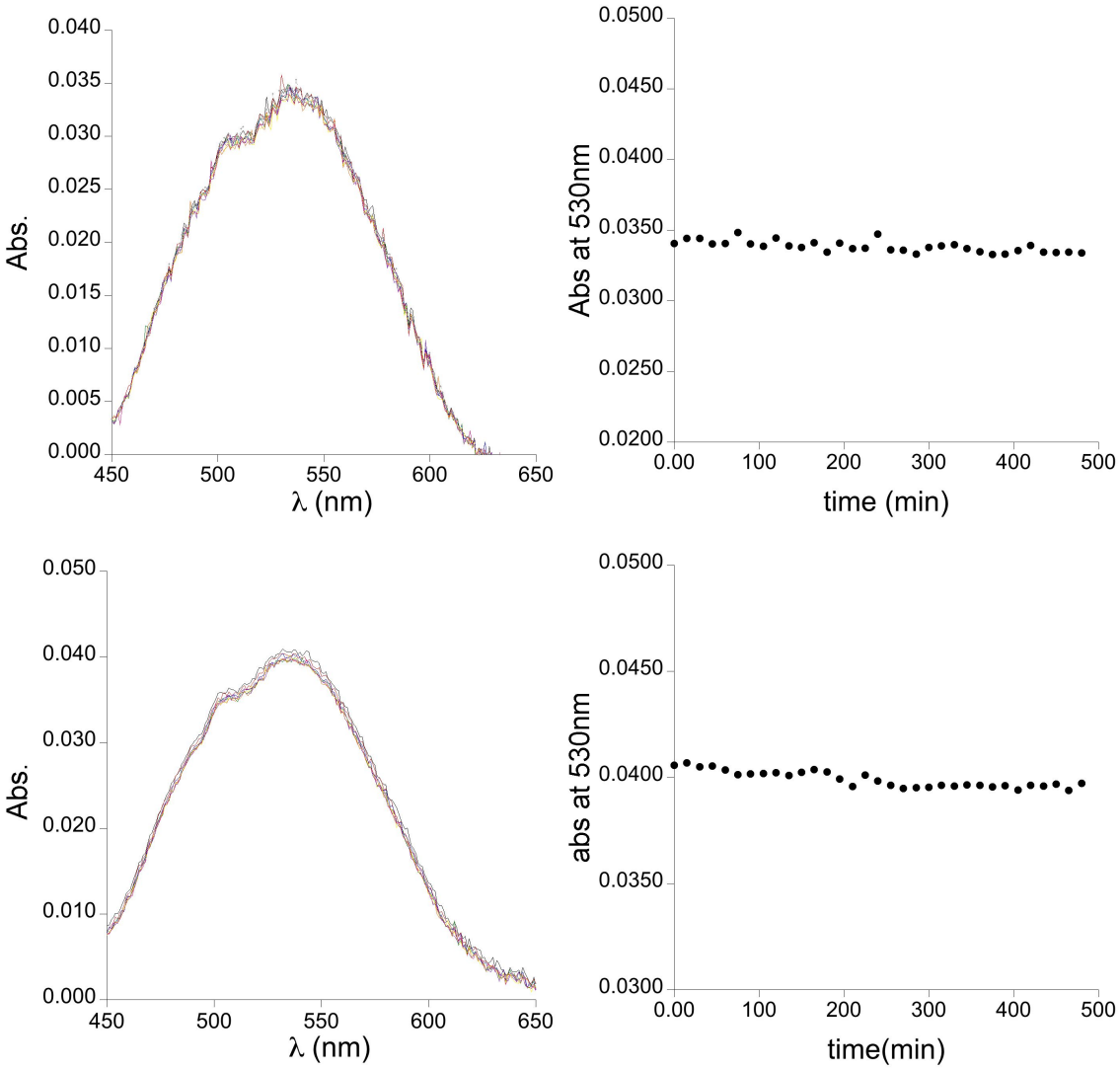

Figure 3.43. *Sequential UV-vis spectra each 15 min during 8h and the corresponding 530 nm absorption evolution with time, for a 200 µM Co9 aqueous solution in (top) 50mM borate buffer at pH = 8 and (bottom) 50mM phosphate buffer at pH = 8.*

UNIVERSITAT ROVIRA I VIRGILI
NOVEL MOLECULAR CATALYSTS FOR WATER OXIDATION: TOWARDS ARTIFICIAL PHOTOSYNTHESIS
Sara Goberna Ferrón
Dipòsit Legal: T.189-2014

buffer	[buffer] mM	TON	CY (%)	TOF (h^{-1})
borate	80	26	1.7	38
"	40	25	1.6	34
"	20	28	1.8	34
"	10	34	2.06	44
phosphate	20	12	0.93	12

Table 3.11. *Turnover numers (TON), Turnover Frequency numbers (TOF) and chemical yield (CY) for homogeneous light–driven water oxidation system using different buffer concentrations and buffer species (6.6 µM* ***Co_9****, 1 mM* $[Ru(bpy)_3]^{2+}$ *and 5 mM* $[S_2O_8]^{2-}$ *at pH = 8).*

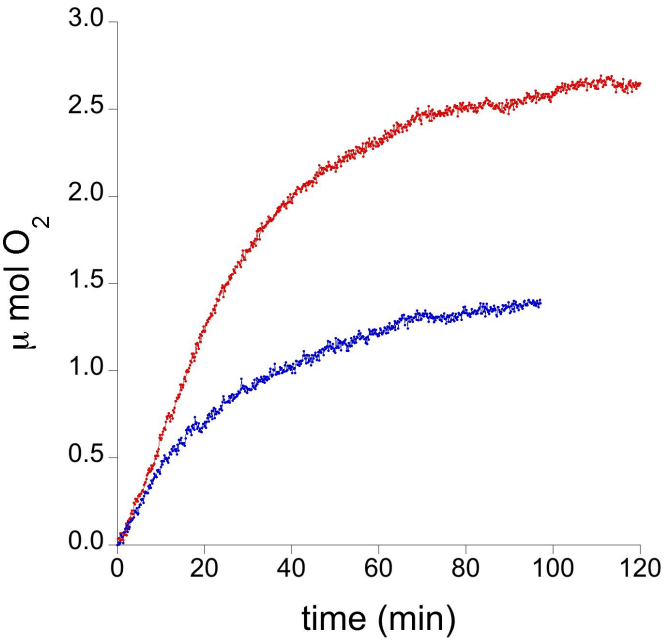

Figure 3.44. *Kinetics of* O_2 *formation upon light irradiation (λ > 400 nm) to the reaction solution containing 6.6 µM* ***Co_9****, 1 mM* $[Ru(bpy)_3]^{2+}$ *and 5 mM* $[S_2O_8]^{2}$ *in (red) 20 mM borate buffer at pH = 8 and (blue) 20 mM phosphate buffer at pH = 8.*

UNIVERSITAT ROVIRA I VIRGILI
NOVEL MOLECULAR CATALYSTS FOR WATER OXIDATION: TOWARDS ARTIFICIAL PHOTOSYNTHESIS
Sara Goberna Ferrón
Dipòsit Legal: T.189-2014

Catalyst Recovery

In all the experiments described above, the catalyst was recovered after the photo−induced water oxidation. The catalyst can be recovered by addition of an excess of $[Ru(bpy)_3]^{2+}$ followed by centrifugation. The IR spectra of the recovered catalyst (Figure 3.45) shows the characteristic bands of a [**Co_9**]-$[Ru(bpy)_3]$ salt (see Figure 3.42). The **Co_9** fingerprint is maintained, confirming its stability. Moreover, EDX microanalysis data present ratios in agreement with the theoretically expected for a $[Co_9(OH)_3(H_2O)_6(HPO_4)(PW_9O_{34})_3][Ru(bpy)_3]_4$ stoichiometry (Table 3.12).

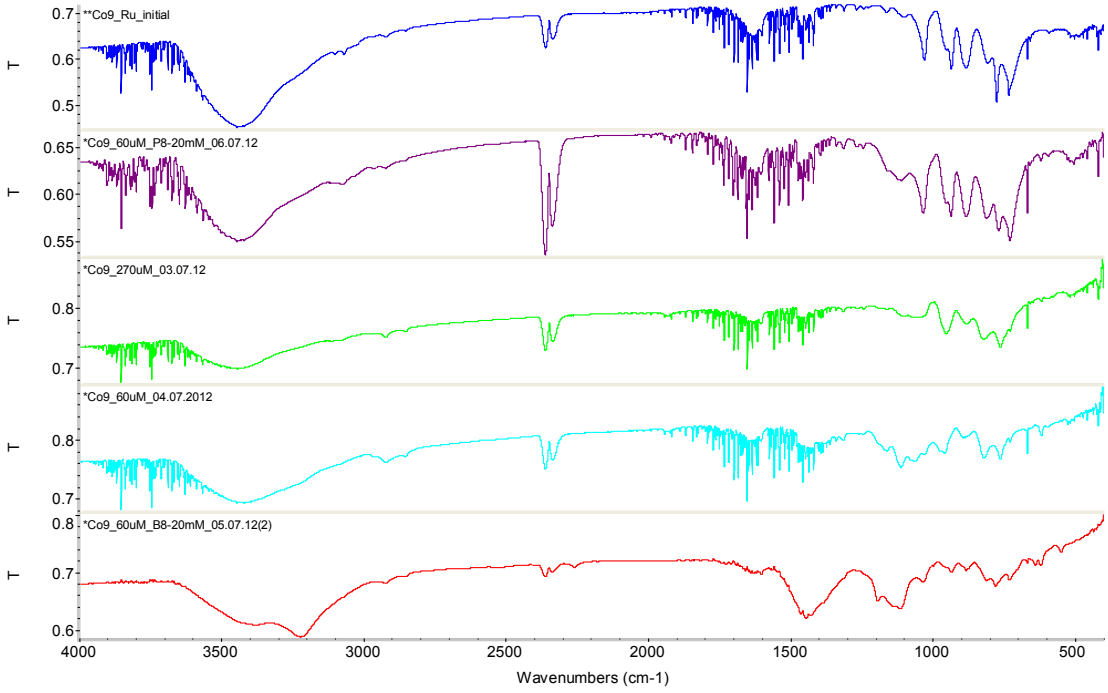

Figure 3.45. *Comparison between the IR spectra of (blue)* ***Co_9***$-[Ru(bpy)_3)]^{2+}$ *adduct prepared by the addition of* $[Ru(bpy)_3)]^{2+}$ *to a* ***Co_9*** *solution; (purple) powder precipitated after catalysis by 6.6 µM* ***Co_9*** *in 20 mM phosphate buffer; (green) powder recovered from the bottom of the reactor after catalysis by 30 µM* ***Co_9*** *in 40 mM borate buffer; (blue) powder precipitated after catalysis by 6.6 µM* ***Co_9*** *in 40 mM borate buffer and (red) powder precipitated after catalysis by 6.6 µM* ***Co_9*** *in 20 mM borate buffer. Solutions at pH = 8 containing 1 mM* $[Ru(bpy)_3]^{2+}$ *and 5 mM* $[S_2O_8]^{2-}$.

UNIVERSITAT ROVIRA I VIRGILI
NOVEL MOLECULAR CATALYSTS FOR WATER OXIDATION: TOWARDS ARTIFICIAL PHOTOSYNTHESIS
Sara Goberna Ferrón
Dipòsit Legal: T.189-2014

	P/Co	P/Ru	P/W
Expected	1.8	1.6	5.4
Prepared Co_9–Ru	1.8	0.97	4.1
After kinetics A	0.8	1.8	7.4
“ B	1.1	1.27	6.7
“ C	1.65	1.4	5.4

Table 3.12. *Metal analysis summary results calculated from EDX analysis of the “recovered” catalysts. A = 60 µM **Co_9** in 40 mM borate; B= 30 µM **Co_9** in 40 mM borate and C= 6.6 µM **Co_9** in 20 mM borate buffer.*

These data indicates that **Co_9** is a robust and stable catalyst also under these photochemical conditions. The kinetics and turnover numbers should be solely limited by the amount of sacrificial electron acceptor and / or photosensitizer used. The insolubility of the [**Co_9**]-[$Ru(bpy)_3$] salt is a drawback, since it limits the concentration in solution of both reagents, the photosensitizer and the catalyst.

UNIVERSITAT ROVIRA I VIRGILI
NOVEL MOLECULAR CATALYSTS FOR WATER OXIDATION: TOWARDS ARTIFICIAL PHOTOSYNTHESIS
Sara Goberna Ferrón
Dipòsit Legal: T.189-2014

3.3 Conclusions

The catalytic activity of a novel cobalt–containing POM, the $[Co_9(H_2O)_6(OH)_3(HPO_4)_2(PW_9O_{34})_3]^{16-}$ cluster, **Co_9** has been investigated. Our experimental data demonstrates that this nonanuclear cobalt cluster, stabilized by a polyoxophosphotungstate moiety, is a true homogeneous WOC at neutral pH.

As an electrocatalyst, decomposition of the POM into a thin cobalt oxide film on the anode occurs. This CoO_x and its catalytic activity has been characterized, showing similar activity that the reported state–of–the–art cobalt oxide.[60,61] Oxide formation can be avoided by the addition of chelating agents. In this conditions, **Co_9** exhibited genuine homogeneous catalytic activity in the absence of any heterogeneous species. **Co_9** is robust and it can be recovered from solution after the catalytic cycles. In diluted conditions, it shows kinetic features competitive to those of cobalt oxides at reasonable overpotentials.

Co_9 is amazingly stable and robust in chemical water oxidation experiments. It is able to catalyze oxygen evolution from a sodium hypochlorite solution in the 7 < pH <9 range for days. It is demonstrate that old **Co_9** solutions present activity identical with that of freshly prepared ones, even after multiple cycles of catalytic oxidation. Compared with **Co_4**, it exhibits a higher activity catalyzing oxygen evolution using

- 3. $\{Co^{II}_9\}$ Polyoxometalate WOC -

NaClO as oxidant; **Co_9** gives up to 10 times the number of cycles and higher rates.

We also discovered that **Co_9**, in combination with $[Ru(bpy)_3]^{2+}$ and persulfate anions, is an efficient and stable molecular catalyst for photodriven water oxidation at neutral pH. The robust and fast kinetics of **Co_9** are limited in this conditions by the decomposition of $Ru(bpy)_3^{3+}$ in neutral pH, and the insolubility of the $[Co_9(OH)_3(H_2O)_6(HPO_4)(PW_9O_{34})_3][Ru(bpy)_3]_4$ salt.

All these features, corroborate that **Co_9** is a viable candidate to be incorporated into an artificial photosynthesis device.

UNIVERSITAT ROVIRA I VIRGILI
NOVEL MOLECULAR CATALYSTS FOR WATER OXIDATION: TOWARDS ARTIFICIAL PHOTOSYNTHESIS
Sara Goberna Ferrón
Dipòsit Legal: T.189-2014

3.4

Experimental

3.4.1 Synthesis and Characterization

All reagents were purchased from Sigma-Aldrich (>99% purity) and used without further purification.

Co_9 was prepared from the literature method.[68] A solution of $Co(OOCCH_3)_2.4H_2O$ (8 g, 32 mmol) in 30 mL of deionized water was added to an aqueous solution of $Na_2WO_4.2H_2O$ (16.5 g, 50 mmol), and Na_2HPO_4 (0.78 g, 5.5 mmol) whose pH was previously adjusted to 7.6 with acetic acid. The resulting red solution was refluxed for 9 h. After that time the resulting mixture was hot filtered, and 5 g of solid $K(OOCCH_3)$ was added. The resulting solution was allowed to cool at room temperature. After several hours small pink needle-shaped crystals of the compound of formula $Na_{(16-x)}K_x[Co_9(OH)_3(H_2O)_6(HPO_4)(PW_9O_{34})_3]$ were obtained through and isolated by filtration, and dried under vacuum to yield 8 g of compound (40%).

Co_4 was prepared the literature procedure.[69] A solution of $Co(OOCCH_3)_2.4H_2O$ (5.5 g, 22 mmol) in 50 mL of deionized water was added to an aqueous solution of $Na_2WO_4.2H_2O$ (33g, 100 mmol), and Na_2HPO_4 (1.5 g, 11 mmol) whose pH was previously adjusted to 6.9 with acetic acid. The resulting solution was refluxed for 2 h. After that time the resulting violet solution was hot filtered, and 4 g of solid $K(OOCCH_3)$ was added. The resulting misture was allowed to cool at room temperature. After several hours prismatic crystals of the $Na_{(10-x)}K_x[Co_4(H_2O)_2(PW_9O_{34})_2]$ salt was obtained, isolated by filtration, and dried under vacuum to yield 14.5 g of compound (50%).

In both reactions a mixture of the $[Co_9(OH)_3(H_2O)_6(HPO_4)(PW_9O_{34})_3]^{16-}$ and $[Co_4(H_2O)_2(PW_9O_{34})_2]^{10-}$ salts were obtained. To separate them, after filtration, cold water is added where the **Co_9** salt is soluble and the **Co_4** salt is insoluble.

Analysis

The counter cations and solvent content were determined by EDX microanalysis and thermogravimetry, respectively. Metal content was analyzed with a Scanning Electron Microscope JEOL-JMS6400 equipped an Oxford EDX analyzer (Oxford Instruments). Thermogrammetry was performed with power samples using a TGA/SDTA851 Mettler Toledo with MT1 microbalance. The molecular formulas are: **$Na_8K_8[Co_9(OH)_3(H_2O)_6(HPO_4)_2(PW_9O_{34})_3].43H_2O$** (**Mw** = 8842.6) (Figure 42 and Table 14) and **$Na_5K_5[Co_4(H_2O)_2(PW_9O_{34})_2]$** (**Mw** = 5599.7) (Figures 3.46-3.49 and Tables 3.13-3.14)

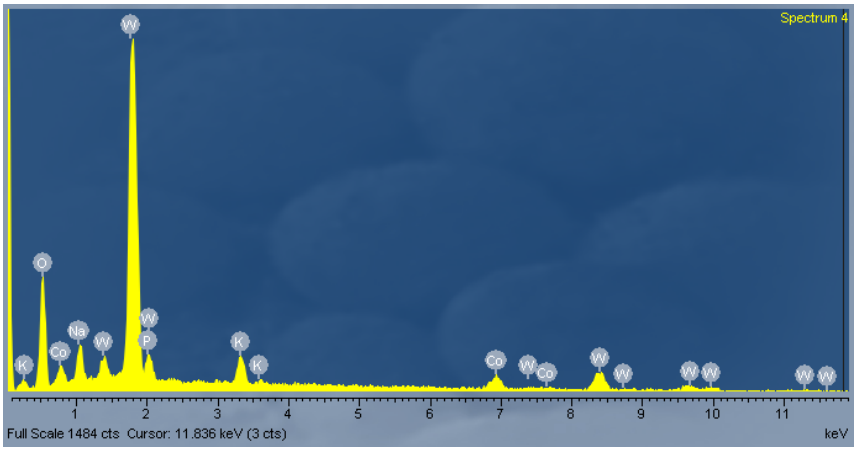

Figure 3.46. *Typical EDX histogram* ***Co_9***

UNIVERSITAT ROVIRA I VIRGILI
NOVEL MOLECULAR CATALYSTS FOR WATER OXIDATION: TOWARDS ARTIFICIAL PHOTOSYNTHESIS
Sara Goberna Ferrón
Dipòsit Legal: T.189-2014

Element	Atomic %	Estimated Stoichiometry	Theoretical Stoichiometry
P	12.98	7	5
K	15.24	8	x
Co	16.99	9	9
W	54.79	29	27

Table 3.13. *Metal analysis summary results calculated from EDX analysis of* ***Co_9***. *The results are an average of three "sites of interest" on the powder analyzed.*

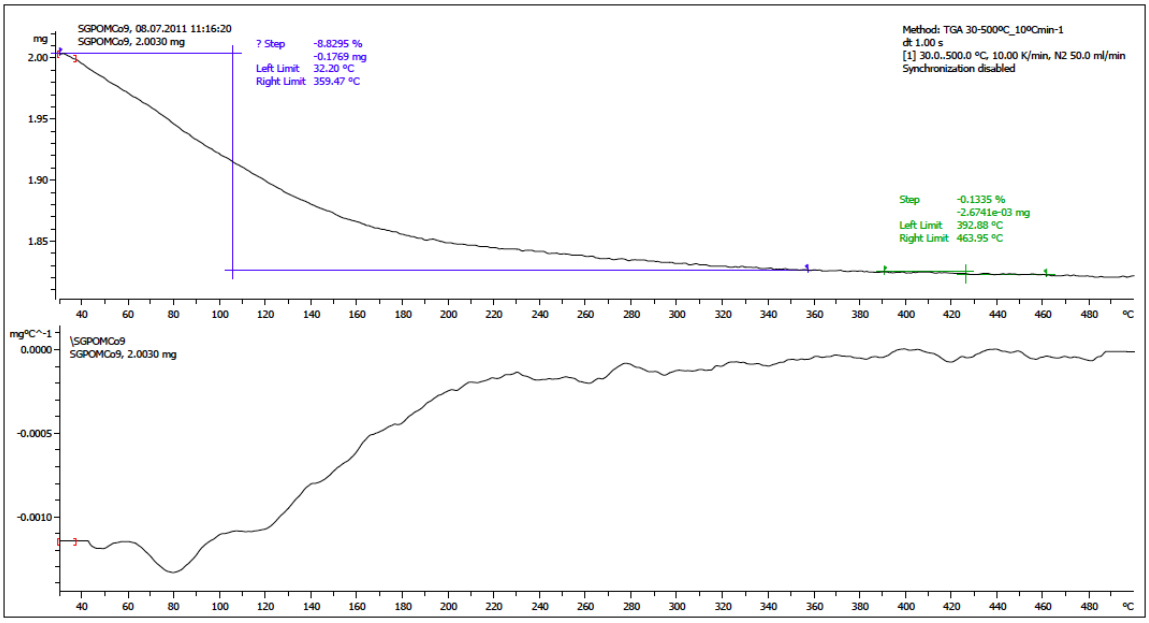

Figure 3.47. *TGA analysis of* ***Co_9***.

UNIVERSITAT ROVIRA I VIRGILI
NOVEL MOLECULAR CATALYSTS FOR WATER OXIDATION: TOWARDS ARTIFICIAL PHOTOSYNTHESIS
Sara Goberna Ferrón
Dipòsit Legal: T.189-2014

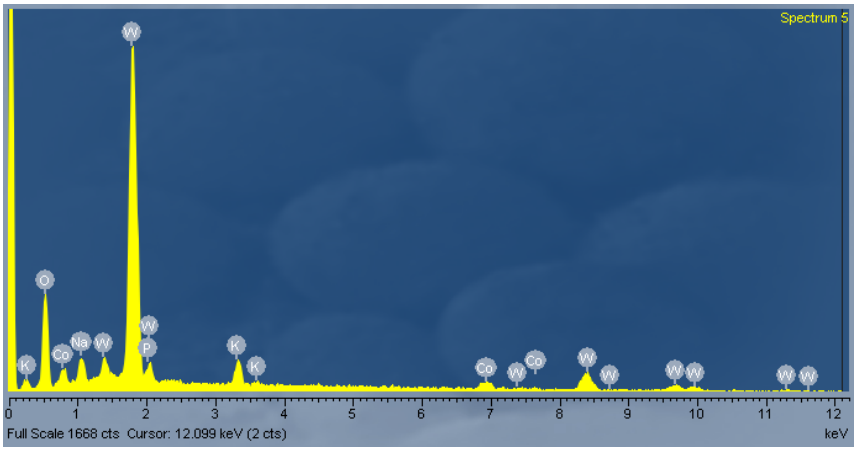

Figure 3.48. *Typical EDX histogram* ***Co_4***

Element	Atomic %	Estimated Stoichiometry	Theoretical Stoichiometry
P	8.67	3	2
K	15.64	5	x
Co	13.10	4	4
W	62.6	19	18

Table 3.14. *Metal analysis summary results calculated from EDX analysis of* ***Co_4***. *The results are an average of three "sites of interest" on the powder analyzed.*

UNIVERSITAT ROVIRA I VIRGILI
NOVEL MOLECULAR CATALYSTS FOR WATER OXIDATION: TOWARDS ARTIFICIAL PHOTOSYNTHESIS
Sara Goberna Ferrón
Dipòsit Legal: T.189-2014

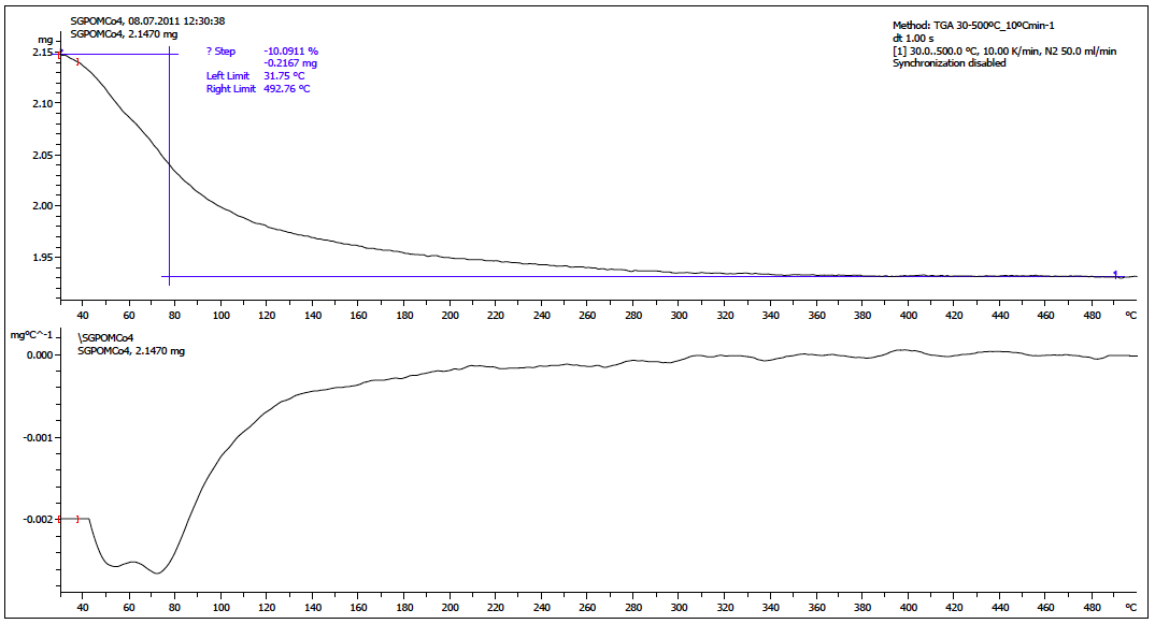

Figure 3.49. *TGA analysis of* ***Co$_4$***.

X Ray Diffraction

Single crystal Xray diffraction of **Co$_9$** and **Co$_4$** was performed with Bruker-Nonius diffractometer equipped with an APPEX 2 4k CCD area detector, a FR591 rotating anode with MoKa radiation, Montel mirrors as monochromator and a Kryoflex low temperature device. Crystal data for **Co$_4$**: monoclinic, **P**2_1/n, **a** = 12.2892(5), **b** = 21.3665(9), **c** = 15.6143(7) Å, β = 92.419(1)°, ***V*** = 4096.31 Å^3. The data confirmed consistent unit cells with the reported literature.[70] Crystal data for **Co$_9$**: hexagonal, **P**6_3**/m**, **a** = 20.243(3), **c** = 20.343(4) Å; **V** = 7220 Å^3 (before) and **P**6_3**/m**, **a** = 20.701(6)**;c** = 20.399(5) Å; **V** = 7571 Å^3 (recrystallized after oxidation catalysis), both isostructural and in agreement with the reported data.[69] The small unit cell differences found are due to different water and alkali cation content.

The compounds were characterized by X-ray powder diffraction with a Bruker D8 Advance Series equipped with a VÅNTEC-1PSD detector (Figure 3.50). The powder patterns are indistinguishable before and after the catalytic oxygen evolution with hypochlorite.

UNIVERSITAT ROVIRA I VIRGILI
NOVEL MOLECULAR CATALYSTS FOR WATER OXIDATION: TOWARDS ARTIFICIAL PHOTOSYNTHESIS
Sara Goberna Ferrón
Dipòsit Legal: T.189-2014

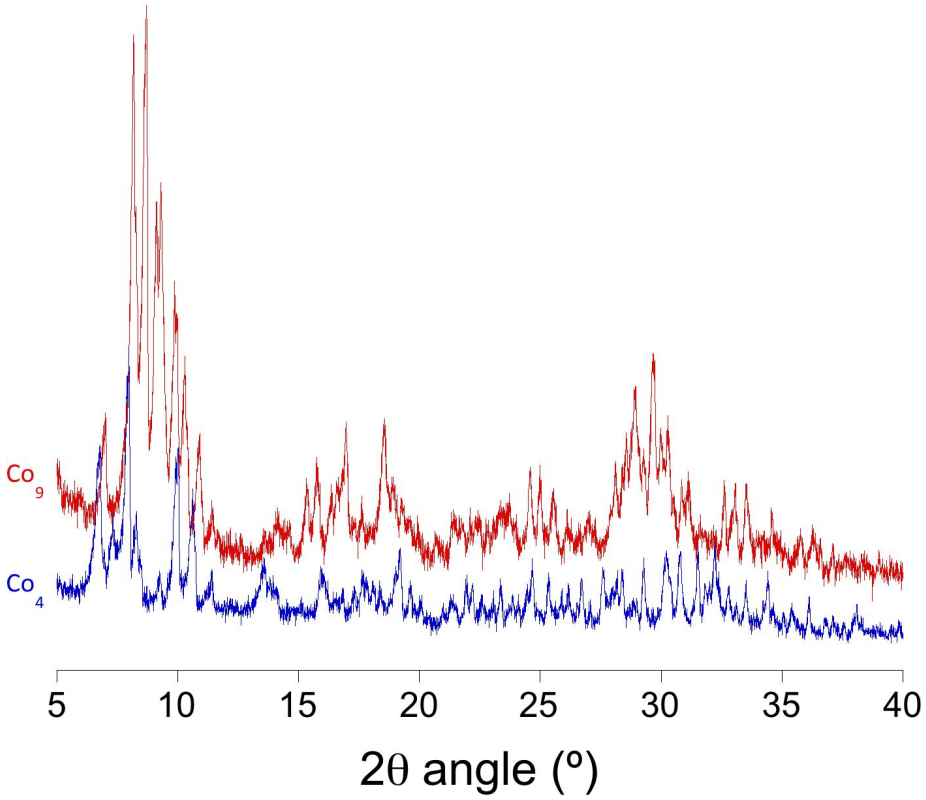

Figure 3.50. *XRD patterns of* ***Co_9*** *(red) and* ***Co_4*** *(blue)*

Infrared spectroscopy

IR spectra for powder samples of **Co_9** and **Co_4** (Figure 3.51) were collected in the 3600-400 cm^{-1} range with a Bruker Optics FTIR Alpha spectrometer equipped with a DTGS detector, KBr beamsplitter at 4cm^{-1} resolution. The main differences are found in the W–O región (600-920 cm^{-1}) where an additional band at 795cm^{-1} is found in the spectra of **Co_9**. The IT spectra are indistinguishable before and after the catalytic oxygen evolution with hypochlorite.

UNIVERSITAT ROVIRA I VIRGILI
NOVEL MOLECULAR CATALYSTS FOR WATER OXIDATION: TOWARDS ARTIFICIAL PHOTOSYNTHESIS
Sara Goberna Ferrón
Dipòsit Legal: T.189-2014

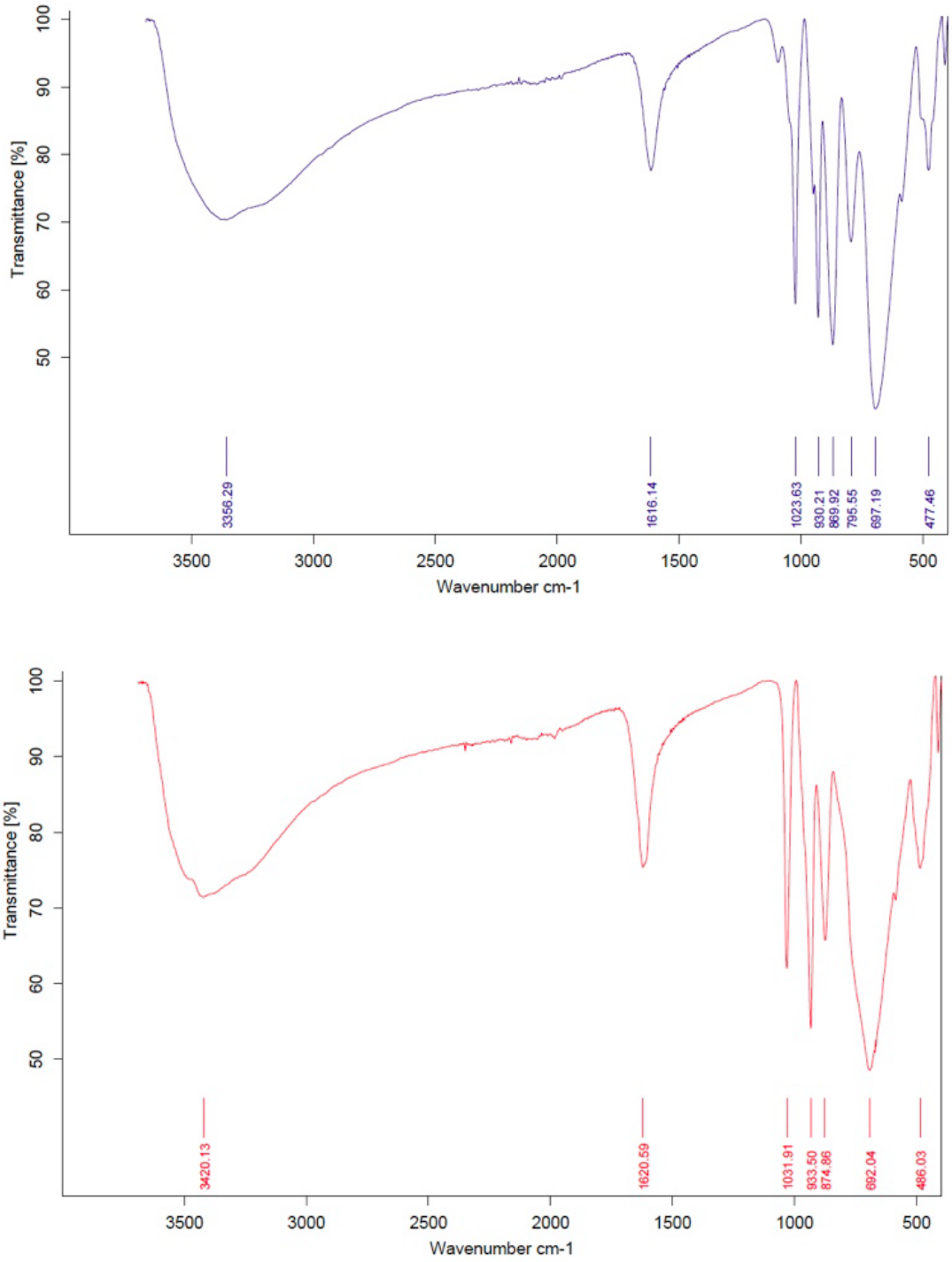

Figure 3.51. *IR spectra for powders samples of* ***Co_9*** *(top in blue) and* ***Co_4*** *(bottom in red)*

Dynamic Light Scattering

UNIVERSITAT ROVIRA I VIRGILI
NOVEL MOLECULAR CATALYSTS FOR WATER OXIDATION: TOWARDS ARTIFICIAL PHOTOSYNTHESIS
Sara Goberna Ferrón
Dipòsit Legal: T.189-2014

The nanoparticles size distribution in a solution of **Co_9** was measured using a Malvern nanoZS analyzer and identical data were found before and after oxygen evolution with hypochlorite (Figure 3.52).

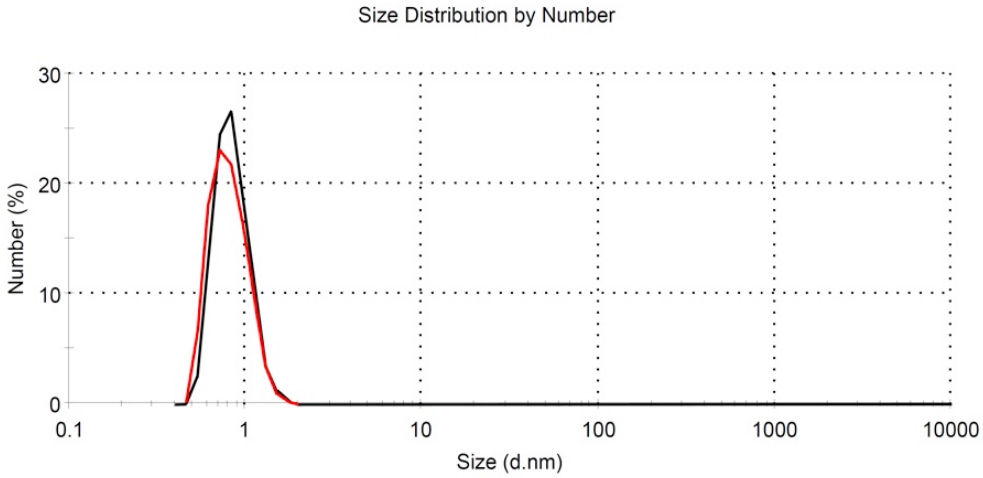

Figure 3.52. *DLS data of a 1.0 mM **Co_9** solution in NaP_i buffer at pH = 7. Before catalytic oxygen evolution (black line) and after complete oxygen evolution from addition of 1000 equivalents of NaClO (red line).*

UV-vis spectroscopy

UV-vis spectroscopy measurements were carried out on a Cary 50 (Varian) spectrophotometer in standard 1 cm Quartz cuvettes. The UV-vis spectra in water for **Co_9** and **Co_4** show a maximum at 530 and 575 nm respectively (Figure 3.53). The UV-vis spectra are indistinguishable before and after the catalytic oxygen evolution.

UNIVERSITAT ROVIRA I VIRGILI
NOVEL MOLECULAR CATALYSTS FOR WATER OXIDATION: TOWARDS ARTIFICIAL PHOTOSYNTHESIS
Sara Goberna Ferrón
Dipòsit Legal: T.189-2014

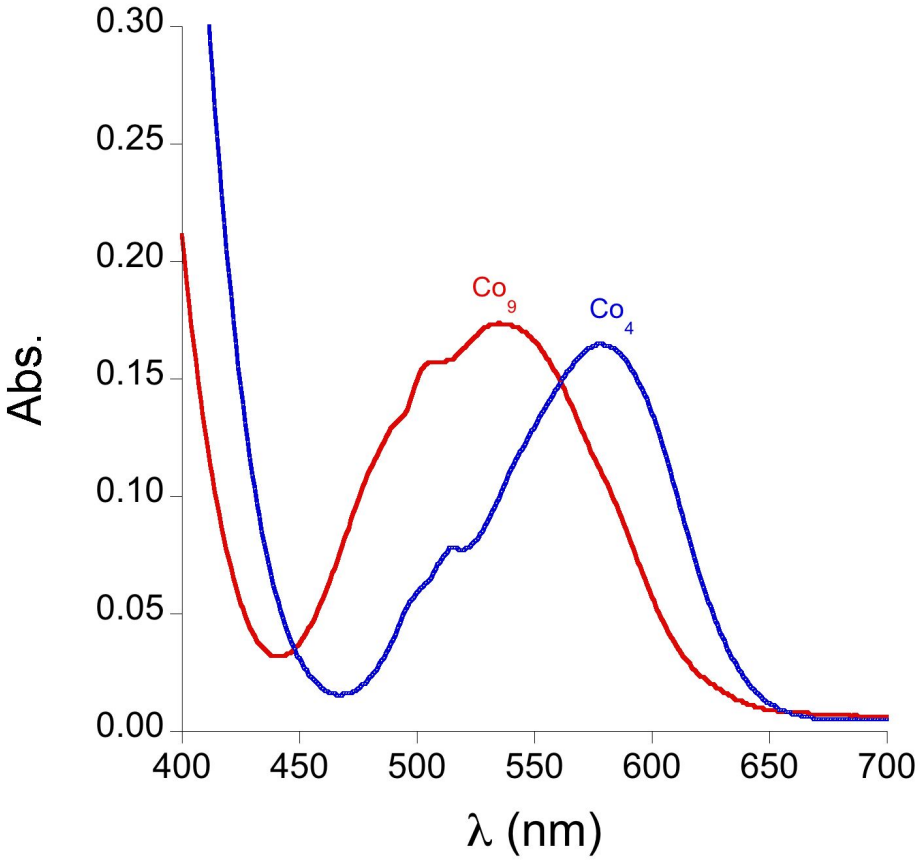

Figure 3.53. *UV–vis spectra of* ***Co₉*** *(red) and* ***Co₄*** *(blue).*

UNIVERSITAT ROVIRA I VIRGILI
NOVEL MOLECULAR CATALYSTS FOR WATER OXIDATION: TOWARDS ARTIFICIAL PHOTOSYNTHESIS
Sara Goberna Ferrón
Dipòsit Legal: T.189-2014

3.4.1 Physical Methods.

Manometric Measurements

Sodium hypochlorite solution was bought from Sigma-Aldrich (16% free chlorine) and the real concentration was determined by thiosulfate titration. Gas evolution profile of catalytic experiments was monitored by a Testo 521 manometer, with an internal differential pressure sensor from 0 to 100 hPa and accuracy within 0.2% of the measurement. One manometer port was connected to a home-made thermostated vessel for the on-line monitoring of the headspace pressure above the catalysis reaction. The other manometer port was connected to another thermostated vessel containing the same solvent and headspace volume as the sample vessel. In a typical catalyzed reaction, a solution of catalyst in of 0.9 M sodium phosphate (NaP_i) buffer at pH = 8 (1.8 mL) was introduced in a vessel and the pressure was stabilized at atmospheric. Then, a solution of NaClO in NaP_i buffer (0.2 mL) were added to the initial solution. All the system was thermostated at the desired temperature between 15 and 35 °C. These experiments were performed at different concentrations of catalyst and NaClO. The system was calibrated using the previous procedure substituting the reaction solutions by water. Different quantities of oxygen (between 50 and 250 μL) were added in the head-space of the sample vessel using a Hamilton gas-tight syringe. After each addition, gas and aqueous phase were stirred until equilibria. The built-in internal pressure data were correlated with the amount of oxygen added. From the calibration slope of the integrated data points, the volume that is occupied by oxygen can be extracted and, thus, the number of moles of oxygen generated in a catalytic reaction can be calculated using the ideal gas law.

UNIVERSITAT ROVIRA I VIRGILI
NOVEL MOLECULAR CATALYSTS FOR WATER OXIDATION: TOWARDS ARTIFICIAL PHOTOSYNTHESIS
Sara Goberna Ferrón
Dipòsit Legal: T.189-2014

Gas Chromatography Measurements

Oxygen content was determined by using a 6890N GC Agilent with a thermal conductivity detector (TCD). In a typical experiment, the desired amount of catalyst was introduced in a 10 mL round-bottom flask and it was extensively degassed under cycles of vacuum and nitrogen for 30 minutes. Then, the catalyst was dissolved in 9 mL of degassed NaP_i buffer solution at pH = 8.0. After this, 1 mL of degassed NaClO solution was added in order to start the catalysis. Samples of 200 µL from the generated gas phase in the reaction flask headspace were taken with a 250 µL Hamilton gas-tight syringe and immediately injected into the instrument for analysis. This experiment was performed for different concentrations of catalyst and NaClO. Calibration of the method was carried out employing the before procedure, using water instead of the reaction mixture. A calibration slope was obtained by additions of different quantities of oxygen (0, 5, 10, 20 and 30 µmol of O_2) in the headspace of the reaction flask. After each addition, gas and aqueous phase were stirred until achieve the equilibria. The integrated data peak was correlated with the amount of oxygen added. The slope from the integrated data points was employed for the quantification of oxygen in the catalysis experiments carried out.

Mass Spectroscopy and ^{18}O-labelling Measurements

Mass spectroscopy measurements were performed using an Omnistar TM GSD 301 C (Pfeiffer) quadrupole mass spectrometer apparatus. All solutions were degassed prior to use. The composition of the gas phase (O_2 *m/z*=32; N_2 *m/z*=28 and CO_2 *m/z*=44) was measured during water oxidation experiments. In a typical procedure, 2 mmol of the complex were dissolved in 1.4 mL of a NaP_i buffer solution and introduced in a vial where the MS-spectrometer cannula is inserted through a septum. Then the water oxidation catalysis was initialized by adding 100 equivalents of NaClO in NaP_i buffer (0.6mL). For ^{18}O-labelling experiments, the NaClO solution consists in a mixture

UNIVERSITAT ROVIRA I VIRGILI
NOVEL MOLECULAR CATALYSTS FOR WATER OXIDATION: TOWARDS ARTIFICIAL PHOTOSYNTHESIS
Sara Goberna Ferrón
Dipòsit Legal: T.189-2014

of 0.2 mL of NaP_i buffer and 0.4 mL of $H_2{}^{18}O$ (water ^{18}O, 97%, Cambridge Isotope Laboratories, Inc). The final ratio of solvent labeled was 19.4% in this case. The same experiment was also performed dissolving the catalyst in $H_2{}^{18}O$ and the oxidant in $H_2{}^{16}O$. The composition of the gas phase ($^{16}O_2$, *m/z* = 32; $^{16}O^{18}O$, *m/z* = 34 and $^{18}O_2$, *m/z* = 36) was monitored by on-line mass spectroscopy. The theoretical isotopic ratios are $^{16}O_2$: (0.806 x 0.806) x 100 = 64.96%, ^{16}O ^{18}O : [(0.806 x 0.194) x 100] x 2 = 31.3% and $^{18}O_2$: (0.194 x 0.194) x 100 = 3.8%. All solutions were prepared in such a way that contained a final 0.9 M phosphate buffer solution at pH = 8.0.

Electrochemistry

Electrochemistry experiments were carried out with a Biologic SP-150 potentiostat. All potentials are reported versus NHE. Typical measurements were performed in a 50 mM sodium phosphate (NaP_i) buffer pH = 7−8 solution with 1 M $NaNO_3$ as electrolyte. All solutions were made with milli Q water.

Cyclic Voltammetry

Cyclic voltammetry experiments were carried out using a standard three-electrode electrochemical cell. As working electrode, 3 mm dia. glassy carbon button electrode or platinum electrode 1.6 mm dia. were used. Pt wire and BASi Ag/AgCl (3 M NaCl) reference electrodes were used as counter and reference electrodes respectively. The working electrodes were polished with 3 µm and 1 µm diamond paste and rinsed with distilled water prior to use.

Bulk Water Electrolysis

Electrolysis experiments are performed by applying a constant external oxidation potential. The ohmic drop was compensated using the positive feedback

UNIVERSITAT ROVIRA I VIRGILI
NOVEL MOLECULAR CATALYSTS FOR WATER OXIDATION: TOWARDS ARTIFICIAL PHOTOSYNTHESIS
Sara Goberna Ferrón
Dipòsit Legal: T.189-2014

compensation implemented in the instrument. The electrodes were allowed to equilibrate with the electrolysis solution for 1 min while being held at the open circuit potential. Moreover, analogous experiments can be performed using a DSSC as source of electrical power. These experiments were carried out with stirring in a two-chamber cell, with a porous frit connecting both chambers. In one chamber, the working and the reference BASi Ag / AgCl (3 M NaCl) electrodes were placed. As working electrode, Fluor Tin Oxide (FTO) coated glass (Pilkington NSG TEC 15A 2.3mm slides with 12-14 W/sq surface resistivity) or 20 x 20 mm Platinum mesh (99.9 % Pt Goodfellow plain weave mesh, 0.25 mm nominal aperture, 0.06 mm wire diameter, 82 x 82 wires/inch, 65 % open area) were used. In the other chamber, a 20 x 20 mm platinum mesh counter electrode was placed. FTO slides were cleaned prior use by sonication for 10 minutes in basic soapy solution (LABWASH classic), deionized water and isopropanol, followed by annealing at 400 ºC during 30 minutes.

In a typical procedure for water electrolysis, the catalyst is placed in the anodic compartment, which is filled with 20 mL of buffered solution. The cathodic compartment is filled with 20 mL buffered solution without catalyst. The electrical current measured corresponds to the electrons removed from water to generate molecular oxygen. For electrodeposition of cobalt oxide film, a FTO working electrode was used as anode for the oxidation process and deposition. A cobalt oxide film is deposited at the anode by applying an oxidation voltage to a 1mM **Co_9** buffered solution.

Preparation of dye-sensitized solar cells (DSSC)

The working and counter electrodes consisted of TiO_2 and thermalized platinum films, respectively, and were deposited onto F-doped tin oxide (FTO, Pilkington Glass Inc., with 15 Ω sq^{-1} sheet resistance) conducting glass substrates. DSSC devices were made using 9 µm thick films consisting of 20 nm TiO_2 nanoparticles (Dyesol© paste) and a scattering layer of 4 µm of 400 nm TiO_2 particles (Dyesol© paste). Prior to the

UNIVERSITAT ROVIRA I VIRGILI
NOVEL MOLECULAR CATALYSTS FOR WATER OXIDATION: TOWARDS ARTIFICIAL PHOTOSYNTHESIS
Sara Goberna Ferrón
Dipòsit Legal: T.189-2014

deposition of the TiO_2 paste, the conducting glass substrates were immersed in a solution of $TiCl_4$ (40 mM) at 70 ºC for 30 minutes and then dried. The TiO_2 nanoparticle paste was deposited onto a conducting glass substrate using the screen printing technique. The TiO_2 electrodes were gradually heated under an air-flow at 325 ºC for 5 min, 375 ºC for 5 min, 450 ºC for 15 min and 500 ºC for 15 min. The heated TiO_2 electrodes were immersed again in a solution of $TiCl_4$ (40 mM) at 70 ºC for 30min and then washed with ethanol. The electrodes were heated again at 500 ºC for 30 min and cooled before dye adsorption. The active area for devices was 1 cm^2. The counter electrode was made by spreading a 5 mM solution of H_2PtCl_6 in isopropyl alcohol onto a conducting glass substrate containing a small hole to allow the introduction of the liquid electrolyte using vacuum, followed by heating at 390 ºC for 15 minutes. The films were sensitized in 0.3 mM C101 dye solution [Na-cis-Ru(4,4'-(5-hexyltiophen-2-yl)-2,2'-bipyridine)(4-carboxylic-acid-4'-carboxylate-2,2'-bipyridine)(thiocyanate)(2)] in ethanol containing 0.3 mM chenoxydecholic acid overnight at 3 ºC. The sensitized electrodes were washed with ethanol and dried under air. Finally, the working and counter electrodes were sandwiched together using a thin thermoplastic (Surlyn) frame that melts at 100 ºC. The electrolyte used consisted of 1 M 1-butyl-3-methylimidazolium iodide (BMII), 0.05 M lithium iodide, 0.03 M iodine, 0.1 M guanidine tiocyanate and 0.5 M tert-butylpyridine in a mixture of acetonitrile:valeronitrile (85:15).

Tafel Plots

Current–potential data were obtained in the same experimental conditions than bulk water electrolysis experiments at a variety of applied potentials. The solution was stirred and steady-state currents were then measured at applied potentials that ascended from 1.05 V to 1.5 V proceeding in 10-25 mV steps. The stable current density (*i*) was measured after 10 minutes of applying a given potential. The obtained

UNIVERSITAT ROVIRA I VIRGILI
NOVEL MOLECULAR CATALYSTS FOR WATER OXIDATION: TOWARDS ARTIFICIAL PHOTOSYNTHESIS
Sara Goberna Ferrón
Dipòsit Legal: T.189-2014

data follows a linear trend that corresponds to a Tafel plot, where overpotential = A + B log (*i*); (see Appendix I for more details regarding Tafel equation and Tafel plots).

Oxygen and Hydrogen evolution measurements

Oxygen evolution in the gas phase was determined with an Ocean Optics NeoFOX oxygen−sensing system equipped with a FOXY probe. Hydrogen evolution in the gas phase was determined with a UNISENSE Clark−type hydrogen microsensor with an internal reference electrode and a sensing anode. Each measurement is performed by inserting the sensor into the anodic compartment of bulk electrolysis experiments through a septum. The system is degassed by an N_2 flow through the gas-space while stirring during 30 minutes to achieve gas−liquid equilibria. In all oxygen and hydrogen determination techniques, the set−up was calibrated using the same procedure substitung the reaction solutions by water. By addition of known quantities of the corresponding pure gas, a calibration slope was obtained. The slope was employed for the quantification of oxygen or hydrogen in the catalysis experiments carried out.

Photo-induced water oxidation measurements

Tris(2,2′-bipyridyl)dichlororuthenium(II) hexahydrate and sodium persulfate were purchased from TCI and Aldrich respectively. In a typical experiment, light-induced water oxidation was performed in a 20 mL schlenck flask. The vessel was filled with 15 mL of buffered (10-80 mM, borate or phosphate, initial pH = 8) solution with 1 mM $[Ru(bpy)_3]^{2+}$, 5 mM $Na_2S_2O_8$ and the desired concentration of **Co_9.** The reaction vessel was then sealed with a screw cap that incorporates the O_2–sensor probe (Ocean Optics NeoFOX oxygen−sensing system equipped with a FOXY probe) and carefully deairated with nitrogen. All procedures were performed with a minimum exposure to ambient light. The reaction was initiated by turning on the blue LED (Wavelength at peak emission = 465 nm; OSRAM Opto Semiconductors) and vigorously stirred to

UNIVERSITAT ROVIRA I VIRGILI
NOVEL MOLECULAR CATALYSTS FOR WATER OXIDATION: TOWARDS ARTIFICIAL PHOTOSYNTHESIS
Sara Goberna Ferrón
Dipòsit Legal: T.189-2014

equilibrate O_2 concentration in liquid and gas phase. The kinetics of oxygen formation was followed continuously in the headspace with the O_2–sensor probe. The reaction was stopped by turning off the blue LED.

The **number of moles of O_2 produced** were calculate following equation 3.14:

$$n_{O2} = \{(\%O_2)n_{N2}/100\} \quad \text{(Eq. 3.14)}$$

Where n_{O2} = number of oxygen moles; $\%O_2$ is given by the oxygen–sensing system and n_{N2} = number of moles of nitrogen (calculated using the Ideal gas law (Eq. 3.15):

$$PV = n_{N2}RT \quad \text{(Eq. 3.15)}$$

Where P = 1atm; V = gas-space volume; n_{N2} = number of N_2 moles; R (gas constant) = 0.083 atmL/molK and T = 298 K.

The **chemical yield** (CY, %) was calculated following equation 3.16:

$$CY = (n_{O2}/2n_{S2O8})100 \quad \text{(Eq. 3.16)}$$

Where n_{O2} = number of oxygen moles and n_{S2O8} is the number of moles of $Na_2S_2O_8$.

The **Turnover number** (TON) was calculated following equation 3.17:

$$TON = n_{O2}/n_{cat} \quad \text{(Eq. 3.16)}$$

Where n_{O2} = number of oxygen moles and n_{cat} is the number of moles of catalyst.

Finally, the **Turnover frequency** (TOF, s^{-1}) was calculated by plotting n_{O2} vs. time; the very beginning of the O_2 evolution follows a linear fit, from the slope (n_{O2}/ time) the TOF can be extracted following equation 3.17:

$$TOF = TON/t = slope/n_{cat} \quad \text{(Eq. 3.16)}$$

UNIVERSITAT ROVIRA I VIRGILI
NOVEL MOLECULAR CATALYSTS FOR WATER OXIDATION: TOWARDS ARTIFICIAL PHOTOSYNTHESIS
Sara Goberna Ferrón
Dipòsit Legal: T.189-2014

3.5

References

1 Long, D. L., Burkholder, E. & Cronin, L. Polyoxometalate clusters, nanostructures and materials: From self assembly to designer materials and devices. *Chem. Soc. Rev.* **36**, 105-121 (2007).

2 Hill, C. L. Progress and challenges in polyoxometalate-based catalysis and catalytic materials chemistry. *J. Mol. Catal. A: Chem.* **262**, 2-6 (2007).

3 Kortz, U., Mueller, A., van Slageren, J., Schnack, J. r., Dalal, N. S. & Dressel, M. Polyoxometalates: Fascinating structures, unique magnetic properties. *Coord. Chem. Rev.* **253**, 2315-2327 (2009).

4 Pope, M. T. *Heteropoly and Isopoly Oxometalates*. (Springer-Verlag, 1983).

5 Hill, C., Weeks, M. & Schinazi, R. Anti-HIV-1 activity, toxicity, and stability studies of representative structural families of polyoxometalates. *J. Med. Chem.* **33**, 2767-2772 (1990).

6 Barnard, D., Hill, C., Gage, T., Matheson, J., Huffman, J., Sidwell, R., Otto, M. & Schinazi, R. Potent inhibition of respiratory syncytial virus by polyoxometalates of several structural classes. *Antiviral research* **34**, 27-37 (1997).

7 Shigeta, S., Mori, S., Watanabe, J., Soeda, S., Takahashi, K. & Yamase, T. Synergistic anti-influenza virus A (H1N1) activities of PM-523 (polyoxometalate) and ribavirin in vitro and in vivo. *Antimicrob. Agents Chemother.* **41**, 1423-1427 (1997).

8 Rhule, J., Hill, C., Judd, D. & Schinazi, R. Polyoxometalates in Medicine. *Chem. Rev.* **98**, 327-358 (1998).

9 Judd, D., Nettles, J., Nevins, N., Snyder, J., Liotta, D., Tang, J., Ermolieff, J., Schinazi, R. & Hill, C. Polyoxometalate HIV-1 protease inhibitors. A new mode of protease inhibition. *J. Am. Chem. Soc.* **123**, 886-897 (2001).

10 Bareyt, S. b., Piligkos, S., Hasenknopf, B., Gouzerh, P., Lacote, E., Thorimbert, S. & Malacria, M. Highly efficient peptide bond formation to functionalized Wells-Dawson-type polyoxotungstates. *Angewandte* **42**, 3404-3406 (2003).

11 Shigeta, S., Mori, S., Kodama, E., Kodama, J., Takahashi, K. & Yamase, T. Broad spectrum anti-RNA virus activities of titanium and vanadium substituted polyoxotungstates. *Antiviral research* **58**, 265-271 (2003).

12 Lee, I., Long, J., Prusiner, S. & Safar, J. Selective precipitation of prions by polyoxometalate complexes. *J. Am. Chem. Soc.* **127**, 13802-13803 (2005).

UNIVERSITAT ROVIRA I VIRGILI
NOVEL MOLECULAR CATALYSTS FOR WATER OXIDATION: TOWARDS ARTIFICIAL PHOTOSYNTHESIS
Sara Goberna Ferrón
Dipòsit Legal: T.189-2014

13 Yanagie, H., Ogata, A., Mitsui, S., Hisa, T., Yamase, T. & Eriguchi, M. Anticancer activity of polyoxomolybdate. *Biomedicine & pharmacotherapy* **60**, 349-352 (2006).

14 Wille, H., Shanmugam, M., Murugesu, M., Ollesch, J., Stubbs, G., Long, J., Safar, J. & Prusiner, S. Surface charge of polyoxometalates modulates polymerization of the scrapie prion protein. *PNAS* **106**, 3740-3745 (2009).

15 Coronado, E. & Day, P. Magnetic molecular conductors. *Chem. Rev.* **104**, 5419-5448 (2004).

16 Coronado, E. & Gómez-García, C. Polyoxometalate-Based Molecular Materials. *Chem. Rev.* **98**, 273-296 (1998).

17 Aldamen, M., Clemente-Juan, J., Coronado, E., Martí-Gastaldo, C. & Gaita-Ariño, A. Mononuclear lanthanide single-molecule magnets based on polyoxometalates. *J. Am. Chem. Soc.* **130**, 8874-8875 (2008).

18 Kögerler, P., Tsukerblat, B. & Müller, A. Structure-related frustrated magnetism of nanosized polyoxometalates: aesthetics and properties in harmony. *Dalton Trans.*, 21-36 (2010).

19 Speldrich, M., Schilder, H., Lueken, H. & Kögerler, P. A Computational Framework for Magnetic Polyoxometalates and Molecular Spin Structures: CONDON 2.0. *Isr. J. Chem.* **51**, 215-227 (2011).

20 Fang, X., Anderson, T., Hou, Y. & Hill, C. Stereoisomerism in polyoxometalates: structural and spectroscopic studies of bis(malate)-functionalized cluster systems. *Chem. Commun.*, 5044-5046 (2005).

21 Lu, M., Kang, J., Wang, D. & Peng, Z. Enantiopure 1,1'-binaphthyl-based polyoxometalate-containing molecular hybrids. *Inorg. Chem.* **44**, 7711-7713 (2005).

22 Long, D.-L., Kögerler, P., Farrugia, L. & Cronin, L. Linking chiral clusters with molybdate building blocks: from homochiral helical supramolecular arrays to coordination helices. *Chem. Asian J.* **1**, 352-357 (2006).

23 Hou, Y., Fang, X. & Hill, C. Breaking symmetry: spontaneous resolution of a polyoxometalate. *Chemistry* **13**, 9442-9447 (2007).

24 Hasenknopf, B., Micoine, K., Lacôte, E., Thorimbert, S., Malacria, M. & Thouvenot, R. Chirality in Polyoxometalate Chemistry. *Eur. J. Inorg. Chem.* **2008**, 5001–5013 (2008).

25 Yan, L., López, X., Carbó, J. J., Sniatynsky, R., Duncan, D. & Poblet, J. M. On the origin of alternating bond distortions and the emergence of chirality in polyoxometalate anions. *J. Am. Chem. Soc.* **130**, 8223-8233 (2008).

26 Jahier, C., Cantuel, M., McClenaghan, N., Buffeteau, T., Cavagnat, D., Agbossou, F., Carraro, M., Bonchio, M. & Nlate, S. Enantiopure dendritic polyoxometalates: chirality transfer from dendritic wedges to a POM cluster for asymmetric sulfide oxidation. *Chemistry* **15**, 8703-8708 (2009).

3. 5. References

27 Carraro, M., Modugno, G., Sartorel, A., Scorrano, G. & Bonchio, M. Optically Active Polyoxotungstates Bearing Chiral Organophosphonate Substituents. *Eur. J. Inorg. Chem.* **2009** (2009).

28 Katsoulis, D. A Survey of Applications of Polyoxometalates. *Chem. Rev.* **98**, 359-388 (1998).

29 Keggin, J. F. Structure of the Molecule of i2-Phosphotungstic. *Nature* **131**, 908-909 (1933).

30 Illingworth, J. W. & Keggin, J. F. 127. Identification of the 12-heteropoly-acids and their salts by means of X-ray powder photographs. *J. Chem. Soc.*, 575-580 (1935).

31 Putaj, P. & Lefebvre, F. Polyoxometalates containing late transition and noble metal atoms. *Coord. Chem. Rev.* **255**, 1642-1685 (2011).

32 Lyons, J. E., Ellis, P. E., Jr. & Durante, V. A. *Studies in Surface Science and Catalysis*. (Elsevier, 1991).

33 Okun, N., Anderson, T., Hardcastle, K. & Hill, C. Cupric decamolybdodivanadophosphate. A coordination polymer heterogeneous catalyst for rapid, high conversion, high selectivity sulfoxidation using the ambient environment. *Inorg. Chem.* **42**, 6610-6612 (2003).

34 Kozhevnikov, I. Catalysis by Heteropoly Acids and Multicomponent Polyoxometalates in Liquid-Phase Reactions. *Chem. Rev.* **98**, 171-198 (1998).

35 Khenkin, A. & Hill, C. Selective homogeneous catalytic epoxidation of alkenes by hydrogen peroxide catalysed by oxidatively-and solvolytically-resistant polyoxometalate complexes. *Mendeleev Commun.* **3**, 140–141 (1993).

36 Rong, C. & Pope, M., T. Lacunary polyoxometalate anions are .pi.-acceptor ligands. Characterization of some tungstoruthenate(II,III,IV,V) heteropolyanions and their atom-transfer reactivity. *J. Am. Chem. Soc.* **114**, 2932–2938 (1992).

37 Neumann, R. & Abu-Gnim, C. Alkene oxidation catalyzed by a ruthenium-substituted heteropolyanion, SiRu(L)W11O39: the mechanism of the periodate-mediated oxidative cleavage. *J. Am. Chem. Soc.* **112**, 6025–6031 (1990).

38 Faraj, M. & Hill, C., L. Sustained catalytic homogenous oxo-transfer oxidation of alkanes. Interaction of alkyl hydroperoxides with transition metal-substituted polyoxometalates. *J. Chem. Soc., Chem. Commun.*, 1487-1489 (1987).

39 Howells, A., Sankarraj, A. & Shannon, C. A diruthenium-substituted polyoxometalate as an electrocatalyst for oxygen generation. *J. Am. Chem. Soc.* **126**, 12258-12259 (2004).

40 Lv, H., Geletii, Y., Zhao, C., Vickers, J., Zhu, G., Luo, Z., Song, J., Lian, T., Musaev, D. & Hill, C. Polyoxometalate water oxidation catalysts and the production of green fuel. *Chem. Soc. Rev.* **41**, 7572-7589 (2012).

UNIVERSITAT ROVIRA I VIRGILI
NOVEL MOLECULAR CATALYSTS FOR WATER OXIDATION: TOWARDS ARTIFICIAL PHOTOSYNTHESIS
Sara Goberna Ferrón
Dipòsit Legal: T.189-2014

41 Geletii, Y. V., Yin, Q., Hou, Y., Huang, Z., Ma, H., Song, J., Besson, C., Luo, Z., Cao, R., O'Halloran, K. P., Zhu, G., Zhao, C., Vickers, J. W., Ding, Y., Mohebbi, S., Kuznetsov, A. E., Musaev, D. G., Lian, T. & Hill, C. L. Polyoxometalates in the Design of Effective and Tunable Water Oxidation Catalysts. *Isr. J. Chem.* **51**, 238 – 246 (2011).

42 Zhu, G., Glass, E. N., Zhao, C., Lv, H., Vickers, J. W., Geletii, Y. V., Musaev, D. G., Song, J. & Hill, C. L. A nickel containing polyoxometalate water oxidation catalyst. *Dalton Trans.* **41**, 13043-13049 (2012).

43 Geletii, Y., Botar, B., Koegerler, P., Hillesheim, D., Musaev, D. & Hill, C. An all-inorganic, stable, and highly active tetraruthenium homogeneous catalyst for water oxidation. *Angew. Chem.* **47**, 3896-3899 (2008).

44 Sartorel, A., Carraro, M., Scorrano, G., De Zorzi, R., Geremia, S., McDaniel, N., Bernhard, S. & Bonchio, M. Polyoxometalate embedding of a tetraruthenium(IV)-oxo-core by template-directed metalation of [gamma-SiW10O36]8-: a totally inorganic oxygen-evolving catalyst. *J. Am. Chem. Soc.* **130**, 5006-5007 (2008).

45 Yin, Q. S., Tan, J. M., Besson, C., Geletii, Y. V., Musaev, D. G., Kuznetsov, A. E., Luo, Z., Hardcastle, K. I. & Hill, C. L. A Fast Soluble Carbon-Free Molecular Water Oxidation Catalyst Based on Abundant Metals. *Science* **328**, 342-345 (2010).

46 Stracke, J. J. & Finke, R. G. Electrocatalytic Water Oxidation Beginning with the Cobalt Polyoxometalate [Co(4)(H(2)O)(2)(PW(9)O(34))(2)](10-): Identification of Heterogeneous CoO(x) as the Dominant Catalyst. *J. Am. Chem. Soc.* **133**, 14872-14875 (2011).

47 Natali, M., Berardi, S., Sartorel, A., Bonchio, M., Campagna, S. & Scandola, F. Is [Co4(H2O)2([alpha]-PW9O34)2]10- a genuine molecular catalyst in photochemical water oxidation? Answers from time-resolved hole scavenging experiments. *Chem. Commun.* **48**, 8808-8810 (2012).

48 Car, P.-E., Guttentag, M., Baldridge, K., K., Alberto, R. & Patzke, G., R. Synthesis and characterization of open and sandwich-type polyoxometalates reveals visible-light-driven water oxidation via POM-photosensitizer complexes. *Green Chem.* **14**, 1680-1688 (2012).

49 Tanaka, S., Annaka, M. & Sakai, K. Visible light-induced water oxidation catalyzed by molybdenum-based polyoxometalates with mono- and dicobalt(III) cores as oxygen-evolving centers. *Chem. Commun.* **48**, 1653-1655 (2012).

50 Weakley, T. J. R. The identification and X-ray structure of the diphosphatotris (nonatungstophosphato) nonacobaltate (II) heteropolyanion. *J. Chem. Soc., Chem. Commun.*, 1406-1407 (1984).

51 Creutz, C. & Sutin, N. Reaction of tris(bipyridine)ruthenium(III) with hydroxide and its application in a solar energy storage system. *N. Proc. Acad. Sci. U.S.A.* **72**, 2858-2862 (1975).

3. 5. References

52 Parent, A. R., Brewster, T. P., De Wolf, W., Crabtree, R. H. & Brudvig, G. W. Sodium Periodate as a Primary Oxidant for Water-Oxidation Catalysts. *Inorg. Chem.* **51**, 6147-6152 (2012).

53 Limburg, J., Vrettos, J. S., Chen, H. Y., de Paula, J. C., Crabtree, R. H. & Brudvig, G. W. Characterization of the O-2-evolving reaction catalyzed by (terpy)(H2O)Mn-III(O)(2)Mn-IV(OH2)(terpy) (NO3) (terpy=2,2 ': 6,2 ''-terpyridine). *J. Am. Chem. Soc.* **123**, 423-430 (2001).

54 Limburg, J., Vrettos, J. S., Liable-Sands, L. M., Rheingold, A. L., Crabtree, R. H. & Brudvig, G. W. A functional model for O-O bond formation by the O-2-evolving complex in photosystem II. *Science* **283**, 1524-1527 (1999).

55 Lister, M. Decomposition Of Sodium Hypochlorite : The Catalized Reaction. *Can. J. Chem.* **34**, 479-488 (1956).

56 Lister, M. & Petterson, R. Oxygen evolution from sodium hypochlorite solutions. *Can. J. Chem.* **40**, 729-733 (1962).

57 Adam, L. & Gordon, G. Hypochlorite Ion Decomposition: Effects of Temperature, Ionic Strength, and Chloride Ion. *Inorg. Chem.* **38**, 1299-1304 (1999).

58 Parent, A., Crabtree, R. & Brudvig, G. Comparison of primary oxidants for water-oxidation catalysis. *Chem. Soc. Rev.* **42**, 2247-2252 (2013).

59 Eisenberg, R. & Gray, H. Preface on making oxygen. *Inorg. Chem.* **47**, 1697-1699 (2008).

60 Kanan, M. W. & Nocera, D. G. In situ formation of an oxygen-evolving catalyst in neutral water containing phosphate and Co(2+). *Science* **321**, 1072-1075 (2008).

61 Surendranath, Y., Kanan, M. W. & Nocera, D. G. Mechanistic Studies of the Oxygen Evolution Reaction by a Cobalt-Phosphate Catalyst at Neutral pH. *J. Am. Chem. Soc.* **132**, 16501-16509 (2010).

62 Gerken, J., McAlpin, J., Chen, J., Rigsby, M., Casey, W., Britt, R. & Stahl, S. Electrochemical water oxidation with cobalt-based electrocatalysts from pH 0-14: the thermodynamic basis for catalyst structure, stability, and activity. *J. Am. Chem. Soc.* **133**, 14431-14442 (2011).

63 Dau, H., Limberg, C., Reier, T., Risch, M., Roggan, S. & Strasser, P. The Mechanism of Water Oxidation: From Electrolysis via Homogeneous to Biological Catalysis. *ChemCatChem* **2**, 724-761 (2010).

64 Pijpers, J. J. H., Winkler, M. T., Surendranath, Y., Buonassisi, T. & Nocera, D. G. Light-induced water oxidation at silicon electrodes functionalized with a cobalt oxygen-evolving catalyst. *Proc. Natl. Acad. Sci.* **108**, 10056-10061 (2011).

65 Henry, S. W., William, G. B. & Allen, J. B. Photochemistry of the tris(2,2'-bipyridine)ruthenium(II)-peroxydisulfate system in aqueous and mixed acetonitrile-water solutions. Evidence for a long-lived photoexcited ion pair. *J. Phys. Chem.* **88**, 1840-1846 (1984).

UNIVERSITAT ROVIRA I VIRGILI
NOVEL MOLECULAR CATALYSTS FOR WATER OXIDATION: TOWARDS ARTIFICIAL PHOTOSYNTHESIS
Sara Goberna Ferrón
Dipòsit Legal: T.189-2014

66 Hara, M., Waraksa, C., C., Lean, J., T., Lewis, B., A. & Mallouk, T., E. Photocatalytic Water Oxidation in a Buffered Tris(2,2'-bipyridyl)ruthenium Complex-Colloidal IrO 2 System. *J. Phys. Chem. A* **104**, 5275-5280 (2000).

67 Pushpito, K. G., Bruce, S. B., Mei, C., Carol, C. & Norman, S. Thermal and light-induced reduction of the ruthenium complex cation Ru(bpy)33+ in aqueous solution. *J. Am. Chem. Soc.* **106**, 4772-4783 (1984).

68 Galán-Mascarós, J. R., Gómez-Garcia, C., J., Borrás-Almenar, J. J. & Coronado, E. High nuclearity magnetic clusters: Magnetic properties of a nine cobalt cluster encapsulated in a polyoxometalate, [Co9(OH)3(H2O)6(HPO4)2(PW9O34)3]16-. *Adv. Mater.* **6**, 221-223 (1994).

69 Weakley, T. J. R. The identification and X-ray structure of the diphosphatotris (nonatungstophosphato) nonacobaltate (II) heteropolyanion. *J. Chem. Soc., Chem. Commun.*, 1406-1407 (1984).

70 Weakley, T. i., J. R, Evans, H., T., Showell, J., S., Tourné, G., F. & Tourné, C., M. 18-Tungstotetracobalto(II)diphosphate and related anions: a novel structural class of heteropolyanions. *J. Chem. Soc., Chem. Commun*, 139-140 (1973).

UNIVERSITAT ROVIRA I VIRGILI
NOVEL MOLECULAR CATALYSTS FOR WATER OXIDATION: TOWARDS ARTIFICIAL PHOTOSYNTHESIS
Sara Goberna Ferrón
Dipòsit Legal: T.189-2014

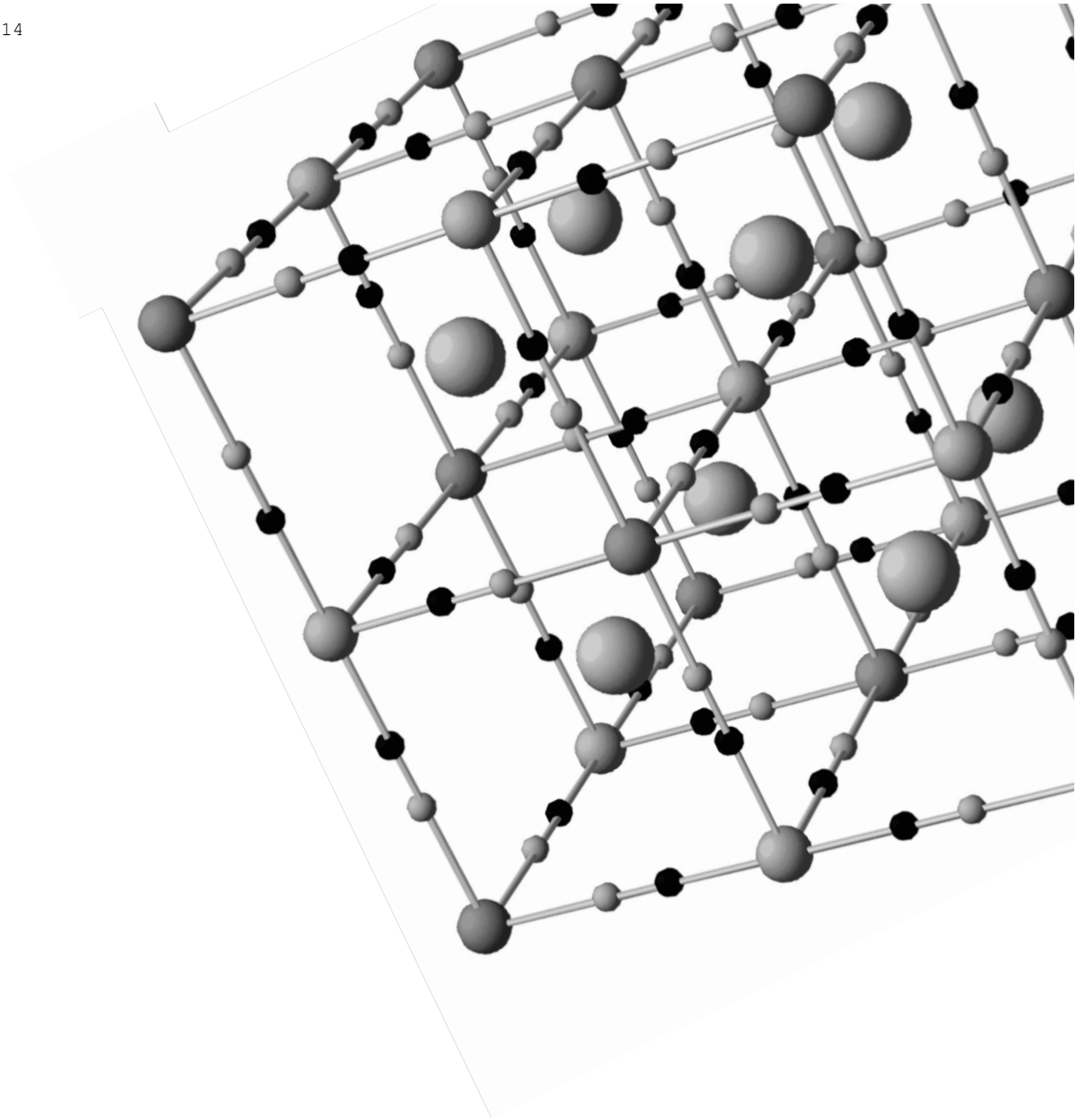

Chapter 4

Prussian Blue Type Water Oxidation Catalyst

UNIVERSITAT ROVIRA I VIRGILI
NOVEL MOLECULAR CATALYSTS FOR WATER OXIDATION: TOWARDS ARTIFICIAL PHOTOSYNTHESIS
Sara Goberna Ferrón
Dipòsit Legal: T.189-2014

UNIVERSITAT ROVIRA I VIRGILI
NOVEL MOLECULAR CATALYSTS FOR WATER OXIDATION: TOWARDS ARTIFICIAL PHOTOSYNTHESIS
Sara Goberna Ferrón
Dipòsit Legal: T.189-2014

4.1

Introduction

Prussian Blue was discovered over 300 years ago as a pigment by the Berlin artist Diesbach.[1] The value of this new pigment was immediately obvious, especially when it was shown to be stable and relatively insensitive to light. As it was much cheaper than alternatives derived from indigo and mineral sources, it has been used by many outstanding artists such as Hokusai and Picasso in his blue period (Figure 4.1).[2] Although it is one of the oldest synthetic coordination compounds recorded in the scientific literature, the field of the cyanide-based compounds has emerged in the last 20 years.[3]

Transition metal hexacyanometallates (MHCM), an important class of mixed−valence compounds, are isostructural to the original Prussian blue,[3] $Fe_4^{III}[Fe^{II}(CN)_6]_3 \times xH_2O$. The crystal structure consists in a cubic arrangement where two octahedral metal centers are bound through cyanide bridges to construct a face−centered cubic unit cell (Figure 4.2).[4] MHCM are known for many combinations of transition metal ions in multiple oxidation states. They are also highly porous because the metal / hexacyanometallate ratio is usually greater than one. This creates vacancies in the $M(CN)_6$ sites and, therefore, open coordination positions in the transition metal that are occupied by solvent molecules. Depending on synthetic conditions, they can also incorporate interstitial alkali metal ions. Despite of their rigid structure, these compounds are usually non−stoichiometric because different non-integer ratios between all components can be accommodated. This chemical variety makes of them a versatile type of coordination materials, indeed MHCM have a wide range of applications. They are room temperature magnets;[5] biosensors;[6] electrochromic displays;[7] possess high hydrogen storage capabilities;[8] negative thermal expansion[9] or

UNIVERSITAT ROVIRA I VIRGILI
NOVEL MOLECULAR CATALYSTS FOR WATER OXIDATION: TOWARDS ARTIFICIAL PHOTOSYNTHESIS
Sara Goberna Ferrón
Dipòsit Legal: T.189-2014

high proton conductivity.[9]

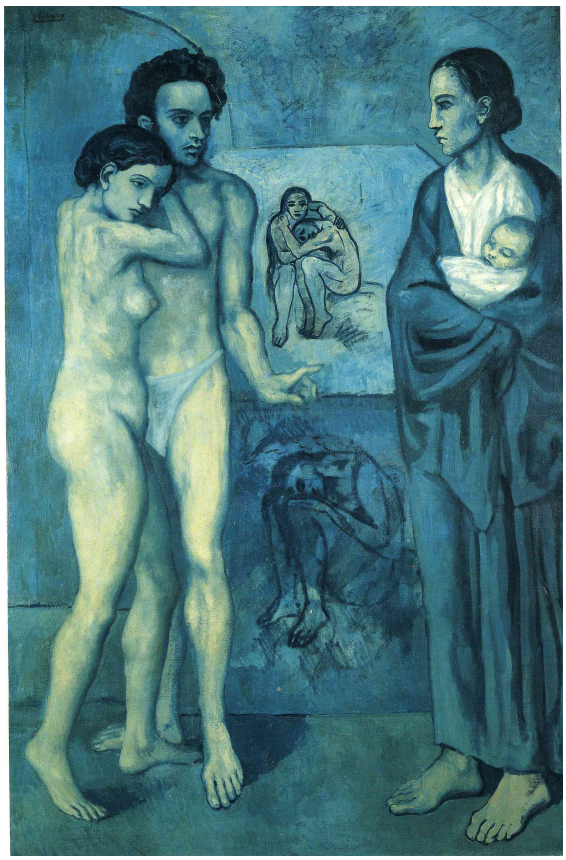

Figure 4.1. *La Vie, 1903. Pablo Picasso (1881–1973). Oil on canvas; 197 x 129 cm. The Cleveland Museum of Art, Gift of the Hanna Fund 1945.24. Picasso subtly varied the Prussian blue, the most prominent color, by adding white in some cases and ocher or yellow in others.*[2]

MHCM have been studied as components of modified electrodes.[10,11] As electrocatalysts, they have been used for the oxidation of organic substrates[12] and even for the catalytic reduction of molecular oxygen.[13] It is surprising that, given the richness and successful electrochemical applications of MHCM, water oxidation catalysis has not been studied or reported. Taking into account that Co centers are the reactive sites in some of the most successful homogeneous and heterogeneous water oxidation catalysts,[14,15] cobalt hexacyanometallates appear to possess all the

UNIVERSITAT ROVIRA I VIRGILI
NOVEL MOLECULAR CATALYSTS FOR WATER OXIDATION: TOWARDS ARTIFICIAL PHOTOSYNTHESIS
Sara Goberna Ferrón
Dipòsit Legal: T.189-2014

requirements of a promising WOC:

. They posses a highly porosity, where the $M(CN)_6$ vacancies are filled by water molecules, some of them directly coordinated to the cobalt (II) centers.

. These compounds are highly insoluble in water at pH > 3, this feature makes them candidates as heterogeneous catalysts.

. MCHM complexes present a high thermal and chemical stability.

. They are easily prepared as thin films on different electrode surfaces.

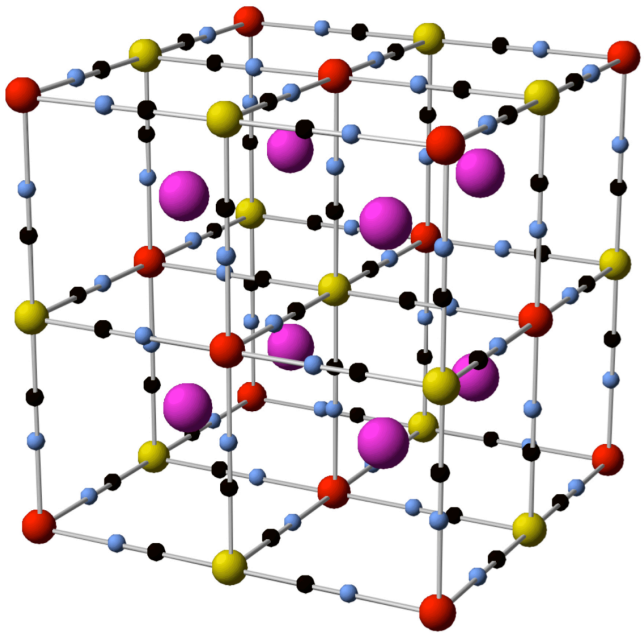

Figure 4.2. *Unit cell representation of the face centered cubic Prussian blue type structure. Yellow and red: transition metal ions; black = carbon atoms; blue = nitrogen atoms; violet: interstitial open sites for alkali metal ions or additional solvent. Yellow, black, blue and violet positions have occupancy factors less than one according to the non-stoichiometric composition.*

In the present chapter, the catalytic activity for water oxidation of a Prussian blue type cobalt hexacyanoferrate (CoHCF) has been explored. In the first section, CoHCF modified electrodes are used for electrochemical water oxidation. In the second

UNIVERSITAT ROVIRA I VIRGILI
NOVEL MOLECULAR CATALYSTS FOR WATER OXIDATION: TOWARDS ARTIFICIAL PHOTOSYNTHESIS
Sara Goberna Ferrón
Dipòsit Legal: T.189-2014

section, bulk CoHCF is used to oxidize water in a heterogeneous light–induced water oxidation system and its activity is compared with other Prussian blue type complexes.

UNIVERSITAT ROVIRA I VIRGILI
NOVEL MOLECULAR CATALYSTS FOR WATER OXIDATION: TOWARDS ARTIFICIAL PHOTOSYNTHESIS
Sara Goberna Ferrón
Dipòsit Legal: T.189-2014

4.2

Results and Discussion

4.2.1 Electrochemical Water Oxidation with CoHCF modified electrodes

The catalytic activity of Prussian blue type cobalt hexacyanoferrate (CoHCF) modified electrodes for electrochemical water oxidation is investigated. The water oxidation reaction is conducted by applying an electrical power source to an aqueous electrolyte solution at neutral pH.

Preparation and Characterization of CoHCF Modified Electrodes

Electrode surfaces can be modified with transition metal hexacyanoferrates (MHCF) by different methods that can be divided into three main groups:[16]

1. By dipping a clean electrode surface in a solution containing cyanoferrates and transition metal ions, allowing formation of insoluble MHCF by a simple chemical reaction or electrochemical reaction, cycling the electrode over a range of potentials.

2. By immersing the transition metal electrode surface, or an electroplated electrode with a transition metal, in a solution containing cyanoferrate ions and then derivatizing the electrode surface to obtain insoluble MHCF by chemical or electrochemical methods.

UNIVERSITAT ROVIRA I VIRGILI
NOVEL MOLECULAR CATALYSTS FOR WATER OXIDATION: TOWARDS ARTIFICIAL PHOTOSYNTHESIS
Sara Goberna Ferrón
Dipòsit Legal: T.189-2014

3. By immobilizing mechanically the metal hexacyanoferrates as microparticles on the surface of an appropriate electrode (paraffin-impregnated graphite, carbon paste or conductive polymer−coated electrodes)

Electrochemical methods provide more stable and reproducible films. However, we had to take into account that high positive voltages could induce the formation of of cobalt oxide impurities. For these reasons, we decided to use method 2,[10,17-19] by derivatization of a cobalt−platted electrode surface, applying a constant positive voltage low enough to preclude the formation of cobalt oxides.

CoHCF was prepared fluoride doped tin oxide (FTO) coated glass electrodes. First metallic cobalt was deposited on the surface of the FTO electrode by applying a reduction potential of −0.695 V to a 10 mM $CoCl_2$ solution in 0.1 M KCl during 1 minute, washed with water and sonicated to eliminate the excess of cobalt that is not purely deposited. In the second step (derivatization), the Prussian blue type film was obtained by applying a positive potential of 0.5 V to the Co^0−covered electrodes in a solution containing 10 mM hexacyanoferrate(III) in 0.1 M KCl . During derivatization, cobalt slowly dissolves under the oxidation potential to be trapped by the formation of the desired CoHCF crystallites, deposited on the surface of the electrode. After derivatization, the CoHCF modified electrodes were sonicated to eliminate excess of CoHCF just adhered to the surface and air dried overnight to avoid the detachment of the film if immediately used. It is important to confirm that no residues of metallic cobalt remain at this stage. Metallic cobalt would lead to cobalt oxides by applying higher oxidation potentials, required for water electrolysis. The absence of metallic cobalt residues after the formation of CoHCF was confirmed by the absence of any sign of the corresponding oxidation wave (Figure 4.3). The cyclic voltammogram of a freshly prepared a CoHCF modified FTO electrode (Figure 4.3, top right) shows the

UNIVERSITAT ROVIRA I VIRGILI
NOVEL MOLECULAR CATALYSTS FOR WATER OXIDATION: TOWARDS ARTIFICIAL PHOTOSYNTHESIS
Sara Goberna Ferrón
Dipòsit Legal: T.189-2014

absence of the the Co / Co^{2+} oxidation band, tat can be observed in a Co^{0}–covered electrode (Figure 4.3, top left).

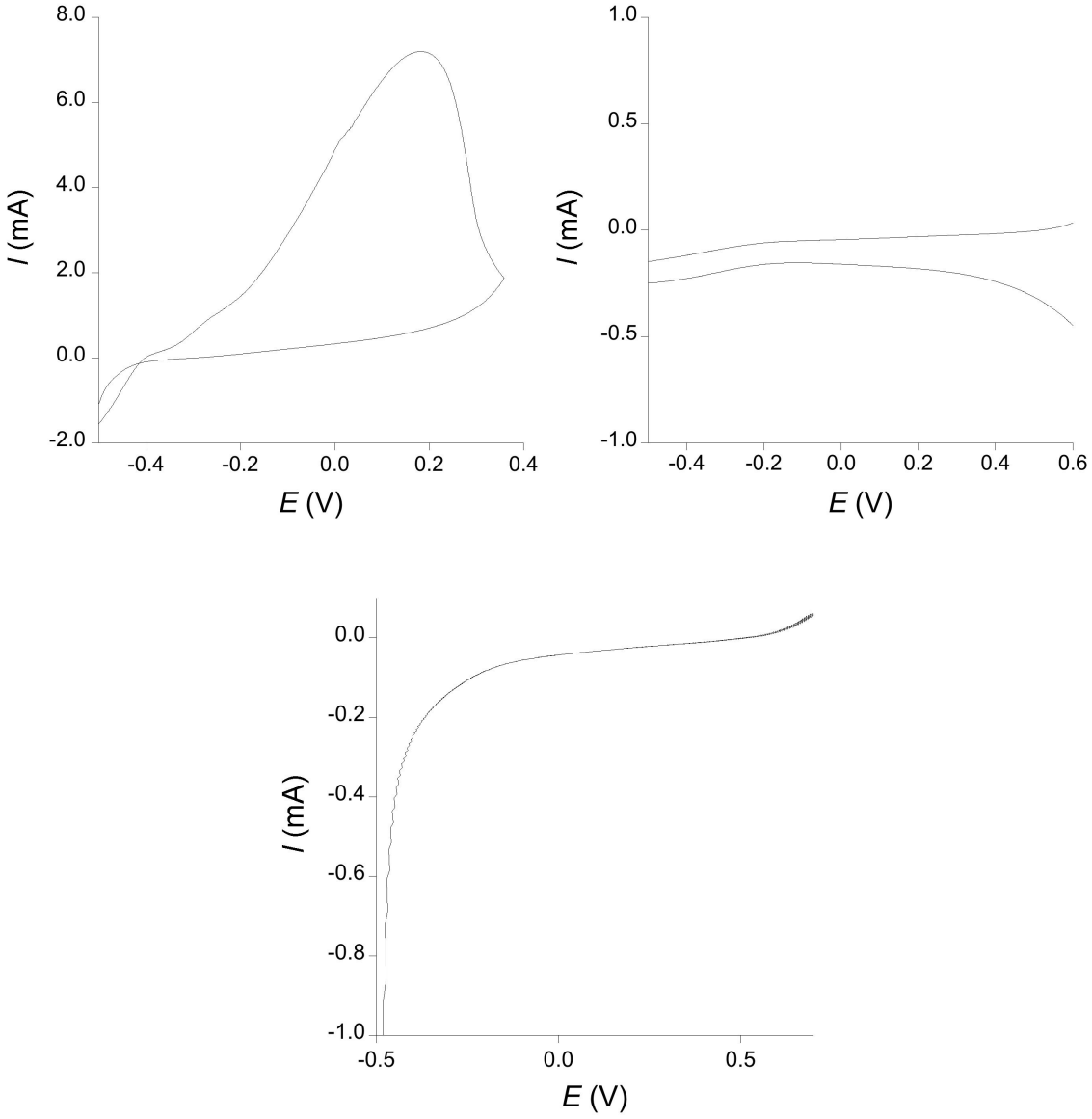

Figure 4.3. ***Top left:*** *Cyclic voltammogram of a FTO electrode platted with metallic cobalt in a neutral 50 mM potassium phosphate (KP_i) water solution containing 1 M KNO_3 as electrolyte, showing the strong Co / Co^{2+} oxidation band.* ***Top right:*** *Detail of the cyclic voltammogram of a CoHCF modified FTO electrode in the same conditions.* ***Bottom:*** *Differential pulse voltammogram of a CoHCF modified FTO electrode in the same conditions, showing the absence of any redox process in the region of the Co / Co^{2+} oxidation band. All potentials reported vs NHE.*

FTO electrodes are optically transparent, allowing for a direct and better characterization of the deposited materials. The CoHCF films deposited on the FTO electrode were characterized by spectroscopy and electron microscopy. The UV−Vis spectra of CoHCF is sensitive to the amount of surface−confined material (on the electrode surface) and its oxidation state.[11] The formation of a thin CoHCF film leads to a highly transparency to visible light. The "as prepared" thin film is transparent with a weak yellow coloring (Figure 4.4). The UV−vis spectra, with the light beam passing through the glass substrate, shows a very low difference in absorbance when compared with a pristine FTO (Figure 4.5, left). By comparing with a Co^0−covered FTO electrode (not transparent), CoHCF−covered FTO electrode shows a minimum transmittance of 70% in the 400−900 nm region without significant absorption bands, while metallic cobalt shows a 30 % of transmittance (Figure 4.5, right). The nominal transmittance of the FTO glass electrodes is 81.5 %.

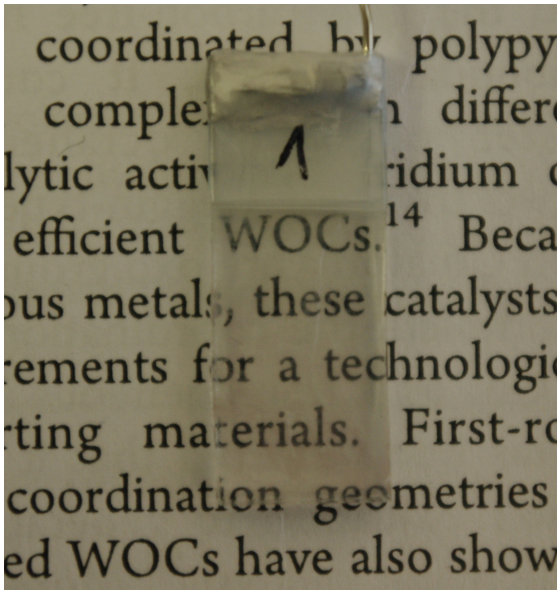

Figure 4.4. *Picture of a freshly prepared CoHCF modified electrode.*

UNIVERSITAT ROVIRA I VIRGILI
NOVEL MOLECULAR CATALYSTS FOR WATER OXIDATION: TOWARDS ARTIFICIAL PHOTOSYNTHESIS
Sara Goberna Ferrón
Dipòsit Legal: T.189-2014

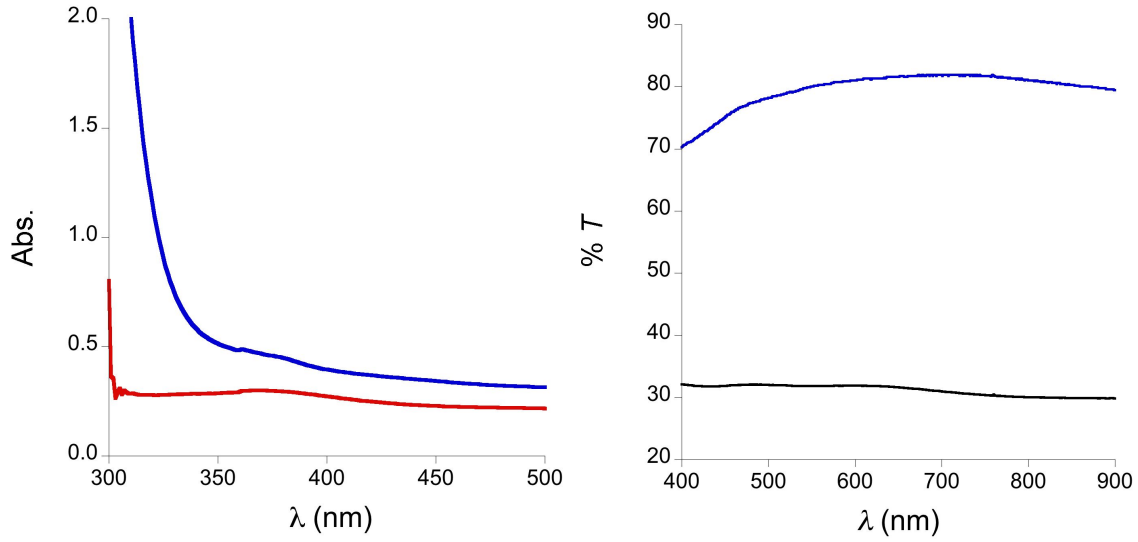

Figure 4.5. ***Left:*** *UV–vis spectra of a pristine FTO (red) and a CoHCF modified FTO (blue).* ***Right:*** *Transmittance of FTO electrodes coated with metallic Co (after paltting) (black) and CoHCF (after derivatization) (red). Nominal 81.5 % transmittance of the FTO glass electrodes has been corrected.*

Energy-dispersive X-ray (EDX) analysis of the CoHCF films indicates the presence of Co, Fe and K (Figure 4.6). Measurements with independently prepared electrodes showed a very high reproducibility. The analysis confirmed a $K_{2x}Co_{(2-x)}[Fe(CN)_6]$ stoichiometry with typical ratios in the (0.85 < x < 0.95) range (Table 4.1).

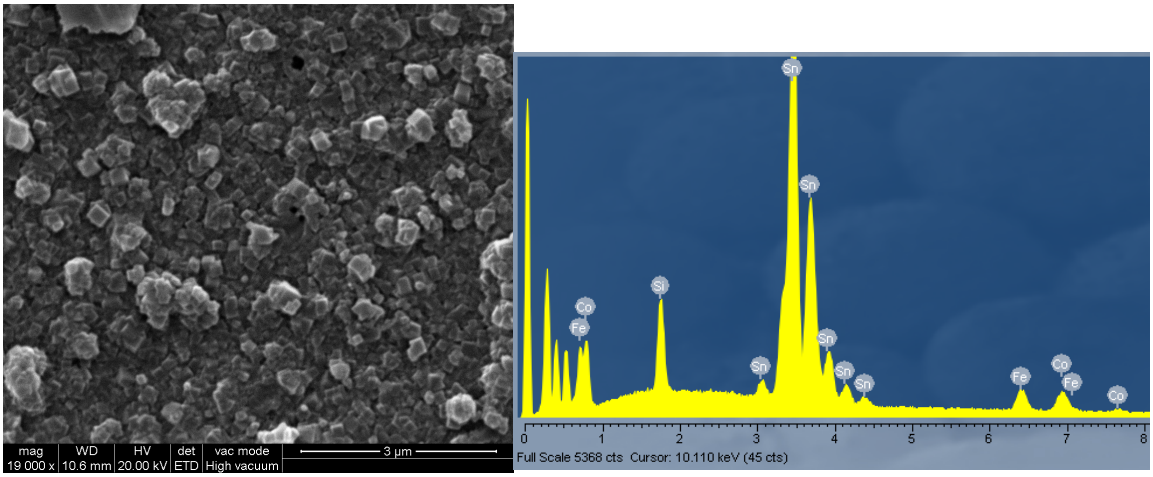

Figure 4.6. *SEM image and EDX analysis of "as prepared" CoHCF grown on a FTO electrode.*

UNIVERSITAT ROVIRA I VIRGILI
NOVEL MOLECULAR CATALYSTS FOR WATER OXIDATION: TOWARDS ARTIFICIAL PHOTOSYNTHESIS
Sara Goberna Ferrón
Dipòsit Legal: T.189-2014

	Fe : Co : K ratio			$K_{2x}Co_{(2-x)[}Fe(CN)_6]$
Electrode	**Fe**	**Co**	**K**	**x**
1	1	1.06	1.88	0.94
2	1	1.14	1.75	0.86
3	1	1.05	1.90	0.95
4	1	1.15	1.74	0.90
5	1	1.05	1.93	0.95
6	1	1.09	1.82	0.91
7	1	1.04	1.90	0.96
8	1	1.14	1.78	0.86
9	1	1.11	1.70	0.88
10	1	1.08	1.86	0.92

Table 1.1. *EDX analysis for a batch of 10 electrodes prepared following the procedure described above. For detail see section: 4.4. Experimental / 4.4.1 Preparation of CoHCF Modified Electrodes.*

The corresponding IR signature for the prepared CoHCF film scrapped from the electrode showed one single band in the cyanide group stretch region at 2076 cm^{-1} (Figure 4.7), characteristic of Fe^{II}–CN–Co^{II} bridges.[11] At the derivation potential, these are the two stable redox states.

The morphology of the electrodes surface was analyzed by Scanning Electron Microscopy (SEM). The FTO surface is covered by a conglomerate of regular cubic-shaped crystallites with maximum edges up to 0.25 μm (Figure 4.6). This shape is typical of Prussian blue crystallites. X-ray powder diffraction of these crystallites shows the typical pattern of a Prussian blue structure (Figure 4.8).[20] The diffraction peaks are broad due to the small particle size and their indexation leads to a face-centered cubic unit cell parameter a = 10.08 ± 0.05 Å.

UNIVERSITAT ROVIRA I VIRGILI
NOVEL MOLECULAR CATALYSTS FOR WATER OXIDATION: TOWARDS ARTIFICIAL PHOTOSYNTHESIS
Sara Goberna Ferrón
Dipòsit Legal: T.189-2014

Figure 4.7. *IR spectra of CoHCF grown on a FTO electrode.*

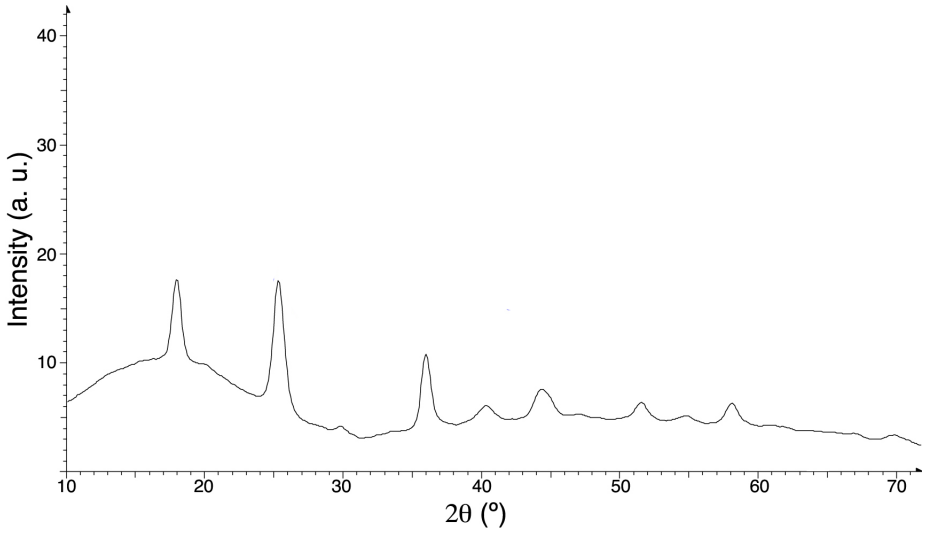

Figure 4.8. *X–ray diffraction pattern for crystallites from a CoHCF modified FTO electrode.*

The cyclic voltammogram of these CoHCF modified electrodes in 50mM potassium phosphate (KP_i) electrolyte at pH = 7 showed a quasi-reversible redox couple with the oxidation peak at 1.04 V and the reduction peak at 0.87 V vs NHE ($E_{1/2}$ = 0.96 V, $E_c - E_a$ = 170 mV) (Figure 4.9, inset). This one electron process can be assigned to the $Co^{II}Fe^{II}$ – $Co^{III}Fe^{II}$ couple.[21] In CoHCF materials, the stability of the two isoelectronic phases $Co^{III}Fe^{II}$ and $Co^{II}Fe^{III}$ depends on stoichiometry, counter cation and preparation. And they can be interconverted through charge transfer induced by external stimuli.[22] With a Co/Fe ratio below 1.15, the $Co^{III}Fe^{II}$ phase is the most stable one.[23] A second oxidation into the $Co^{III}Fe^{III}$, expected a higher oxidation potentials, was not observed since a strong characteristic catalytic water oxidation wave appears above 1.2 V, suggesting a catalytic process (Figure 4.9).

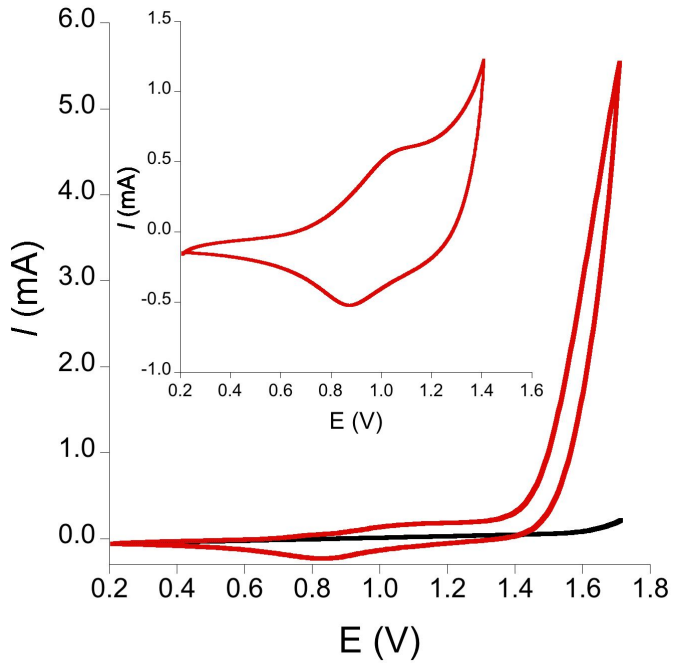

Figure 4.9. *Cyclic voltammogram of a CoHCF modified FTO electrode in 50 mM KP_i buffer solution containing 1 M KNO_3 as electrolyte at pH = 7 (red), and profile of a pristine FTO electrode (black), with a 50 mV s^{-1} sweep rate. Inset: Detail of the 0.2 – 1.4 V range with a 100 mV s^{-1} sweep rate. Pt wire counter electrode and Ag/AgCl (NaCl 3 M) reference electrode. Potentials reported vs NHE.*

UNIVERSITAT ROVIRA I VIRGILI
NOVEL MOLECULAR CATALYSTS FOR WATER OXIDATION: TOWARDS ARTIFICIAL PHOTOSYNTHESIS
Sara Goberna Ferrón
Dipòsit Legal: T.189-2014

In addition to the CoHCF redox activity, a minor irreversible oxidation wave at 0.7 V was observed in the first voltammetry cycles without an associated cathodic process. This irreversible oxidation disappears after several cycles, or after applying an oxidation potential for a few minutes. Since CoHCF exhibits reversible redox chemistry, this weak oxidation can be attributed to the FTO substrate.

The $Co^{II}Fe^{II}$ – $Co^{III}Fe^{II}$ redox pair can be used to calculate the surface coverage (Γ_0, mol cm^{-2}) on the electrode. Cyclic voltammograms at different scan rates were recorded in the 0.2 − 1.6 V potential window. By plotting the peak current and the scan rate (υ), a linear trend is observed (Figure 4.10). From the slope of this relationship it is possible to extract the value of surface concentration, following equation 4.1 (see Appendix II).

$$slope = \frac{n^2 F^2 A \Gamma_0}{4RT} \qquad \text{(Eq. 4.1)}$$

Where n = 1 (1 e^-–redox process), F = faraday's constant, A = surface area, Γ_0 = surface concentration (mol cm^{-2}), R = ideal gas constant and T = temperature. The coverage of redox active Co centers on the electrode is Γ_0 = 1.4 ± 0.2 nmol cm^{-2}, averaged from several independently prepared CoHCF modified electrodes.

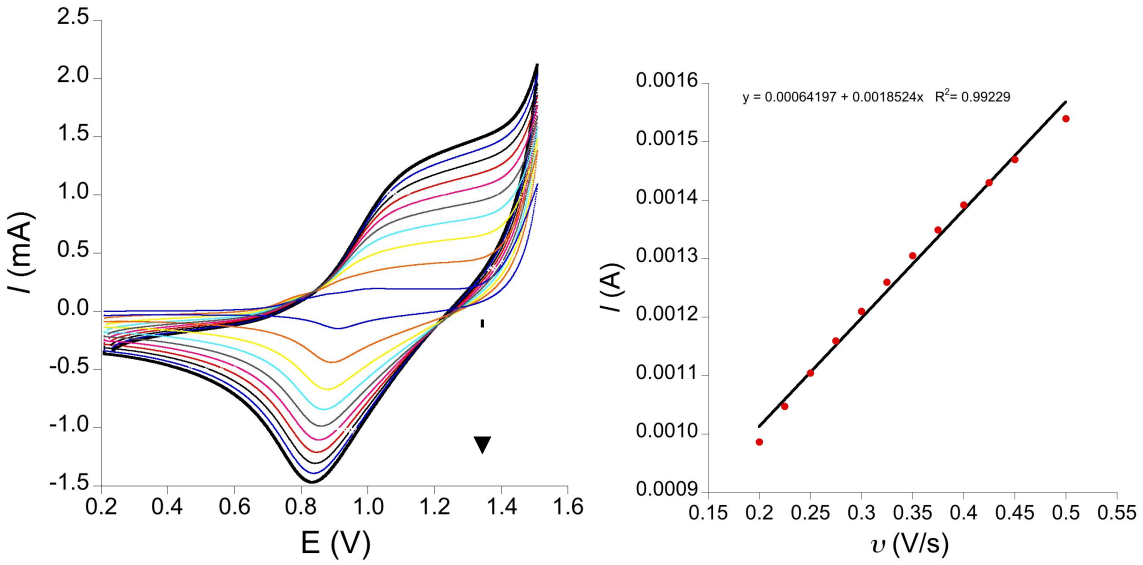

Figure 4.10. ***Left:*** *Cyclic voltammograms of a CoHCF modified FTO electode in 50 mM KP_i buffer solution containing 1 M KNO_3 as electrolyte at pH = 7 at different scan rates (υ), the arrow indicates from 25 to 500 mV s^{-1}.* ***Right:*** *Linear dependence of the peak current of the Co^{3+} / Co^{2+} reduction wave vs scan rate. The concentration of redox active sites was calculated from the slope (Eq.4.1) as described in Appendix II.*

All the characterization experiments were performed with at least three CoHCF modified electrodes, and consistent results were found.

Catalytic activity of the CoHCF modified FTO anodes.

We tested the catalytic activityof the CoHCF modified electrodes for controlled potential water electrolysis. Steady current density (j) was measured at different constant applied potentials in a two−compartment cell, with a glass-frit separating the anode and cathode, in a well-stirred 50 mM KP_i buffer solution containing 1 M KNO_3 as electrolyte at pH = 7. CoHCF modified FTO was used as working electrode. Significant current was detected above 1.10 V. The Tafel plot (Figure 4.11), that relates catalytic current and overpotential (**η**), shows linear behavior for intermediate potentials, with slopes in the 85−100 mV $decade^{-1}$ range, confirming the catalytic

UNIVERSITAT ROVIRA I VIRGILI
NOVEL MOLECULAR CATALYSTS FOR WATER OXIDATION: TOWARDS ARTIFICIAL PHOTOSYNTHESIS
Sara Goberna Ferrón
Dipòsit Legal: T.189-2014

process. This slope is between the expected values for a chemical and electrochemical rate–limiting step.[24] A current density of 1 mA cm^{-2} would theoretically require η ≈ 600 mV. In these experiments, 1 mA/cm^2 catalytic current needed η > 650 mV because the η vs log *j* deviates from linearity above 1.37 V (η = 550 mV) suggesting the appearance of mass transport issues. Indeed, at these high potentials, the electrodes are completely covered by gas bubbles (Figure 4.12) and this should affect the apparent kinetics of the catalysis.

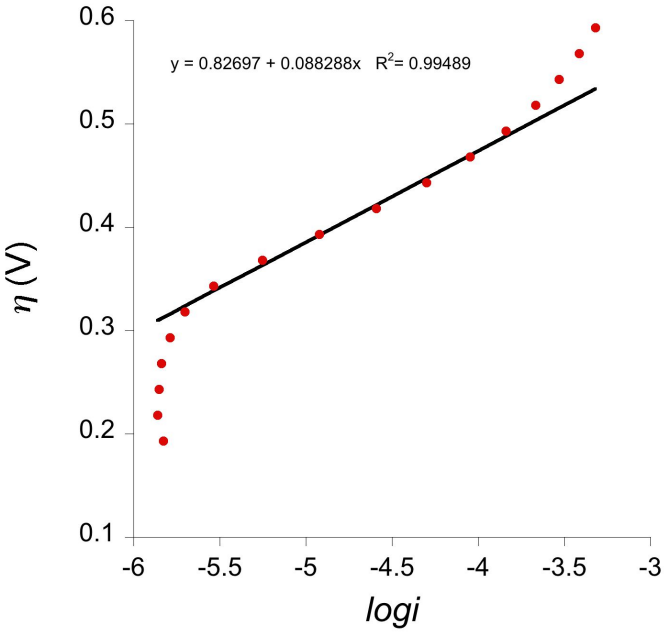

Figure 4.11. *Tafel plot of the steady state current density in 50 mM KP_i buffer solution containing 1 M KNO_3 as electrolyte at pH = 7. Calculated slope = 88 mV $decade^{-1}$.*

UNIVERSITAT ROVIRA I VIRGILI
NOVEL MOLECULAR CATALYSTS FOR WATER OXIDATION: TOWARDS ARTIFICIAL PHOTOSYNTHESIS
Sara Goberna Ferrón
Dipòsit Legal: T.189-2014

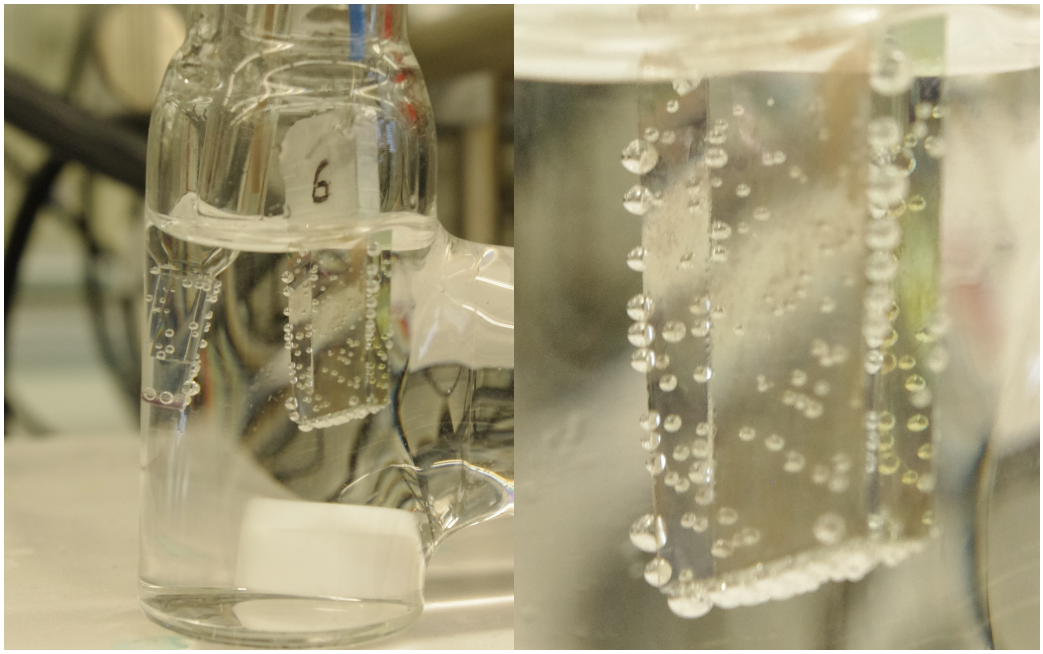

Figure 4.12. ***Left:*** *Picture of an anode compartment in a typical experiment applying a constant potential of 1.4 V with CoHCF modified FTO electrode.* ***Right:*** *Detail of the CoHCF modified FTO electrode covered by gas bubbles.*

The lower limit catalytic rates for these CoHCF modified electrodes can be estimated by using the surface coverage (Γ_0) of the electrodes following equation 4.2.

$$TOF = \frac{Q}{4t\Gamma_0} \qquad \text{(Eq. 4.2)}$$

Where Q = integrated charge througha CoHCF modified FTO (C cm^{-2}), t = time (s), Γ_0 = surface concentration (mol cm^{-2}) and 4 corresponds to the e^- needed to oxidize water into O_2.

This is an upper limit to the real number of catalytic sites, since heterogeneous catalysis should occur only on the surface of the crystallites, whereas the bulk material is electroactive. With the coverage numbers applied to the linear Tafel region, the turnover frequency (TOF) shows values between 2×10^{-3} s^{-1} at **η** = 300 mV and 0.5 s^{-1} at **η** = 550 mV (Figure 4.13).

UNIVERSITAT ROVIRA I VIRGILI
NOVEL MOLECULAR CATALYSTS FOR WATER OXIDATION: TOWARDS ARTIFICIAL PHOTOSYNTHESIS
Sara Goberna Ferrón
Dipòsit Legal: T.189-2014

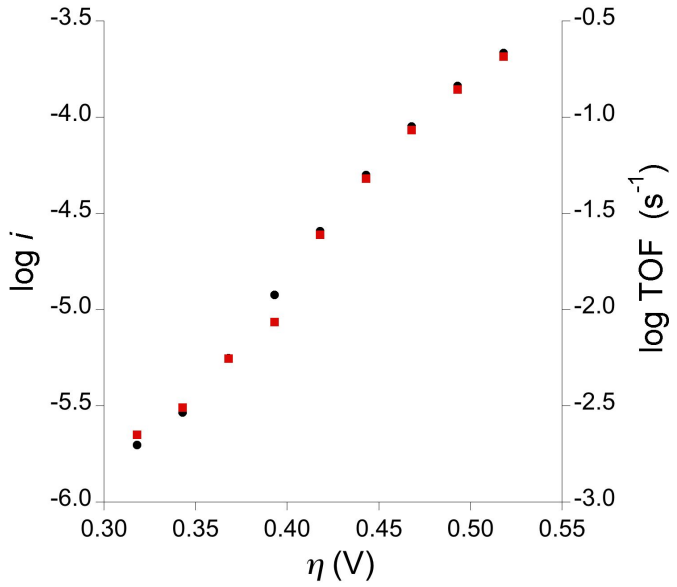

Figure 4.13. *Estimated TOF in the Tafel region at neutral pH (50 mM KP_i buffer solution containing 1 M KNO_3 as electrolyte).*

Catalytic bulk water electrolysis

In order to characterize the stability of the CoHCF modified FTO electrodes we test them for long–term bulk water electrolysis experiments. These measurements were carried out under a constant applied potential of 1.4 V in the same experimental conditions described before (Figure 4.14, left). After a short induction period due to capacitance, the current reaches a more stable state after 1 hour. The induction period is not related to any decomposition or change in the films. Indeed, if the electrolysis is stopped and started again, the same spike appears in multiple cycles (Figure 4.14, right).

UNIVERSITAT ROVIRA I VIRGILI
NOVEL MOLECULAR CATALYSTS FOR WATER OXIDATION: TOWARDS ARTIFICIAL PHOTOSYNTHESIS
Sara Goberna Ferrón
Dipòsit Legal: T.189-2014

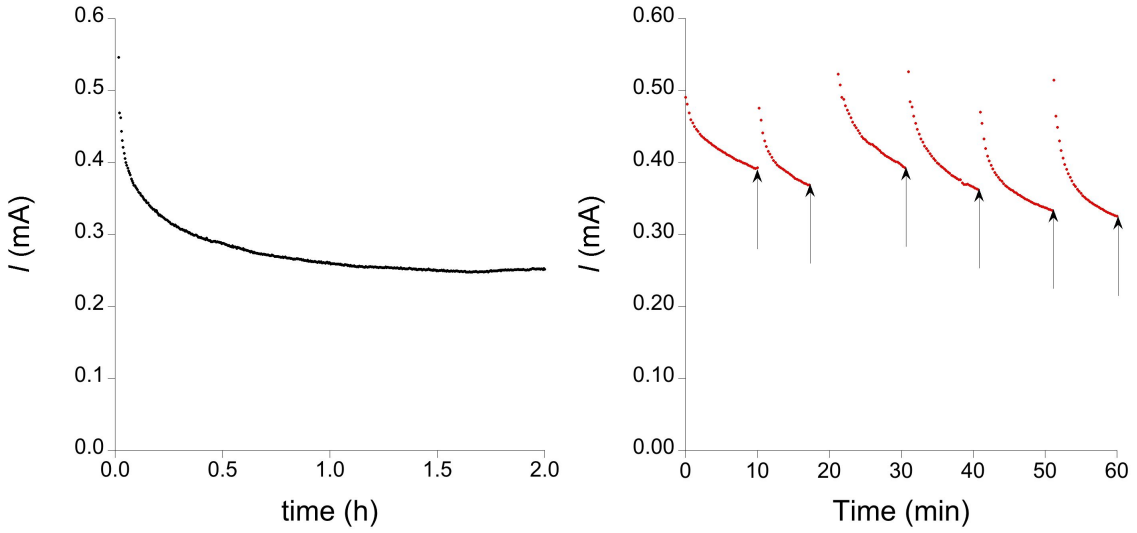

Figure 4.14. ***Left:*** *Current profile during bulk electrolysis at constant voltage = 1.4 V of a CoHCF modified FTO electrode in 50 mM KP_i buffer solution containing 1 M KNO_3 as electrolyte at pH = 7.* ***Right:*** *Successive bulk water electrolysis in the same conditions, the arrows indicate when the circuit was open to re−start the electrolytic current. This plot shows the consistent current and initial spike of current density. Pt mesh counter electrode and Ag/AgCl (NaCl 3 M) reference electrode. Potentials reported vs NHE.*

The stability of the catalytic process is remarkable. Continuous long−term water electrolysis was performed for days (Figure 4.15). Taking the current after one hour as initial value, to avoid the capacitance contribution at very short times, current (*I)* decreases slowly to reach a stable regime at 35−40% of the initial catalytic current after one day. This deactivation only occurs in brand new electrodes. Although some catalyst deterioration might occur, this decrease in activity after very long periods of time can be attributed to the mechanical loss of poorly attached crystallites, changes in pH (the solution pH decreases below 6 during long electrolysis), and to the gas bubbles that accumulate on the surface. Catalytic deactivation or poisoning would be a non-stop monotonic process, and it should continue at a constant pace through the active life of the catalyst. However, the stable catalytic current persists in the long term, without any further sign of deterioration. When electrolysis is stopped after 92 hours, and the same modified electrode is used for a second bulk electrolysis in a new buffer solution, the initial activity after 1 hour corresponds to 48 % of the original

UNIVERSITAT ROVIRA I VIRGILI
NOVEL MOLECULAR CATALYSTS FOR WATER OXIDATION: TOWARDS ARTIFICIAL PHOTOSYNTHESIS
Sara Goberna Ferrón
Dipòsit Legal: T.189-2014

value. Successive electrolysis in new buffer solutions reach consistent stable currents right after capacitance (Figure 4.15), and *I* follows a very slow deactivation rate of < 3% per day.

Regarding turnover frequency values, the data is in good agreement with the data obtained from the previously described Tafel plot experiments (0.5 s^{-1} at **η** = 550 mV). For bulk electrolysis at η = 590 mV, catalytic water oxidation rates up to TOF = 0.5 s^{-1} were observed in a 2−hour electrolysis (averaged for the 2 hours electrolysis), yielding a total turnover number of TON ≈ 3600. In 12−hour bulk electrolyses, TOF values about 0.30 s^{-1} were found, for a total TON ≈ 13000. Remarkably, in the 120−hours electrolysis previously described, over 70000 TON were produced. Usually, TON is reported at the time the catalyst is deactivated, but at this point CoHCF was still active, retaining a stable TOF of 0.15 s^{-1} after 5 days of continuous performance. The number of redox active sites on the modified electrode after this long catalytic cycle were calculate again, and it was found that Γ_0 decreases about one order of magnitude, but its activity accounts for 1/3 of the initial TOF. The final and robust TOF estimated after 5 days according to the final coverage (Γ = 0.30±0.06 nmol cm^{-2}) corresponds with TOF = 0.7 s^{-1} (> 2500 h^{-1}).

It is remarkable to note that consistent Tafel plots were found for the same modified electrodes before and after 12−hours bulk electrolysis experiments (Figure 4.16). This is an additional evidence of the robustness of the catalytic process.

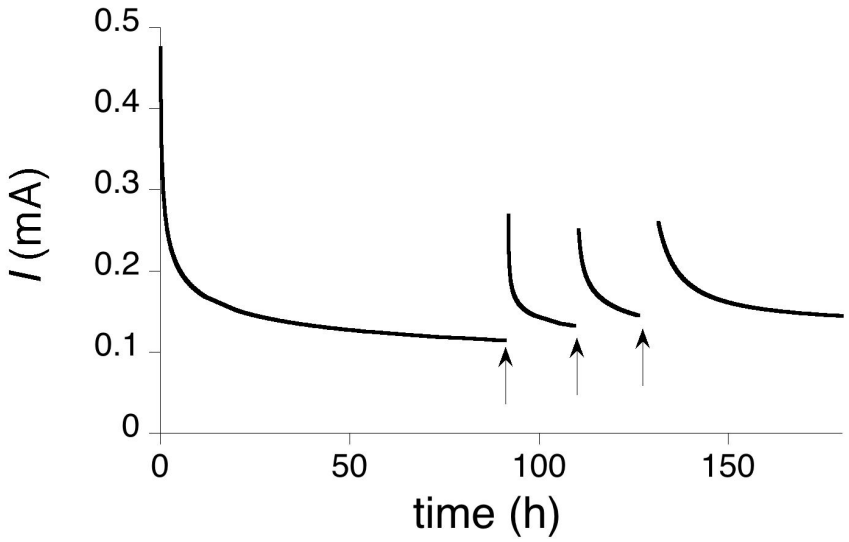

Figure 4.15. *Current profile during 1 week–bulk water electrolysis at 1.4 V of a CoHCF modified FTO electrode in 50 mM KP_i buffer solution containing 1 M KNO_3 as electrolyte at pH = 7. The arrows indicate the moment when electrolysis was stopped and the electrode changed to a new buffer solution. Pt mesh counter electrode and Ag/AgCl (NaCl 3 M) reference electrode. Potentials reported vs NHE.*

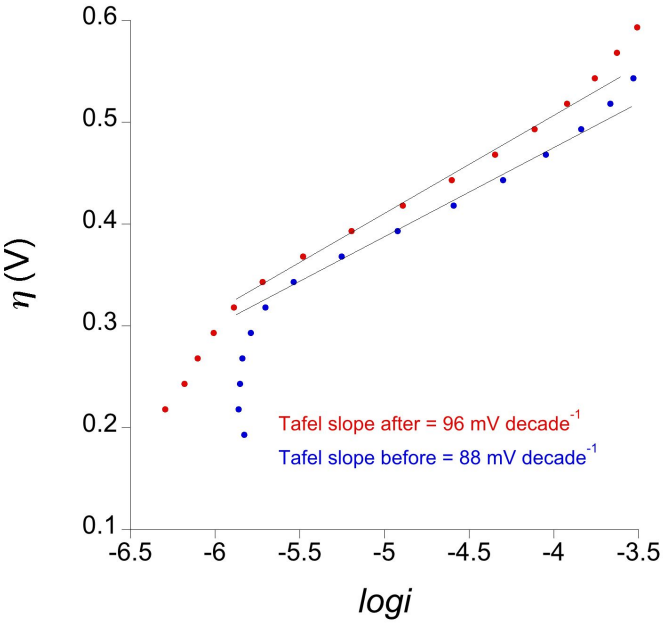

Figure 4.16. *Tafel plot of the steady state current density in 50 mM KP_i buffer solution containing 1 M KNO_3 as electrolyte at pH = 7, before (red) and after (blue) 12*

UNIVERSITAT ROVIRA I VIRGILI
NOVEL MOLECULAR CATALYSTS FOR WATER OXIDATION: TOWARDS ARTIFICIAL PHOTOSYNTHESIS
Sara Goberna Ferrón
Dipòsit Legal: T.189-2014

hours–bulk water electrolysis at constant voltage = 1.4V.

Oxygen evolution was monitored and quantified with a fluorescence probe during bulk water electrolysis experiments at constant applied potential of 1.41 V. The efficiency of the process is quantitative. O_2 evolution matches the theoretical amount calculated from Faraday's law (Figure 4.17, left) for a $4e^-$ redox process. This confirms that no competing redox reactions are taking place, and that *I* is quantitative for oxygen production. The gas content in the gas space was also analyzed by mass spectroscopy. Oxygen was the only component increasing its content during electrolysis. No traces of CO_2 or any other small molecule was found (Figure 4.17, right).

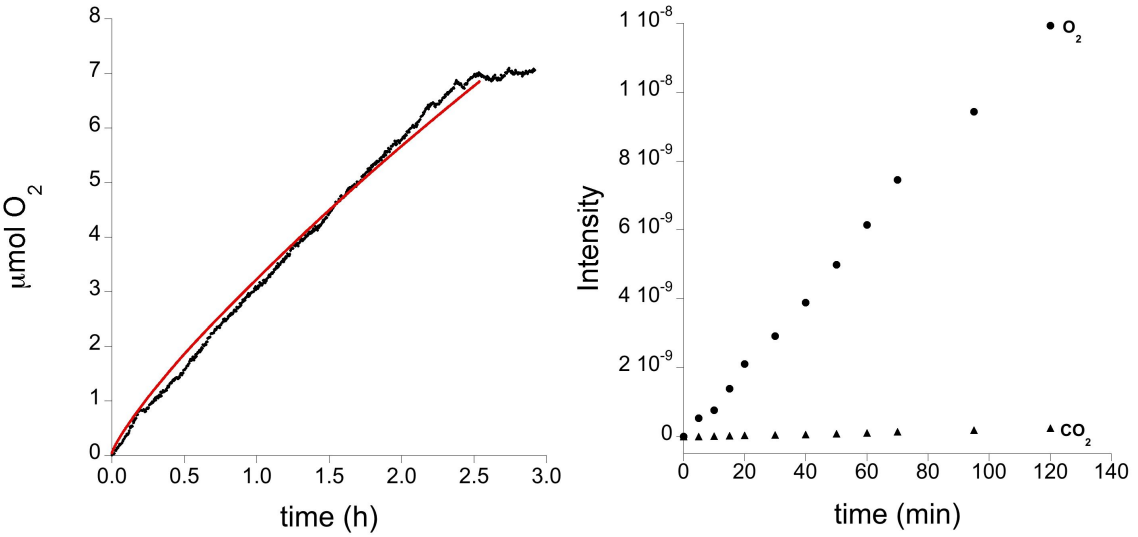

Figure 4.17. ***Left:*** *Catalytic O_2 evolution (black) during bulk electrolysis at 1.4 V of a CoHCF modified FTO electrode in 50 mM KP_i buffer solution containing 1 M KNO_3 as electrolyte at pH = 7, and theoretical O_2 assuming Faradaic behavior (red).* ***Right:*** *Mass spectra of O_2 (m/z=32) and CO_2 (m/z=44) obtained in the same reaction conditions.*

Stability of the CoHCF modified electrodes

The stability of the CoHCF films has also been confirmed by characterization of the electrodes after water oxidation experiments. After bulk water electrolysis, the

UNIVERSITAT ROVIRA I VIRGILI
NOVEL MOLECULAR CATALYSTS FOR WATER OXIDATION: TOWARDS ARTIFICIAL PHOTOSYNTHESIS
Sara Goberna Ferrón
Dipòsit Legal: T.189-2014

CoHCF electrodes have lower density of crystallites, which now show rounded edges. EDX analysis indicates that the Fe/Co ratio remains unchanged, and no traces of phosphate appear (Figure. 4.18). CoO_x films incorporate phosphate from solution during water oxidation, in a self–repairing process.[14] Therefore, the absence of a P absorbance peak is another experimental evidence of no oxide participation. The X-ray powder diffraction pattern shows good crystallinity and only two small differences. The diffraction peaks are displaced to higher angles, leading to a smaller unit cell a = 9.90±0.05 Å, and the reflection (220) has decreased its relative intensity (Figure 4.19). Both can be attributed to the oxidation of CoHCF. Co^{III} centers possess smaller radii, and their presence requires the loss of interstitial potassium cations, that scatter in phase with the reflection (220).[20] In its oxidized state, the electrodes show purple color (Figure 4.20), and the IR spectra shows two bands in the cyanide stretch region (Figure 4.21) at 2076 cm^{-1} and 2125 cm^{-1}, the latter assigned to the Fe^{II}–CN–Co^{III} bridge.[21] The original color is recovered by reduction at derivatization potential, and the oxidized or reduced forms exhibit the same catalytic performance.

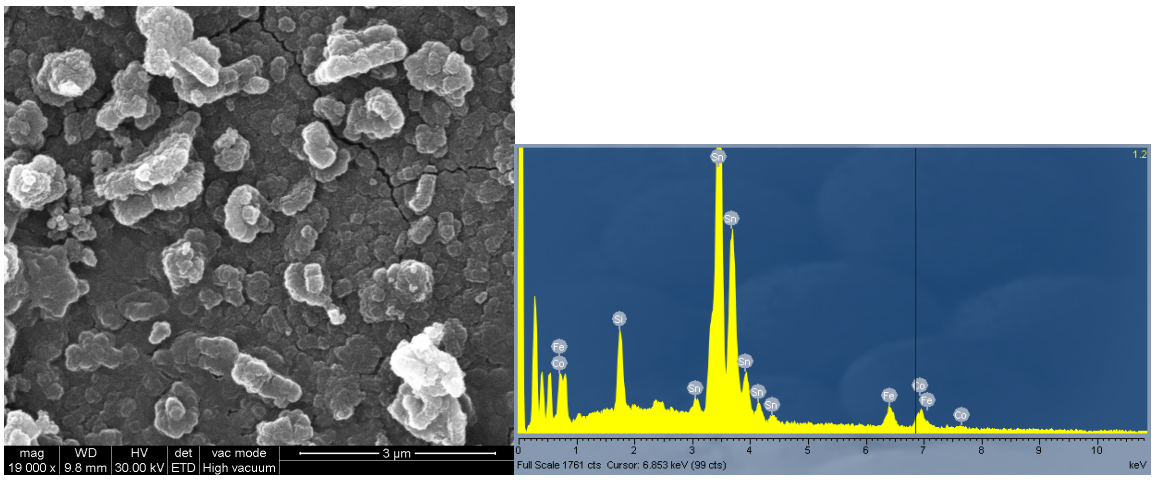

Figure 4.18. SEM image and EDX analysis of "*as used*" CoHCF grown on a FTO electrode after 12 hours–bulk electrolysis.

UNIVERSITAT ROVIRA I VIRGILI
NOVEL MOLECULAR CATALYSTS FOR WATER OXIDATION: TOWARDS ARTIFICIAL PHOTOSYNTHESIS
Sara Goberna Ferrón
Dipòsit Legal: T.189-2014

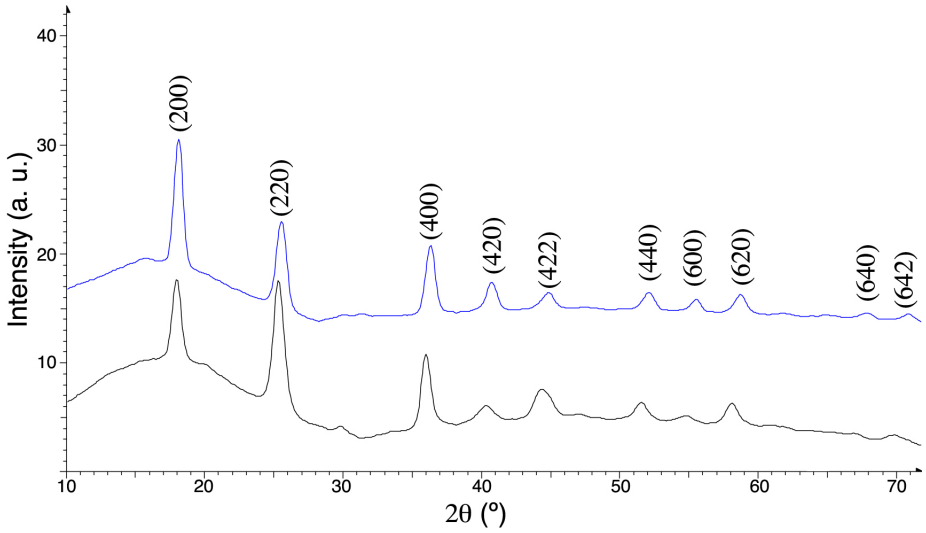

Figure 4.19. X−ray diffraction pattern for crystallites from a CoHCF modified FTO electrode before (black) and after (blue) 5 hours−bulk water electrolysis.

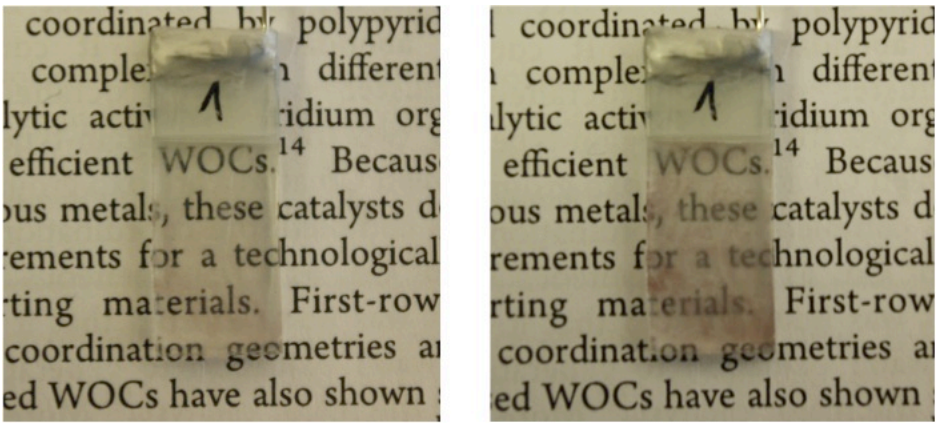

Figure 4.20. Picture of a CoHCF modified electrode before (left) and after (right) 1 day−bull water electrolysis.

UNIVERSITAT ROVIRA I VIRGILI
NOVEL MOLECULAR CATALYSTS FOR WATER OXIDATION: TOWARDS ARTIFICIAL PHOTOSYNTHESIS
Sara Goberna Ferrón
Dipòsit Legal: T.189-2014

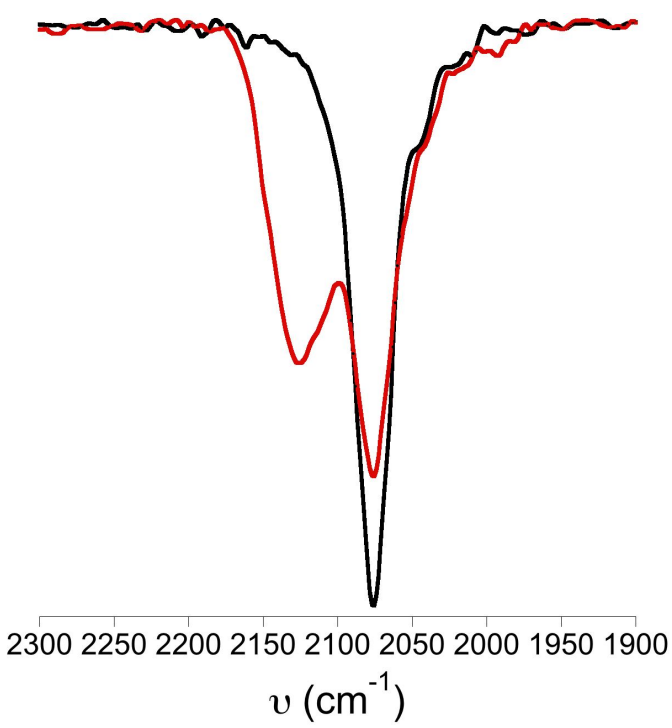

Figure 4.21. IR spectra of CoHCF grown on a FTO electrode, before (black) and after (red) 12 hours–bulk electrolysis.

CoHCF modified electrodes exhibits the stability advantages of heterogeneous catalysts with the tunability and other advantages of homogeneous catalysts, as well as being transparent, low density and stable at neutral pH and room temperature. All these features make Prussian blue analogous promising WOCs. For this reason, it is interesting to test the catalytic activity of other Prussian blue analogous compounds and compare it with CoHCF. For this purpose, the bulk compounds were synthetized and the catalytic activity was tested in a photo–induced water oxidation system. Bulk synthesis is easier than electrodeposition, and light–driven water oxidation is a good approach in order to compare O_2 evolution catalyzed by different WOCs.

Effect of pH and buffer on catalytic activity

An important variable in electrochemical water oxidation is pH. As described in equation 4.3, the water oxidation potential is pH–dependent.

UNIVERSITAT ROVIRA I VIRGILI
NOVEL MOLECULAR CATALYSTS FOR WATER OXIDATION: TOWARDS ARTIFICIAL PHOTOSYNTHESIS
Sara Goberna Ferrón
Dipòsit Legal: T.189-2014

$E = +1.23 – 0.059(pH)$ V vs (NHE) at 25°C (Eq. 4.3)

The effect of pH on the activity of CoHCF was examined. The catalyst film was introduced into a KP_i buffered solution, oxidation potential was held constant at 1.4 V and the pH of the solution was increased from 4 to 10 (Figure 4.22, left). Current density showed a sinusoidal dependence with little variations below pH 5 and then a rapid and continuous increase reaching maximum values at pH 9, probably due to decomposition and / or detachment of the CoHCF film. The difference between minimum and maximum is of one order of magnitude. Identical behaviour was found using NaP_i buffer instead of KP_i. It is known that Na^+ is easily transported in and out the CoHCF.[11] Cation exchange of K^+ by Na^+ occurs in NaP_i buffer, but no differences in the pH–dependence were found. A similar trend was observed using sodium borate (NaB) buffer (Figure 4.22, right). In this case, the current density increases from pH 5 to pH 10 less rapidly and a maximum is observed at pH 10, where it starts to stabilize.

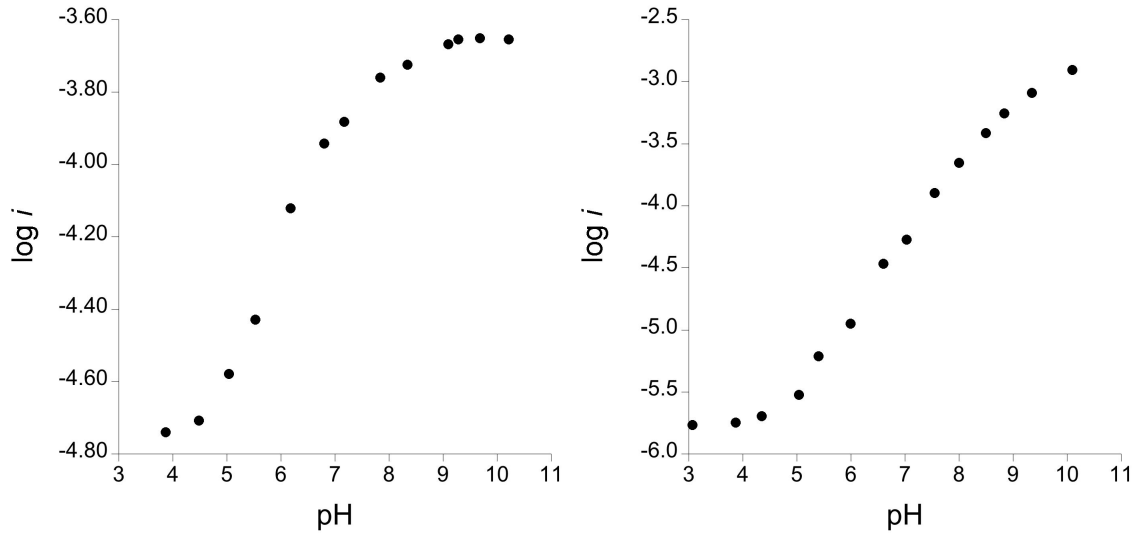

Figure 4.22. *Dependence of current density vs pH in bulk water electrolysis with a CoHCF modified FTO electrode at 1.4 V in 50 mM KP_i buffer solution containing 1 M KNO_3 as electrolyte (**left**) and 50 mM NaBorate buffer solution containing 1 M $NaNO_3$ as electrolyte (**right**).*

UNIVERSITAT ROVIRA I VIRGILI
NOVEL MOLECULAR CATALYSTS FOR WATER OXIDATION: TOWARDS ARTIFICIAL PHOTOSYNTHESIS
Sara Goberna Ferrón
Dipòsit Legal: T.189-2014

Comparison between CoHCF and Cobalt Oxides

Some comparisons between the activity of CoHCF and cobalt oxides,[25] arguably the best heterogeneous WOCs reported to date, can be derived. A TOF = 2.6 × 10^{-3} s^{-1} was reported for a cobalt oxide film at pH 7 and η = 410 mV. CoHCF catalyst exhibits already the same TOF at just η = 305 mV. Of course, this comparison is quite rough because of the very different morphology of the films. In both cases TOF is referred to bulk content, and a different surface to bulk ratio would significantly affect the results. Still, our data shows that CoHCF is at least competitive in kinetic terms with respect to the oxide counterparts. However, the reported maximum current densities for oxides are higher. We rationalize this because of the higher surface coverage. CoO_x films reach 1 mA cm^{-2} just above 410 mV, but with loadings in the μmol cm^{-2} range. Whereas Γ is below 0.5 nmol in the CoHCF films. We can estimate that 1 mA would be reached at just 400 mV overpotential with CoHCF coverages about 2.5 nmol cm. The strong dependence of the Tafel slope with pH is also a very special feature of CoHCF. In the case of oxides, Tafel slope is consistent above pH 5.5.[24] The linear increase of current with pH is also very distinct. There is a different slope in the linear region (1 vs 0.5) and oxides deviate from linearity above pH = 8, whereas the current density keeps increasing up to pH = 14 for CoHCF. Such high current densities found in alkali media cannot be yielded by traces of an oxide[25], since oxides need much higher surface coverage to reach analogous activity. The participation of any adventitious cobalt oxide on the CoHCF modified electrodes can be ruled out according to several experimental evidences. The films exhibit all the expected features of a Prussian blue material, including spectroscopic and crystallographic data. Cobalt oxide cannot form at the derivatization potential, since a higher potential is needed for Co oxide formation.[25] No metallic cobalt remains on the electrode after derivatization, as confirmed by cyclic and differential pulse

UNIVERSITAT ROVIRA I VIRGILI
NOVEL MOLECULAR CATALYSTS FOR WATER OXIDATION: TOWARDS ARTIFICIAL PHOTOSYNTHESIS
Sara Goberna Ferrón
Dipòsit Legal: T.189-2014

voltammetry. Current intensity does not increase during water electrolysis, and this also discards the in situ hypothetical formation of a more active catalyst.[26] The distinct Tafel slope of CoHCF when compared with Co oxides also suggests a different catalytic mechanism. And the apparently faster catalytic activity found for CoHCF indicates that major oxide contamination would be needed to match these results, and this is inconsistent with all the structural, spectroscopic and electrochemical data. Therefore, the participation of any adventitious cobalt oxide on the CoHCF modified electrodes is discarded and, besides, CoHCF catalytic activity is comparable with the state−of−the art metal oxide catalysts.

UNIVERSITAT ROVIRA I VIRGILI
NOVEL MOLECULAR CATALYSTS FOR WATER OXIDATION: TOWARDS ARTIFICIAL PHOTOSYNTHESIS
Sara Goberna Ferrón
Dipòsit Legal: T.189-2014

UNIVERSITAT ROVIRA I VIRGILI
NOVEL MOLECULAR CATALYSTS FOR WATER OXIDATION: TOWARDS ARTIFICIAL PHOTOSYNTHESIS
Sara Goberna Ferrón
Dipòsit Legal: T.189-2014

4.2.2 Photo–Induced Water Oxidation with Prussian Blue (PB) type WOCs.

In photo–induced water oxidation, the electron scavenging is a photochemically generated oxidant that oxidizes water in the presence of a catalyst (Equations 4.4–4.7 and Figure 4.23). In a heterogeneous photo–induced system using $Ru(bpy)_3^{2+}$ as the photosensitizer and $S_2O_8^{2-}$ as sacrificial acceptor, the oxidation of water to O_2 is produced at the surface of colloidal / bulk particles of the catalysts.

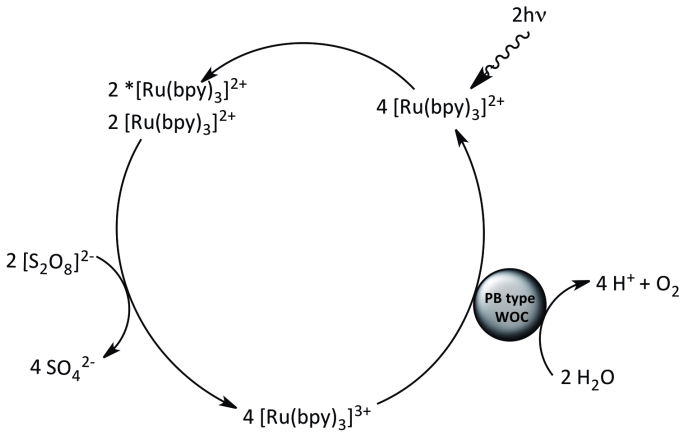

Figure 4.23. *Schematic representation of the photo–induced oxidation of water*

$Ru(bpy)_3^{2+} + h\nu \rightarrow {}^*Ru(bpy)_3^{2+}$ (Eq. 4.4)

$^*Ru(bpy)_3^{2+} + S_2O_8^{2-} \rightarrow Ru(bpy)_3^{3+} + SO_4^{2-} + SO_4^{-\bullet}$ (Eq. 4.5)

$Ru(bpy)_3^{2+} + SO_4^{-\bullet} \rightarrow Ru(bpy)_3^{3+} + SO_4^{2-}$ (Eq. 4.6)

$Ru(bpy)_3^{3+} + 2H_2O + \text{catalyst} \rightarrow 4\,Ru(bpy)_3^{2+} + 4H^+ + O_2$ (Eq. 4.7)

UNIVERSITAT ROVIRA I VIRGILI
NOVEL MOLECULAR CATALYSTS FOR WATER OXIDATION: TOWARDS ARTIFICIAL PHOTOSYNTHESIS
Sara Goberna Ferrón
Dipòsit Legal: T.189-2014

Photo–induced catalytic water oxidation with CoHCF

Given the results of CoHCF as electrocatalyst for water oxidation when deposited on a FTO electrode, the study of the catalytic activity of CoHCF in a heterogeneous photo–induced system has been investigated following the same procedure described in section 3.3.3. Bulk CoHCF was synthetized by precipitation following the method described by Berrettoni et al.[27] (see details and characterization in section 4.4 Experimental).

The time evolution of molecular oxygen production occurring in a 12.5 mL containing $[Ru(bpy)_3]^{2+}$ (1.0 mM) , sodium persulfate (5.0 mM) and 10 mg of CoHCF, at pH = 7 in 40 mM potassium phosphate (KP_i) buffer upon light irradiation ($\lambda > 400$ nm) was monitored using a fluorescence probe (Figure 4.24), oxygen evolution reaches values of 7 µmol of O_2 in 1.5 hours. As a control experiment, the same procedure was repeated with 10 mg of Co_3O_4 oxide (cubic phase from Sigma-Aldrich, nanopowder S_{BET} 40-70 m^2/g) (Figure 4.24), in this case the oxygen generation only reaches 5 µmol of O_2. When the comparison is made in terms of turnover frequency values, the difference is clear: The TOF per number of cobalt atoms calculated for CoHCF is one order of magnitude bigger than the calculated for Co_3O_4 oxide (3.0×10^{-4} s^{-1} and 4.2×10^{-5} s^{-1}, respectively)

UNIVERSITAT ROVIRA I VIRGILI
NOVEL MOLECULAR CATALYSTS FOR WATER OXIDATION: TOWARDS ARTIFICIAL PHOTOSYNTHESIS
Sara Goberna Ferrón
Dipòsit Legal: T.189-2014

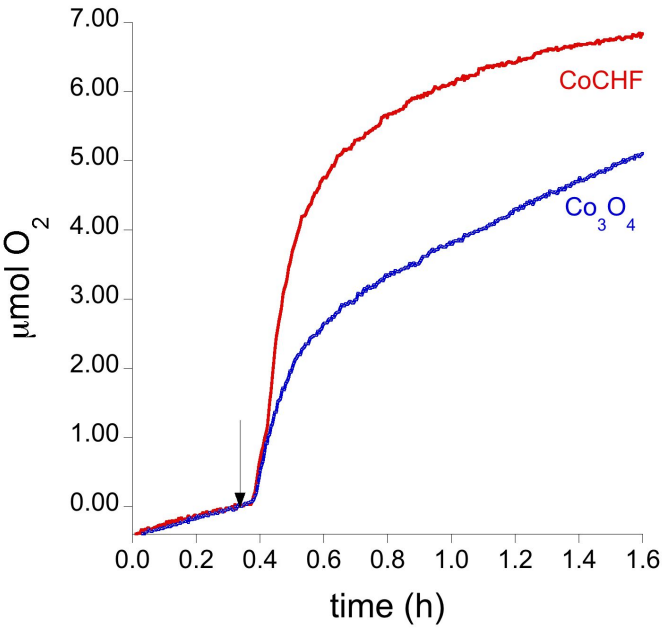

Figure 4.24. *Kinetics of O_2 formation upon light irradiation (λ > 400 nm) to the reaction solution containing 1 mM $[Ru(bpy)_3]^{2+}$, 5 mM $[S_2O_8]^{2-}$ and 10 mg of CoHCF (red line) or 10 mg of Co_3O_4 (blue line), at pH = 7 in 40 mM KP_i buffer. The arrow indicates when the light was turned on.*

Analogous and independent experiments were performed with reaction solutions without each of the key components of the photocalytic system (catalysts, $Ru(bpy)_3^{2+}$, light, persultafe) yielding no oxygen evolution. From these results the catalytic activity towards water oxidation of CoHCF is corroborated in a heterogeneous light–induced system.

We also optimized the reaction conditions regarding the relative reagents concentration: $[Ru(bpy)_3]^{2+}$, $S_2O_8^{2-}$ and CoHCFe (Table 4.2 and Figure 4.28). The parametric study was performed modifying the selected variable while maintaining the others constant. The reaction rate (TOF) strongly depends on the Co / Ru ratio employed (Figure 4.28, top). The lower the CoHCFe catalyst / $[Ru(bpy)_3]^{2+}$ ratio used, the higher the TOF value obtained. These results points out the relevance of the contact catalyst–sensitizer as the rate–determining step during the 4-e^- water

UNIVERSITAT ROVIRA I VIRGILI
NOVEL MOLECULAR CATALYSTS FOR WATER OXIDATION: TOWARDS ARTIFICIAL PHOTOSYNTHESIS
Sara Goberna Ferrón
Dipòsit Legal: T.189-2014

oxidation process. Further studies should be addressed in order to maximize the contact catalyst–sensitizer and / or improves the diffusion of the Ru complex to the catalyst's active places. On the other hand, the increment of the persulfate concentration in the reaction media also enhances the reaction rate of oxygen evolution (Figure 4.28, bottom). Nevertheless, with the reaction conditions used in these experiments, such positive effect reaches a maximum with a concentration of 7.5 mM $S_2O_8^{2-}$. In this case is the $[Ru(bpy)_3]^{2+}$ is limiting the reaction step previously described by the equation 4.5.

CoHCF (mg)	**$[Ru(bpy)_3]^{2+}$ (mM)**	**$S_2O_8^{2-}$ (mM)**	**TOF (s^{-1})***
0.0	1.0	5.0	-
10.0	1.0	0.0	-
10.0	0.0	5.0	-
5.0	1.0	5.0	5.5×10^{-4}
10.0	"	"	3.0×10^{-4}
15.0	"	"	2.0×10^{-4}
20.0	"	"	4.0×10^{-5}
10.0	0.5	5.0	1.8×10^{-4}
"	1.5	"	3.6×10^{-4}
"	2.0	"	4.1×10^{-4}
10.0	1.0	2.5	8.3×10^{-5}
"	"	7.5	4.8×10^{-4}
"	"	10.0	3.7×10^{-4}

Table 4.2. *TOF values calculated from O_2 formation upon light irradiation (λ > 400 nm) to the reaction solution containing different $[Ru(bpy)_3]^{2+}$ / $[S_2O_8]^{2-}$ / CoHCF ratios, at pH 7 in 40 mM KP_i buffer. TOF calculated from the slope in the very initial O_2 evolution kinetics and expressed per moles of cobalt.*

UNIVERSITAT ROVIRA I VIRGILI
NOVEL MOLECULAR CATALYSTS FOR WATER OXIDATION: TOWARDS ARTIFICIAL PHOTOSYNTHESIS
Sara Goberna Ferrón
Dipòsit Legal: T.189-2014

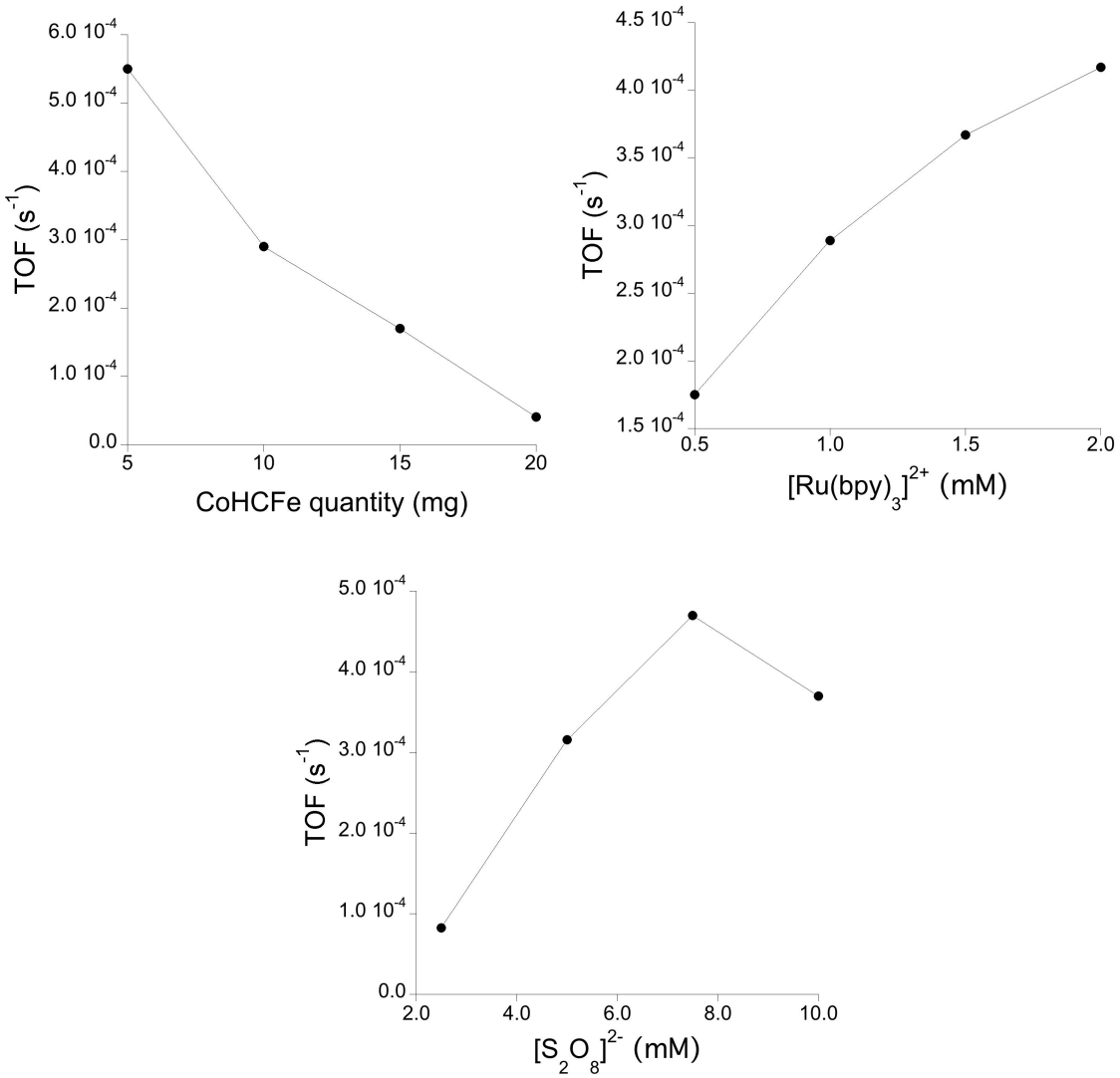

Figure 4.28. *TOF values calculated from O_2 formation upon light irradiation (λ > 400 nm) to the reaction solution at pH 7 in 40 mM KP_i buffer containing:* ***Top left****: 1 mM $[Ru(bpy)_3]^{2+}$, 5 mM $[S_2O_8]^{2-}$ and different quantities of CoHCF.* ***Top right****: 5 mM $[S_2O_8]^{2-}$, 10 mg of CoHCF and different concentrations of $[Ru(bpy)_3]^{2+}$ and* ***Bottom****: 1 mM $[Ru(bpy)_3]^{2+}$, 10 mg of CoHCF and different concentrations of $[S_2O_8]^{2-}$. TOF calculated from the slope in the very initial O_2 evolution kinetics and expressed per moles of cobalt.*

UNIVERSITAT ROVIRA I VIRGILI
NOVEL MOLECULAR CATALYSTS FOR WATER OXIDATION: TOWARDS ARTIFICIAL PHOTOSYNTHESIS
Sara Goberna Ferrón
Dipòsit Legal: T.189-2014

Stability of CoHCF in Photo–induced Water Oxidation Conditions

Although the stability of CoHCF under electrochemical conditions has been demonstrated in the previous section. The distinct conditions in the light–induced water oxidation require additional catalyst stability experiments. In order to determine if the catalyst is being decomposed or deactivated during photo–induced water oxidation reaction, a second water oxidation is performed by adding an extra amount of $S_2O_8^{2-}$ in the same reaction solution after three hours reaction. After that, the system was again purged with N_2 until baseline stabilization and then, the light–induced reaction was re–started to complete a second cycle reaction with the same CoHCF catalyst (Figure 4.29). The kinetics of O_2 evolution using CoHCF after one use showed very similar kinetics, the TOF value calculated during the first cycle corresponds to 4.6 x 10^{-4} s^{-1}. Nevertheless, after renovation of the persulfate concentration and re–starting the second cycle, the TOF was slightly affected, reaching a value of 1.9 x 10^{-4} s^{-1}, suggesting that the catalyst remains active and is stable under these photochemical conditions. Instead of decomposition of the catalyst, the most likely scenario is that the photosensitizer decomposition in neutral or basic conditions, which depends on pH and buffer nature[28] (Equation 4.8) competes with electron transfer from the catalyst (Equation 4.7), and a significant decomposition of the photosensitizer will reduce the efficiency.

$Ru(bpy)_3^{3+}$ + nucleophiles (*i.e.*, OH^-) → decomposition products (Eq. 4.8)

It has been reported that turnover numbers and decomposition of the sensitizer under light–induced conditions are strongly dependent on the pH and composition of the buffers. Na_2SiF_6–based buffers are supposed to improve TON and increase the lifetime of the photosensitizer. However, no catalytic activity was observed using Na_2SiF_6–based buffer. Additional experiments regarding the effect of buffer nature,

UNIVERSITAT ROVIRA I VIRGILI
NOVEL MOLECULAR CATALYSTS FOR WATER OXIDATION: TOWARDS ARTIFICIAL PHOTOSYNTHESIS
Sara Goberna Ferrón
Dipòsit Legal: T.189-2014

concentration and pH should be considered. Furthermore, it would be interesting to characterize the catalyst after the water oxidation reaction and study the possibility of catalyst recovery.

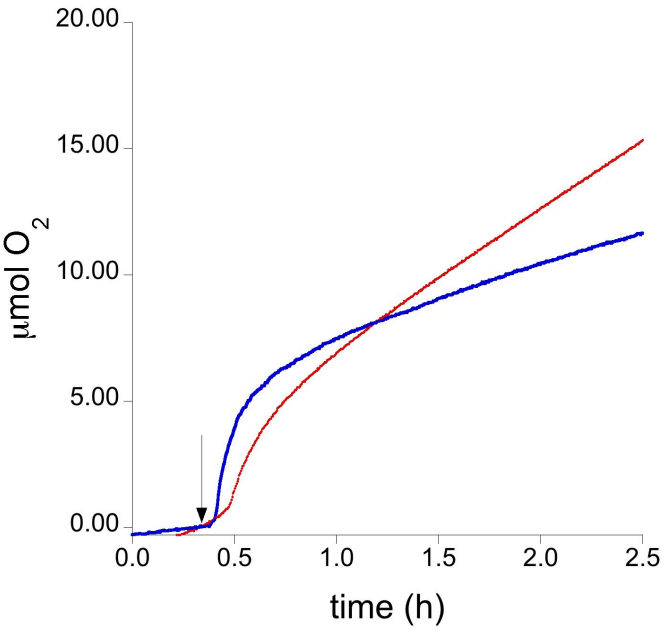

Figure 4.29. *Kinetics of O_2 formation of the first run (blue line) and the second run (red line) upon light irradiation (λ > 400 nm) to the reaction solution containing 2 mM $[Ru(bpy)_3]^{2+}$, 7.5 mM $[S_2O_8]^{2-}$ and 10 mg of catalyst, at pH 7 in 40 mM KP_i buffer. After the completion of the first run, 7.5 mM of $[S_2O_8]^{2-}$ was added to the reaction solution.*

Thus, Co-based PB analogs (N−coordinated Co^{2+} ions) are active and stable catalysts for water oxidation under light-driven conditions. In addition, the possibility to synthetize these materials by electrodeposition on the surface of electrodes, makes them attractive materials for electrochemical or photo−electrochemical water oxidation applications.

UNIVERSITAT ROVIRA I VIRGILI
NOVEL MOLECULAR CATALYSTS FOR WATER OXIDATION: TOWARDS ARTIFICIAL PHOTOSYNTHESIS
Sara Goberna Ferrón
Dipòsit Legal: T.189-2014

Other MHCM as water oxidation catalysts

After confirming the catalytic activity of CoHCF in heterogeneous photo−induced conditions, we decided to test the complete series of MHCM. In this case the materials do not need to be grown on an electrode, as required for electrocatalysis, and thus the rest of the series is easily accessible.

First we studied the series of hexacyaferrates, substituting the Co^{2+} center by other transition metals: $M_3[Fe(CN)_6]_2 \times H_2O$ (M = Mn, Fe, Ni and Cu). These complexes were synthetized following exactly the same procedure than for CoHCF substituting $CoCl_2$ by the corresponding metal chloride (see details and characterization in section 4.4 Experimental).

The same water oxidation experiments described above were performed using the different metal hexacyanoferrate (MHCF) compounds monitoring the O_2 generation (Figure 4.25). The Fe, Ni and Cu derivatives showed negligible catalytic activity. MnHCF shown significant oxygen evolution although much slower than CoHCF.

From these results, we concluded that cobalt was the best candidate of Prussian blue compounds as WOCs. The we studied the series of cobalt hexacyanometalates: $Co_3[M(CN)_6]_2 \times H_2O$ (M = Cr, Co).

The catalytic performance of CoHCCo and CoHCCr compounds was tested in the same conditions described above and compared with the activity of CoHCF (Figure 4.26). The very initial kinetics of the oxygen evolving reaction obtained with CoHCFe, CoHCCo and CoHCCr compounds after turning on light are very similar each other.

UNIVERSITAT ROVIRA I VIRGILI
NOVEL MOLECULAR CATALYSTS FOR WATER OXIDATION: TOWARDS ARTIFICIAL PHOTOSYNTHESIS
Sara Goberna Ferrón
Dipòsit Legal: T.189-2014

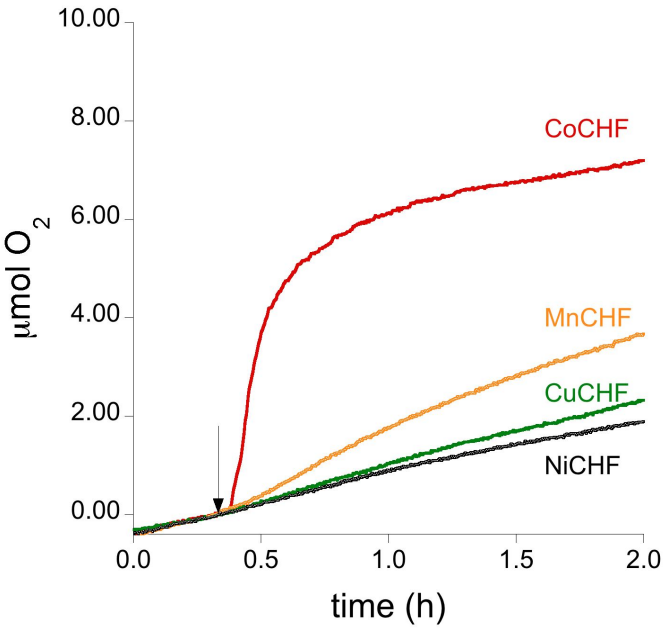

Figure 4.25. *Kinetics of O_2 formation upon light irradiation (λ > 400 nm) to the reaction solution containing 1 mM $[Ru(bpy)_3]^{2+}$, 5 mM $[S_2O_8]^{2-}$ and 10 mg of MHCF (M = Co, Cu, Mn and Ni), at pH 7 in 40 mM KP_i buffer. The arrow indicates when the light was turned on.*

Nevertheless, from the TOF values calculated, CoHCCo seems to be the most efficient one with a TOF above 5.3 x 10^{-4} s^{-1} compared to those obtained for CoHCFe and CoHCCr (3.0 x 10^{-4} s^{-1}, and 2.8 x 10^{-4} s^{-1}, respectively). Considering that these TOF values were calculated as a function of the numbers of Co moles N-coordinated (M-type cations in the general formula $M_3[M'(CN)_6]$, the TOF obtained for CoHCCo may have been overestimated. Then, considering the total number of Co moles in CoHCCo material, the new TOF calculated corresponds to 2.8 x 10^{-4} s^{-1}, which is very similar to the TOF values reported for the other cobalt–hexacyanometallates.

UNIVERSITAT ROVIRA I VIRGILI
NOVEL MOLECULAR CATALYSTS FOR WATER OXIDATION: TOWARDS ARTIFICIAL PHOTOSYNTHESIS
Sara Goberna Ferrón
Dipòsit Legal: T.189-2014

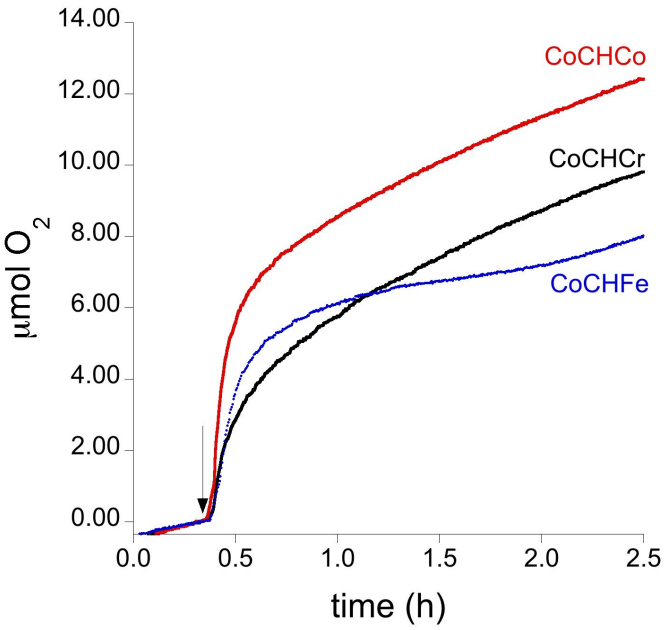

Figure 4.26. *Kinetics of O_2 formation upon light irradiation (λ > 400 nm) to the reaction solution containing 1 mM $[Ru(bpy)_3]^{2+}$, 5 mM $[S_2O_8]^{2-}$ and 10 mg of catalyst, at pH 7 in 40 mM KP_i buffer. The arrow indicates when the light was turned on.*

Thus, it is clear the beneficial effect of Co cations in Prussian blue type structures for the water oxidation reaction. However, the nature of the Co coordination (to occur through the N or C ions associated to the CN ligand) could be also important for the catalytic activity of these materials. In order to obtain additional insights about this specific topic, a supplementary MHCM was synthesized allowing an opposite metal-ligand coordination to that characteristic of the CoHCFe material (Co−C instead of Co−N). Thus, the Fe(II) hexacyanocobaltate (FeHCCo) was tested in the light-induced water oxidation reaction. This material resulted non−active for the water oxidation process under the reaction conditions employed in this work.

Considering these results, it seems that to get active catalysts for the oxygen evolution reaction by using Prussian blue (PB) type analogs, the Co coordination in the structure must occurs through the N atoms of the CN ligand. It means the presence of Co(II) species in a high spin configuration.

UNIVERSITAT ROVIRA I VIRGILI
NOVEL MOLECULAR CATALYSTS FOR WATER OXIDATION: TOWARDS ARTIFICIAL PHOTOSYNTHESIS
Sara Goberna Ferrón
Dipòsit Legal: T.189-2014

In a similar photo−induced system but using a colloidal $IrO_x.nH_2O$ as WOC, the rate-determining step in the process was reported to be the electron transfer between $[Ru(bpy)_3]^{3+}$ and surface Ir(IV) (see Equation 4.7), occurring with a second-order rate constant.[29] Therefore, the efficiency of the cobalt−based catalysts used in this work may be limited by the accessibility of the $[Ru(bpy)_3]^{3+}$ molecules to the Co−active sites in the materials structure. Although the establishment of a mechanism reaction by using the Co−based PB type complexes is far away from the aims of this thesis, a general mechanism where the Co(II) species in a high spin configuration can be oxidized by $Ru(bpy)_3^{3+}$, generating high-valence Co ions (Co^{III}/Co^{IV}) could be proposed. Then, these cobalt species could induce the water oxidation reaction to evolve O_2, re−changing into the Co(II) electronic state. As described before, these solids are characterized by a lacunary structure where the $[Fe(CN)_6]$ vacancies (in the case of the hexacyanoferrates) are filled by molecules of water, some of them directly coordinated to the Co(II) ions (Figure 4.27).[30] Thus, the cobalt−OH_2 coordinated units could be considers as a metal-oxo core where the H---O---H re−arrangements needed for the oxygen evolution reaction can take place in a similar way as described for Co-Pi catalysts.[25,31]

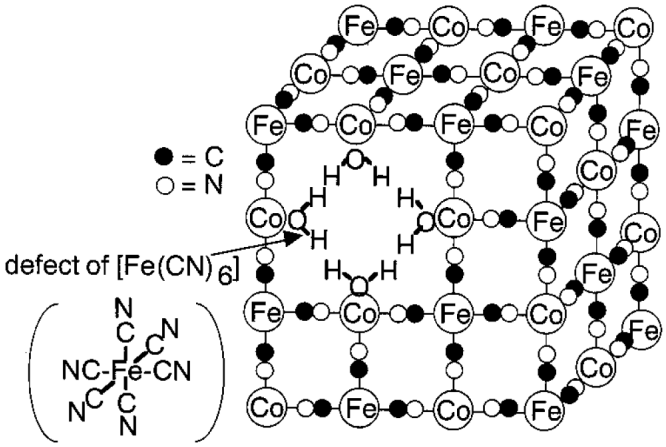

Figure 4.27. *Unit cell of cobalt-iron cyanide with a lacunary $[Fe(CN)_6]$ structure*.

UNIVERSITAT ROVIRA I VIRGILI
NOVEL MOLECULAR CATALYSTS FOR WATER OXIDATION: TOWARDS ARTIFICIAL PHOTOSYNTHESIS
Sara Goberna Ferrón
Dipòsit Legal: T.189-2014

UNIVERSITAT ROVIRA I VIRGILI
NOVEL MOLECULAR CATALYSTS FOR WATER OXIDATION: TOWARDS ARTIFICIAL PHOTOSYNTHESIS
Sara Goberna Ferrón
Dipòsit Legal: T.189-2014

4.3

Conclusions

Metallic hexacyanometallates represent a completely novel type of heterogeneous water oxidation catalysts and a new attractive area of research for artificial photosynthesis applications. Cobalt hexacyanoferrate matches most of the features of metal oxides: it is formed from Earth-abundant metal ions in aqueous solution, it is extremely robust in turnover conditions, it is fast enough to compete with state–of–the–art cobalt oxides, and it works at neutral pH and ambient conditions. CoHCF modified electrodes promote water oxidation for days, maintaining constant high rates at low overpotentials. At the same time, CoHCF modified electrodes offers additional advantages of molecule-based materials. Unlike oxides, thin films of CoHCF are transparent to visible light, of particular interest to be incorporated into photo anodes and light–harvesting devices. CoHCF can be prepared in aqueous solution from its molecular building blocks, offering unique processing versatility. It possesses a well-defined crystal structure that will help to understand the mechanism of the catalytic process. Although total current densities are low for the requirement technological targets, this should be overcome by increasing surface coverage, improving processing on more compatible electrodes surfaces or as amorphous films. All of this is currently under study in our group.

Photo–induced water oxidation allows demonstrating that the CoHCF bulk material is also active under photodriven conditions. Even having similar physicochemical properties, only the cobalt–based Prussian blue type compounds (Co ions N–coordinated) were active for water oxidation. These experiments allow to determinate which Prussian blue type catalysts are plausible to be studied in other strategies such as electrochemical or photoelectrochemical water oxidation systems.

UNIVERSITAT ROVIRA I VIRGILI
NOVEL MOLECULAR CATALYSTS FOR WATER OXIDATION: TOWARDS ARTIFICIAL PHOTOSYNTHESIS
Sara Goberna Ferrón
Dipòsit Legal: T.189-2014

These new type of WOCs meet most of the requirements demanded to be incorporated into a reliable photosynthetic system.

UNIVERSITAT ROVIRA I VIRGILI
NOVEL MOLECULAR CATALYSTS FOR WATER OXIDATION: TOWARDS ARTIFICIAL PHOTOSYNTHESIS
Sara Goberna Ferrón
Dipòsit Legal: T.189-2014

4.4

Experimental

4.4.1 Electrochemical Water Oxidation with CoHCF modified electrodes

Preparation of the CoHCF modified FTO electrodes

All chemicals were commercially available (> 99.9 %, Sigma-Aldrich) and were used without further purification. All solutions were prepared with Milli-Q water (typically 18.2 MΩ−cm resistivity). As fluorine-doped tin oxide coated glass slides (FTO) we used Pilkington NSG TEC 15A 2.2 mm slides with 12v14 Ω/sq surface resistivity, and 80.0−81.5 % transmittance. FTO slides were cleaned prior use by sonication for 10 minutes in basic soapy solution, deionized water and isopropanol, followed by annealing at 400 °C during 30 minutes. Electrodeposition was performed with a Biologic SP-150 potentiostat, a ALS Ag/AgCl (3.5 M KCl) reference electrode and a Pt mesh counter electrode. Potentials are reported vs NHE reference scale using **E**(NHE) = **E**(Ag/AgCl) + 0.209 V.

For the preparation of catalyst modified electrodes, 1 x 2.5 cm FTO electrodes were used as working electrodes, but only a surface of 1 x 1.5 cm was immersed in the solution. The first step was the platting of the electrode with metallic cobalt at constant voltage of –0.695 V with stirring in a KCl (0.1 M) water solution containing Co^{2+} ions (10 mM) during 1 minute. A dark covering was observed on the FTO surface as metallic cobalt is deposited. After deposition, the slides were sonicated for 15 seconds in deionized water. The second step, namely derivatization, was also carried out with a potentiostatic method by applying a constant voltage of +0.508 V with the

UNIVERSITAT ROVIRA I VIRGILI
NOVEL MOLECULAR CATALYSTS FOR WATER OXIDATION: TOWARDS ARTIFICIAL PHOTOSYNTHESIS
Sara Goberna Ferrón
Dipòsit Legal: T.189-2014

metallic cobalt-covered electrode immersed in a KCl 0.1 M water solution containing 10 mM $K_3[Fe(CN)_6]$. During this process, cobalt slowly dissolves under the oxidation potential to be trapped by the formation of the desired CoHCF. Derivatization time is usually 5 hours long. The time required is determined by the total charge used in the platting process. At least the same charge should pass through the electrode in the derivatization to assure that no traces of metallic cobalt remain. After derivatization, the electrodes were sonicated again for 15 seconds and dried in air overnight.

Characterization of the CoHCF modified electrodes

- **UV-Vis spectroscopy** data was acquired with a Cary 50 (Varian) UV-Vis spectrometer. The modified FTO electrodes were placed in the standard cuvette holder, with the light beam perpendicular to the electrode, passing through the deposited CoHCF, the FTO coating and the glass substrate.
- **IR spectroscopy** data was acquired with an Alpha Bruker FTIR equipped with Attenuated Total Reflectance (ATR) sample holder.
- **X-ray powder diffraction** data was acquired by supporting crystallites from the surface of a CoHCF modified electrode with paratone oil on a Kapton tip. The tip was mounted on a Bruker Kappa APEX II DUO diffractometer equipped with an APPEX 2 4K CCD area detector, a Microsource with $Mo_{K\alpha}$ radiation and an Oxford Cryostream 700 low temperature device. Data collection was performed at 100 K with the Apex2 V2012.2-0 program (Bruker AXS 2010), and integrated with Pilot plug-in from Apex2 V2012.2-0.
- **Scanning Electron microscopy (SEM)** images and EDX spectra were obtained with an Environmental Scanning Electron Microscope JEOL-JMS6400 equipped with an Oxford Instruments X-ray elemental analyzer. The peaks corresponding to K, Fe and Co were integrated. Each electrode surface was analyzed in multiple points and the mean value was calculated to determine the stoichiometry.

UNIVERSITAT ROVIRA I VIRGILI
NOVEL MOLECULAR CATALYSTS FOR WATER OXIDATION: TOWARDS ARTIFICIAL PHOTOSYNTHESIS
Sara Goberna Ferrón
Dipòsit Legal: T.189-2014

Electrochemical methods

All electrochemical experiments were performed with a Biologic SP-150 potentiostat, a ALS Ag/AgCl (3.5 M KCl) reference electrode and a Pt wire or mesh counter electrode. All potentials reported in this manuscript were converted to the NHE reference scale using **E**(NHE) = **E**(Ag/AgCl) + 0.209 V. Unless otherwise stated, the buffer electrolyte used for bulk water electrolysis was prepared at 50 mM potassium phosphate (KP_i), and 1 M KNO_3 as electrolyte.

Bulk water electrolysis was carried out with stirring in a two−chamber cell, with a porous frit connecting both chambers. In one chamber we placed a Pt mesh counter electrode, and in the other chamber a 1 cm x 1.5 cm CoHCF modified FTO working electrode and a BASi Ag/AgCl (KCl 3.5 M) reference electrode. A solution of 50 mM KP_i (1 M KNO_3) at the desired pH was used as electrolyte. Ohmic drop was compensated using the positive feedback compensation implemented in the instrument. **Oxygen evolution** was determined with an Ocean Optics NeoFOX oxygen−sensing system equipped with a FOXY probe inserted into the head−space of the anodic compartment. The solution head−space was purged with high purity nitrogen gas for 30 minutes with vigorous stirring. Once the nitrogen gas stream is stopped, the oxygen fluorescence signal was allowed to stabilize. The residual oxygen signal in the absence of an applied potential was recorded for 20 minutes, although it becomes constant after ~5 minutes. This confirms the cell is gas-tight. Then the desired potential was applied. The Faradaic oxygen evolution was calculated taking into account that 4 e^- are needed to produce one molecule of O_2. The fluorescence data measured was transformed into µmols of O_2 after a five−point calibration of the same electrochemical cell by addition of known quantities of high purity oxygen gas. **Mass spectroscopy** measurements were performed using an Omnistar TM GSD 301 C (Pfeiffer) quadrupole mass spectrometer apparatus. The solution head−space was purged with high purity nitrogen gas for 30 minutes with vigorous stirring. Once the nitrogen gas stream is stopped, the composition of the gas phase (O_2 *m/z*=32; N_2

UNIVERSITAT ROVIRA I VIRGILI
NOVEL MOLECULAR CATALYSTS FOR WATER OXIDATION: TOWARDS ARTIFICIAL PHOTOSYNTHESIS
Sara Goberna Ferrón
Dipòsit Legal: T.189-2014

m/z=28 and CO_2 *m/z*=44) was measured during bulk water oxidation experiments. For this purpose a vial sealed with a septum was degassed during 30 minutes, and the MS-spectrometer cannula was inserted through the septum. Then, samples of 200 µL from the generated gas phase in the anodic compartment of the bulk electrolysis experiment headspace were taken with a 250 µL Hamilton gas-tight syringe and immediately injected into the vial through the septum.

Tafel analysis were carried out by obtaining steady current density data from bulk water electrolysis at different applied potentials. A well−stirred 50 mM KP_i (1 M KNO_3) at the desired pH was used as electrolyte in the same set−up than the described for bulk electrolysis experiments. The current of electrolysis were used as steady state data. All measurements were made three times and averaged. The variation found in different runs was always less than 5 %.

4.1.2 Photo−Induced Water Oxidation with Prussian Blue (PB) type WOCs.

Synthesis and Characterization of Prussian Blue Type Complexes

Potassium hexacyanoferrate $K_3[Fe(CN)_6]$ (Acros Organics, 98%), potassium hexacyanocobaltate $K_3[Co(CN)_6]$ (Acros Organics, 98%), potassium hexacyanochromate $K_3[Cr(CN)_6]$ (SAFC, 99,99%), cobalt chloride hexahydrate $CoCl_2.6H_2O$ (Fluka, ≥ 98%), niquel chloride hexahydrate $NiCl_2.6H_2O$ (Fluka, ≥ 98%), manganese chloride tetrahydrate $MnCl_2.4H_2O$ (Sigma-Aldrich, 98%+), cupper chloride dihydrate $CuCl_2.2H_2O$ (Sigma-Aldrich, 98%+). All the solutions were prepared with Milli-Q water (typically 18.2 MΩ−cm resistivity).

Synthesis procedure:

The materials were synthesized by precipitation employing the “drop by drop” (DbD) methodology described by Berrettoni et al.[1] In a typical synthesis, 100 mL of an

UNIVERSITAT ROVIRA I VIRGILI
NOVEL MOLECULAR CATALYSTS FOR WATER OXIDATION: TOWARDS ARTIFICIAL PHOTOSYNTHESIS
Sara Goberna Ferrón
Dipòsit Legal: T.189-2014

aqueous solution of 0.01M $K_3[M(CN)_6]$ (M = Fe, Co or Cr) was added drop by drop to 100 mL of an aqueous solution of 0.02 M of the respective metal chloride, at room temperature (25 °C aprox.) and stirring constant. After total addition of hexacyanometallate solution, the obtained slurry was keeped under stirring during one hour and then was washed with Milli-Q water three times, by centrifugation. The execss of water was removed from the obtained solid at 40 °C, under vacuum. Finally, the collected powder was leaved at 40 °C during 2 hours in an oven.

The obtained materials were named according to the nature of the metal transition cations used for the sythesis and the corresponding hexacyanometallante (HC-metalate), as follow: MHCF, MHCCo and MHCCr where M corresponds to Co, Cu, Mn or Ni.

Characterization:

- **X- ray diffraction**: The compounds were characterized by X-ray powder diffraction with a Bruker D8 Advance Series equipped with a VÅNTEC-1PSD detector (Figure 4.30). Assuming the space group Fm3m (a face centered cubic structure), all the reflections can be indexed and no additional reflections were observed. There is not preferential orientation in the polycrystalline samples; nevertheless, the intensity, position and width of the reflections depend of the transition metal cation occupying the nitrogen-coordinated position in the lattice (Co, Cu, Mn or Ni). The observed smaller 2θ angle for the MnHCF compound corresponds with a bigger unit cell edge, related with the bigger size of the Mn^{2+} ion.

UNIVERSITAT ROVIRA I VIRGILI
NOVEL MOLECULAR CATALYSTS FOR WATER OXIDATION: TOWARDS ARTIFICIAL PHOTOSYNTHESIS
Sara Goberna Ferrón
Dipòsit Legal: T.189-2014

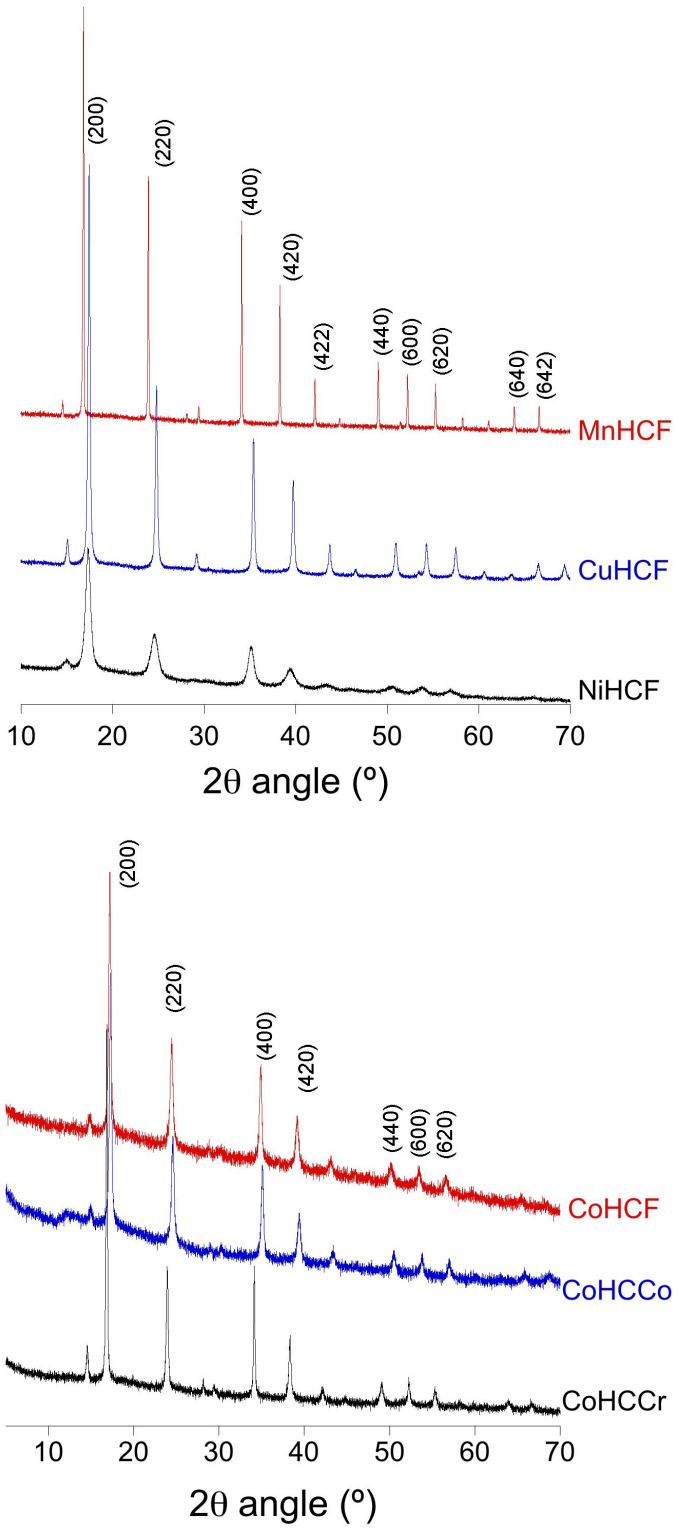

Figure 4.30. *XRD patterns of the synthetized materials.*

UNIVERSITAT ROVIRA I VIRGILI
NOVEL MOLECULAR CATALYSTS FOR WATER OXIDATION: TOWARDS ARTIFICIAL PHOTOSYNTHESIS
Sara Goberna Ferrón
Dipòsit Legal: T.189-2014

- **Thermal Gravimetric Analysis** (TGA): The solvent content was determined by thermogravimetry (Table 3.3). TGA was performed with power samples using a TGA/SDTA851 Mettler Toledo with MT1 microbalance.

Code	H_2O per formula unit
CoHCF	$Co_3[Fe(CN)_6]_2.14H_2O$
CuHCF	$Cu_3[Fe(CN)_6]_2.12H_2O$
MnHCF	$Mn_3[Fe(CN)_6]_2.12H_2O$
NiHCF	$Ni_3[Fe(CN)_6]_2.15H_2O$
CoHCCo	$Co_3[Co(CN)_6]_2.16H_2O$
CoHCCr	$Co_3[Cr(CN)_6]_2.12H_2O$

Table 4.3. *Solvent content summary determined by TGA*.

About the thermal stability of these types of solids (Figure 4.31), it has been reported to be mostly related to the release of the coordinated and zeolitic water from the materials structure and the decomposition of the ferricyanide complex to ferrocyanide, liberating C_2N_2.[32,33] The evolution of crystal water is normally described at temperatures below 100 °C, implying a weight loss close to 30%. The relatively easy dehydration of these compounds is related to their open channel framework, which even allows the evolution of water at room temperature under vacuum conditions. The depletion of water from the materials studied take place in a wide range of temperature from 100 to 200 °C, depending on the metal transition cation involved in their structures. For CoHCF, CoHCCo and CoHCCr materials does not exist a thermal event related to the cyano-ligand decomposition (above 280 °C), this behavior have been explained by a heat-induced charge transfer that allows the occurrence of an

UNIVERSITAT ROVIRA I VIRGILI
NOVEL MOLECULAR CATALYSTS FOR WATER OXIDATION: TOWARDS ARTIFICIAL PHOTOSYNTHESIS
Sara Goberna Ferrón
Dipòsit Legal: T.189-2014

inner redox reaction with the formation of a mixed valence Co(II)Co(III) ferrocyanide, with a relatively improved thermal stability.[32,34]

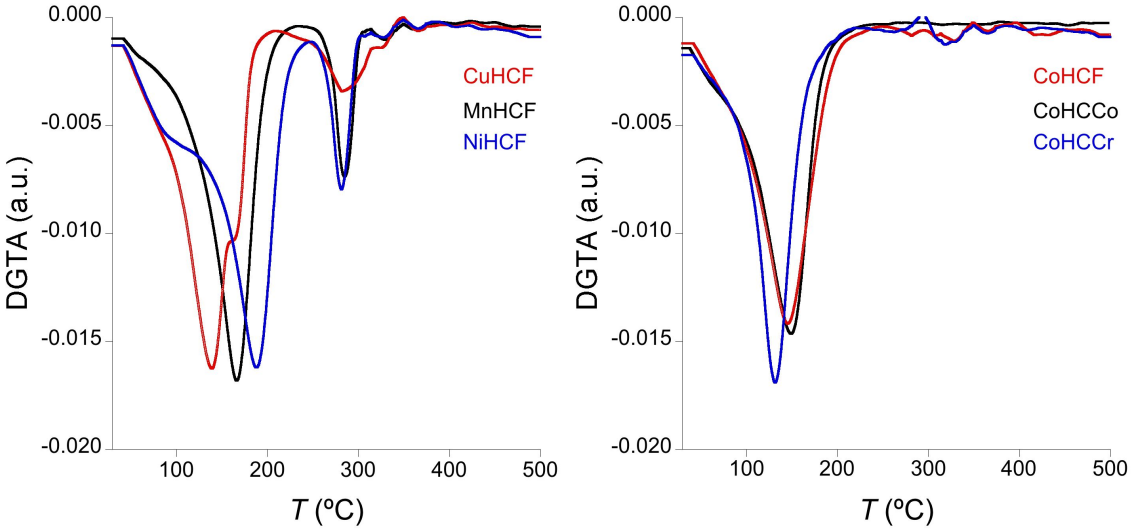

Figure 4.31. *Differential thermal analysis (DGTA) of $M_3[M'(CN)_6]$.* ***Left:*** *M = Cu; Mn and Ni, M' = Fe.* ***Right:*** *M = Co, M' = Fe; Co and Cr.*

❖ **EDX microanalysis**: Metal content was analyzed with a Scanning Electron Microscope (SEM) JEOL-JMS6400 equipped an Oxford EDX analyzer (Oxford Instruments) (Table 4.4). In all the MHCF synthesized materials, the obtained M/Fe molar ratio is very close to the target one (1.5), which is expected to promote the generation of a lacunary structure materials where the $[Fe(CN)_6]$ vacancies are filled by water molecules.[35] The low content of K in these materials (K/(M+Fe)) is also in good agreement with this structural feature. In addition, SEM images of the MnHCF compound, which is the only one composed by well–defined micrometric cubes, were taken (Figure 4.32).

Code	M/Fe	K / (M+Fe)

UNIVERSITAT ROVIRA I VIRGILI
NOVEL MOLECULAR CATALYSTS FOR WATER OXIDATION: TOWARDS ARTIFICIAL PHOTOSYNTHESIS
Sara Goberna Ferrón
Dipòsit Legal: T.189-2014

	molar ratio	molar ratio
CoHCF	1.19	0.0084
CuHCF	1.60	0.0038
MnHCF	1.47	0.033
NiHCF	1.64	0.014

Table 4.4. *Metal analysis summary results calculated from EDX analysis.*

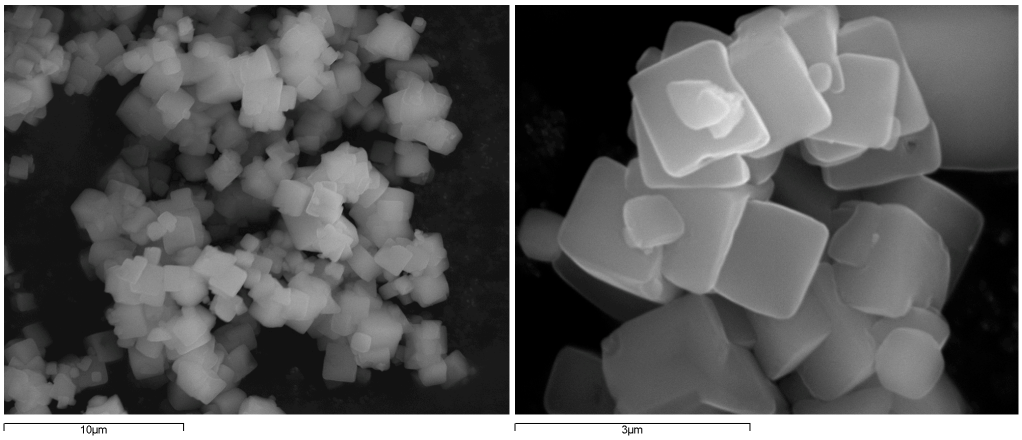

Figure 4.32. *SEM images obtained for MnHCF solid.*

- **IR spectroscopy**: IR spectra for powder samples of the synthetized compounds were collected in the 3600-400 cm^{-1} range with a Bruker Optics FTIR Alpha spectrometer equipped with a DTGS detector, KBr beamsplitter at 4cm^{-1} resolution (Figure 4.33). The region in the 2000 to 2250 cm^{-1} shows the characteristic M^{II}–CN–M'^{III} ($M_3[M'(CN)_6$) vibrational mode between 2147 and 2172 cm^{-1} and additional vibrational bands in between 2125 and 2050 cm^{-1}. These additional bands correspond to different electronic configurations: M^{III}–CN–M'^{II} and M^{II}–CN–M'^{II}.

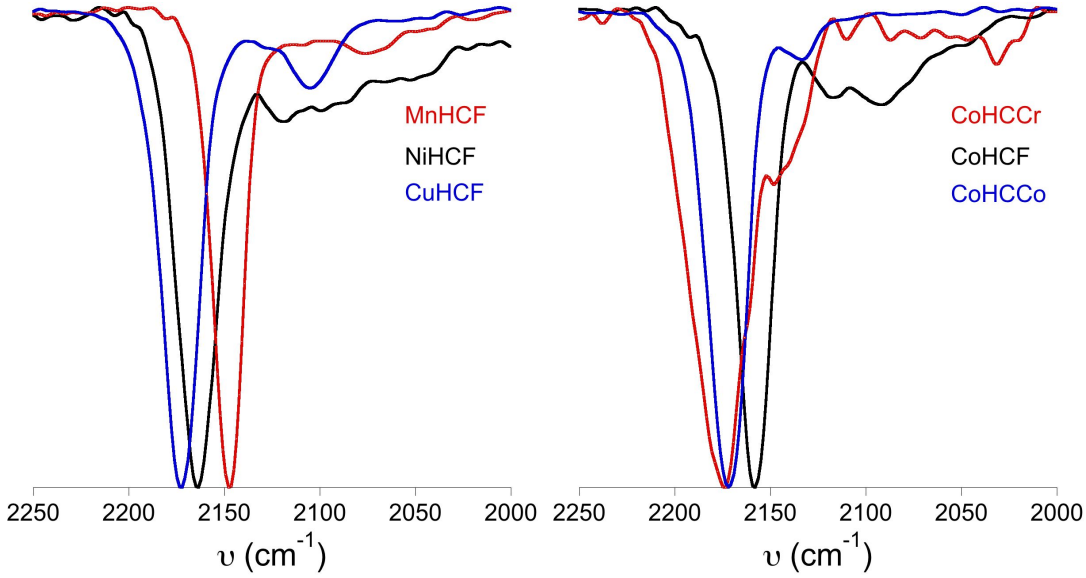

Figure 4.33. *Normalized IR spectra of the υ(CN) region.*

Photo–induced Water Electrolysis Measurements

Tris(2,2′-bipyridyl)dichlororuthenium(II) hexahydrate and sodium persulfate were purchased from TCI and Aldrich respectively. In a typical experiment, light–induced water oxidation was performed in a 20 mL schlenck flask. The vessel was filled with a solution with 1 mM $[Ru(bpy)_3]^{2+}$, 5 mM $Na_2S_2O_8$ and 10 mg of catalyst. The final reaction volume was 12.5 mL of 40 mM potassium phosphate buffer (KaPi), initial pH = 7. The reaction vessel was then sealed with a septum that incorporates the O_2–sensor probe (Ocean Optics NeoFOX oxygen–sensing system equipped with a FOXY probe), carefully deairated with nitrogen and vigorously stirred to equilibrate O_2 concentration in liquid and gas phase. All procedures were performed with a minimum exposure to ambient light. The reaction was initiated by turning on the blue LED (Wavelength at peak emission = 465 nm; OSRAM Opto Semiconductors) and vigorously stirred to equilibrate O_2 concentration in liquid and gas phase. The kinetics of oxygen formation was followed continuously in the headspace with the O_2–sensor

UNIVERSITAT ROVIRA I VIRGILI
NOVEL MOLECULAR CATALYSTS FOR WATER OXIDATION: TOWARDS ARTIFICIAL PHOTOSYNTHESIS
Sara Goberna Ferrón
Dipòsit Legal: T.189-2014

probe. The reaction was stopped by turning off the blue LED.

The **number of moles of O_2 produced** were calculate following equation 3.14:

$$n_{O2} = \{(\%O_2)n_{N2}/100\} \quad \text{(Eq. 3.14)}$$

Where n_{O2} = number of oxygen moles; $\%O_2$ is given by the oxygen−sensing system and n_{N2} = number of moles of nitrogen (calculated using the Ideal gas law (Eq. 3.15):

$$PV = n_{N2}RT \quad \text{(Eq. 3.15)}$$

Where P = 1atm; V = gas-space volume; n_{N2} = number of N_2 moles; R (gas constant) = 0.083 atmL/molK and T = 298 K.

The **Turnover frequency** (TOF, s^{-1}) was calculated by plotting n_{O2} vs. time; the very beginning of the O_2 evolution follows a linear fit, from the slope (n_{O2}/ time) the TOF can be extracted following equations 3.17-3.17:

$$TON = n_{O2}/n_{cat} \quad \text{(Eq. 3.16)}$$

$$TOF = TON/t = slope/n_{cat} \quad \text{(Eq. 3.16)}$$

Where *TON* = turnover number; n_{O2} = number of oxygen moles and n_{cat} is the number of moles of catalyst.

UNIVERSITAT ROVIRA I VIRGILI
NOVEL MOLECULAR CATALYSTS FOR WATER OXIDATION: TOWARDS ARTIFICIAL PHOTOSYNTHESIS
Sara Goberna Ferrón
Dipòsit Legal: T.189-2014

UNIVERSITAT ROVIRA I VIRGILI
NOVEL MOLECULAR CATALYSTS FOR WATER OXIDATION: TOWARDS ARTIFICIAL PHOTOSYNTHESIS
Sara Goberna Ferrón
Dipòsit Legal: T.189-2014

4.5

References

1 Woodward, J. Praeparatio Caerulei Prussiaci Ex Germania Missa ad Johannem Woodward, M. D. Prof. Med. Gresh. R. S. S. *J Philos Trans* **33**, 15-17 (1724).

2 Dabrowski, M. *et al.* (ed The Metropolitan Museum of Art) (New York, 2010).

3 Durnbar, K. R. & Heintz, R. A. Modern Perspectives in Cyanide Chemistry. *Prog. Inorg. Chem.* **45**, 283-391 (1997).

4 Buser, H. J., Schwarzenbach, D., Petter, W. & Ludi, A. The crystal structure of Prussian Blue: Fe4[Fe(CN)6]3.xH2O. *Inorg. Chem.* **16**, 2704–2710 (1977).

5 Ferlay, S., Mallah, T., Ouahes, R., Veillet, P. & Verdaguer, M. A room-temperature organometallic magnet based on Prussian blue. *Nature* **378**, 701-703 (1995).

6 Wang, J. Electrochemical glucose biosensors. *Chem. Rev.* **108**, 814-825 (2008).

7 DeLongchamp, D. M. & Hammond, P. T. High-Contrast Electrochromism and Controllable Dissolution of Assembled Prussian Blue/Polymer Nanocomposites. *Adv. Funct. Mater.* **14**, 224-232 (2004).

8 Kaye, S. S. & Long, J. R. The role of vacancies in the hydrogen storage properties of Prussian blue analogues. *Catal. Today* **120**, 311-316 (2007).

9 Ohkoshi, S. *et al.* High proton conductivity in prussian blue analogues and the interference effect by magnetic ordering. *J. Am. Chem. Soc.* **132**, 6620-6621 (2010).

10 Itaya, K., Uchida, I. & Neff, V. D. Electrochemistry of polynuclear transition metal cyanides: Prussian blue and its analogues. *Acc. Chem. Res.* **19**, 162-168 (1986).

11 de Tacconi, N., R, Rajeshwar, K. & Lezna, R., O. Metal Hexacyanoferrates: Electrosynthesis, in Situ Characterization, and Applications. *Chem. Mater.* **15**, 3046-3062 (2003).

12 Chen, S. Preparation, characterization, and electrocatalytic oxidation properties of iron, cobalt, nickel, and indium hexacyanoferrate. *J. Electroanal. Chem.* **521**, 29-52 (2002).

13 Itaya, K., Shoji, N. & Uchida, I. Catalysis of the reduction of molecular oxygen to water at Prussian blue modified electrodes. *J. Am. Chem. Soc.* **106**, 3423–3429 (1984).

14 Kanan, M. W. & Nocera, D. G. In situ formation of an oxygen-evolving catalyst in neutral water containing phosphate and Co(2+). *Science* **321**, 1072-1075 (2008).

UNIVERSITAT ROVIRA I VIRGILI
NOVEL MOLECULAR CATALYSTS FOR WATER OXIDATION: TOWARDS ARTIFICIAL PHOTOSYNTHESIS
Sara Goberna Ferrón
Dipòsit Legal: T.189-2014

15 Yin, Q. S. *et al.* A Fast Soluble Carbon-Free Molecular Water Oxidation Catalyst Based on Abundant Metals. *Science* **328**, 342-345 (2010).

16 Pournaghi-Azar, M. H. & Sabzi, R. Preparation of a cobalt hexacyanoferrate film-modified aluminum electrode by chemical and electrochemical methods: enhanced stability of the electrode in the presence of phosphate and ruthenium(III). *J. Solid State Electrochem.* **6**, 553–559 (2002).

17 Pournaghi-Azar, M. H. & Sabzi, R. Preparation of a cobalt hexacyanoferrate film-modified aluminum electrode by chemical and electrochemical methods: enhanced stability of the electrode in the presence of phosphate and ruthenium(III). *J. Solid State Electrochem.* **6**, 553-559 (2002).

18 Xun, Z., Cai, C., Xing, W. & Lu, T. Electrocatalytic oxidation of dopamine at a cobalt hexacyanoferrate modified glassy carbon electrode prepared by a new method. *J. Electroanal. Chem.* **545**, 19-27 (2003).

19 Heli, H., Eskandari, I., Sattarahmady, N. & Moosavi-Movahedi, A. A. Cobalt nanoflowers: Synthesis, characterization and derivatization to cobalt hexacyanoferrate, Electrocatalytic oxidation and determination of sulfite and nitrite. *Electrochim. Acta* **77**, 294-301 (2012).

20 Bleuzen, A. *et al.* Photoinduced Ferrimagnetic Systems in Prussian Blue Analogues C I x Co 4 [Fe(CN) 6] y (C I = Alkali Cation). 1. Conditions to Observe the Phenomenon. *J. Am. Chem. Soc.* **122**, 6648-6652 (2000).

21 Lezna, R., O, Romagnoli, R., de Tacconi, N., R & Rajeshwar, K. Cobalt Hexacyanoferrate: Compound Stoichiometry, Infrared Spectroelectrochemistry, and Photoinduced Electron Transfer. *J. Phys. Chem. B* **106**, 3612-3621 (2002).

22 Sato, O., Iyoda, T., Fujishima, A. & Hashimoto, K. Photoinduced Magnetization of a Cobalt-Iron Cyanide. *Science* **272**, 704-705 (1996).

23 Shimamoto, N., Ohkoshi, S.-i., Sato, O. & Hashimoto, K. Control of charge-transfer-induced spin transition temperature on cobalt-iron Prussian blue analogues. *Inorg. Chem.* **41**, 678-684 (2002).

24 Gerken, J. B. *et al.* Electrochemical Water Oxidation with Cobalt-Based Electrocatalysts from pH 0–14: The Thermodynamic Basis for Catalyst Structure, Stability, and Activity. *J. Am. Chem. Soc.* **133**, 14431-14442 (2012).

25 Surendranath, Y., Kanan, M. W. & Nocera, D. G. Mechanistic Studies of the Oxygen Evolution Reaction by a Cobalt-Phosphate Catalyst at Neutral pH. *J. Am. Chem. Soc.* **132**, 16501-16509 (2010).

26 Stracke, J. J. & Finke, R. G. Electrocatalytic Water Oxidation Beginning with the Cobalt Polyoxometalate [Co(4)(H(2)O)(2)(PW(9)O(34))(2)](10-): Identification of Heterogeneous CoO(x) as the Dominant Catalyst. *J. Am. Chem. Soc.* **133**, 14872-14875 (2011).

27 Berrettoni, M., Giorgetti, M., Zamponi, S., Conti, P., Ranganathan, D., Zanotto, A., Saladino, M. L. & Caponetti, E. Synthesis and Characterization of

Nanostructured Cobalt Hexacyanoferrate. J. Phys. Chem. C 114, 6401-6407 (2010).

28 Michikazu, H., Chad, C. W., John, T. L., Bradley, A. L. & Thomas, E. M. Photocatalytic Water Oxidation in a Buffered Tris(2,2'-bipyridyl)ruthenium Complex-Colloidal IrO 2 System. *J. Phys. Chem. A* **104**, 5275-5280 (2000).

29 Morris, N. D., Suzuki, M. & Mallouk, T. E. Kinetics of Electron Transfer and Oxygen Evolution in the Reaction of [Ru(bpy) 3] 3+ with Colloidal Iridium Oxide. *J. Phys. Chem. A* **108,** 9115-9119 (2004).

30 Sato, O., Einaga, Y., Fujishima, A. & Hashimoto, K. Photoinduced Long-Range Magnetic Ordering of a Cobalt-Iron Cyanide. *Inorg. Chem.* **38**, 4405-4412 (1999).

31 Mattioli, G., Risch, M., Amore Bonapasta, A., Dau, H. & Guidoni, L. Protonation states in a cobalt-oxide catalyst for water oxidation: fine comparison of ab initio molecular dynamics and X-ray absorption spectroscopy results. *Phys. Chem. Chem. Phys* **13**, 15437-15441 (2011).

32 Balmaseda, J., Reguera, E., Rodriguez-Hernandez, J., Reguera, L. & Autie, M. Behavior of transition metals ferricyanides as microporous materials. *Microporous Mesoporous Mater.* **96**, 222-236 (2006).

33 Roque, J. *et al.* Porous hexacyanocobaltates (III): Role of the metal on the framework properties. *Microporous Mesoporous Mater.* **103**, 57-71 (2007).

34 Martínez-Garcia, R., Knobel, M. & Reguera, E. Thermal-induced changes in molecular magnets based on prussian blue analogues. *J. Phys. Chem. B* **110**, 7296-7303 (2006).

35 Ludi, A. & Gudel, H. U. *Structure and Bonding*. Vol. 14 (1973).

UNIVERSITAT ROVIRA I VIRGILI
NOVEL MOLECULAR CATALYSTS FOR WATER OXIDATION: TOWARDS ARTIFICIAL PHOTOSYNTHESIS
Sara Goberna Ferrón
Dipòsit Legal: T.189-2014

UNIVERSITAT ROVIRA I VIRGILI
NOVEL MOLECULAR CATALYSTS FOR WATER OXIDATION: TOWARDS ARTIFICIAL PHOTOSYNTHESIS
Sara Goberna Ferrón
Dipòsit Legal: T.189-2014

Chapter 5

General Conclusions And outlook

UNIVERSITAT ROVIRA I VIRGILI
NOVEL MOLECULAR CATALYSTS FOR WATER OXIDATION: TOWARDS ARTIFICIAL PHOTOSYNTHESIS
Sara Goberna Ferrón
Dipòsit Legal: T.189-2014

UNIVERSITAT ROVIRA I VIRGILI
NOVEL MOLECULAR CATALYSTS FOR WATER OXIDATION: TOWARDS ARTIFICIAL PHOTOSYNTHESIS
Sara Goberna Ferrón
Dipòsit Legal: T.189-2014

5.1

General Conclusions and Outlook

The beginning of my studies coincided with an incremented interest in the search for new alternatives of classic molecular water oxidation catalysts. Moreover, the discovery that some molecular WOCs decompose into catalytically metallic oxides was an important concern for new and known molecular WOCs.[1-10] Therefore, stability investigations are needed on each newly discovered catalyst for their optimal characterization.

With the aim to explore new molecular WOCs with improved features we decided to investigate complexes that posses the requirements for a viable WOC: stability, multiple and accessible oxidation states and low cost elements.

Among molecular homogeneous WOCs, ruthenium complexes are of high importance, but they are usually based on organic ligands, which are vulnerable to oxidative degradation. These WOCs are easily and rapidly deactivated. We found, and it was descripted in Chapter 2, the catalytic activity of a Ru-Ru bonded complex that is stabilized by acetate ligands, more stable and inexpensive than organic groups. The $[Ru_2(\mu\text{-}O_2CCH_3)_4]$ (**Ru_2**), with the axial positions available for water ligation, was found to be an active WOC in a wide pH range, an uncommon feature among molecular Ru-WOCs. We used two methodologies to estimate limiting turnover frequencies values in electrochemical conditions, a maximum value of 77 s^{-1} and a value of 7 s^{-1} during bulk electrolysis in our experimental conditions were found. Those TOFs suggests that our catalyst is one of the fastest reported among Ru-WOCs. We performed stability tests in order to rule out the possibility of decomposition into catalytically active

UNIVERSITAT ROVIRA I VIRGILI
NOVEL MOLECULAR CATALYSTS FOR WATER OXIDATION: TOWARDS ARTIFICIAL PHOTOSYNTHESIS
Sara Goberna Ferrón
Dipòsit Legal: T.189-2014

RuO_2. Although we observed a slow decomposition via acetate loss, the black powder formed, probably ruthenium oxide, is not participating in the catalysis.

Numerous directions could conceivably be investigated; increasing M-M bond stability could be achieved by using other bridging ligands and / or other transition metals. Preferably, we will focus on Earth-abundant metals and inorganic ligands as phosphate. The stability and redox activity of M-M bond complexes can be easily adjusted by modifications of the bridging ligands and, therefore great opportunities to reach technological needs are expected for this new family of WOCs.

In terms of new directions, another possibility to improve the stability of these species would be the implementation on surface electrodes. M-M bonded catalyst could be supported in polymer membranes, such as Nafion by electrostatic interactions or adsorbed on a heterogeneous matrix, such as clays or attached to electrode surfaces. To demonstrate water oxidation in such heterogeneous media, chemical or electrochemical water oxidation will be used. This strategy will play an important role in the development of water splitting devices.

The final step towards an artificial photosynthetic system would be the use of photosensitizers, such as $Ru(bpy)_3^{2+}$, coupled with the M-M bonded catalysts in order to use light directly to induce water oxidation in the presence of a sacrificial oxidant, such as $S_2O_8^{2-}$.

We have discovery the first M-M bonded WOC, opening a new area of investigation for the M-M bond community and new perspectives to the WOC community.

Polyoxometalate-based WOCs is currently one of the most controversial research areas in water oxidation catalysis. Since the publication in 2010 of the homogeneous catalytic activity of the first carbon-free and earth abundant WOC, $[Co_4(H_2O)_2(PW_9O_{34})_2]^{10-}$ (**Co_4**)[11], the number of papers questioning the nature of the true catalyst continue increasing. We have experienced the general distrust towards new molecular cobalt-based WOCs. In Chapter 3 it has been discussed the

UNIVERSITAT ROVIRA I VIRGILI
NOVEL MOLECULAR CATALYSTS FOR WATER OXIDATION: TOWARDS ARTIFICIAL PHOTOSYNTHESIS
Sara Goberna Ferrón
Dipòsit Legal: T.189-2014

homogeneous catalytic activity of a new Co-based WOC from POM chemistry: $[Co_9(H_2O)_6(OH)_3(HPO_4)_2(PW_9O_{34})_3]^{16-}$ **Co_9**. We demonstrated that in electrochemical conditions **Co_9**, as reported for **Co_4**[6], decomposes forming a cobalt oxide film on the electrode. The origin of the CoO_x species is not decomposition of the supporting ligand but the solution equilibria that liberate traces of free Co^{2+} ions as precursors for the oxide. Indeed, the use of chelating agents able to trap free Co^{2+} ions precludes the formation of any oxide, and the optimal characterization of the homogeneous catalytic activity of **Co_9** was performed. The kinetics features of **Co_9** at neutral pH are similar to those of cobalt oxides[12]. We observed Tafel slopes of 55-65 mV $decade^{-1}$ in diluted conditions, corresponding to a chemical rate-limiting step.

Furthermore, chemical water oxidation was used to test the stability of **Co_9** using sodium hypochlorite as sacrificial oxidant at pH close to neutrality. We observed that **Co_9** catalyzes water during days with any sign of fatigue or decomposition. Here we have found another concern: hypochlorite can exchange its oxygen with bulk water, leading to concerns that the oxygen produced was result of hypochlorite disproportionation rather than water oxidation.[13] To solve this issue we designed an ^{18}O-labelled solvent experiment that give us insights about the origin of the O_2 produced. Although it is not possible to unambiguously determinate the origin of the oxygen evolved, the most plausible hypothesis regarding our results is that the main source of O_2 is water.

We also tested the catalytic activity of **Co_9** under light-induced conditions; our results indicate that **Co_9** is also a homogeneous WOC under these conditions. As preliminary results we observed a good performance and possibility of catalyst recovery. Additional studies regarding the stability of **Co_9** in a photo-driven water oxidation system is currently topic of research collaboration.

Regarding future perspectives, our group has already demonstrate that homogeneous molecular WOCs from POM chemistry are also active catalysts in the

UNIVERSITAT ROVIRA I VIRGILI
NOVEL MOLECULAR CATALYSTS FOR WATER OXIDATION: TOWARDS ARTIFICIAL PHOTOSYNTHESIS
Sara Goberna Ferrón
Dipòsit Legal: T.189-2014

solid state.[14] The insoluble salt of **Co_9** can be incorporated into a solid−state matrix to promote heterogeneous catalytic water electrolysis at wide pH range, high activity was found in acidic media (pH ≤ 1) where metal oxides are unstable. Moreover, our group collaborates with the research group of Prof. J. M. Poblet (Universitat Rovira i Virgili, Tarragona) performing DFT calculations to model the electronic structure POMs in order to obtain some insight into mechanisms and into the most important features needed for performance optimization.

All the efforts of our group will be addressed on heterogeneously supported POMs for water oxidation, which provides improved stability, easy recovery of the catalyst and broader reaction conditions. This will lead to the construction of an artificial photosynthetic system comprising a dye-sensitized solar cell connected to a H-type electrochemical cell. After irradiation, the voltage produced will oxidize water into molecular oxygen and hydrogen ions in the POM-modified anode, while hydrogen ions and electrons will be combined in the cathode to produce hydrogen.

Heterogeneous catalysts have the advantage of higher stability and easier implementation in devices. However, they are usually slow since only part of the surface is active. Most heterogeneous WOCs reported to date are transition metal oxides. In Chapter 4 it has been discussed the catalytic activity of a new class of heterogeneous WOCs: Prussian blue (PB) type polymers. With respect to other solid-state materials currently being used, PB type compounds present some advantages including porosity (larger active surface area) and chemical versatility to tune the redox properties. We characterize the catalytic activity of cobalt hexacyanoferrate (CoHCF) modified electrodes for water oxidation, this catalyst is formed from earth-abundant materials and it is stable under turnover conditions. CoHCF oxidizes water when a reasonable overpotential is applied and it is fast enough to compete with state−of−the−art cobalt oxides, as well as being transparent, low density and stable at neutral pH and room temperature. Moreover, as a cobalt-containing WOC, we fully

UNIVERSITAT ROVIRA I VIRGILI
NOVEL MOLECULAR CATALYSTS FOR WATER OXIDATION: TOWARDS ARTIFICIAL PHOTOSYNTHESIS
Sara Goberna Ferrón
Dipòsit Legal: T.189-2014

characterize the electrode composition after catalytic water oxidation to rule out the possibility of decomposition into cobalt oxide. We take care of the deposition process to avoid cobalt oxide impurities and we performed control experiments that confirm that CoHCF is the true active catalyst.

We demonstrate through photo-induced water oxidation that only cobalt-containing Prussian blue complexes are suitable for water oxidation. Our group will work in electrochemical or photoelectrochemical water oxidation systems containing these new type of WOCs. Deposition of these compounds in other substrates than FTO is currently under investigation, specially into amorphous carbon and TiO_2.

This promising new class of WOCs is an attractive are of investigation for artificial photosynthesis applications.

In general, all water oxidation catalysts presented in this thesis are significantly a breakthrough in the research area. From new applications of M-M bonded and cyanide complexes to new perspectives in POM-based WOCs.

UNIVERSITAT ROVIRA I VIRGILI
NOVEL MOLECULAR CATALYSTS FOR WATER OXIDATION: TOWARDS ARTIFICIAL PHOTOSYNTHESIS
Sara Goberna Ferrón
Dipòsit Legal: T.189-2014

UNIVERSITAT ROVIRA I VIRGILI
NOVEL MOLECULAR CATALYSTS FOR WATER OXIDATION: TOWARDS ARTIFICIAL PHOTOSYNTHESIS
Sara Goberna Ferrón
Dipòsit Legal: T.189-2014

5.2

References

1 Savini, A., Belanzoni, P., Bellachioma, G., Zuccaccia, C., Zuccaccia, D. & MacChioni, A. Activity and degradation pathways of pentamethyl-cyclopentadienyl-iridium catalysts for water oxidation. *Green Chem.* **13**, 3360-3374 (2011).

2 Grotjahn, D. B., Brown, D. B., Martin, J. K., Marelius, D. C., Abadjian, M.-C., Tran, H. N., Kalyuzhny, G., Vecchio, K. S., Specht, Z. G., Cortes-Llamas, S. A., Miranda-Soto, V., van Niekerk, C., Moore, C. E. & Rheingold, A. L. Evolution of Iridium-Based Molecular Catalysts during Water Oxidation with Ceric Ammonium Nitrate. *J. Am. Chem. Soc* **133**, 19026-19027 (2011).

3 Schley, N. D., Blakemore, J. D., Subbaiyan, N. K., Incarvito, C. D., D'Souza, F., Crabtree, R. H. & Brudvig, G. W. Distinguishing Homogeneous from Heterogeneous Catalysis in Electrode-Driven Water Oxidation with Molecular Iridium Complexes. *J. Am. Chem. Soc.* **133**, 10473-10481 (2011).

4 Blakemore, J. D., Schley, N. D., Olack, G. W., Incarvito, C. D., Brudvig, G. W. & Crabtree, R. H. Anodic deposition of a robust iridium-based water-oxidation catalyst from organometallic precursors. *Chemical Science* **2**, 94-98 (2011).

5 Natali, M., Berardi, S., Sartorel, A., Bonchio, M., Campagna, S. & Scandola, F. Is [Co4(H2O)2([alpha]-PW9O34)2]10- a genuine molecular catalyst in photochemical water oxidation? Answers from time-resolved hole scavenging experiments. *Chem. Commun.* **48**, 8808-8810 (2012).

6 Stracke, J. J. & Finke, R. G. Electrocatalytic Water Oxidation Beginning with the Cobalt Polyoxometalate [Co(4)(H(2)O)(2)(PW(9)O(34))(2)](10-): Identification of Heterogeneous CoO(x) as the Dominant Catalyst. *J. Am. Chem. Soc.* **133**, 14872-14875 (2011).

7 Artero, V. & Fontecave, M. Solar fuels generation and molecular systems: is it homogeneous or heterogeneous catalysis? *Chem. Soc. Rev.* **42**, 2338-2356 (2013).

8 Hintermair, U., Hashmi, S., Elimelech, M. & Crabtree, R. Particle formation during oxidation catalysis with Cp* iridium complexes. *J. Am. Chem. Soc.* **134**, 9785-9795 (2012).

9 Hong, D., Murakami, M., Yamada, Y. & Fukuzumi, S. Efficient water oxidation by cerium ammonium nitrate with [IrIII(Cp*)(4,4[prime or minute]-bishydroxy-2,2[prime or minute]-bipyridine)(H2O)]2+as a precatalyst. *Energy Environ. Sci.* **5**, 5708-5716 (2012).

UNIVERSITAT ROVIRA I VIRGILI
NOVEL MOLECULAR CATALYSTS FOR WATER OXIDATION: TOWARDS ARTIFICIAL PHOTOSYNTHESIS
Sara Goberna Ferrón
Dipòsit Legal: T.189-2014

10 Hong, D., Jung, J., Park, J., Yamada, Y., Suenobu, T., Lee, Y.-M., Nam, W. & Fukuzumi, S. Water-soluble mononuclear cobalt complexes with organic ligands acting as precatalysts for efficient photocatalytic water oxidation. *Energy Environ. Sci.* **5**, 7606-7616 (2012).

11 Yin, Q. S., Tan, J. M., Besson, C., Geletii, Y. V., Musaev, D. G., Kuznetsov, A. E., Luo, Z., Hardcastle, K. I. & Hill, C. L. A Fast Soluble Carbon-Free Molecular Water Oxidation Catalyst Based on Abundant Metals. *Science* **328**, 342-345 (2010).

12 Surendranath, Y., Kanan, M. W. & Nocera, D. G. Mechanistic Studies of the Oxygen Evolution Reaction by a Cobalt-Phosphate Catalyst at Neutral pH. *J. Am. Chem. Soc.* **132**, 16501-16509 (2010).

13 Limburg, J., Vrettos, J. S., Chen, H. Y., de Paula, J. C., Crabtree, R. H. & Brudvig, G. W. Characterization of the O-2-evolving reaction catalyzed by (terpy)(H2O)Mn-III(O)(2)Mn-IV(OH2)(terpy) (NO3) (terpy=2,2 ': 6,2 ''-terpyridine). *J. Am. Chem. Soc.* **123**, 423-430 (2001).

14 Soriano-López, J., Goberna-Ferrón, S., Vigara, L., Carbó, J., Poblet, J. M. & Galán-Mascarós, J. R. Cobalt polyoxometalates as heterogeneous water oxidation catalysts. *Inorg. Chem.* **52**, 4753-4755 (2013).

UNIVERSITAT ROVIRA I VIRGILI
NOVEL MOLECULAR CATALYSTS FOR WATER OXIDATION: TOWARDS ARTIFICIAL PHOTOSYNTHESIS
Sara Goberna Ferrón
Dipòsit Legal: T.189-2014

Appendix I

Tafel equation and Tafel plots

Tafel equation governs the irreversible behavior of an electrode. Considering the general mechanism of electron transfer to an electrode:[1]

$$O + ne^- \rightleftharpoons R \qquad \text{(Eq. AI.1)}$$

Where O is oxidized and R is reduced species present in equilibrium and stable in the solution.

The equilibrium for an electrode reaction is characterized by the Nernst equation, which relates the electrode potential to the bulk concentrations of the components:

$$E = E^0 + \frac{RT}{nF}\ln\frac{C_O^*}{C_R^*} \qquad \text{(Eq. AI.2)}$$

Where C_O^* and C_R^* are O and R concentrations respectively and they are very low; E^0 is the formal potential; R is the universal gas constant, R = 8.314 472(15) J K^{-1} mol^{-1}; T is the absolute temperature; F is the Faraday's constant, F = 9.648 533 99(24)×10^4 C mol^{-1} and n is the number of electrons involved in the electrode reaction.

The equilibrium mentioned above is dynamic. Although no net current flows across the electrodes, both reduction and oxidation takes place at equal rate, so that the composition of the electrolyte does not change. The exchange current density, j_0 is defined as dynamic flow of electrons or charge in both directions per unit area when an electrode reaction is at equilibrium.

The well-known Butler-Volmer equation is expressed as:

$$j = j_0 \exp\frac{(\alpha n F \eta_A)}{RT} + \exp\frac{(-\alpha n F \eta_C)}{RT} \qquad \text{(Eq. AI.3)}$$

Where the overpotential, η, is the difference between the potential at equilibrium and that applied by the driving power source (almost always a *potentiostat*) and α is the charge transfer barrier (symmetry coefficient).

The previous form of Butler–Volmer equation is valid when the electrode reaction is controlled by electrical charge transfer at the electrode (and not by the mass transfer to or from the electrode surface from or to the bulk electrolyte). This is for a well–stirred solution, or with currents so low that the surface concentrations do not differ appreciably from the bulk values.

By applying a high positive overpotential the anodic current density increases while cathodic current density becomes negligible. Therefore, the second term in equation **AI.3** becomes negligible. The equation can be written as:

$$j = j_0 \exp \frac{(\alpha n F \eta)}{RT} \quad \text{(Eq. AI.4)}$$

$$\log j = \log j_0 + \frac{(\alpha n F \eta)}{2.303 RT} \quad \text{(Eq. AI.5)}$$

Equation **AI.5** is called the **anodic Tafel equation**.

In the same way, at negative overpotentials, cathodic current density is much higher than anodic and the anodic current density becomes negligible:

$$\log j = \log j_0 - \frac{(\alpha n F \eta)}{2.303 RT} \quad \text{(Eq. AI.6)}$$

Equation **AI.6** is called the **cathodic Tafel equation**.

The usual form of Tafel's equation is **η = *a* + *b* log *j*** , where:

$$b = \frac{2.303 RT}{\alpha n F} \quad \text{(Eq. AI.7)}$$

$$a = -\frac{2.303 RT}{\alpha n F} \log j_0 \quad \text{(Eq. AI.8)}$$

Log *j* values are plotted against overpotential to get Tafel plots (Figure AI.1).

b and j_0 are obtained by extrapolation of the linear region of the curve to η = 0.

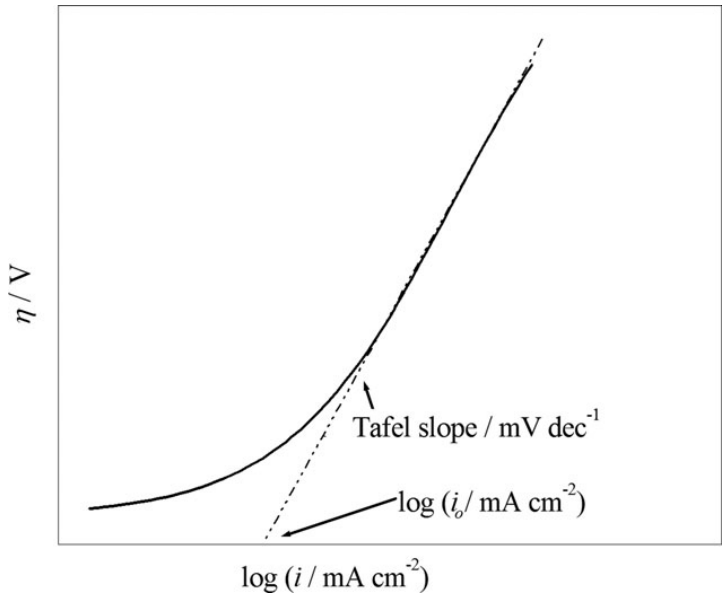

Figure AI.1. *A typical Tafel plot for an electrode reaction, from which exchange current density and Tafel slope can be determined.*[2]

While j_0 is a useful parameter for comparing different catalysts, an electrode material must possess a high j_0 in addition to a low Tafel slope (that means high *j* at low overpotentials) in order to be useful at the operational current densities required for a given energy storage application. Virtually any current can be obtained with any catalyst material if a sufficiently large electrode is used. For this reason, usually current densities are normalized to geometric surface area. Even with this normalization, the performance of a catalyst is enhanced by using a high surface area substrates or catalyst.

The Tafel slope, *b* (mV decade^{-1}) is an important experimental parameter commonly used to probe the mechanism of an electrode reaction and identify the rate determining step of the overall reaction. In electrochemical water oxidation it has been reported that:[3,4]

- Tafel slope ≈ 60 mV decade^{-1} is consistent with a mechanism involving a rate-limiting chemical step.
- Tafel slope ≈ 120 mV decade^{-1} is consistent with a mechanism involving rate-limiting one-electron transfer.

Thus, the Tafel relation between potential and the current density provides a basis for mechanistic interpretation of the catalytic water oxidation.

References Appendix I:

1 Bard, A. J. & Faulkner, L. R. *Electrochemical Methods: Fundamentals and Applications*. (JOHN WILEY & SONS, INC., 2001).

2 Zhao, F., Slade, R. C. T. & Varcoe, J. R. Techniques for the study and development of microbial fuel cells: an electrochemical perspective. *Chem. Soc. Rev.* **38**, 1926–1939 (2009).

3 Surendranath, Y., Kanan, M. W. & Nocera, D. G. Mechanistic Studies of the Oxygen Evolution Reaction by a Cobalt-Phosphate Catalyst at Neutral pH. *J. Am. Chem. Soc.* **132**, 16501-16509 (2010).

4 Gerken, J., McAlpin, J., Chen, J., Rigsby, M., Casey, W., Britt, R. & Stahl, S. Electrochemical water oxidation with cobalt-based electrocatalysts from pH 0-14: the thermodynamic basis for catalyst structure, stability, and activity. *J. Am. Chem. Soc.* **133**, 14431-14442 (2011).

Appendix II

Adsorbed Species and Surface Coverage

Considering that only the absorbed species on the electrode surface are electroactive, the diffusive transport plays no role and the general mechanism of electron transfer to an electrode is:[1]

$O_{adsorbed} + ne^- \rightleftharpoons R_{adsorbed}$ (Eq. AII.1)

Where $O_{adsorbed}$ is oxidized and $R_{adsorbed}$ is reduced species adsorbed on the surface of the electrode.

When this happens the adsorption phenomenon follows the Langmuir isotherm, and in cyclic voltammograms the current intensity at the maximum of the forward peak is correlated with the parameter Γ_0 (surface concentration) and with the scan rate according to the relationship:

$$i = \frac{n^2 F^2 \Gamma_0 A}{4RT} \upsilon \quad \text{(Eq. AII.2)}$$

Where n = number of electrons involved in the electrode reaction; F = Faraday's constant; A = surface area; Γ_0 = surface concentration (mol cm^{-2}); R = ideal gas constant; T = temperature and υ = potential scan rate (V s^{-1}).

This equation is derived from Nerst equation:

$$E = E^0 + \frac{RT}{nF} \ln \frac{C_O(t)}{C_R(t)} \quad \text{(Eq. AII.3)}$$

Where E^0 is the formal potential of the redox couple and $C_O(t)$ and $C_R(t)$ are O and R time−dependent concentrations.

Since there is no bulk concentration, the current (i) can be expressed in terms of the change of concentration of the oxidized species:

$$i = -nFV \left[\frac{dC_O(t)}{dt}\right] \quad \text{(Eq. AII.4)}$$

Where n = number of transferred electrons; *V* = volume and *t* = time. Since the total concentration is constant:

$$C_T = C_O(t) + C_R(t) \quad \text{(Eq. AII.5)}$$

And an expression for $C_O(t)$ can be obtained as a function of applied potential *E*:

$$C_O(t) = \frac{C_T \exp\left[\frac{nF(E-E^0)}{RT}\right]}{1+\exp\left[\frac{nF(E-E^0)}{RT}\right]} \quad \text{(Eq. AII.6)}$$

Differentiating this equation with respect to *t*, and substituting in **Eq. AII.4**:

$$i = \frac{n^2F^2VC_t\upsilon}{RT}\frac{\exp\left[\frac{nF(E-E^0)}{RT}\right]}{\left\{1+\exp\left[\frac{nF(E-E^0)}{RT}\right]\right\}^2} \quad \text{(Eq. AII.7)}$$

Where the scan rate is $\upsilon = -\frac{dE}{dt}$. At peak current, $E = E^0$, and then:

$$i = \frac{n^2F^2\mathrm{V}C_T}{4RT}\upsilon \quad \text{(Eq. AII.8)}$$

And replacing VC_T by $A\Gamma_0$, equation **AII.2** is obtained.

In cyclic voltammetry experiments, the slope of the linear *i* vs υ plot is used to calculate the surface concentration of active redox centers, Γ_0 (mol cm^{-2}):

$$slope = \frac{n^2F^2\Gamma_0 A}{4RT} \quad \text{(Eq. AII.9)}$$

References Appendix II:

1 Zanello, P. *Inorganic electrochemistry : theory, practice and applications*. (The Royal Society of Chemistry: Cambridge, UK, 2003).